PREDICTING THE MECHANICAL BEHAVIOUR OF SMART TEXTILES

DHIFAF AL-AMEEDI

A THESIS SUBMITTED TO

AUCKLAND UNIVERSITY OF TECHNOLOGY

IN FULFILLMENT OF THE REQUIREMENTS FOR THE DEGREE OF

DOCTOR OF PHILOSOPHY (PH.D.)

2025

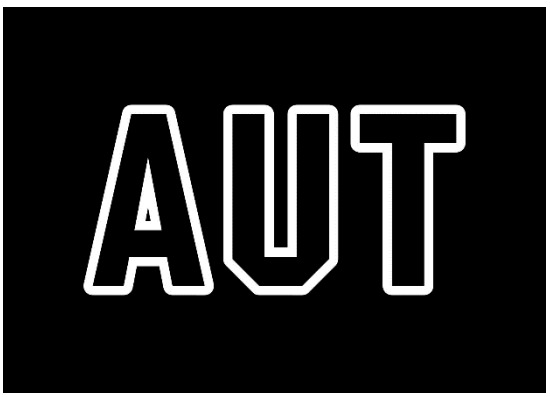

School of Engineering, Computer and Mathematical Sciences

Faculty of Design and Creative Technologies

Supervisors: Prof Andrew Lowe, Prof Frances Joseph

Abstract

Textiles are being progressively explored for use as transducers. Transducers convert energy or variations in physical quantities, such as pressure or brightness, into electrical signals or vice versa. Textile transducers facilitate prompt implementation in the biomedical range because they are correlated with soft constructions suitable to conform to anatomical shapes. Textile transducers classically combine conventional and non-conventional yarns and depend on carefully tailored yarn combinations and structuring of different materials. However, investigations in this field tend to be based on empirical techniques to characterise the functioning of specific textile transducers, meaning that this information cannot be generalised. This study aims to develop a model for predicting the mechanical performance of knitted textile materials by observing the characteristics of textiles to eliminate the need for designers to develop their prototypes using trial-and-error processes. The key objective of this study is to understand and predict the mechanical behaviour of smart knitted textiles by developing and testing a theoretical model.

This research focuses on the behaviour of plain weft knitted textiles using a single conductive yarn type and nonconductive yarn when applying a uniaxial mechanical load. Particle Image Velocimetry (PIV) was used to precisely measure the dynamic movement and stretching of fabrics during mechanical strain. The information gained from this process informed the development of a theoretical framework based on energy conservation principles. A range of empirical tests were used to validate the theoretical model. The model was further used to inspect the effect of different conductive and nonconductive yarns and stitch arrangements on the structure of the knitted textile.

The findings offer valuable insights into the mechanical properties and potential uses of smart knitted textiles, underscoring their exceptional flexibility, stretchiness, and integration capabilities in comparison to woven and non-woven fabrics. the contributions of this research seem to focus on both the theoretical understanding and practical applications of smart knitted textiles, specifically regarding their mechanical behaviour, flexibility, and potential uses as

sensors. These contributions could be grouped into larger subjects if they share a common goal. Here's how they might come together:

- Mechanical Properties and Integration: Explain how the study discovers the specific mechanical properties (such as stretchiness or flexibility) possessed by smart knitted textiles and which can be integrated into such textile construction. It is possible that knitted fabrics can be made for sensor applications than woven or non-woven ones.

- Theoretical and Practical Advancement: The development of predictive models and the connections of theory with the practice has been successful while the thesis also contributes to the field of textile engineering which may motivate further development into smart textile technology.

This work responds to the growing need for innovative, multifunctional textile designs, offering a solid starting point for advancing wearable technology and smart textile applications. By delving into the connections between material composition, stitch patterns, and mechanical behaviour, this research enhances our theoretical understanding of textile mechanics while showcasing its practical value for everyday use and future innovations.

Acknowledgments

In the name of Allah, the most gracious and most merciful. I begin with a heartfelt gratitude to Almighty Allah for bestowing upon me the strength, knowledge, ability, and opportunity to embark on and successfully complete this study.

I extend my sincere appreciation to my esteemed advisor, Prof. Andrew Lowe, whose unwavering support, patience, motivation, and profound knowledge have been instrumental in guiding my Ph.D. journey. His invaluable mentorship has shaped this thesis, and I am truly grateful for his guidance.

I also wish to express my deepest gratitude to my second advisor, Prof. Frances Joseph, whose kindness, encouragement, and insightful guidance were pivotal in making this work possible. Their combined wisdom and contributions have significantly enriched my research, and I am deeply thankful for their support.

My gratitude extends to the Faculty of Design and Creative Technology for providing funding that enabled my studies at the Department of Engineering, Auckland University of Technology (AUT). The collaborative experience between these departments has been remarkable, and I am indebted to everyone at the Textile and Design Lab, particularly Peter Heslop, Gordon Fraser, and Yasir, for their unwavering assistance throughout the research project.

Special thanks are owed to my close friends, whose unwavering encouragement and support bolstered my confidence and provided me with solace during challenging times throughout my Ph.D. journey.

Finally, I offer my profound gratitude to the souls of my parents, whose presence has always been with me, and to my sisters, Suha, Luma, Hadeel, Rana, and Rouaa, as well as my brothers Waleed and Zaid and their families. I am immensely grateful for the unwavering support and love from my two beloved daughters, Fatima and Rahma, who have been my pillars of strength and joy, especially during the most trying moments.

Table of Contents

List of Figures

List of Tables

Chapter One: Introduction

1.1 Overview

The development of smart textiles that can convert mechanical changes into electrical signals represents a growing field around material design. Few studies on the mechanical conduct of smart knitted textiles have been published. In published reports, the differences between theoretical and experimental (practical) results are not accounted for. This project seeks to better understand the mechanical behavior of plain weft knitted fabrics represented by conductive and non-conductive yarns. This chapter outlines the context of the research, the aims and objectives, the rationale of the study, and a summary of the structure of this project.

1.2 Background of the research

Textiles are among the first technologies developed in human history and have been an integral part of daily human existence for thousands of years. Like a second skin (Flint, 2012), textiles provide insulation, protection, and comfort, and are also often used for symbolic purposes. The basic methods of constructing textiles have barely changed over the centuries. However, advances in mechanical and computerized manufacturing technologies have increased speed and capacity, and production rates have reached levels that were unthinkable 200 years ago. One of the most complicated fabrics to develop/ construct is knitted textiles, which have structural characteristics that distinguish them from other textiles. The construction of knitted textiles can be considered more complex than other materials as the structural characteristics are quite specific.

The development of new materials such as conductive yarns, size reduction, and increased compatibility of electronic components have led to the development of smart, electronic, and e-textiles. E-textiles enable sensing and communication between users, for example, a smart fitness shirt, this type of shirt is embedded with sensors that monitor vital signs like heart rate, breathing rate, and body temperature. When worn on the body, they are more conformable and less intrusive than the traditional hardware solutions. Developing e-textiles is necessarily a

multidisciplinary activity that involves (Kirstein, 2013); however, knowledge in this area tends to be bifurcated between scientific and design disciplines. These two disciplines, though both essential to advancing e-textiles, often have different priorities and approaches. As a result, bridging the gap between the two areas can be tricky. Inconsistent theoretical underpinnings and lack of a shared language have been identified as key problems in multidisciplinary research fields (Milligan et al., 1999).

This research project seeks to close the gap between textile engineering and design by clearly defining important textile terminology for engineers and explaining engineering concepts in a way that's accessible to designers.

The current study focuses on knitted textiles due to their unique structural properties that directly affect the electronic behaviour of e-textiles. The mechanical features of knitted fabrics like flexibility, stretchability, and multilayered construction make them ideal for seamless integration of technology. Unlike other types of textiles, knitted fabrics can be manufactured as continuous, uninterrupted sheets, facilitating the incorporation of electronic components. The upcoming sections will compare the construction and technological properties of knitted textiles with those of woven and felted fabrics to emphasize these differences.

1. Construction: Knitted textiles are multilayered constructions made of interlocking yarn loops, creating a fabric with meshes that can move relative to each other. This allows for dimensional changes and stretch capabilities, making knitted fabrics more flexible than woven and felt fabrics.

2. Continuous Sheets: Knitted textiles can be produced as individual continuous sheets of fabric, without seams or joints. This seamless construction facilitates the integration of technological components within the fabric structure by providing a smooth and uninterrupted surface for embedding sensors, conductive threads, or other electronic elements.3. Stretchability: Compared to woven textiles, knitted fabrics have a higher likelihood of achieving stretchable deformations. The interlocking loops in knitted textiles allow for greater elasticity and flexibility, making them ideal for applications where stretchability is required (Niu et al., 2020).

4. Comfort and Fit: Knitted textiles offer a comfortable fit because of their ability to conform closely to the body's contours. Researchers at the MIT Media Lab have developed novel fabrication processes that create smart textiles capable of comfortably fitting the user's body while sensing movements.

5. Integration Potential: The multilayered structure of knitted fabrics provides ample space for the seamless integration of technological components within the textile itself. This enables the creation of smart garments with functionalities such as biometric monitoring or interactive features (Zewe, 2022).

In summary, compared to woven and felt fabrics, knitted textiles stand out because of their multilayered construction, ability to be produced as continuous sheets without seams or joins, stretchability, comfort fit, and potential for seamless integration of technological components within the fabric structure. These unique characteristics make knitted textiles an excellent choice for various applications in smart textiles and wearable technologies.

The significance of e-textiles is further discussed in the literature review (Chapter Two). This research project aims to enhance our understanding of knitted e-textile behaviour, providing deeper theoretical insights into the material that hold significant value in both design and engineering domains.

1.2.1 Types of Textiles

Textile Classes

Textile construction can be separated into four classes: woven, knitted (warp and weft), braided, and nonwoven fabrics (see Figure 1 for an illustration of woven, knitted, and braided textiles).

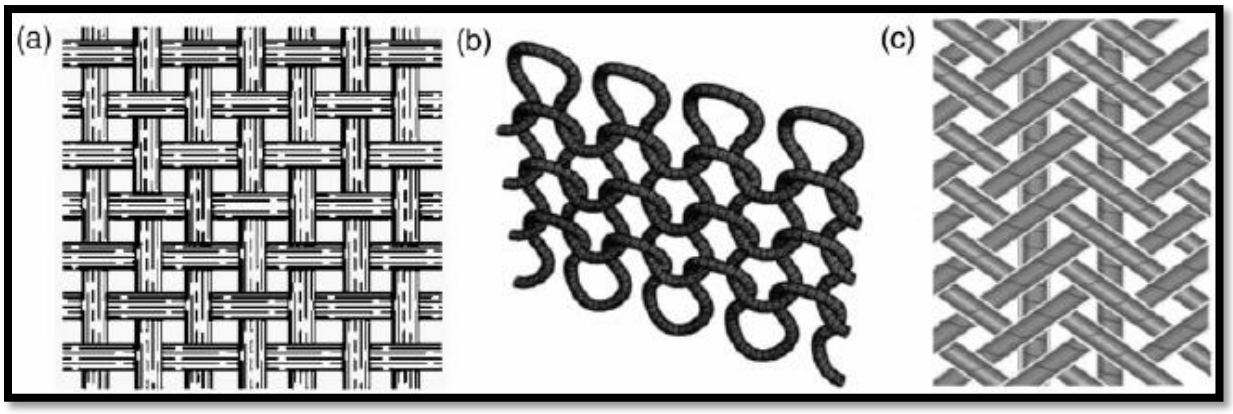

Figure 1: The two-dimensional (a) woven, (b) knit, and (c) braid structures (Ma & Gao, 2015)

Woven textiles were fabricated using a weaving technique. Woven fabrics are generally produced on a loom and made of threads aligned along a weft and warp. These threads are then configured to interlace with each other over and under perpendicular angles. This process produces stable behaviour for the textile against the load, the woven textile structure is shown in Figure 2.

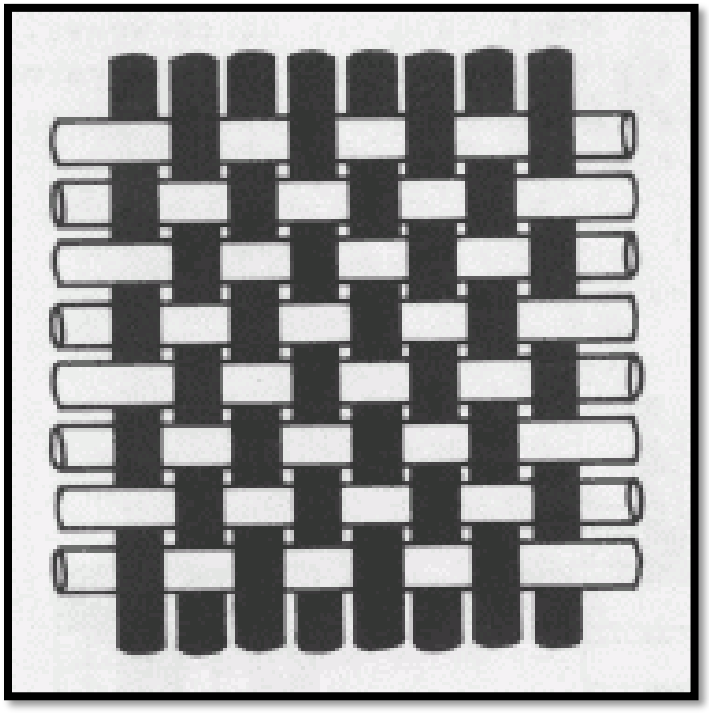

Figure 2: Woven textile structure (Rajak, 2021)

Braided textiles are composed of a structure shaped by interlinking three or more threads of flexible materials such as wires or yarns (see Figure 3 for an illustration of a braided textile). This interpolation of rectangular groups of yarn produces the fibre construction of braided fabrics and provides high stiffness and structural integrity, making them useful for an extensive collection of implementations in areas including automobiles, reinforced hoses, train components, and medicine (Zohoori, 2017).

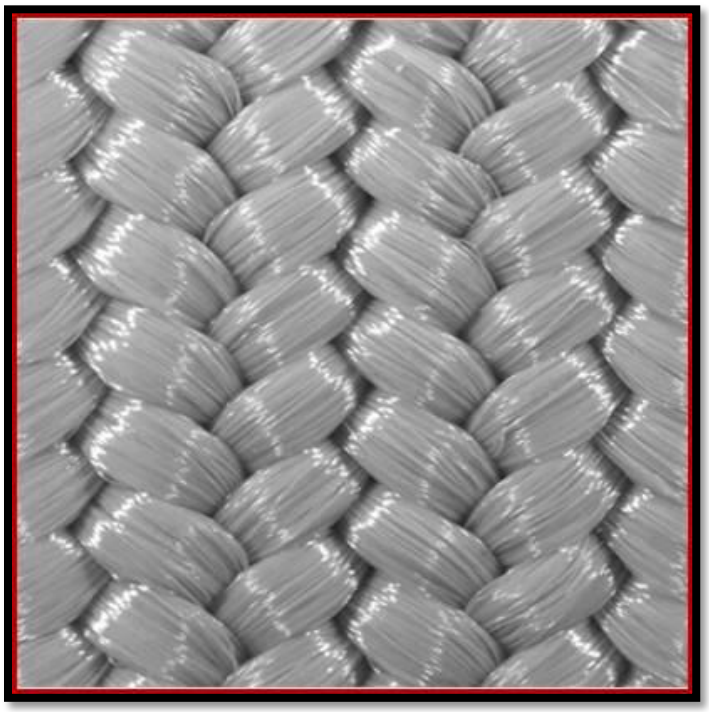

Figure 3: Braided textile structure (ATEX Technologies Inc., 2016)

Non-woven or felted textiles are manufactured by matting, consolidating, and compressing fibres. The main attribute is that they are not made from yarns. Felt textiles can be produced using natural fibres, such as wool, or synthetic fibres, such as acrylics. Felt cuts with a clean edge and does not unravel or fray. The felt cut is flexible and compact, and it is reconstituted frequently without disfigurement. Many types of felt are used in industrial, technical, design, and crafts applications. The entangled structure of the felt is illustrated in Figure 4.

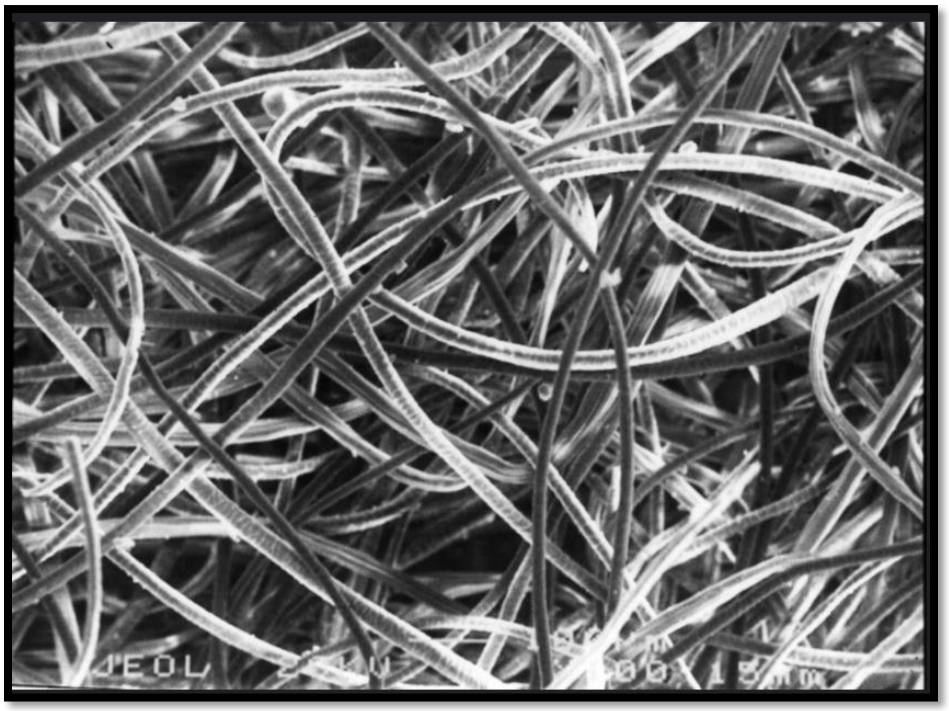

Figure 4: Non-woven textile structure (CORE-Materials, 2010)

Weft Knit vs Warp Knit

According to Tao (2015), knitted textiles result from knitting, a process that creates a two-dimensional continuous fabric from one-dimensional yarn or thread. Thus, knitting describes the technique of constructing textile structures by forming continuous yarn lengths into columns of vertically intermeshed loops. This relies heavily on the availability of fine, strong, and uniformly spun yarn. The knitted fabric yarn follows a winding path (a course), fabricating evenly proportioned loops over and under the median path of the yarn. Knitted fabrics have a much greater elasticity than woven fabrics due to the interlocked loops that can be easily stretched in different directions. As a result, knitted apparel can extend up to 500 %, as determined by yarn variety and knit design (Knitted Fabric, 2021). Behaviorally, knitted materials are super stretchy; however, they are also characterised by an unpredictable load response.

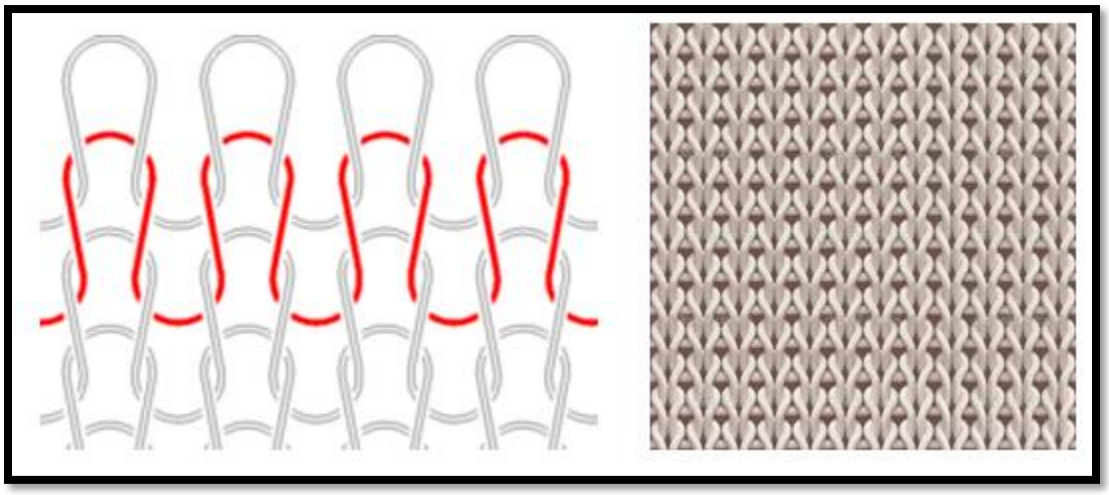

Figure 5: Knitted textile structure (Kiron, 2014a)

knitted textiles can be divided into two structural types, weft knit, and warp knit, which are distinguished by the order in which the fabric is looped from the yarns.

Both the warp and weft knitting techniques are used in the production of knitted fabrics. Warp knitting involves the use of multiple individual yarns threaded into knitting equipment, allowing for a wide range of design options and producing fabrics that are less prone to unravelling. Weft knitting, including circular knitting, is characterised by yarns being knitted in a horizontal direction, resulting in a different fabric structure with distinct properties for some reasons: In horizontal (weft) knitting, loops are interconnected side-to-side, resulting in greater lateral stretch and flexibility and horizontal knits, especially lighter fabrics like jersey, often have edges that curl due to the tension in the knitting. This curling can influence design choices. The discussion below is relevant only to weft knitting, which is the focus of the comparison with continuous woven fabric. The distinct structure of weft knitting imbues the fabric with elasticity and stretchiness, making it suitable for a wide range of applications, including the production of e-textiles and fabric-based electronic components.

Weft knitted textiles consist of columns and rows. Horizontal rows of stitches, also known as courses, are connected to each other perpendicularly in what is referred to as the wale direction. perpendicularly to form columns or wales as shown in Figure 6.

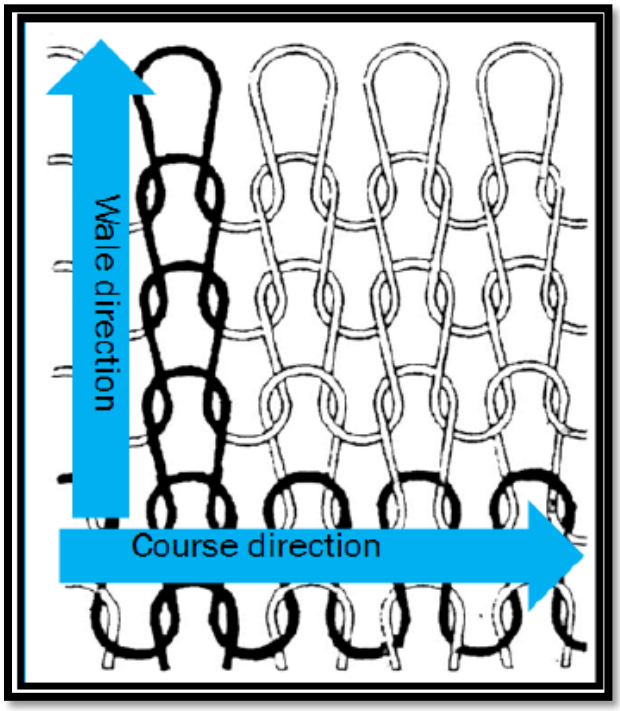

Figure 6: Wale and course directions (Ghapanvari et al., 2015a)

Weft Knitting Techniques

Knitted textiles incorporate a wide range of crafted fabrics using diverse techniques. These include jersey, purl, rib, interlock, and tubular knits. The different techniques and subsequent variations in their construction and appearance lend themselves to a broad spectrum of use and design options.

1. Flat or Jersy knit fabric: A single jersey fabric is a versatile and widely used type of knit fabric known for its excellent stretch in both length and width, although the stretch in width is typically greater (Sheryll, 2021). Its single-knit structure, shown in

Figure 7, is formed from an array of yarns, including cotton, viscose, and wool, resulting in a fabric with one smooth and one piled side. The smooth surface has a flat appearance, whereas the other side has prominent horizontal ribs. This lightweight and breathable fabric is a popular choice for a variety of garments, such as T-shirts, tops, and dresses, because it offers optimal stretching and comfort. The weight, stretch, drape, and stability of a single jersey fabric can differ depending on the type of yarn used, providing greater versatility. Overall, this fabric is the popular choice owing to its versatility and ability to provide both comfort and flexibility (Eysan_ac, 2019).

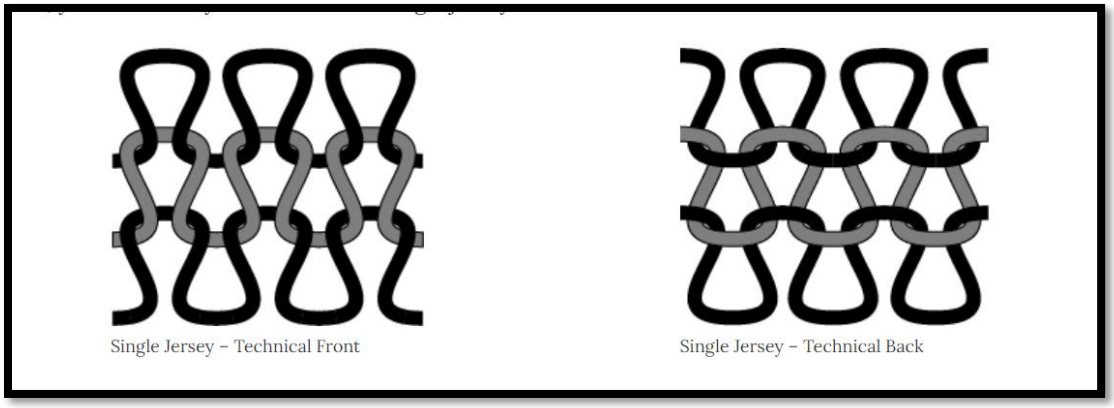

Figure 7: Single Jersy knit fabric structure (Sheryll, 2021)

2. Purl-knit fabric: Purl-knit fabric is a unique textile created by knitting yarn using alternating knit and purl stitches in a single row, as shown in Figure 8. This technique creates a reversible fabric with identical patterns on both the front and back. Unlike other knitted fabrics, purl knit fabric is flat and does not curl, giving it a smooth and even appearance (Kelly Mitchell, 2023). Stretchability is greater in the length direction, making it an ideal choice for certain clothing designs. However, because of its slower production speed, the cost per kilogram of the purl knit fabric is higher than that of other knitted fabrics. Despite this, purl knit fabric is a popular choice for creating thick sweaters, cardigans, pullovers, and children's clothing. It is also widely used for crafting various accessories such as scarves, hats, gloves, and headbands.

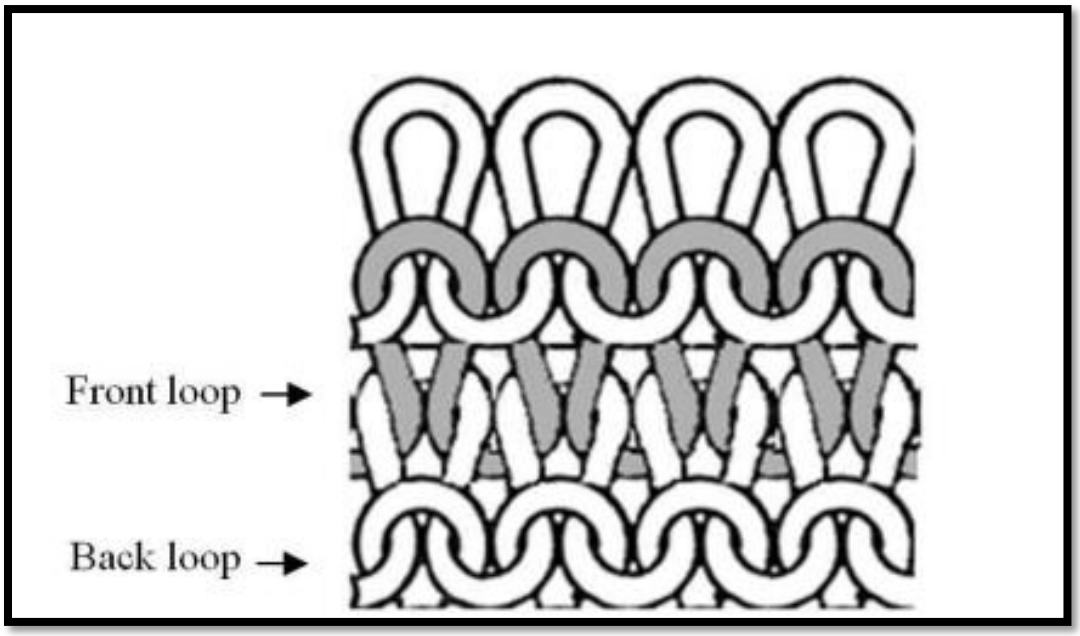

Figure 8: Purl knit fabric structure (W. Choi & Lee, 2010)

3. Rib-stitch knit fabric: A rib knit, also referred to as ribbing, is a highly versatile and durable type of knitted fabric. It features vertical textured lines created by alternating knit and purl stitches, resulting in a distinctive raised ribbed effect (Knitting, 2002), as shown in Figure 9. The specific type of rib knit is determined by the number of knits and purl stitches used, such as 1 × 1, 2 × 2, or 3 × 3. This fabric is particularly well suited for cuffs, bands, and neck lines owing to its elastic nature and resilience.

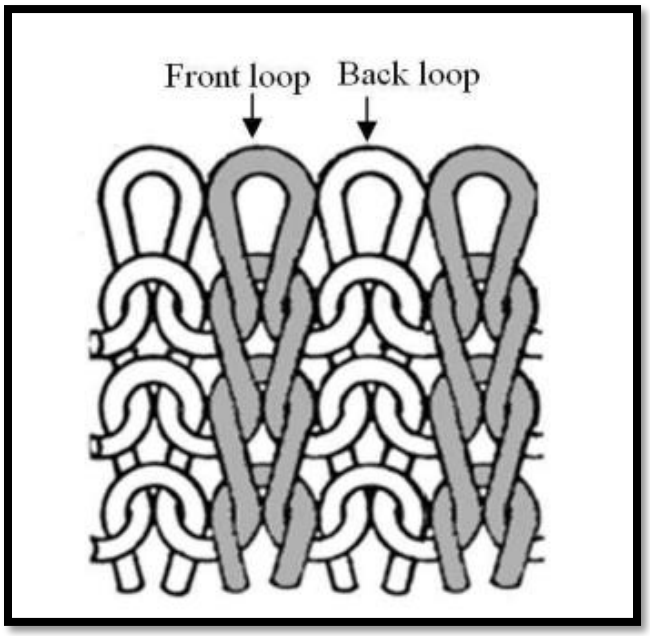

Figure 9: Rib knit fabric structure (W. Choi & Lee, 2010)

4. Interlock knit fabric: Interlock knit fabric is a type of double-knit fabric that offers a luxurious and practical alternative to regular knit fabric. Using two rows of interlocking stitches, this fabric becomes thicker and more absorbent, creating a soft and smooth texture that is perfect for active wear (Mathews, 2023), as shown in Figure 10. Not only does the interlocking of the stitches provide stretchiness and breathability, also ensures that the fabric retains its shape even after stretching. In addition, its strong construction means that it is resistant to running and will not unravel or curl at the edges. The versatility of interlock knit fabric makes it is a popular choice for a wide

range of clothing items including T-shirts, dresses, babywear, and sportswear

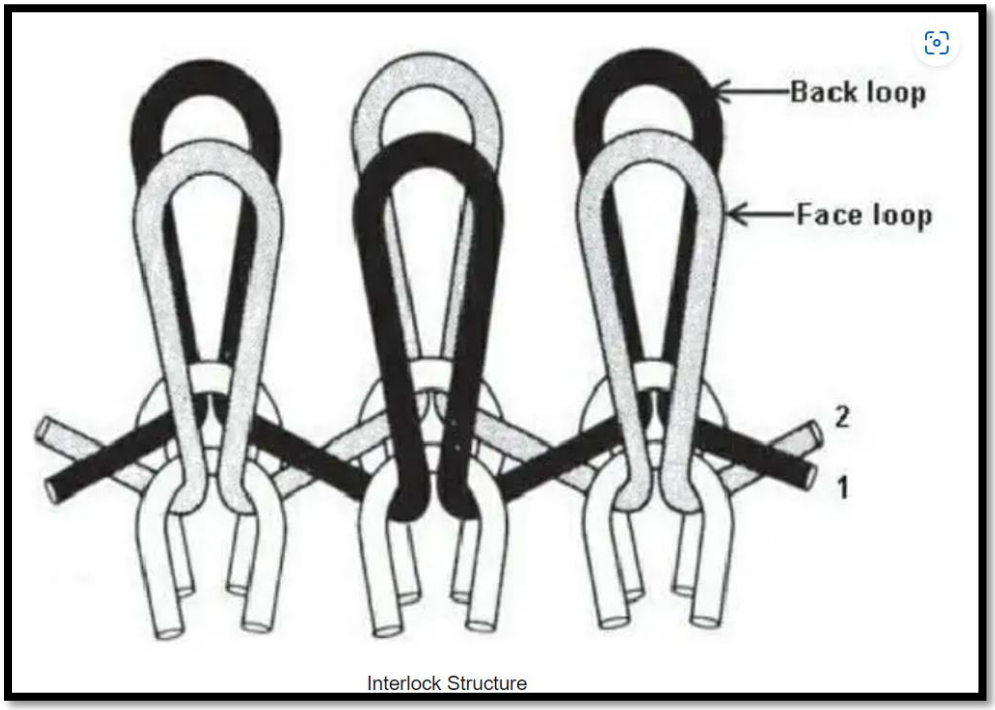

Figure 10: Interlock knit fabric structure (Weft Knitting Structure, 2013)

5. Tubular knit fabric: Tubular knit fabric is a specialised type of knit material that is made without any seams, resulting in a seamless, tube-like structure, as shown in Figure 11. This unique production method is achieved using specialised knitting machines that create interlocked loops of yarn, forming vertical wales and horizontal courses (H. Liu et al., 2021). Its seamless construction makes the tubular knit ideal for comfortable items, such as T-shirts, turtlenecks, and socks. By eliminating the need for side seams, the fabric is not only smooth against the skin but also minimises the need for additional stitching. Tubular knit structures offer distinct advantages in garment construction and are a unique and noteworthy method for producing knit fabrics.

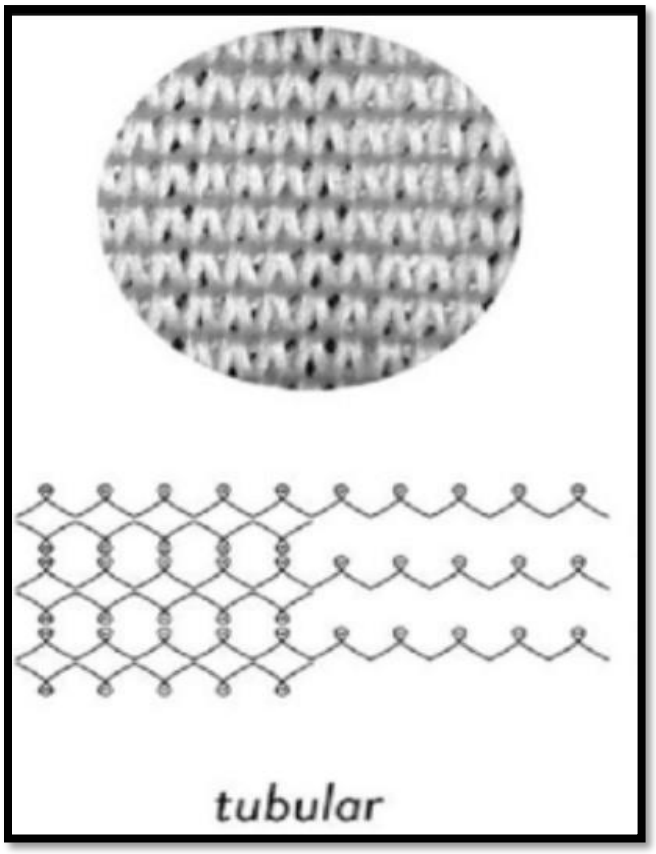

Figure 11: Tubular knit fabric (Tamke et al., 2021).

Weft Knit vs Warp Knit Part 2

Warp-knit structure: Warp knitting utilises a collection of knitting techniques in which the yarn travels back and forth along the length of the fabric, following columns of loops rather than individual rows. This is made possible by a warp beam that holds numerous threads, each designated for a specific column, to direct the yarn's journey through the fabric (Figure 12).

Weft–knit structure**:** This is an uncomplicated approach for transforming yarn into fabric. The technique of weft knitting includes each needle forming a loop that connects with the loops from the previous row, creating a series of interconnected loops that make up the fabric. The horizontal feeding of yarn allows for the creation of rows, which can be built upon to create various patterns and textures. In this procedure, a singular weft thread is fed at a 90°

angle in the direction in which the fabric is created. The individual course of the weft knit depends on the preceding knit course (Figure 13).

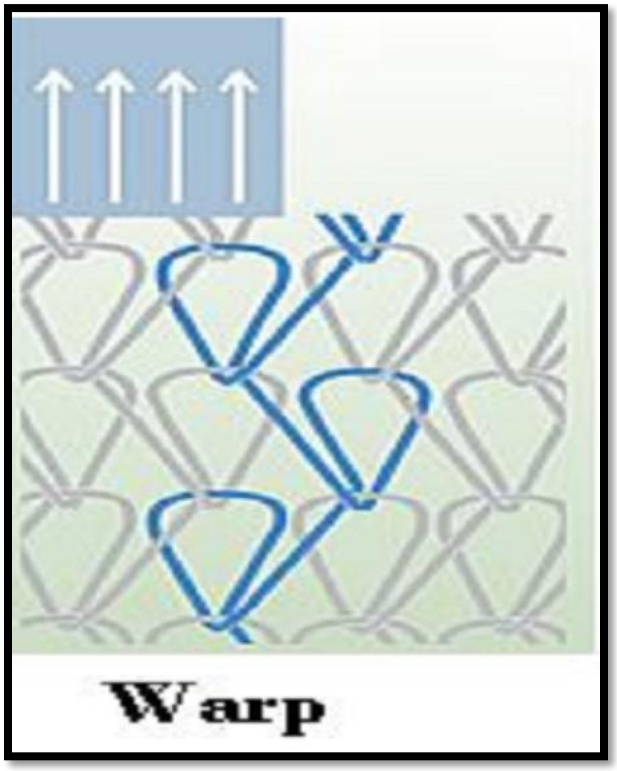

Figure 12: Warp knit structure (Tex Education, 2015)

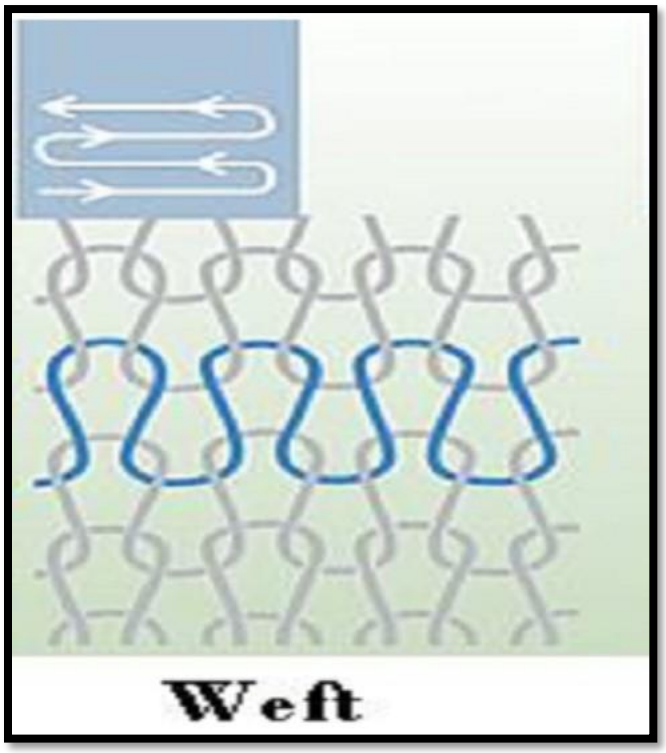

Figure 13: Weft knit structure (Tex Education, 2015)

Weft-knitted structures include plain, rib, purl knit, interlock, and tuck structures. This thesis focuses on the creation and modelling of a plain flat-knitted fabric in addition to a tubular flat.

This section describes the different classes, techniques, and production forms of knitted fabrics. It discussed how using different stitch structures and yarn types produces a wide range of knitted textile types with vastly different haptic and behavioural characteristics, resulting in variations in the textile parameters. Owing to their stretching properties, smart knitted fabrics are being increasingly invested for use as transducer which is a device that transforms one form of energy or signal into another. In the context of smart knitted fabrics, transducers can change mechanical changes—such as stretching or pressure—into electrical signals. This capability is particularly beneficial for smart clothing, enabling the fabric to track physical movements or physiological signals from the wearer.

1.3 Aim and Objective

Few investigations on the mechanical and electrical behaviours of smart knitted textiles have been published. In the papers identified in the literature review, the differences between theoretical and experimental (practical) results were not accounted for. This project focuses on investigating the mechanical behaviour of knitted textile materials as they are relevant to the sensing properties. The research analysis was as follows:

- Particle image velocimetry (PIV) was used to precisely measure the dynamic motion of textiles subjected to mechanical strain. By employing PIV technology, the intricate movements and deformations within the fabric can be accurately quantified, providing invaluable insights into its mechanical behaviour under various conditions.

- An energy-conservation-based approach was used to model mechanical behaviour.

- The evolving behaviour of knitted textiles under repeated extension and its correlation with forming techniques and material properties was demonstrated.

1.4 Thesis Structure

Chapter 1: Introduction

This chapter contextualises research within the domain of smart knitted textiles, providing a clear understanding of the study's focus on mechanical properties. It succinctly outlines the aims and objectives and offers a complete overview of the research's purpose and importance to the field of textile engineering.

Chapter 2: Literature Review

This chapter offers a comprehensive overview of the relevant literature, encompassing articles, journals, and books that delve into the intricate realm of the mechanical behaviour exhibited by different materials and fabrics. By identifying the synthesis of these sources, valuable insights into multifaceted factors such as reliability, sensitivity of the fabric, strain, and contact

resistance can be gained. These factors exert a significant impact on fabric behaviour, shaping the trajectory of research in mathematical modelling methodologies and sophisticated image-processing methods employed in practical image velocimetry (PIV) analysis.

Chapter 3: Experimental Model

This chapter describes the experimental tests conducted on textile samples, providing a detailed account of the equipment setup, sample manufacturing, testing procedure, and subsequent analysis of sample behaviour. Additionally, this chapter encompasses a dedicated section that elucidates the complexities of the image-processing techniques employed in this study.

Chapter 4: Mathematical Model

This chapter establishes a comprehensive theoretical model that explains the fundamental principles of the conservation of energy methods. This chapter investigates the intricacies of modelling simulating tensile tests conducted on textiles, offering a detailed exploration of the underlying principles and methodologies used.

Chapter 5: Discussion and Conclusion

Chapter 5 synthesis the findings of this study and offers an in-depth interpretation and discussion. These findings are compared with those of previous studies, highlighting the novel contributions of this study. This chapter also addresses the limitations of this research and identifies areas that require future exploration. Finally, it presents the conclusions drawn from the investigation, providing an overview of the study's significance and implications.

Chapter Two: Literature Review

2.1 Introduction

This chapter aims to review the existing knowledge relevant to this research study, establish its context, and identify the gap it seeks to address. A new model is developed, informed by the observed behaviour of a subset of knitted textiles, marking a significant advancement over previous models that focused solely on the properties of a single stitch.

(Kirstein, 2013) emphasized that the development of smart textiles is inherently multidisciplinary. While this project originates from the field of electrical engineering, it draws upon insights from various disciplines, including textile design and material science.

The literature review begins with an examination of smart clothing and e-textiles, exploring their functionalities and applications. It then discusses the geometric properties of fabrics, followed by an analysis of the parameters affecting textile structures.

The review encompasses the following sections:

2.2 Smart Clothing and E-Textiles
2.3 Geometric Properties of Fabric
2.4 Parameters Affecting Textile Structures
2.5 Theoretical and Experimental Mechanical Models
2.6 Literature Review of Knitted Fabric Modelling
2.7 Bending and Curling of Knit Fabric
2.8 The Energy Method
2.9 Particle Image Velocimetry (PIV)

2.2 Smart Clothing and E-textiles

2.2.1 Smart Clothing

Smart clothing, also called high-tech clothing, smart garments, or smart wear, are clothes that have been enhanced with technology to add functionality beyond that of established use (Stephenson, 2021).

Many smart garments incorporate complex textiles with interlacing circuitry, commonly known as smart, electronic, or e-textiles. To achieve true smart functionality, these garments must integrate sensors and additional hardware components effectively. Various smart clothing devices can connect to apps or programs on other devices via Wi-Fi or Bluetooth. However, simply having a wireless connection is not sufficient to classify a garment as a smart textile.

To be considered a smart textile, a garment must meet specific criteria beyond connectivity. It should be capable of performing designated functions, such as monitoring health metrics or responding to environmental changes.

In summary, while basic connectivity is essential, it is the combination of functionality, integrated technology, durability, and user interactivity that truly defines a garment as a smart textile.

According to the Editorial Department at SSAW Studio (2016), which specializes in fashion, technology, art direction, and graphic design, smart clothing can estimate vital signs, such as breathing patterns, ECG, perspiration, breathing rate, bodily electrical activity, skin temperature, gesture, body motion, and bodily electrical activity. The use of smart clothing within the health sector to monitor vital signs is promising but still in its infancy.

Stoppa and Chiolerio (2014) noted that textile transducers are becoming increasingly popular in the healthcare field due to their ability to conform comfortably to patients' bodies, providing a more pleasant experience. These innovative textiles are crafted from materials that

incorporate conductive fibres or smart materials, enabling them to offer electronic functionalities while maintaining the softness required for patient comfort.

There are several techniques to integrate these advanced materials into textiles, including embroidery, sewing, weaving, knitting, coating or laminating, printing, and chemical treatments. Each method contributes to developing intricate textile structures that can function as electrical circuits.

Smart textiles utilize various techniques and materials, including textile-like fibres, filaments, and yarns, combined with knitted, woven, or non-woven structures. These textiles are designed not only for durability and functionality but also for optimal interaction with their environment and the people using them. This thoughtful integration of technology and comfort holds great promise for enhancing patient care and improving health outcomes (Stoppa & Chiolerio, 2014).

Smart textiles are designed to sense and respond to environmental changes, adjusting their properties in real time based on thermal, magnetic, mechanical, and electrical conditions (Kun et al., 2009). These innovative materials feature responsive elements that react to external stimuli—such as heat, pressure, or electric fields—by altering their shape, colour, conductivity, or texture. This adaptability is often achieved using specialized materials, including shape-memory alloys and conductive polymers, which allow the textiles to dynamically respond to their surroundings. The potential applications for these smart textiles are vast, ranging from medical monitoring devices to adaptive clothing, enhancing comfort, functionality, and user interaction. Integrating functionalities into a textile structure can involve the use of both traditional and non-traditional materials. Textile transducers typically combine traditional and nontraditional yarns (Jansen, 2020). Firms like Ireland Yarns and The Great British Yarn Company are known for their traditional cotton yarn products. The Apache wool/copper yarn produced by Volt yarns, on the other hand, is an example of a non-traditional yarn. It is made up of a blend of traditional fibers (wool 29.6%, polyester 31.8%) and nontraditional fibers (stainless steel wire 16.3%, copper wire 16.6%) (staff, 2018); naturally, these different material combinations have other properties than traditional yarns. The structure of a textile, determined by various techniques for manipulating and organizing fibers and yarns into cloth, also influences its properties and behavior.

2.2.2 E-Textiles

Smart textiles include specific domains such as e-textiles or electronic textiles and others functional subgroups providing different technological capabilities and applications. As shown in (Figure 14), the e-textile. (Yang et al., 2019) defined e-textiles as fabrics containing electronic elements. Electronic textiles can be used in wearable technologies, which is a broader term for computer-powered devices or equipment that users can wear, such as clothing, watches, and glasses. When an e-textile is integrated with electronic components, it can sense variations in the environment and react, for instance by giving off sound, light, or radio waves, this is possible because e-textiles are made of conductive yarns. E-textiles seamlessly incorporate woven electronics by integrating components and interconnections within the fabric. This design ensures that they are discrete and significantly less susceptible to tangling or snagging. They offer the potential for less intrusive wearable technologies, which are better integrated into everyday items such as clothing and homeware. The introduction of computing technology and sensory materials in textile structures can enhance textiles with a new type of behaviour and functionality. In addition to sensing, responding, and conducting electricity, materials can also perform computational operations. Smart fabrics represent a transformative shift in the textile industry, moving from traditional, passive materials with limited functionality such as cotton and polyester to dynamic products with enhanced and effective capabilities.

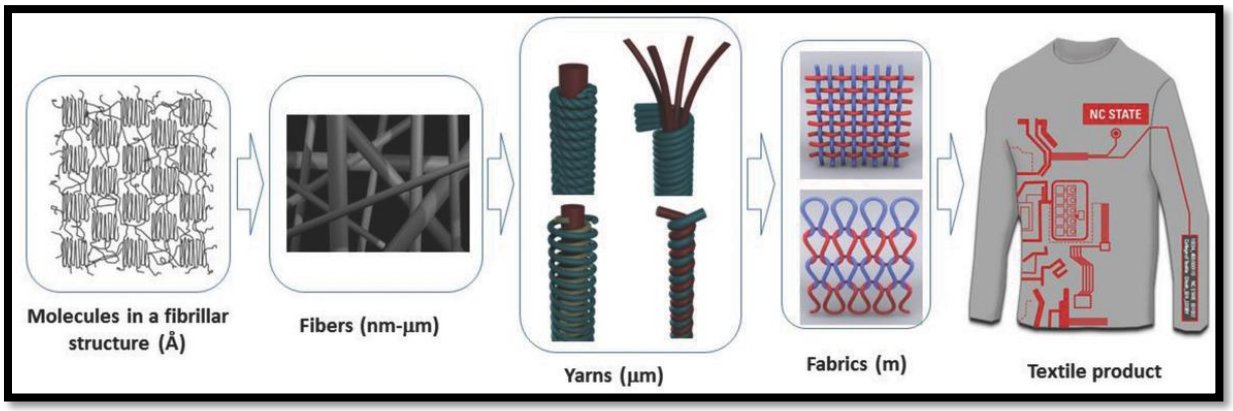

Figure 14: E-Textile (Agcayazi et al., 2018)

2.2.3 Smart Textile Applications

Over the past 10 years, the body of literature on smart textiles has grown significantly (Atalay et al., 2013). Much of the literature in this area has focused on studying the behaviour of prototype components or specific applications rather than developing more generalised models of theorisation. For instance, Atalay et al (2013), introduced the design of a textile-based strain sensor that can be optimized by understanding how fabric parameters affect its sensing capabilities. This optimization allows for accurate measurement of human body movements, making it valuable for applications in health monitoring. Essentially, the study demonstrates the potential of using fabric characteristics to enhance sensor performance in wearable technology. This sensor was developed on a basic fabric created with elastomeric yarns of various linear yarn densities structured in an interlock arrangement. They found a convincing association between the base fabric features and base detection limits and experimentally established this relationship.

Another study that focused on conductivity presented by (Abreu et al., 2010), investigated the development of sensors in two contrasting ways, the first method utilized typical electronics, and the second tried to use textiles with embedded electronics as sensors. These two facets are two different ways of sensing conductivity, using different materials and different degrees of integration. The contacts between the conducting fibres determine the electrical resistance of the sensor. They also explored the possibility of creating a textile elongation sensor, a type of sensor embedded in or made from textile material that measures stretch or elongation. This sensor could be used in a smart shirt to monitor breathing, using fabric knitted from stainless steel. The special textile detects the expansion and contraction of the chest during breathing, enabling real-time monitoring. An experiment was conducted to test the time dependence and elongation dependence of the electrical impedance of knitted fabrics with dissimilar structures.

Abreu et al. (2010) found that the best way to integrate a sensor into an entire garment that is organised, such as a medium stitch size cardigan, is to orient the elongation direction path in the course direction.

Gilmore (1998) investigated fibre-meshed transducers for garment computing applications in order to established two strategies for transducer structures using knit technology. One was a displacement transducer, and the other was a strain gauge. He discovered that a wearable real-time personalised information gathering system, such as a physiological condition monitoring system, can be made using a strain gauge.

Petersen et al. (2011) utilised a fabric to develop an electrical resistor by sewing an extremely conductive mineral laminated yarn into lower conductive fabric. Petersen et al. (2011) contrasted three functional strategies to estimate the electrical impedance and features of the fabric's surface resistivity. They concluded their research by considering that stitch lengths of 1.5–2 mm were preferred for less connection resistance, and the sewn connection strategy was stable for a significant time.

Meyer et al. (2006) used textile sensors to estimate the pressure of the human upper arm's muscle activity. Researchers have utilised a longitudinal precision of 2 cm × 2 cm and an accuracy rate of less than 4% within the measurable scope of 0-10 N/cm^2 to develop multiple textile sensors. The textile pressure sensor was applied to the upper arm, and the muscle bend was caused by forearm deflection between 0° and 135°. An elastic band was placed with a sensor on the biceps and triceps on the muscle part which led to pressure with a high level of discrepancy. On the upper arm, it was possible to detect muscle activity to observe the sensing part force; therefore, the compressible divider was positioned under the electrodes. The authors concluded that the textile pressure sensor is effective in detecting and quantifying pressure on the human body. Its sensitivity and responsiveness suggest potential applications in wearable health monitoring, ergonomic assessments, and smart clothing aimed at tracking body mechanics or posture.

Many studies on e-textiles have focused on medical applications. One study by Rattfält et al. (2007) demonstrated the electrical characteristics of conductive yarn and textile electrodes that touch human skin, thereby producing an actual ECG registration state. The researchers investigated the electrical properties of three different conductive yarns (impedance) and three other textile electrodes that are placed on the skin (impedance and polarisation potential) to identify their appropriateness as ECG electrodes. The outcome indicated that an unmixed stainless-steel electrode was the best steady option for ECG electrodes. In the ECG

measurements, the resistance of the pure stainless-steel electrode was lower in frequency, and the electrode resistance was in series with the input impedance of the dissimilar amplifiers. The yarn displayed purely resistive properties and low impedance.

Paradiso et al. (2005) developed a comfortable health system based on a textile garment interface by integrating electrodes, connections, and sensors in fabric form. They developed futuristic telecommunication systems and signal-processing techniques. The strategy included conductive fabric electrodes represented by a yarn in which two stainless steel wires were twisted around a viscous textile yarn. Hydrogel membranes were used to improve the electrical signal quality under dynamic conditions. An advanced system was designed to monitor individuals affected by cardiovascular diseases. Based on the findings, the researchers concluded that a sensing garment where the bus structure, electrodes, and sensors were all incorporated into the textile material could be worn while engaging in everyday activities. Simultaneously, a consultant to ensure that the people with cardiovascular diseases were not endangered using the garment and the consultant did not observe any distress among the participants.

The above studies on textile sensors and smart textile applications indicate the range and focus of enquiry in the smart textile field in sensor design and medical application areas. However, as can be seen from the synopses presented above, studies in this field tend to focus on studying the behaviour of prototype components or specific applications. Like other studies in this field, this research does not extend its results to broader, generalised models or theoretical frameworks. This gap in theoretical development influenced the focus of my research.

2.3 The Geometric Properties of the Fabric

The mechanical properties of textiles are subject to a multitude of factors, including their geometric and informational characteristics. These important elements can be investigated by using various models and methods. Some of the primary factors that affect the mechanical behaviour of textiles are fabric structure, yarn behaviour, geometric parameters, fibre material, and geometric fabrics. The concept of geometric fabrics, a modern extension of classical mechanics, offers a unique perspective on understanding the behaviour of textiles. Using this approach, it is possible to create systems that overcome the limitations of

traditional mechanical systems in practical applications. In this section, prior research on the geometric properties of fabrics is explored.

2.3.1 Understanding Dimensional Stability in Warp Knit Fabrics Through Geometric Modelling and Relaxation Treatments

Grosberg (1964) presented two examples to illustrate the geometric properties of a 2-bar full-group warp knit fabric, one of which captures the friction between the two sides of the warp knit loop and then separates them while the other assumes that friction is not negligible. According to the influence of abrasion resistance, simple warp and knit fabrics are divided into two groups: fabrics of the first class are relatively rigid in shape, while the second group includes fabrics that typically maintain their form under constant conditions.
Based on the findings, Grosberg's (1964) developed a model that accounts for factors such as a yarn size, packing density, and geometric differences within the fabric. the model assumes uniformity in yarn properties, meaning it doesn't account for variations between yarns at the loop and cross-link.
Fixed and unfixed fabrics were also analysed separately, in terms of the relationship between course spacing and wale spacing. Theoretical models help us understand the bending moments and forces in the fabric system, predict the behaviour of fabric properties at relaxation, provide insight into fabric behaviour, and help in optimising fabric design for various applications.

Grosberg's (1964) model distinguishes between rigid fabrics, which tend to protect their path gaps, and unstable fabrics that do not. An empirical correction of 10 % must be made to accurately predict the course-to-wale spacing ratio for both stable and non-stable fabrics. This theoretical model provides a framework for understanding fabric behaviour and can be used to design optimal fabrics for various applications.

A quantitative analysis of the theoretical changes in plain-woven fabrics was performed by Postley (1968). The analysis included a wide variety of synthetic fibres and natural polymeric fibres induced by various relaxation treatments. This study contributes to the understanding of the properties of woven fabrics, including the effects of relief treatment on, the fabric's shrinkage, shape deformation, and flexibility.

Thus, Grosberg's (1964) model demonstrates that knitting conditions relaxation of the dimensions, and potential shrinkage of a knitted fabric can be influenced by its composition as well as its shape retention properties. Wet relaxation treatments do not allow the fabric material to achieve complete relaxation or dimensional stability. It also highlights the difficulty in manufacturing knitted fabrics that retain their dimensions after knitting without the use of a wet finishing process.

2.3.2 The Impact of Yarn Diameter on Dimensions

The aim of the studies presented by Gowers and Hurt (1978) was to evaluate the effect of yarn diameter on the dimensions of relaxed plain knitted fabrics and to investigate how variations in dimensions under different conditions affected the properties of relaxed fabrics. Fabrics from a variety of low-twist-energy yarns (cotton, acrylic fibres, and worsted) were knitted to reduce the main problem of ordinary plain-knitted fabrics, represented by the effect of spirality.

Gowers and Hunt's (1978) study investigated the wet-relaxed properties of knitted fabrics created from worsted, cotton, and acrylic fibre yarns, with a focus on their small elastic recovery force. They highlighted the critical role of yarn diameter in determining the dimensions of woven fabrics, as evidenced by the correlation between intercepts and yarn diameter. These results offer valuable insights into how the yarn size directly affects fabric measurements and relaxation.

2.3.3 Key Factors Influencing Loop Length in Knitted Fabrics

This section investigates the key factors that influence loop length, exploring insights from recent studies and models that quantify the effects of variables like yarn tension, bending properties, and machine adjustments. By understanding these factors, designers and manufacturers can better control fabric attributes and meet desired performance standards.

2.3.3.1 Deterministic Model for Loop Length in Single Jersey Fabrics

Banerjee and Ghosh (1999) developed a deterministic model to predict loop length in single jersey fabrics, accounting for the influence of yarn, machinery, and process variables. Their model includes software capable of simulating how changes in these factors affect loop formation. In one section of their study, Banerjee and Ghosh explore the impact of yarn-

bending properties on loop length, providing both qualitative and quantitative evidence to demonstrate that yarn flexibility significantly influences the stability and length of loops in the fabric. Understanding the influence of the yarn bending strength on the needle force and loop creation is crucial. An increase in bending rigidity significantly affects the energy exerted by the needles and the resulting tension in the yarn, ultimately affecting the formation of loops. The relationship between loop length and yarn tension at the knitting point was well reflected by Banerjee and Ghosh's model. Their study provides a clear understanding of single-jersey loop manufacturing technology and the factors affecting it by measuring loop length accurately and qualitatively.

Factors that affect the loop length, such as yarn input tension and cam settings, were considered in the current study. As observed in this study, the loop length increases linearly with an increase in stitch-cam settings until, at some point, the rate of change slows down when the cam setting rises. In addition, this data touches on the impact of the yarn bend properties of the loop length that generates larger actual loops for a thick yarn.

2.3.3.2 Curling Tendencies in Rib-Knitted Fabrics

The purpose of the study introduced by Singhal et al. (2021) was to enhance our knowledge on mechanical and physical properties exhibited by knitted fabrics, especially about curling tendencies found in rib-knitted fabrics. In addition, it introduced the concept of de-curling energy which is an innovative method for measuring rib curling.

Singhal et al. study used Autodesk Inventor Pro 2019 to create CAD models of knitted fabrics with respect to a known loop structure. These models are important for determining the mechanical and physical characteristics of fabrics, particularly as they pertain to the curling potential of rib-knitted fabrics. The findings of their research indicated that "de-curling energy can be utilised to assess curling in ribbed fabrics and emphasise the practical implications of these results in terms of the mechanics and physical attributes of rib-knitted materials.

2.3.3.3 Mathematical Modelling and Visualization of Knitted Fabrics

The purpose of Demiroz and Dias's (2000a) project was to develop a cohesive mathematical framework and innovative software tool to produce vibrant three-dimensional visuals of plain-knitted designs. Emphasising the critical role of fabric characteristics and the constraints of current knitting computer-aided design (CAD) systems, this analysis also included comprehensive formulas and explanations for stitch dimensions within various segments of the structure of a stitch.

In addition, Demiroz and Dias (2000b) presented an experimental analysis and computer simulation-based mathematical modelling of simple woven structures. Moreover, beyond offering insights into the effects of yarn and weave variations on fabric properties and patterns, the research aimed to develop a mathematical model for generating diagrams of standard woven materials, allowing fabric parameter values to be visually represented on a computer screen.

2.3.3.4 Experimental Analysis of Woven Structures

The study is being described is by Demiroz and Dias (2000b). They conducted an experiment involving the fabrication of complex weaves using cotton polypropylene yarn on a 12-gauge Stoll CMS flat-bed knitting machine, followed by a drying period of seven days under standardised conditions. The dimensions and structural characteristics of each stitch were carefully recorded using state-of-the-art charge-coupled-device cameras. The experiment conducted for the current study encompassed a range of fibres, such as cotton, wool, and acrylic, as well as various yarn patterns. Through meticulous comparison with the theoretical values, the interplay between these elements within various knitted structures was successfully illuminated.

The research faced limitations such as the following:

1. Two-dimensional images: Fabric dimensions are measured based on 2-D images displayed on a computer screen, but these measurements may differ slightly from the actual physical dimensions of the fabric.

2. Symmetry assumption: The parameter values are not uniform within the same structure, which leads to possible inaccuracies.
3. Simplifications and assumptions: The mathematical model of cloth geometry, which included simplifications and assumptions, yielded unsatisfactory results when compared to actual knitted structures.

The results showed that the experimental values did not exactly match the theoretically calculated values because of the complexity of plain knitted fabrics and some influential yarn and knitting variables on fabric properties and dimensions, as concluded in Demiroz and Dias (2000b) study.

2.3.4 Spirality

Sarker et al. (2022) investigated the impact of spirality and shrinkage on a single jersey fabric by examining different parameters such as yarn count, stitch length, machine speed, and knitting tension. The term "spirality" refers to the propensity of knitted fabric to twist or distort, leading to uneven wales and deformed seams in clothing, as shown in Figure 15.

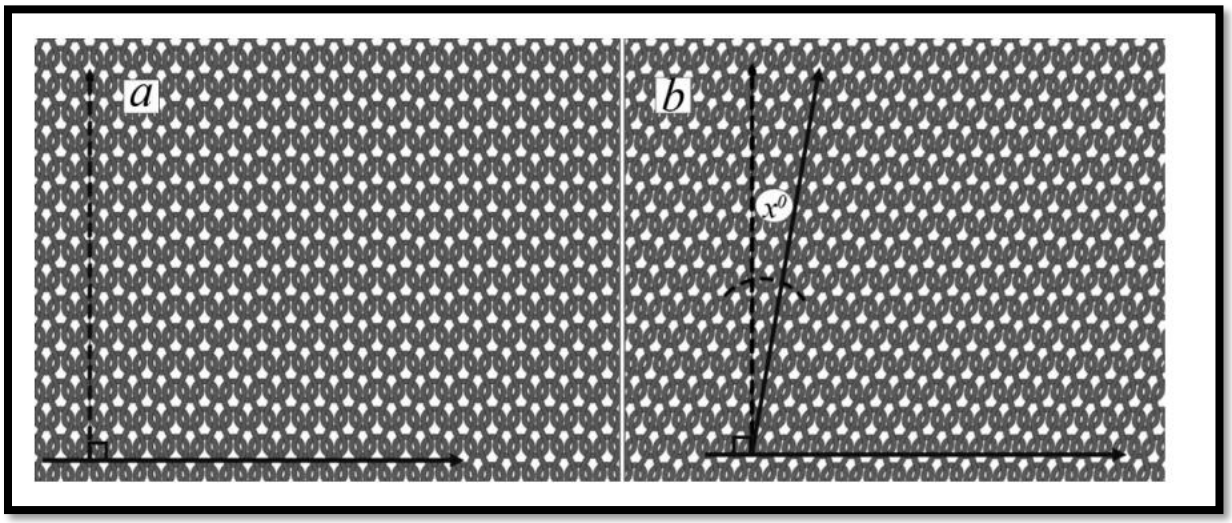

Figure 15: The locations of courses and wales in knit fabrics can be classified into two categories: (a) those that do not have spirality and (b) those that do have spirality (Sarker et al., 2022)

Several experimental models and methods have been used to investigate the factors that affect the spirality of single-jersey fabrics. These include the use of regression models, image analysis, genetic programming, and artificial neural network (ANN) models. Murrell et al. (2009) developed an ANN model to examine the impact of yarn count, tightness factor, and

other variables on fabric spirality. Their findings showed a strong correlation between predicted and measured spirality values, with a correlation coefficient of 0.976, suggesting that yarn count and tightness factor significantly affect both spirality and shrinkage.
The results of this study showed that the yarn count and tightness factor have a remarkable effect on spirality and shrinkage in a single jersey fabric. Furthermore, this study also showed that stitch length, fabric weight, needle gauge, and feeding rate significantly influence spirality.

Single jersey fabrics are characterized by their lightweight and stretchy nature, with factors like yarn type, knitting technique, and fabric weight critical for ensuring dimensional stability and minimizing spirality. In contrast, full cardigan patterns feature a different knitting technique that results in thicker, more textured fabrics, offering improved stability and suitability for applications like outerwear. The choice between these fabric types depends on the specific properties needed for their intended use.

In the following section, I'll provide a detailed explanation of the full cardigan design.

2.3.5 Full Cardigan Design

The full cardigan design is conventionally used to produce outwear-knitted clothes and sportswear. The full cardigan design, as shown in Figure 16, and the use of composite materials that feature a zigzag shape created by the intersection of two yarns can be beneficial in providing resistance to external forces. This was demonstrated in a study conducted by Kurbak and Alpyildiz (2009), who presented a geometric model of the full cardiac structure inspired by Kurbak & Alpyildiz (2009) , loop model for plain knitting. The model incorporates ellipses to depict the loop and tuck heads in a two-dimensional form, derived from parameters obtained through the analysis of medium-tightness wool fabric in its relaxed, post-wash state. The model was brought to life through expert computer-generated illustrations using 3DSMax software.

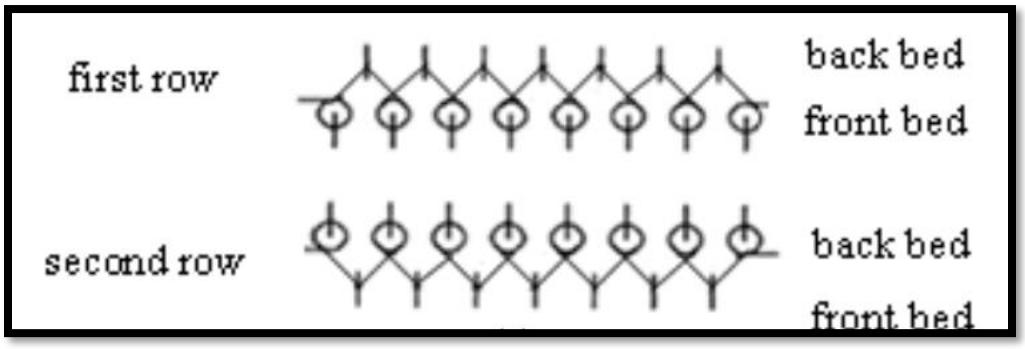

Figure 16: Full cardigan knitting design (Kurbak & Alpyildiz, 2009)

The experimental work involved knitting the samples on a knitting machine with a 10-gauge V-bed using three distinct types of yarns: 28/2 Nm acrylic, 16/2 Ne cotton, and 28/2 Nm wool. Each type of yarn had a specific weight and structure, with 28/2 Nm wool being a 2-ply yarn that contained 28,000 m/kg. The knitting process was performed under five different cam settings and take-down tensions while maintaining a constant yarn tension. The study found that the cardigan design, which utilised wash-relaxed wool fabric with a medium level of tightness, closely resembled the fabric structures observed in both machine-knitted and hand-knitted samples.

2.3.6 Geometric Models for Ribbed Knitted Textiles

The primary objective of the research established by Kurbak and Soydan (2009) was to generate geometric models for well-balanced ribbed knitted textiles, particularly for $2\ x\ 2, 3\ x\ 3, 4\ x\ 4, and\ 5\ x\ 5$, rib fabrics. These patterns were derived from visual images and various parameters, offering valuable information regarding the structure and attributes of the ribbed knitted fabrics. The $m\ x\ m$ rib fabrics (such as $2\ x\ 2\ or\ 3\ x\ 3$ patterns) were chosen primarily for decorative knits, stretchable fabrics, and specialised textile applications They are acquired on a dual bed knitting apparatus by picking needles in a precise sequence. Following the knitting process, the textiles coil inward in the direction of the course and decrease in width.

Kurbak and Soydan's (2009) study proposed a geometrical model that visually depicted $2\ x\ 2, 3\ x\ 3, 4\ x\ 4, and\ 5\ x\ 5$, rib fabrics. This model was constructed by examining the lateral curvature of each fabric through photographs and creating visualisations of the gaps among the $1\ x\ 1$ rib sections and the plain knitting's curled sections using a sophisticated

graphic programme. These models generated closely resemble the actual shapes of rib-knitted fabrics and offer valuable insights into their construction and unique properties.

2.3.7 Lateral Rolling of Simple Knit Materials

Building on this investigation into knit structures, Kurbak and Ekmen (2008) developed a geometric representation to illustrate the lateral rolling of simple knit materials. Its objective was to simulate $m\ x\ n$ rib fabrics and smaller tubular fabrics. This study discussed the implications of edge curling of plain knit textile materials, and suggestions are made to overcome the problems associated with edge curling spinning, which creates an unbalanced bending moment in the yarn. This was found to cause curling at the upper and lower edges on the front side, resulting from their three-dimensional structure, and at the left and right edges on the backside. Despite its desire to remain straight, the yarn is disrupted by neighbouring loops, ultimately causing edge curling. This can pose challenges when creating plain-knit clothing.

The knitting model used for the width-wise curling of plain-knitted fabrics is dependent on, Kurbak and Ekmen (2008) original plain knit model. This model involves depicting the transformation of loop shapes and pinpointing the specific locations within the loop where yarn energy is altered. The use of the 3DS-MAX computer graphics programme enabled the precise creation of a scale model that closely resembled the loop shapes found in real rib fabrics. In addition to its visual representation, this model also offers precise calculations of loop parameters, radii of curvature, and torsions for both the original plain knit and the curled loop.

The research demonstrates how the model can effectively be utilised to comprehend alterations in the loop shape and the dispersion of yarn energy. The study also underscores the significant decrease in torsional and bending energies caused by width-wise curling, particularly in the middle areas of the loop arms.

2.3.8 Loop Length

The intricate geometry of the knitted loops is a prominent feature of knitted fabrics. The main factor that defines the nature of a knitted fabric is the length of the loops. To quantify the loop length of traditional yarn-based knitted fabrics, measuring techniques have been continually refined. This study builds on a comprehensive review of prior research (Pavko-

Cuden & Sluga, 2015) to develop knitted samples with varying degrees of structural density by using yarns that exhibit different elongation, elasticity, and relaxation characteristics. These samples were produced on a flat weft knitting machine by employing various spinning and twisting techniques as well as a range of colour options. The study aims to evaluate how different relaxation conditions affect the dimensional properties of knitted fabrics

Findings from previous studies suggest that knitted materials made with elastic yarns show minimal changes in loop length after relaxation, with a reduction of less than 5%.

Pavko-Cuden & Sluga (2015) also found significant differences in loop length measurements when calculated using different models, highlighting the importance of establishing an accurate model for determining loop length in elasticised knitted fabrics.

Postle and Munden (1967a) examined the knitted loop structure when it was dry and relaxed to understand the forces acting on the loop within the fabric surface as well as the balance of its components. Their study also explored the loop's unique asymmetrical configuration when subjected to a three-dimensional bend and presented the concept of fabric cover, which refers to the portion of fabric occupied by yarn. This study explored the intricacies of Leaf's model (Leaf, 1958), which offers insight into the structure of a perfectly even elastic rod wrapped in a loop in a single plane. Furthermore, Leaf's model (1958) also highlights the crucial role of interlocking points in maintaining yarn formation that is accomplished through the application of couples.

Postle and Munden (1967a) research has shown that the knitted loop, when dry and relaxed, operates as a system driven by force and can be studied by considering the forces present on the fabric's surface at the points where the loops connect. Furthermore, the study identified specific situations in which this examination can be applied, depending on the circumstances in which the structure is confined to either its width or length.

In the second part of study Postle and Munden (1967b) demonstrated the intricacies of the three-dimensional dry-relaxed knitted-loop setup, taking it beyond its traditional two-dimensional understanding, as shown in Figure 17. The knitted loop was analysed in three

dimensions to carefully examine the forces, couples, curvature, and torsion acting on it, as well as the behaviour of the loop outside the fabric plane.

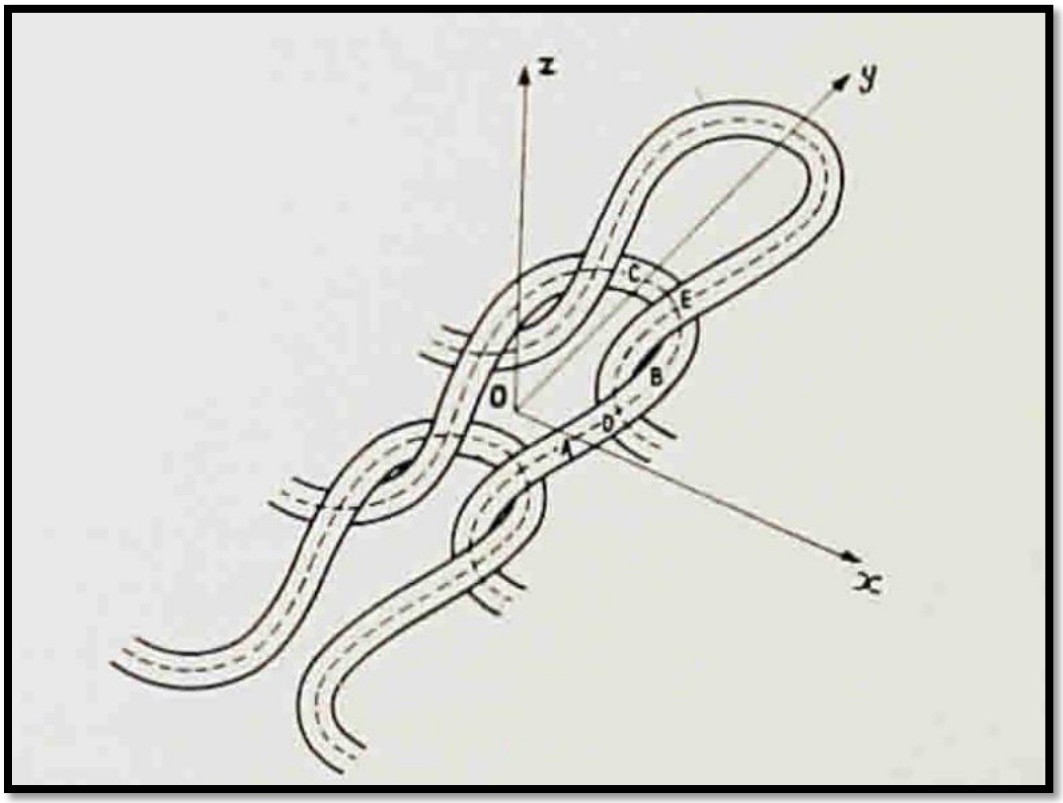

Figure 17: 3D plain-knitted structure. (Postle & Munden, 1967)

The investigators highlighted a particular limitation: the assumption of a precisely symmetrical structure for a relaxed knitted loop. This assumption may not entirely reflect the actual structure. It has been suggested that a stable knitted loop may exhibit a slight skew. The impact of twisting on knitted fabric is illustrated by introducing opposite twists on each side of the loop, as shown in Figure 18. Their study aimed to explore the simplifications that result from assuming a uniform effective yarn diameter across the entire loop, as well as to assess the consequences of localised forces and couples at the interlocking points. Nevertheless, it should be acknowledged that these assumptions may not precisely represent the complex force distribution and variations in yarn diameter that can take place.

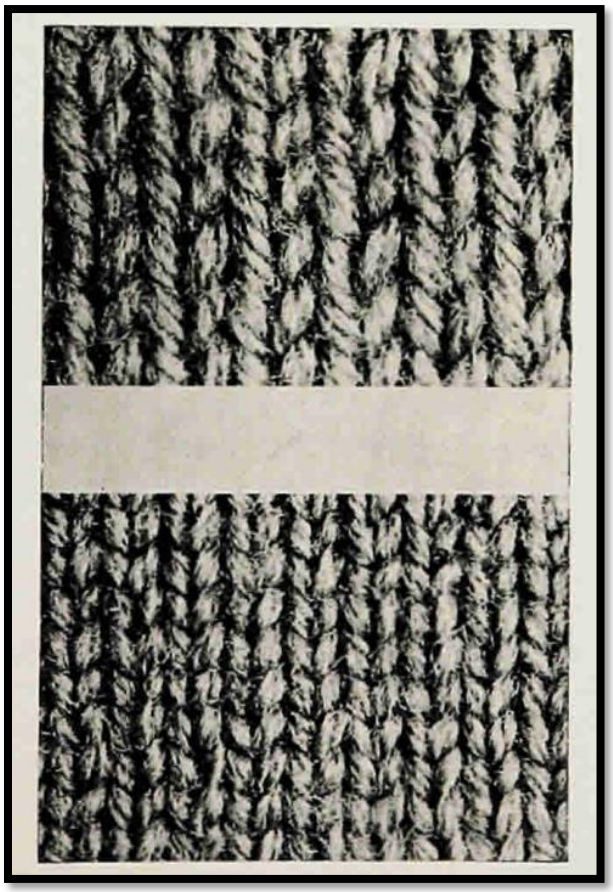

Figure 18: The effect of twisting on knitted fabric is demonstrated by creating opposite twists on each side of the knitted loop. Photographs taken at the same time magnification show two fabrics, one tightly knitted and the other loosely knitted, both made from the same wool directions on either side of the knitted loop. The (Postle & Munden, 1967)

Postle and Munden (1967b) emphasised the importance of additional enquiries and the potential for applying the analysis to other knitted designs and states of relaxation.

Building on Postle and Munden's foundational work on the structural forces within knitted loops, Shanahan and Postle (1974) extended this understanding to examine how these structural characteristics influence the broader mechanical properties of knitted fabrics, particularly under load-extension conditions in the course direction.

Shanahan and Postle's (1974) research advanced the understanding of the mechanical properties of plain-knitted fabrics, with a particular focus on load-extension curves related to fabric extension in the course direction. Their study examined the influence of yarn

compressibility and lateral yarn compression on the initial portions of the load-extension curves, which represent the nearly straight sections of the curves for fabric expansion in the direction of the course. Moreover, this study provides valuable insights into the mechanical properties of nylon and wool plain-knitted fabrics by comparing theoretical calculations with experimental data.

The purpose of Shanahan and Postle's (1974) study was to establish a theoretical framework to capture the load-extension curves for weft fabric extension. This model incorporated several variables, including yarn compressibility, lateral yarn compression, and extended-loop configuration. Additionally, this study examined the impact of machine settings on fabric tensile performance aiming to enhance clarity and precision in describing the model without altering its intended meaning.

Olofsson's (1964) model, introduces the concept of "form factor", defined as the ratio of the yarn's cross-sectional area to its perimeter to examine the mechanical behaviour of woven fabrics. This model accurately predicts key fabric properties, such as bending and stretching, by considering resistance to extension resulting from changes in yarn formation within knitted loops, excluding any slipping, stretching, or side compression. It also incorporates yarn flexural rigidity, impacting the fabric's stretchability, and emphasize the role of fabric relaxation or treatment in reducing internal forces, particularly in bending. The alignment of experimental results with theoretical calculations confirms the model's reliability, making it a valuable tool for understanding fabric behaviour. The accuracy is significant for its practical applications in textile engineering and design, aiding in the development of fabrics with specific mechanical properties like stretchability and flexibility. Additionally, the model serves as a foundation for further research, enabling more precise predictions for novel fabric types and manufacturing techniques.

2.3.9 Milano Rib

Various knitted fabric structures are preferred for specific applications, with the Milano rib being one notable example. Milano knit fabric is constructed from two sets of crosswise knitted yarns, giving it unique characteristics suited to certain uses. The geometric model of the Milano rib-knit structure is illustrated in Figure 19 . The face of the Milanese knit fabric has thin perpendicular ribs and the opposite has a crosswise structure. Milano rib constructions can be practically utilised as functional textiles, for instance, by adding wires,

water pipes, electrical cables, and yarn. Under regular tight circumstances, Kurbak and Amreeva (2006) developed a geometric model for the Milano rib fabric and provided valuable insights into its structure. This model was based on the Kayacan and Kurbak (2008) model for plain-knit fabric construction and has the goal of accurately representing the structural parameters and minimum course spacing. An advanced 3DS MAX computer graphics program was used to visualise the shape of the fabric. Furthermore, the model considers small compressions in the yarn at interlocking points and a 50% increase in yarn size away from these points.

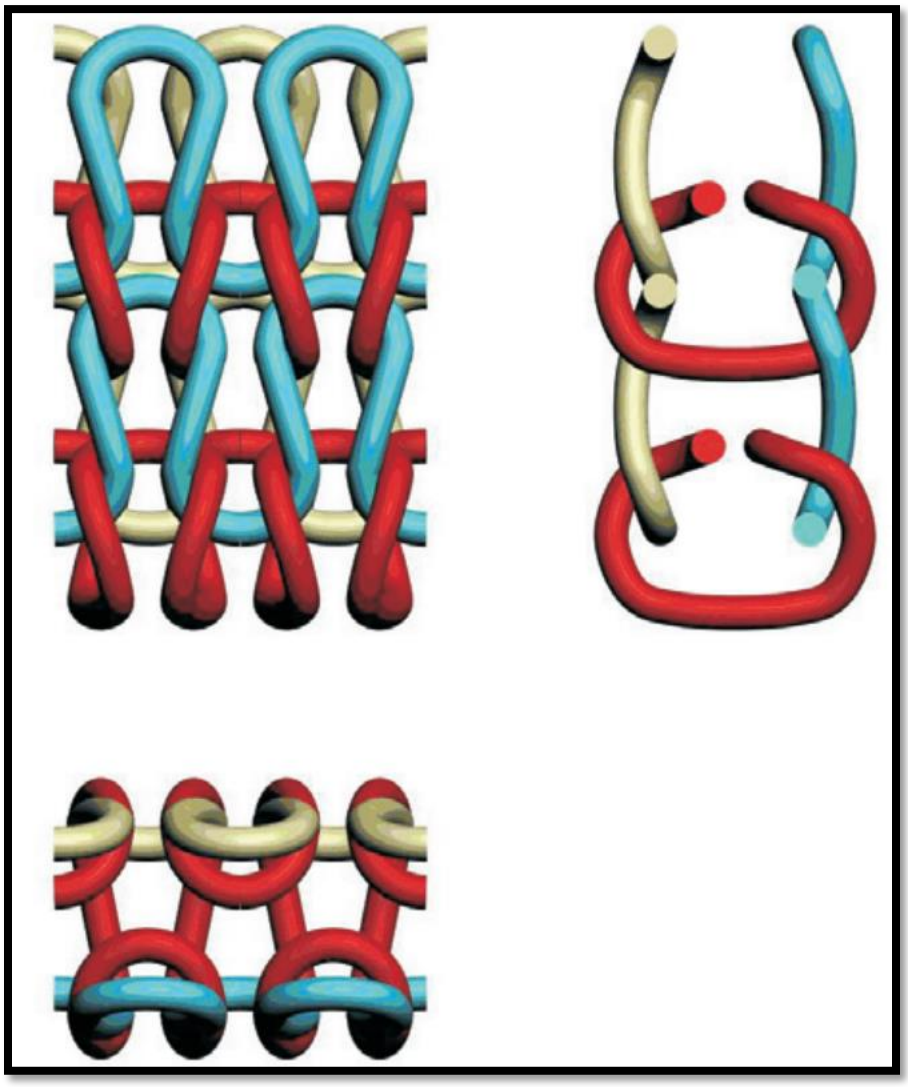

Figure 19: Current geometric model of Milano rib-knitted fabric (Kurbak & Amreeva, 2006)

Upon comparing the experimental data for the Milano knit sample, it was determined that the calculated parameters of the model, such as the structural parameters and minimum course spacing, were consistent with the observed dimensions of the fabric.

Ajeli et al. (2009) undertook a theoretical and experimental investigation of twisted elastica shapes. Specifically, when a perfectly elastic bar is subjected to appropriate amounts of force and torque at its ends, it assumes a unique shape known as an elastica, as shown in Figure 20. This structure is often used to represent a knitted loop and is a crucial part of the examination of knitted fabrics. The elastica dimensions were determined using bending rigidity and torsional rigidity ratios. This study explored the relationship between the twist angle at the ends of the bar and the dimensions that affect the magnitude of twisted couples, which are pairs of forces working in opposition rather than in parallel. These forces are indicative of the forces exerted on the bar and can be used to model the loop shape and fabric measurements using mathematical equations.

For experimental confirmation, four popular textile material bars, created from polypropylene, nylon 6, polyethylene, and polyester, all of which had a circular diameter of approximately 5 mm, were employed. Using a digital camera and additional tools, the experimental arrangement facilitated buckling and twisting of the bar ends. Strikingly accurate agreement between the theoretical and experimental results was revealed by comparing the resulting measurements with the calculated values.

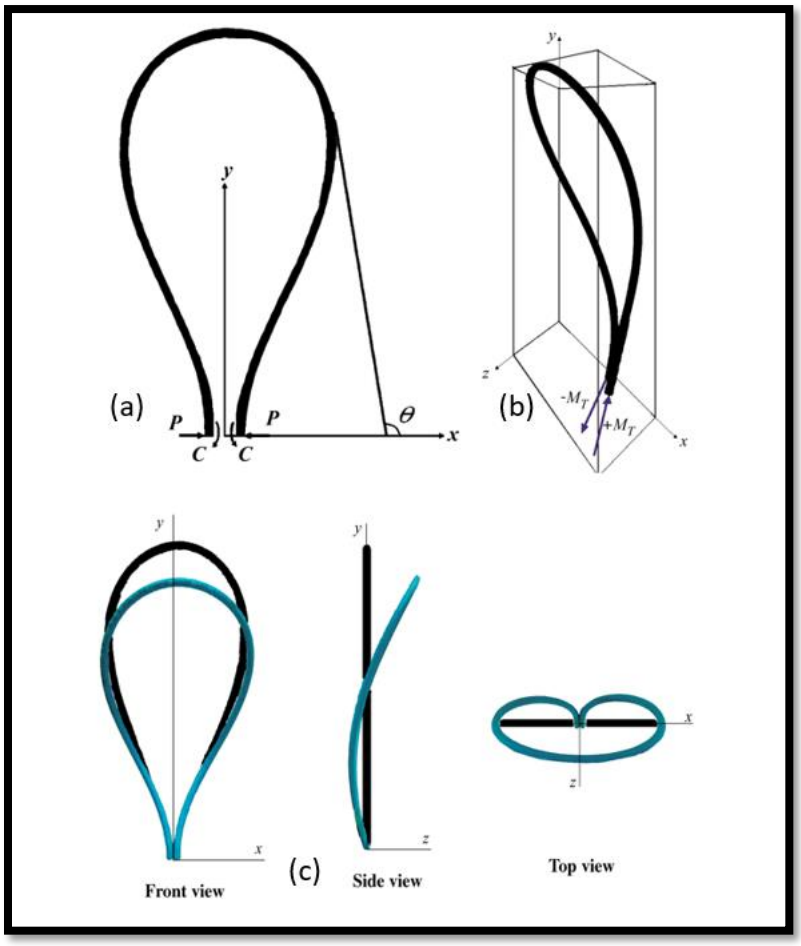

Figure 20: (a) Elastic shape, (b) three-dimensional form of a buckled and rotated electrical bar, (c) graphic shapes of the buckled bar (dark colour) contrasted with the buckled and rotated form (light colour) (Ajeli et al., 2009)

2.3.10 Weft Knitted Fabrics

There are various types of weft-knitted fabric structures such as ribs, interlocks, and plains, each of which has its geometrical relationships. Some of these structures have been examined for separation and their geometries have been explored. Nutting and Leaf (1964) explained the basic structure of weft-knitted fabrics and examined the importance of the relaxed state idea and its effect on fabric geometry. Their research explored both experimental and theoretical models, focusing on the shape of the elastic rod deformation and its dependence on the proportion of flexural to torsional rigidities. Although the investigators acknowledged the initial stage of their work and the speculative nature of some of their ideas, they emphasised the need for more research in this area.

Song and Turner (1968) conducted their study to develop a new technique for accurately measuring the density of plain-knit weft-knitted fabrics and to introduce the idea of a "tightness factor" as a more effective alternative to traditional density measurements. This study built upon previous research on plain and 1 × 1 rib weft-knitted wool fabrics by incorporating half- and full-cardigan constructions and examined the effect of relaxation temperature and conditions on fabric geometry.

The "tightness factor" relates to the connection between the quantity of stitches per unit of fabric and the loop length of the fabric. Although it is a convenient and easily computable metric that has significant promise for use in manufacturing settings, it should not be mistaken as a measure of fabric coverage. Rather, it offers information on the relative firmness or looseness of a fabric's structure.

This research produced significant insights into the geometry and behaviour of weft-knitted fabrics, with loop length being a critical factor in all such structures. Additionally, the study found that the loop shape stability was based on the yarn utilised and the fabric relaxation approach. The size of the relaxed fabric was determined by the balance between the length and shape of the loop. This study also emphasised the importance of qualitative analysis of complex equations that aim to connect stitch density, loop length, and yarn weight. The findings of this research consistently showed how relaxation values are affected by tightness factors, and how they significantly affect the properties of wool fabrics created using weft knitting techniques.

This section’s discussion of the geometric properties of fabrics highlights key findings from the literature on geometric modelling and textiles. Numerous studies have focused on accurately simulating each stitch or unit cell within the textile structure. Such simulations provide a comprehensive understanding of textile functionality, offering valuable insight into the mechanics of stitching and how textiles respond to external forces. The dynamic fusion of computer graphics and visualisation techniques has greatly propelled the evolution of geometric modelling in textiles. In this section, various models were discussed that primarily focus on how geometric and informational characteristics affect the mechanical behaviour of textiles. These models also consider the energy exerted by needles and the resulting tension in yarn, providing valuable insights into fabric behaviour for different uses. In this thesis, Chapter 4 Mathematical Model), takes a distinct approach by examining the overall energy response of

textiles after fabrication, rather than focusing solely on the internal energy within individual unit cells, as seen in previous studies. Prior research often models textiles at the unit cell level, analysing the energy dynamics of individual loops or stitches in isolation. While these models provide insights into localised behaviours, they fail to account for the cumulative interactions across the fabric, which are crucial for understanding the textile's behaviour under real-world conditions. The unit cell-based approach fails to account for the interconnections between loops in fabrics, resulting in an incomplete understanding of their collective energy response during larger deformations or repeated stress. Therefore, predictions based only on individual unit cells can be inaccurate in real-world situations, where fabrics function as interconnected systems.

In contrast, this thesis presents a holistic energy-based model that evaluates the fabric's overall response after it's made. This model considers the combined effects of strain, bending, torsion, and friction across the entire textile surface, allowing for more accurate predictions of mechanical behaviour. By adopting this wider perspective, we gain better insight into smart textiles' performance, durability, flexibility, and resilience across different applications.

This new approach improves fabric design optimization by providing a comprehensive understanding of the factors affecting mechanical performance. The thesis explores geometric modelling and textile structures, drawing from a wide array of research, including individual stitch modelling and multiscale methods. This work yields valuable insights into the mechanical properties of fabrics and their responses to external forces.

2.4 Parameters Affecting Knitted Textile Structure

Some parameters that play a vital role in influencing the mechanical and electrical functions of knitted textile structures have been identified in research to date. Zhang et al. (2006) identified the critical factors that determine the reliability, sensitivity, and accuracy of sensors by constructing two textile structures to investigate the characteristics of contact resistance. The investigators found that the key factor promoting the resistance-strain response was the contact electrical resistance. The sensitivity of the knitted structure gauge was identified by the

construction of the fabric, and the gauge sensitivity was more affected by the temperature than the strain rate.

Wang et al. (2014) suggested that the vital factor for the sensitivity of elastic fabric sensors was yarn segment transfer that caused impedance changes. As the strain increased, the resistance also increased linearly. The researchers concluded that the key factor influencing the equivalent resistance of the knitted sensor was the fabric distortion associated with the length impedance.

Zhang et al. (2005) identified that a key factor that governs the sensitivity of knitted fabric sensors was the yarn contact resistance–load relationship. To improve the sensitivity of the fabric sensor, linearisation of the relationship between the contact resistance and load of the two overlapping yarns was the preferred method used by Zhang et al. (2005). Their results showed that the change in contact resistance, which transfers the yarn length in each loop segment, leads to a variation in the knitted fabric resistance.

2.5 Theoretical and Experimental Mechanical Models

Previous research has focused on the mechanical behaviour of knitted textile structures that were used to develop theoretical and experimental models. For example, Choi and Ashdown (2000) focused on the mechanical properties of weft knit wear as a function of the knit structure and density and the relationships between hand (or texture), density, and construction of the textile. To isolate the effects of these variables, they reduced the variables using engineering samples in which only the knit structure and density varied. They observed many changes in the mechanical properties of the knit, such as tensile and bending stiffness, average shear strain, softness, and smoothness. This analysis of the desired properties of knitted fabrics can be used to select knitting structures and densities of double weft knit fabrics for wear during the winter season, depending on the current preferred properties of the market.

The initial test of the hand value demonstrated that a double knit is greater than a single knit because the knit density increases with the hand value (Choi and Ashdown, 2000). The knit structure incorporating miss and tuck stitches demonstrates features particularly suitable for

winter and outwear. This structure provides improved stretch and flexibility, especially in the course direction, although it cannot absorb external stress along this axis. In contrast, the interlock fabric structure in the course direction showed exceptional stretching properties, making it a strong candidate for applications where durability and flexibility are required.

Nocent et al. (2001) developed a method for simulating cloth dynamics in computer animation that enhances computational efficiency and visual realism. They simplified the cloth's internal structure by reducing its dimensional space and minimizing parameters, particularly through decreased degrees of freedom, while maintaining the fundamental lattice structure. This approach enabled high-quality animations that preserved physical integrity without demanding extensive computational resources, making it particularly suitable for real-time applications in gaming and virtual environments where detail and efficiency are essential.

Nocent et al. (2001) explored the physical properties of cloth by simulating the interactions between yarns using contact constraints, which are crucial for accurately modelling how cloth behaves. They faced challenges with high computational demands, especially when trying to animate larger cloth surfaces. To address this issue, the researchers developed a method to streamline the computational complexity by reducing the number of parameters required for animation. They implemented a detailed approach that employed a parametric bounding volume, enabling the simulation to effectively capture significant macroscopic behaviours of cloth while using fewer, strategically selected parameters. This work highlights the balance between realism and computational efficiency in cloth simulation.

Chen et al. (2013) presented an initial investigation into how to measure the yarn contact area between single yarns for two dissimilar stitch designs in knitted (intelligent sensor) fabrics and determined the suitability of a visual viewpoint to evaluate the area. The investigators desired to develop an understanding of how dissimilar yarn structures perform by selecting two types of yarn: shielding and silver. Each sample had four different stitch patterns along its length and two knit structures. The silver yarn fabric was much more open with a larger unit width and height that were produced with a smaller diameter yarn, whereas the shielding yarn fabric was quite stiff. Chen et al. (2013) estimated that the contact area for silver fabric was uncomplicated, and when the fabric was distorted, the self-contact of the yarn accumulated.

Chen et al.'s (2013) study showed that the shielding fabric exhibited properties opposite to those of the silver fabric under the same conditions. While this work led to the development of a simple model for understanding the contact areas in knitted structures, the researchers concluded that more research was required to better understand and model this phenomenon, mainly as it varied significantly concerning the physical structure of the different yarn types.

2.6 Literature Review of Knitted Fabric Modelling

Some studies have focused on the mechanical characteristics of knitted fabrics, which are influenced by tensile and shearing loads. Dinh et al. (2018) established the fabric yarn level's discrete structure, presenting a numeric scheme to forecast the mechanical behaviour of the knitted fabrics. The homogenisation approach for cyclical materials was exploited according to the systematic yarn-loop distribution of the knitted structure. This means that a less mathematically critical analysis can be performed on a repeated unit cell (RUC) rather than taking into account the entire fabric sample under the load, the repeated unit cell (RUC) and its orientation in the course and wale directions, is illustrated in (Figure 21 and Figure 22). Depending on the organised sample parameters of the knitted loops, a repeated unit cell was created.

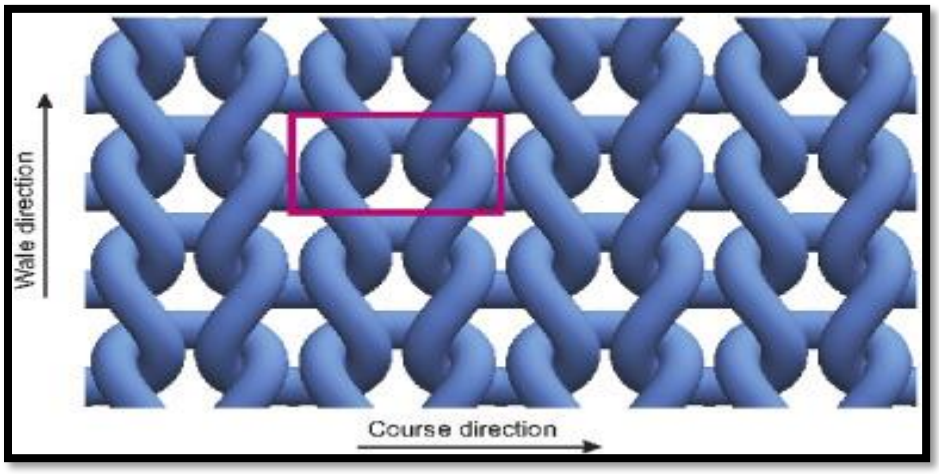

Figure 21: Repeated unit cell (RUC) (Dinh et al., 2018)

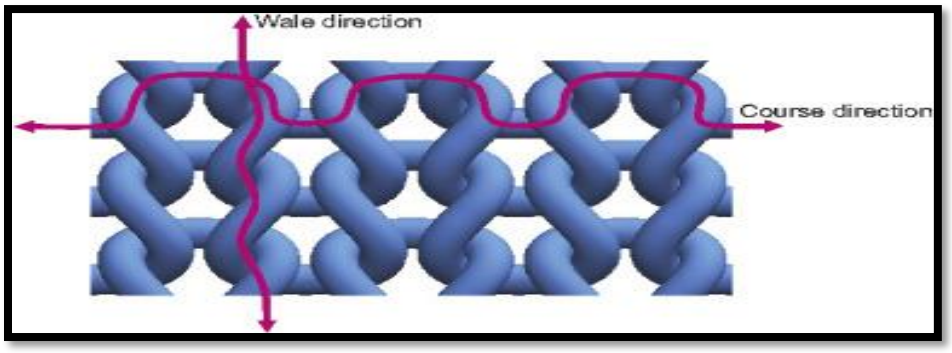

Figure 22: Course and wale direction for the (RUC) (Dinh et al., 2018)

To specify the stress ranges in the RUC below the shearing and tensile loads, a nonlinear finite element analysis was performed. Dinh et al. (2018) used periodic boundary conditions (PBCs) and the arithmetical homogenisation technique to interchange particulars at the macro and textile mesoscale. The macroscopic conductivity was based on the functioning of the yarns and matrix at the mesoscale (scale of the textile unit cell). Likewise, the conduct of the unit cell at the mesoscale was based on the interaction of fibres with fibres and the matrix on the border at the micro-scale level, which represented the boundary conditions of the (RUC) using the axis system. They concluded that it is complex to phenomenologically model knitted fabrics if they consider the fibres or yarn and limited heterogeneities clearly in the configurational investigation. The researchers suggested that multiscale modelling could be a potential solution to this issue.

Essentially, the research by Dinh et al. (2018) showed that the proposed structures' physical accuracy was validated by close agreement between the model's predictions and actual empirical measurements. This good agreement indicates that the structure behaves in practice as it was expected to theoretically, reinforcing the model's validity for representing real-world fabric properties, as shown in the graph represented in (Figure 23 and

Figure *24*).

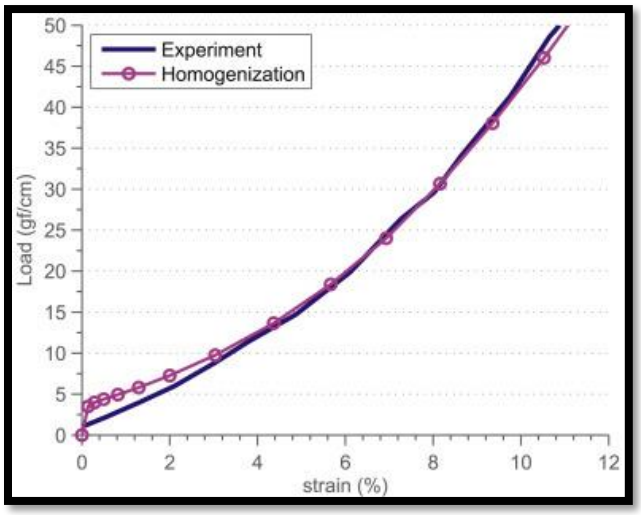

Figure 23: In the wale-wise tensile test, the homogenized load-strain arch predicted the RUC and the measuring empirical data (Dinh et al., 2018)

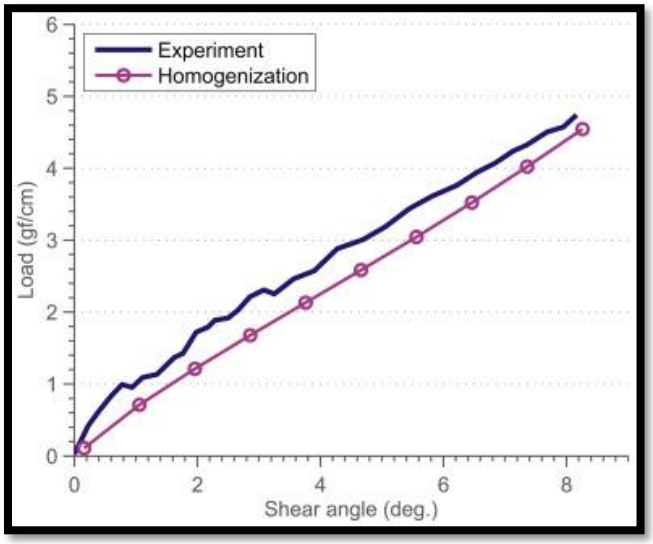

Figure 24: In the shear test, the homogenised load-shear angle and measuring empirical data (Dinh et al., 2018)

2.6.1 Finite Element Modelling of Tensile Properties in Knitted 1×1 Rib Fabrics

A novel 3D geometric model was created by Abghary et al. (2016) to obtain the tensile features of a traditional knitted $1\ x\ 1\ rib$ fabric, a diagram of this $1\ x\ 1\ rib$ structure is shown in (Figure 25) for use in functional implementations. A streamlined model containing the fabric is a sustained homogenous membrane-like material that cannot precisely explain its mechanical properties. This is because the geometrical sophistication of the knitted fabric yarn elongation and curvature within the malformation procedure and the involvement phenomena between yarns in the touching areas significantly affect the mechanical test of knitted fabrics. In Abghary et al.'s (2016) study, they used the finite element method (FEM) to numerically simulate the tensile stress-strain relationship in the course and wale trends. The finite element method (FEM) is a computational mechanical testing instrument that requires accurate geometrical impersonation of the bodies, configuring the complicated microstructure of textile fabrics. The employment of this technique was based on the resolution of the geometrical model of the fabric. The stress-strain relationship counterpart to the wale-wise and course-wise trends for an assumed knitted fabric was simulated by the finite element approach and contrasted with empirical outcomes. The accuracy of the geometrical model used was measured by comparing the simulated tensile stress-strain arch of the model to an estimated arch. The results demonstrated a good level of agreement between the simulated and empirical relationships for the two different rib fabrics. The results generated by Abhary et al. (2016) show that the suggested geometrical model can obtain the tensile behaviour of the 1 × 1 rib construction, as shown in Figure 26.

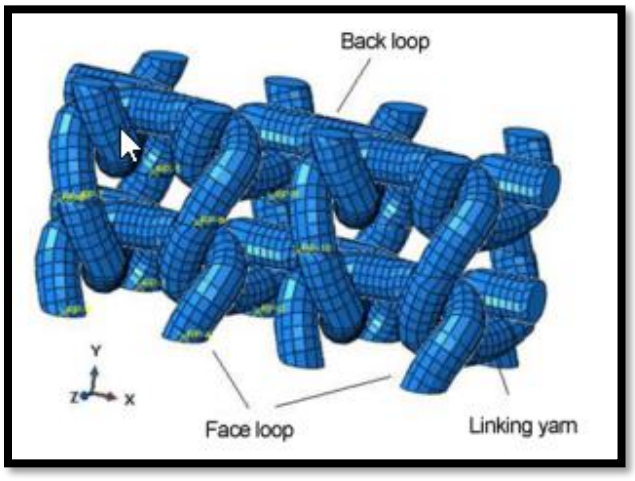

Figure 25: A 1×1 rib construction diagrammatic (Abghary et al., 2016)

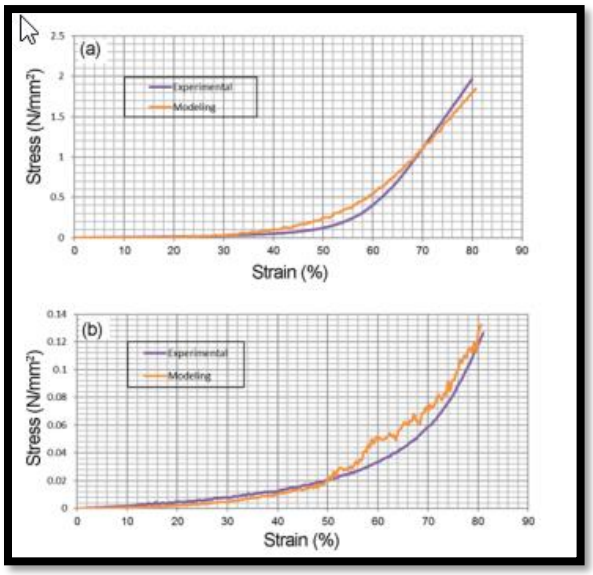

Figure 26: Stress-strain arch predicted from the empirical and modelling approach in wale-wise (a) and course-wise (b) loading (Abghary et al., 2016)

2.6.2 Woven Fabric Draping

A model of woven fabric draping was presented by Sharma and Sutcliffe (2004), who utilised two main strategies: an inclusive finite element model and kinematic modelling (the features of this model are a very simple and quick calculation process). The strategy of this method is to model the fabric using a mesh of basic truss components attached through diagonals by smooth components. This process serves to simulate the material's shear stiffness by employing the unit cell finite element model (FE).

The model developed by Sharma and Sutcliffe (2004) exploits the unit cell performance of the fabric's unit cell, with material properties derived from the basic tests, The material behaviour of the unit cell model is illustrated in (Figure 27). Sharma and Sutcliffe (2004) proposed that the unit cell is composed of a mesh of pin-jointed taut trusses as a pin join net (PJN), with shear hardness displayed through diagonal bracing components.

Bias extension tests were performed to extract an appropriate stress-strain curve for the diagonal components. The hardness of the trusses was predicted using suitable bias extension standards over the entire length of the sample. The estimations of the deformation of the bias extension sample away from the gauge section had perfect concurrence with the measurements.

For the influence of the in-plane forces on the two slippages and shear malformation, the unit cell model introduced the capability to signify an impact.

Sharma and Sutcliffe (2004) used their pin-jointed net (PJN) model with a finite element (FE) framework to simulate the draping behaviour of fabric over an ellipsoid, essentially testing the model's practical application. The ideal procedure here implies that the model was effectively suited to represent the draping mechanics realistically. The computational efficiency allowed the simulation to be run quickly, enabling detailed studies on fabric elasticity and deformation with only moderate computing resources.

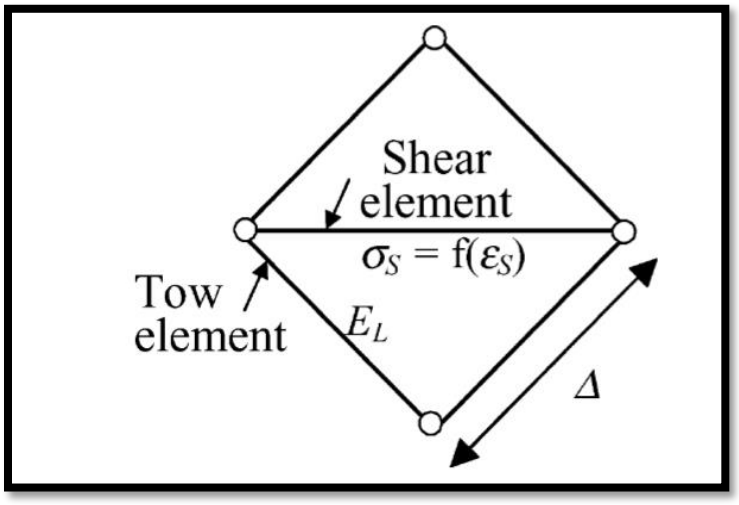

Figure 27: The material behaviour of the unit cell model (Sharma & Sutcliffe, 2004)

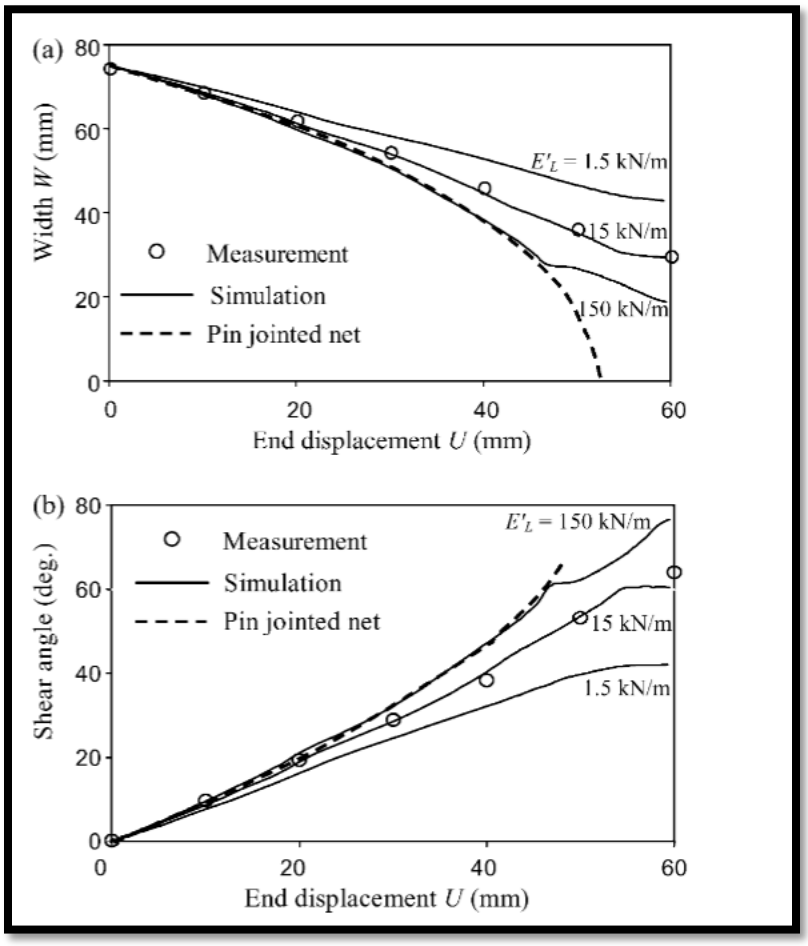

Figure 28: During the bias extension test, Sharma and Sutcliffe (2004) compared theoretical predictions with measured values by analysing the geometry of the sample. This involved evaluating (a) the displacement U across the entire sample, (b) the width W of the central gauge section, and (c) the shear angle within the gauge section (Sharma & Sutcliffe, 2004)

This research and the plot presented in Figure 28 above showing X demonstrate that the sample width decreases with an increase in displacement because the sample in this research was between two grips that secured the fabric. The research shows that the theoretical method represented by PJN (Figure 28) predicts the deformation of the bias extension sample away from the gauge section and is in perfect agreement with the measurement.

Abghary et al. (2016) and Sharma and Sutcliffe (2004) both employed a novel approach using the finite element modelling (FEM) method to analyse and predict the mechanical behaviour of fabrics across various FEM providing a shift from traditional mathematical models by enabling advanced simulations of fabric mechanics. However, this PhD research adopts an energy-based approach. To support this method, a bias extension testing technique was developed to assess the behaviour of dry-knitted fabrics. Securing the fabric ends between two grips ensures accurate measurements, which were then used to calibrate and validate the energy-based model.

2.6.3 The Vassiliadis and Savvas (2007) Model

Vassiliadis and Savvas (2007), proposed a new mathematical model for single jersey fabrics. Their model assumes that the yarns are uniform, behave like ideal elastic materials, and naturally settle into a relaxed state by minimizing stored elastic energy. These assumptions simplify the computational process but may not fully account for the complexities of real-world yarns.

The Vassiliadis and Savvas model employs an iterative calculation procedure for loop formation, correlating with the shorted loop length. This approach reflects the model's assumption that the fabric reaches a stable confirmation by minimizing the elastic energy of the yarns. To validate their model, the study also applied existing geometrical models to the same dataset, calculated the loop length for all models, and compared these results to experimental measurements. By using loop length as a standard, the accuracy of their model was assessed. this accuracy is essential for ensuring the success of the mechanical simulation of knitted fabric.

These researchers proposed a new model designed to reduce errors, based on rotational principles such as the minimisation of energy. The success of this model is related to the resulting computational description of the knitted fabric structure for a single jersey. This is relevant to my project because they have used a similar modelling method to accurately predict the result and minimise errors across the various steps of mechanical analysis. However, Vassiliadis and Savvas's (2007) research represented the model for the knitted fabric's structure for a single jersey with the greatest achievable accuracy, in which different fabrics

and materials stretched under known strain values were used to estimate the mechanical features of these fabrics.

Bassett et al. (1999) investigated a traditional fabric analysis with several specifics for biaxial tension and shear. This work is a review of the study of different experimental techniques that can be utilised to estimate the mechanical characteristics of fabrics, which is fundamental in garment handling, involving the parameters of biaxial tension and in-plane shear.

This research examined fundamental issues which can be encountered during fabric tests. Subsequently, the shear fabric test and the present biaxial tension were displayed and analysed critically. The shear features of garment fabrics are normally estimated under heterogeneous uniaxial tensile stress. This test is unable to provide precise estimations of the correlation between shear strain and shear stress and its reliance on strain conditions and tensile stress.

Based on the above research, the investigators established several issues based on the analysis of the fabric type. The research goal was to employ the shear stress and biaxial tensile stress to the specimen; the researchers discovered in the case of shear stress that when they tested the knit fabric to estimate the shear and tensile stress, results were not precise. In addition, the woven fabric test remained unexplained because the stress of the tensile distribution was inhomogeneous and undefined during the examination.

The investigators recognised that they needed to construct a new test method to determine the fabric tensile and shear stress properties. Initially, they exploited a rectangular sample with each rectangular side gripped by a clamping system such that the distributive force of the monolithic edge was placed along each side of the specimen, with grips on the middle points of the sides as shown in Figure 29.

Symmetrically, the opposite sides were subjected to equal loading. the clamping system was autonomously designed to differentiate between the three elements of stress, strain, and shear, acting along the three degrees of flexibility at the fabric’s edges. in the traditional shear test, the strain and shear stress at the upper end were influenced by the initial twist or torsional state of the material. This starting twist was required to be resilient ensuring the material could endure the applied forces during the test without excessive deformation. To supply the

foundational features of fabric as a starting point for a garment model, data from the appliance could be employed to assist in explaining the behaviour of fabrics under shear stress. Based on these instructions, a new examination based on Bassett's understanding was suggested, in which shear and tensile forces may be employed concurrently. Based on the results which are supposed to be time-independent, when the test started, it was agreed to have up to three different stress (or strain) elements synchronously. This required different tests to trace different paths such that a wide distribution of strain component combinations was generated by the test series.

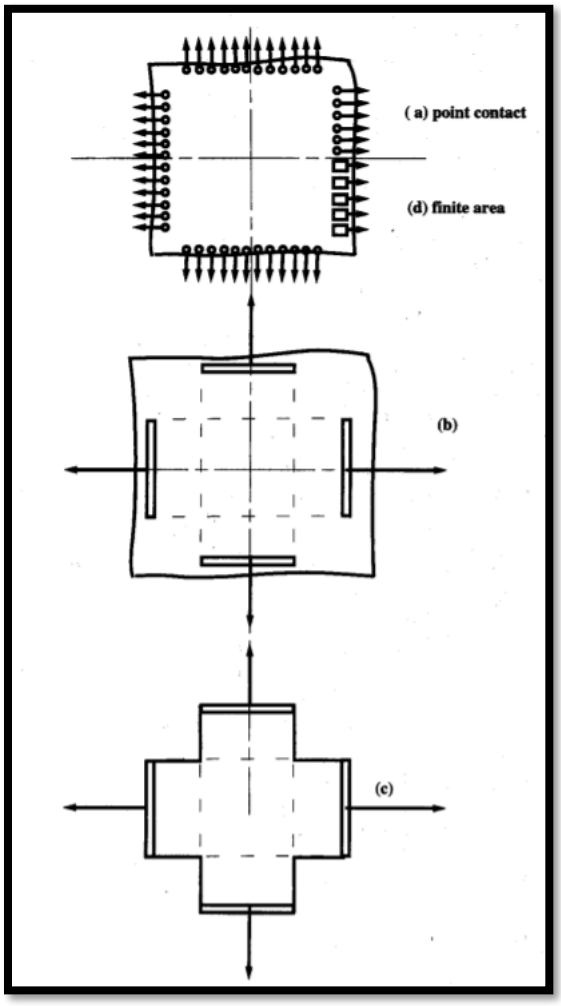

Figure 29: A biaxial fabric tester with different types of fabric clamping (a) point contact (b) graph exam (c) cruciform exam (d) segments clamps (Bassett et al., 1999)

Because the investigators faced some problems when they applied biaxial tensile stress to the woven fabrics, the tensile stress distribution within the test was heterogeneous and undefined. Because of the inconvenient properties of the woven fabrics during the experimental test, I decided to choose a different type of fabric represented by plain knitted fabrics with different yarn materials to overcome this problem during the experimental test for the chosen sample in this research.

2.6.4 Woven Fabric Laminates

Carvelli and Poggi (2001) presented a strategy for numerically assessing the mechanical characteristics of woven fabric laminates. Normally, woven fabric yarns (warp and weft) overlap perpendicularly, and for composite yarns, the distribution of the fibres can be regarded as more systematic. To determine the strength and stiffness of the woven fabric laminates, a three-dimensional (3D) finite element model was utilised for two strides. This model involved all the fundamental parameters which affect the mechanical conduct, such as the yarn direction, fibre volume, woven fabric laminate thickness, and mechanical properties of the elements (Figure 30).

By examining the elastic behaviour of a woven fabric laminate shown in Figure 31, Carvellin and Poggi (2001) empirically validated the possibilities of the numerical model and determined and analysed the final strength of a glass fabric laminate. Based on the hypothesis of the cyclic distribution of the fibres within the yarn and the systematic arrangement for strengthening yarns in the fabric, Carvellin and Poggi (2001) suggest a homogenization process. This homogenisation approach for repeated media was initially applied to the yarns of fibre-strengthened composites and then later extended to the homogenised yarns of the woven composite, though it is not explicitly clear whether this was conducted by Carvellin and Poggi (2001). The process verified the elastic subject against other investigative solutions. The next step was to realise and parse the non-linear conduct of a fabric composite experimentally. The strategy was then applied to a business finite-element code. A manufacturing designer might quickly select a similar advance to study and improve the composite material using different keys that affect the mechanical features. This model demonstrates that it is an effective tool for the determination of woven textile composites.

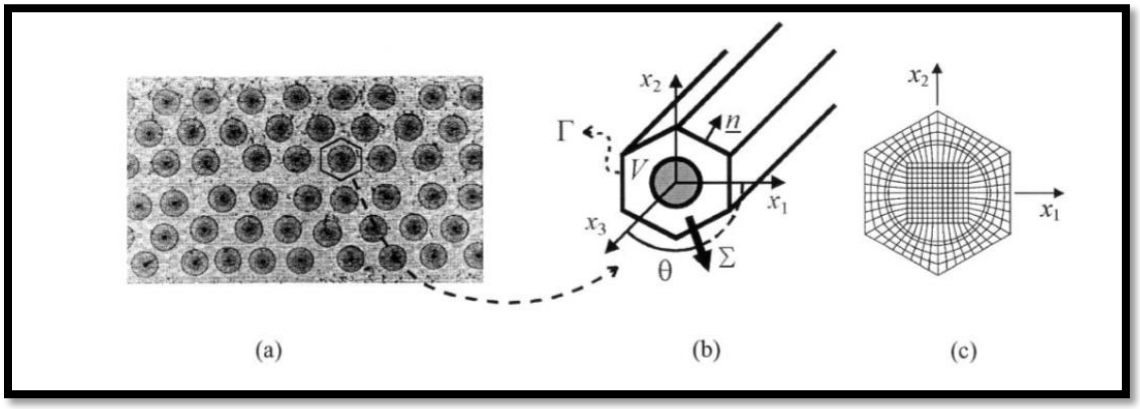

Figure 30: (a) fibre-reinforced composite has all fibres aligned in one direction, offering maximum strength and stiffness along that line. (b) represented volume (c) 3D finite element mesh's front view displayed in the numeric homogenisation of the yarns (Carvelli & Poggi, 2001)

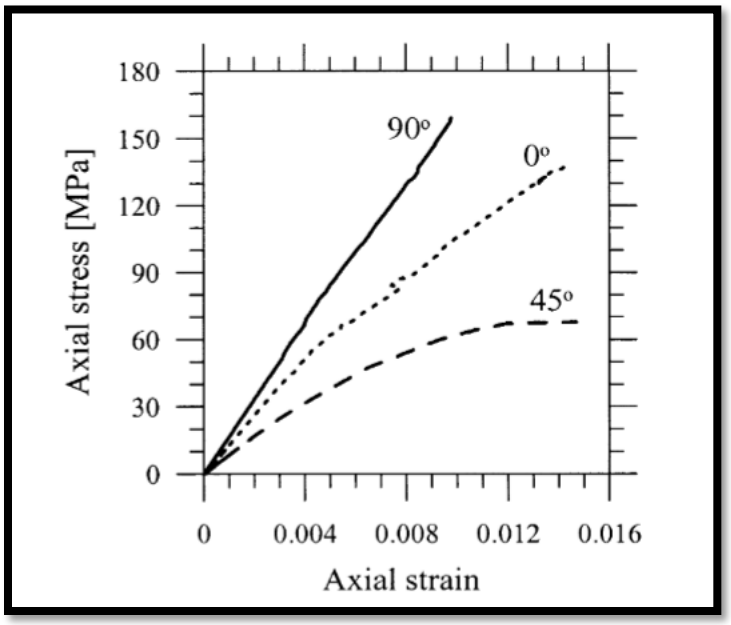

Figure 31: Empirical tensile tests showing stress-strain curves (Carvelli and Poggi, 2001)

The Carvelli and Poggi (2001) used the (3D) Finite Element (FE) model as an arithmetic model to anticipate the most critical parameters that affect the mechanical conduction of the woven

fabric. They found that this composite would first be verified in the elastic field against other investigative solutions and through the nonlinear conduct of a fabric composite. This model helps the study of the mechanical properties of composite materials which are affected by different factors. The project by Carvelli and Poggi (2001) has helped identify the parameters that influence the mechanical features of textiles, even if the model is dissimilar in mechanical structure.

Using textile fabric-enhanced composites has increased the structural implementation of the automotive, recreational, and aerospace industries. The difficulty in the mechanical conduct of textile fabric composites is based on various scale materials. The unit cell conducted at the mesoscale (scale of the textile unit cell) is dependent on the fibre interactions, knitted fabric, and knitted textile composite. Jacques et al. (2014) developed and defined a method for constructing mesoscale finite element models of textile-enhanced composites utilising interval terms on manifold part meshes (ORAS). The approach was validated through comparative empirical results and state-of-the-art verified models (WisTex/Mesh-Tex) , especially for a 5H, 5-harness stain weave unit cell, where the fill yarn floats under one warp yarn and over four warp yarns. Once the technique is understood, mastering the art of curling and playing with the pattern feels effortless. Figure 32, illustrates the geometrical model of a 5-harness stain weave (RUC), created using CAD software, showing the precise arrangement of wrap and fill yarns. Current ORAS software permits inequivalent meshes at opposite faces and numerous meshes. The empirical test is labour- and time-intensive. Numeric diagnoses utilising the Repeated Unit Cell (RUC) and Finite Element (FE) approach for predicting elastic materials have invariably been demonstrated to be acceptable. The results of the mesoscale FE method employed in the RUC by utilising ordinary limit conditions with macro homogenisation received with the recent approach are in perfect agreement with those that received displayed art approaches and empirical data.

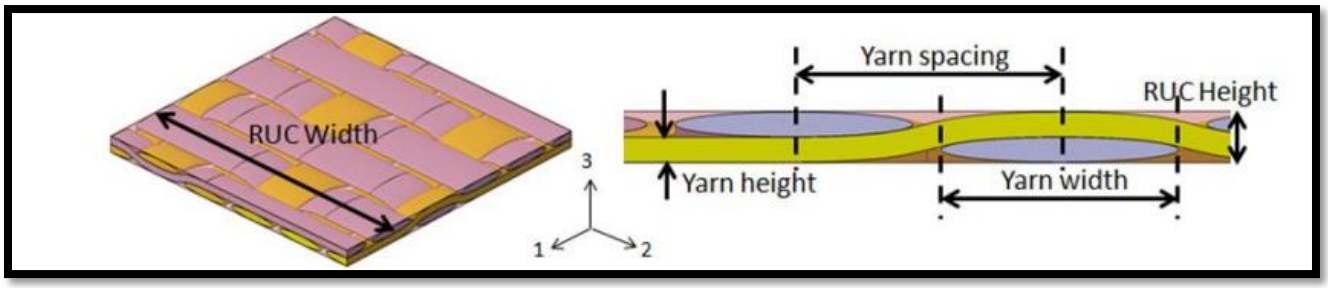

Figure 32: RUC created with CAD software for the geometrical model of a 5H-Satin weave (Jacques et al., 2014)

Lomov et al. (2008) discussed three implementations of the full field strain deformation measurements. Their examination of the tensile and shear distortions of textiles (biaxial extension analyses and picture framework) utilised a visual extensometer, permitting the precise examination of the sample distortion which may have a significant difference from the distortion employed by the testing instrument. The investigators reported textile distortion mechanisms on the gauge of the textile unit cell and single yarns via micro- and meso-gauge full-field strain estimations. Additionally, they estimated the distribution of the local distortion and 3D disfigurement, such as the textile strengthening of the shear angles after wrapping. The provided input for verifying material wrap models and predicting the performance of the consolidated part through structural finite element analysis. Figure 33, illustrates the distribution of shear angles and the local distortion and the textile material in two blank directions (0^{o} and 45^{o}) as predicted by the kinematic model. it also highlights how the material deforms (3D disfigurement) and shows the measurement of deformation along the distance of apex, as indicated by the insets.

Lomov et al. (2008) provided samples of investigations of glass/PP (polypropylene), non-crimp (Carbon), and woven glass textile strengthening deformation. The authors concluded their research by estimating the full field for the regional distortions on a composite part after shaping and supplied a suitable tool for the resolution of the shear angles and the regional directions of the fibre above the specified part and for helping the variation of draping expectations by shaping software mimicking.

This project provided a comprehensive overview of the micro- and meso-examinations of the fabric's strain on the gauge level of the unit cell supply visuals into the fabric's action via distortion and the mechanism revealed by the yarn's reaction. It is essential to emphasise that in this PhD project, my focus was on examining the deformation within the structure of the fabric, rather than at the micro-level.

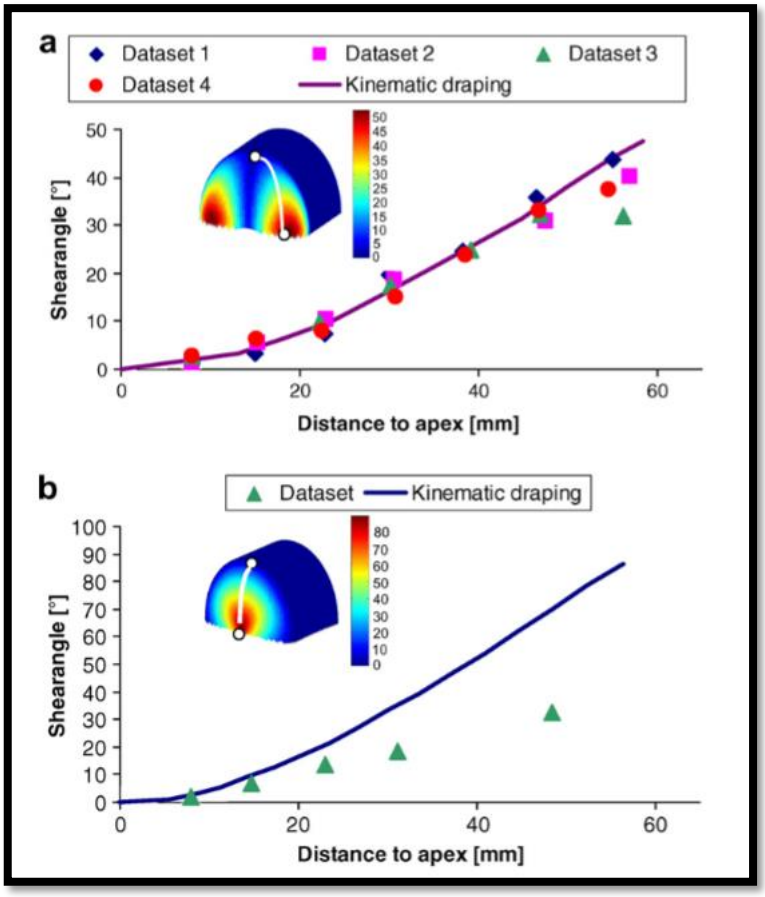

Figure 33: Estimated differentiation of achievements and shear angles through kinematic modelling method for two blank directions: (a) 0°and (b) 45°. The "distance to apex" refers to the distance along the arches introduced in the insets (Lomov et al., 2008)

Research on the mimicking of bending, tensile, and shear of the plain-weft knitted fabric's distortion was conducted analogously to the test performed using the Kawabata Evaluation System (KES-F) for the objective estimation of the mechanical characteristics and the measurement of the fabric by hand as presented by Vassiliadis et al. (2007). KES-F is a series

of tools that are utilised to estimate the textile material features that enable the expectation of the qualities considered by the touch of humans (hand textiles) (NC State University, 2021).

The Kawabata system measures several fabric properties that influence tactile sensation and how fabrics behave under manipulation with lower forces. These properties include shear stiffness (which affects the drape of the fabric), tension (related to how much the fabric stretches), bending rigidity, compression, flexing, and surface friction. In addition, properties such as thickness, softness, and roughness (as they fell against the skin) all contribute to the sensitivity of touch when interacting with the fabric. KES can not only account for human reaction but also supply an explanation of how the variables of yarn, fabric construction, fibre, and the end use contribute to the relation of comfort.

The Kawabata Evaluation System (KES) evaluates the mechanical properties of fabrics, including bending, uniaxial tensile, and shear behaviour. These tests are conducted separately for the course (horizontal) and the wale (vertical) directions of the fabric. By analysing these directions individually, the system identifies differences in fabric performance based on orientation. The results from the course and wale directions are then compared to provide a comprehensive understanding of how the fabric behaves under various conditions, ultimately contributing to the realisation of comfort in the final product. Additionally, the tensile examiner assesses bending, uniaxial tensile, and shear properties for both directions simultaneously and compares their orientations. For a complete evaluation of fabric hand, it is crucial to estimate the friction coefficient, surface roughness, weight per unit area, and fabric thickness. (Kawabata, 1980).

Regarding contact phenomenality, the test simulation depends on the model of the fabric microstructure, the equivalent load which matches each mechanical examination, and the application of the boundary conditions. A 3D model configuration of three connected bodies were used by authors to characterise the unit cells of the fabric microstructure. Based on the complexity of the fabric structure, a finite element analysis was employed to determine the performance of the fabric. The interface phenomenon among the yarns in the interaction areas and the yarn's anisotropic characteristics prevented the union of logical approaches.

The results of each simulation and laboratory test were closely correlated, underscoring the effectiveness of using computational data as a robust tool for analysing textile patterns. This suggests that the accurate identification of the appropriate load and boundary conditions is crucial for faithfully simulating mechanical exams during the testing process.

2.7 Bending and Curling of Knit Fabrics

2.7.1 Description of Phenomena

As discussed earlier in section 2.3 The Geometric Properties of the Fabric), knitting involves the interlocking of yarn loops to create fabric structures. This process forms a series of interconnected loops, which serve as the building blocks of the fabric. In this section (2.7.1 Description of Phenomena

These loop types are created using a single thread running horizontally across the fabric, enabling a wide range of textures and patterns to be incorporated into the design (Kabir et al., 2023). This flexibility allows for both functional and decorative variations in fabric construction, as illustrated in Figure 34.

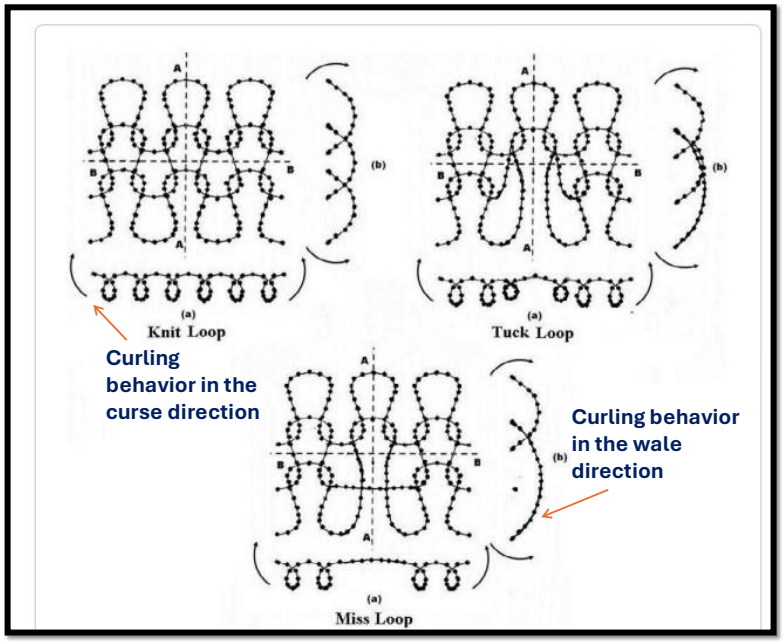

Figure 34: Cross-section of fabric showing curling patterns, the image shows fabric loops with arrows highlighting curling in the course and wale directions. and wale directions (Hasani, 2014a)

2.7.2 Curling

Curling is a common phenomenon in knitted fabrics and occurs in different manners, depending on the course and wale directions. This phenomenon is consistent with whether the edge of the fabric is a self-edge or a cut edge. Curling in knitted fabrics occurs because of their intricate geometry, which can lead to both visual and physical complexity (Sperl et al., 2021). One of the various factors that contribute to curling in knitted fabrics is the knitting structure. In weft knitting, where the yarn runs along the width wise direction of the fabric, curling can occur because of the way the loops are formed and interlocked, as shown in Figure 35. This curling behaviour in weft-knitted fabrics has been extensively studied by researchers. Hamilton (1975) analysed the curling behaviour of plain-knitted fabrics and investigated the influence of yarn elasticity, flexural rigidity, and torsion rigidity on this phenomenon. Hasani (2014) developed a test method for measuring the self-edge curling of plain-knitted fabrics. The self-edge (or selvedge) refers to the edge of fabric that is finished during the knitting or weaving process to prevent it from unravelling. In plain knitted fabrics, the self-edge is the natural edge created by the loops at the end of each row, as shown in Figure 36. Furthermore, Kurbak and Ekmen (2008b) presented a geometrical model for the width-wise curling of plain-knit fabrics. The curling effect in knitted fabrics is not only significant from an engineering perspective but also has practical applications and aesthetic attributes (Yan et al., 2021a). Studies have explored the application-oriented aspects of curling in knitted fabrics, focusing on the unique characteristics and auxetic effects that can be created.

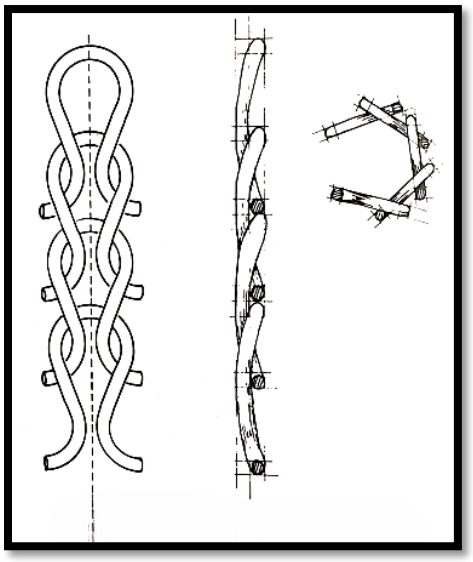

Figure 35: Plain fabric curling towards the face (Bhosale & Jadhav, 2015)

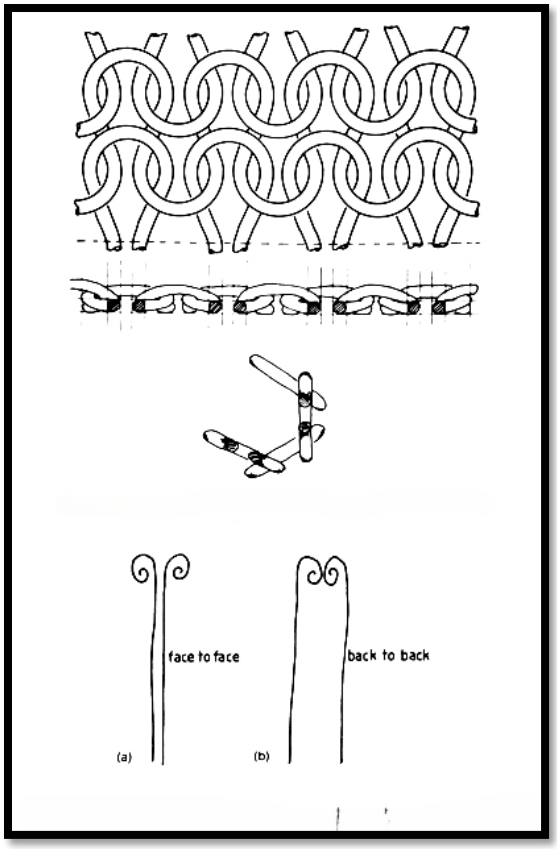

Figure 36: The plain fabric's self-edge curls towards the back during seaming, either facing each other (a) or back to back (b)(Bhosale &Jadhav, 2015)

Curl is a peculiar type of knitted textile. A cut of the porous textile fabric was described as a square sample with alternating corners attempting to roll upward and downward, southwest and northeast bends rolling along the same path. In contrast, southeast and northwest bends rolled in the opposite direction. Some samples rolled only slightly. while others roll so forcefully that they bend upward diagonally, forming a duplex scroll as illustrated in Figure 37, (Go & Shinohara, 1959).

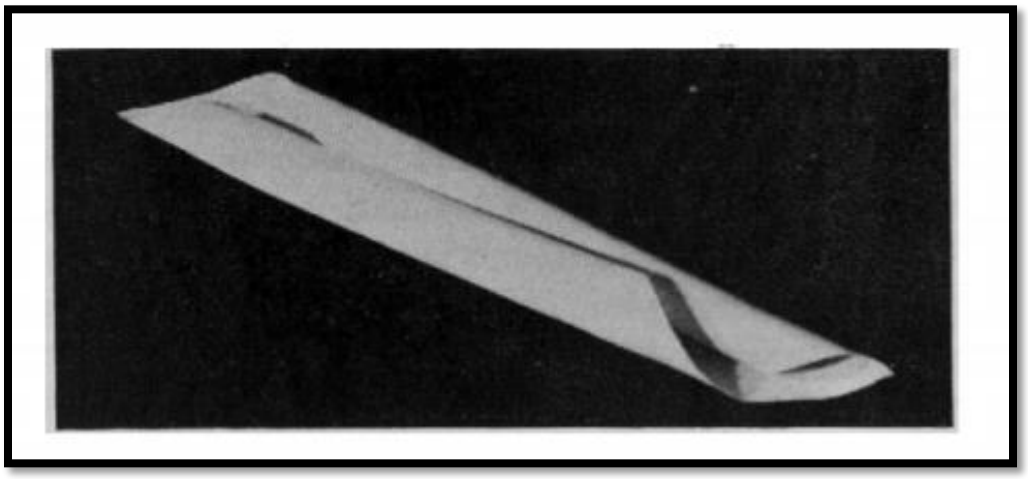

Figure 37: Rolling corners curling fabric into a duplex scroll (Go & Shinohara, 1959)

Virtually all single-knitted fabric edges curl. When a fabric is cut, it is common for the edges to curl. This is because the tension held within the fibres is released, creating a natural curling effect. However, even without cutting, some fabrics may still curl at the edges because of various factors such as tension in the fibres or changes in the environment. Circular knitting machines can create single-knit fabrics using either one or two sets of needles. A single set of needles, such as those used in circular knitting, generally produces tubular fabric (Joy, 2021). In contrast, two sets of needles, as used in flat knitting machines or with straight needles, produce a flat fabric with two distinct edges (Lundström & Lu, 2021). For example, circular needles can create flat or tubular fabric, depending on their use. The fabric structure, appearance, and properties (like curling edges) depend on various factors, including the knitting pattern, yarn type, and finishing processes, not just the number of needle sets used.

The plain knitted fabric samples tested in this thesis curls properly at the edges when free to move. The top and bottom curling sides can be prevented by adding a border of a different yarn type. Figure 38 below shows a stainless-steel sample from this thesis, where curling is visible along the right and left edges. The polyester yarn was added to the top and bottom of the sample for two reasons. First, single knits with a rib structure provide stability to the fabric and effectively prevent curling. The incorporation of polyester yarn on the edges heightens the non-curling capability as polyester and stainless-steel yarns offer distinct properties in the main fabric. In addition, by clamping the non-curl edges during tensile testing, the fabric sample could be securely held in a fully taut and straight position. Consequently, more precise, and consistent measurements of the stretch, recovery, and other mechanical properties of the fabric could be obtained.

Figure 38: Stainless steel sample curling edges

2.7.3 Bending Rigidity

Bending rigidity, which measures a fabric's resistance to bending, is closely related to curling, particularly in knitted fabrics. Curling occurs when there is an imbalance in tension between

the fabric's face and back, leading to edges that roll inward or outward. Fabrics with high bending rigidity are more resistant to deformation and thus less prone to curling, as their stiffness helps maintain structural stability. Conversely, fabrics with low bending rigidity are more flexible and susceptible to curling, as they easily deform under tension imbalances. By modifying bending rigidity through adjustments in yarn type, fabric structure, or stabilizing elements like borders, curling can effectively minimize, improving edge stability and fabric usability.

2.7.4 Previous Research on Bending Rigidity and Curling

This section focuses on previous research findings related to bending rigidity and its role in curling behaviour with knitted fabrics.

The curling behaviour of the fabric edges was described in detail by Walker and Doyle (1952). During knitting, the yarn is bent into a loop according to its elasticity. If the fabric's edge is unbonded, it will uncurl itself out, and all loop forces can be satisfactory for elevating the fabric and shaping it into a roll. This response is illustrated in Figure 39 and Figure 40 (a), which demonstrates the protruding bend in the Z plane according to the enactment of the yarn around the loop neckline of the next course.

The edge rolling of the fabric and the flexible forces acting on it help to minimise the curvature (Hasani, 2014a). Additionally, the edges of the fabric curling in upward and downward directions occur concerning the yarn's bend in the Y plane (Barburski & Lomov, 2016). The bending trend in the X- plane conflicts with that of the Y-plane, resulting in an opposing trend. This influence is illustrated in Figure 40 (b). These illustrations demonstrate the fundamental influence of the geometrical construction of the loop on yarn diameter. The degree of curvature is significantly affected by the yarn diameter in the loop neckline and the partition between neighbouring courses which has been explained for the two cases. Therefore, with a small yarn diameter and very slow-moving knitting, we could only have a small curvature and the lowest inclination to curl. When rib knitting is used, the opposite stitches are flipped, effectively counteracting any curling forces and producing a flat fabric.

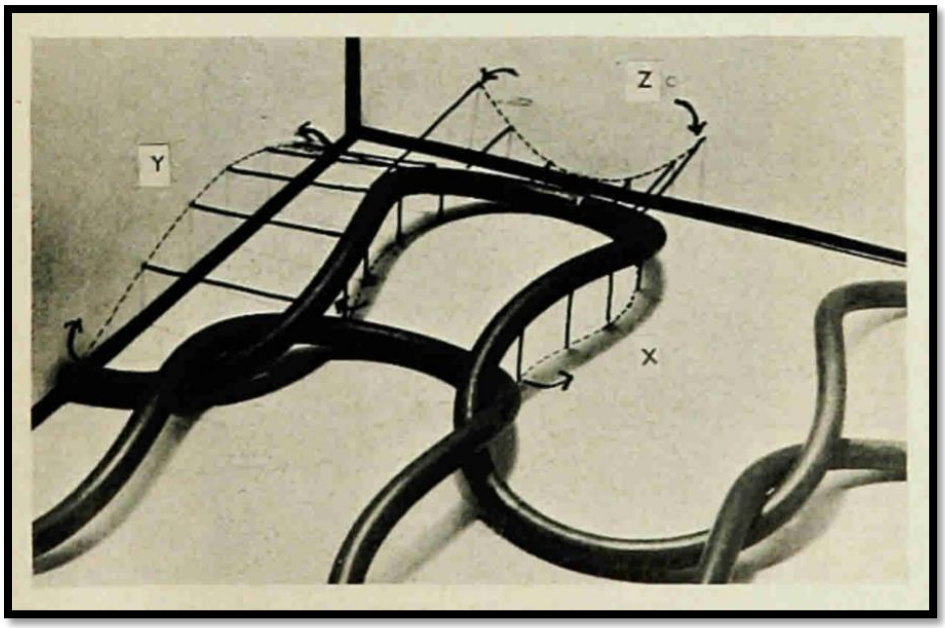

Figure 39: Model of knitted fabric. Arrows signify the orientation of forces of elastic revival (Walker & Doyle, 1952)

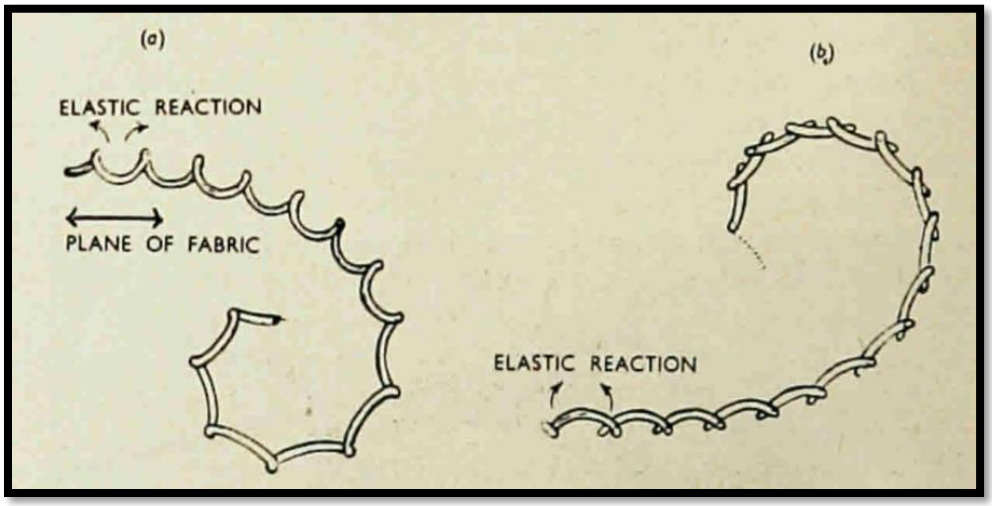

Figure 40: plot demonstrating the act of fabric in curling. (a) View along Wales with predictable bend on Z-plane. (b) View beside courses with predictable bend on Y-plane (Walker & Doyle, 1952)

Researchers have investigated the curling behaviour of single-jersey-knitted fabrics. Walker and Doyle's (1952) study demonstrated that fabric curling is influenced by factors such as bending rigidity, torsion stiffness, and yarn elasticity.

In this thesis, the fabric samples used, such as stainless steel, silver, and polyester, exhibited curled edges on the right and left sides, because of the elastic reaction of the yarn.

Hamilton and Postle (1974) proposed an approach for estimating the tendency of a knitted fabric to curl or roll at the edges due to imbalanced structural deformations within the course and wale directions., also known as the curling couple. This occurs because the loops at the edges of the knitted fabric are not interlocked on all sides, allowing them to deform more than loops within the frame of the fabric. Hamilton and Postle (1974) were the first to examine the phenomena of a negative bend, noting that it occurs without the jamming of the plain-knitted structure.

Jamming of plain-knitted production refers to the phenomenon where the yarns in a knitted fabric are tightly packed and interlocked, resulting in a solid, stable structure. This can occur in various varieties of weft-knitted systems, including simple-knitted fabrics (Shanahan & Postle, 1973). Jamming can affect the overall mechanical performance of the fabric, as it can increase the rigidity and strength of the material (Balea et al., 2014). Jamming can be affected by factors such as course spacing, stitch length, yarn type and size, and knitting method. The condition of jamming occurs when the fabric is bent. Inspection of the fabric geometry (see

Figure *41*) demonstrates that no loop jamming must occur in the state of a negative fabric bend and that there would be a usual opening out of the course through the construction. The bending resistance is believed to be primarily caused by the bending and sliding of yarns, rather than compression or strain.

When a bending moment (the measure of force causing the bending of an object) is applied parallel to the course, it becomes necessary to deform two yarns per loop, thereby increasing the resistance to bending. This suggests that the resistance to bending primarily arises from yarn deformation rather than from other factors such as compression or tension.

The bending behaviour of plain knitted fabric typically exhibits negative curvature when it is relaxed and bent along the course direction. However, when the fabric is not relaxed and is bent differently, the bending process becomes more complex, involving multiple aspects such as flexing and other types of bends. The bending along the course direction. However, when the fabric is not relaxed and flexing and other influencers like

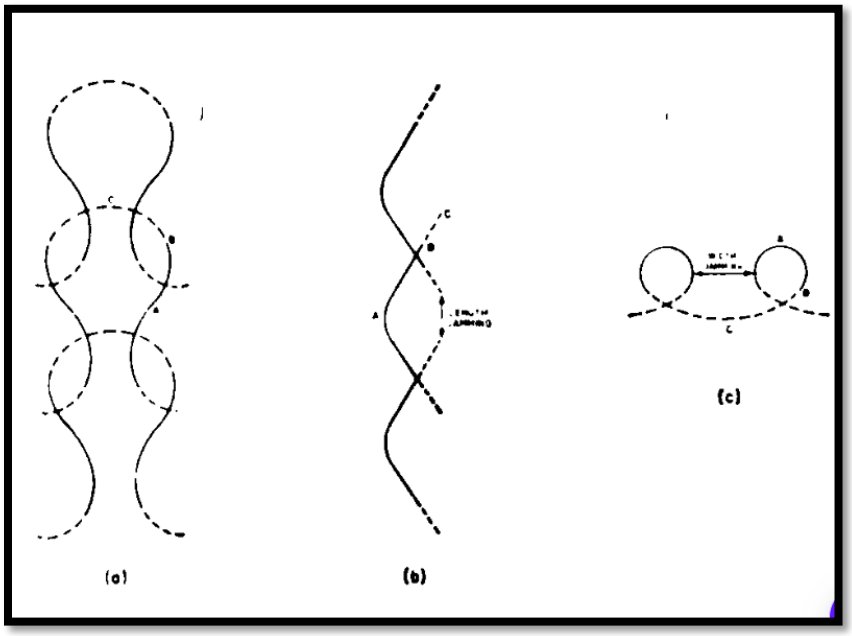

Figure 41: A geometrical model of the plain-knitted construction demonstrating the circumstances of jamming which happens when the fabric is bent, (a) plain view, (b) side elevation- no loop jamming is expected to occur for negative fabric curvature, and (c) end elevation- jamming in the figure occurs between adjacent wales for negative curvature bending ((Hamilton & Postle, 1974)

The curling of the edges of the plain-knitted fabric showed a different propensity. Four parameters were utilised to identify the bending behaviour of every fabric in every main direction: B_1 and B_2 curling stiffnesses, M_o hysteresis at zero bend, M_c and M_w curling couple.

After fabric recreation, the greatness of each limit was established to decrease significantly, and the average exceeding each limit with the tightness key also decreased. The result of the study for the relaxed fabric is that the curling couple must be zero, the amount of hysteresis at

the zero bend M_o must be the lowest and nearly impartial of the fabric tightness key, and the different fabric stiffnesses should assume their lowest levels.

Hamilton and Postle (1974) concluded their research by examining the bending and recovery characteristics of plain-knitted wool fabrics from both geometric and rheological perspectives. They predicted hysteresis bends for sequences of relaxed and unrelaxed fabrics and estimated the bending limits based on two main trends.

Hamilton and Postle's study can be extended to include knitted structures beyond plain fabrics, fibre types other than wool, and bending in a biased direction. Such an expansion would further advance understanding and clarify systematic bending behaviour observed during knitted construction.

For this PhD thesis, the information outlined above was used to investigate the factors influencing edge curvature, including the sample's bending and recovery properties in both relaxed and unrelaxed states. in Hamilton and Postle's research, however, the yarn used was wool, while the current project employs a smart yarn, which exhibits distinct properties compared to stainless steel, silver, and polyester.

Phukan and Subramaniam (1995) investigated the grade and consistency of the flat set (the extent to which a knitted fabric retains its flatness after deformation, such as bending) in plain knitted fabrics made from polyester/cotton, polyester/viscose, cotton, and polyester for both ring- and rotor-spun yarns. They described the flat set as resulting from the compound bending behaviour of the fabric, which arises from the combined effects of bending hysteresis on the technical front and back sides. These bending behaviours were analysed along the wale (vertical loops) and course (horizontal loops) directions, with the integration of the bending hysteresis curves in these directions contributing to the overall flat set.

Phukan and Subramaniam (1995) examined the bending hysteresis trends along the wale and course directions in blends of cotton and polyester. They observed that Plain-knitted constructions are characterised by greater elasticity when bending occurs around an axis parallel to the wale direction, compared to the course direction. To explain the bending recovery and stability of the set, the authors proposed the following equation.

bending recovery $= \frac{maximum\ curvature - resdual\ curvature}{maximum\ curvature}$ and

stability of set $= \frac{bending\ recovery\ after\ wet\ tretment}{bending\ recovery\ before\ treatment}$

The investigators concluded that there were minimal differences in the flat set grades of fabric specimens made from ring-spun yarns compared to those made from open-end spun yarns. Furthermore, the overall flat set grades for the group of fabric specimens were found to be similar. The curling couple highlighted the impact of different finishing treatments on the identification and characteristics of the fabric group. these treatments did not reduce the curling tendency of the plain-knitted fabric. Instead, they primarily enhanced the fabric's appearance and texture, suggesting that the focus of the treatments was more on improving the look and feel of the fabric rather than its flatness.

The curling space of the dry-relaxed cotton plain knitted fabric was modelled by employing a manifold regression examination Ucar (2000b). A single group of limits utilised in manifold regression examination is the moment on the loop that forces the fabric to curl. The study developed theoretical equations to describe the forces and moments responsible for curling. In a dry-relaxed state, various forces act on the loops within the knitted fabric. These forces originate from tension-applied knitting, jamming, and the bending and twisting required to transform straight yarn into loops. The energy sorted in the loops due to those forces leads to issues such as shrinking, curling, and spirality.

The real loop in the fabric is a three-dimensional construction, as illustrated in Figure 28, and the section (BE) of the loop is twisted downward and the section (BN) is twisted upward by the forces which arise from the interactions with neighbouring loops.

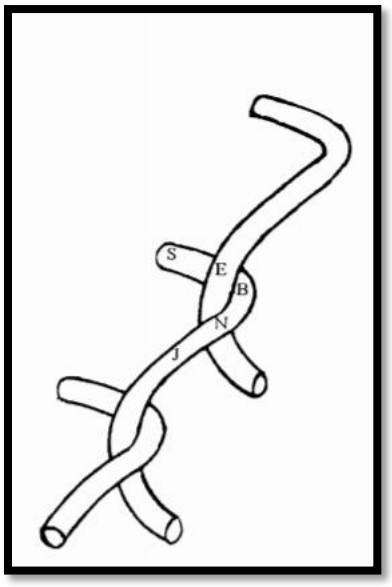

Figure 42: Schematic illustration of the loop in three-dimensional (Ucar, 2000b)

Ucar (2000b) identified that the loop head and legs were bent out of the fabric plane by the force F_z (Figure 43). This bending causes energy accumulation in the loop. Therefore, when the fabric was snipped and crimped at the edges, it began with energy clearing. At the high and low edges of the fabric, curling occurs from the backside to the front side; however, at the fabric's sides, crimping occurs from the back and front (as shown in Figure 43 a and b).

This is because the bending stiffness for the negative bend is less than the consistent value for the positive bend when the bending moment is displayed on the axis counterpart to the course. For the negative bend, the face of the fabric was on the concave side of the bend fabric. The conflict is correct for a positive bend. The bending stiffness for the positive bend was inferior to the corresponding value for the negative bend. The reason for this difference in deformation is the orientation and arrangement of yarns in the fabric. When the bending moment is applied around the axis parallel to the wales, it affects the two yarns in each loop, causing more deformation. However, when the moment is applied around the axis parallel to the course, it only affects one yarn in each loop, resulting in less deformation.

This difference in deformation indicates that the fabric is more resistant to bending moments around the y-axis than around the x-axis. This could be due to the inherent properties of the yarns and their arrangement in the fabric structure. Therefore, the value of the moment of the

x-axis can be higher than the value of the moment of the y-axis, based on the fabric's response to bending.

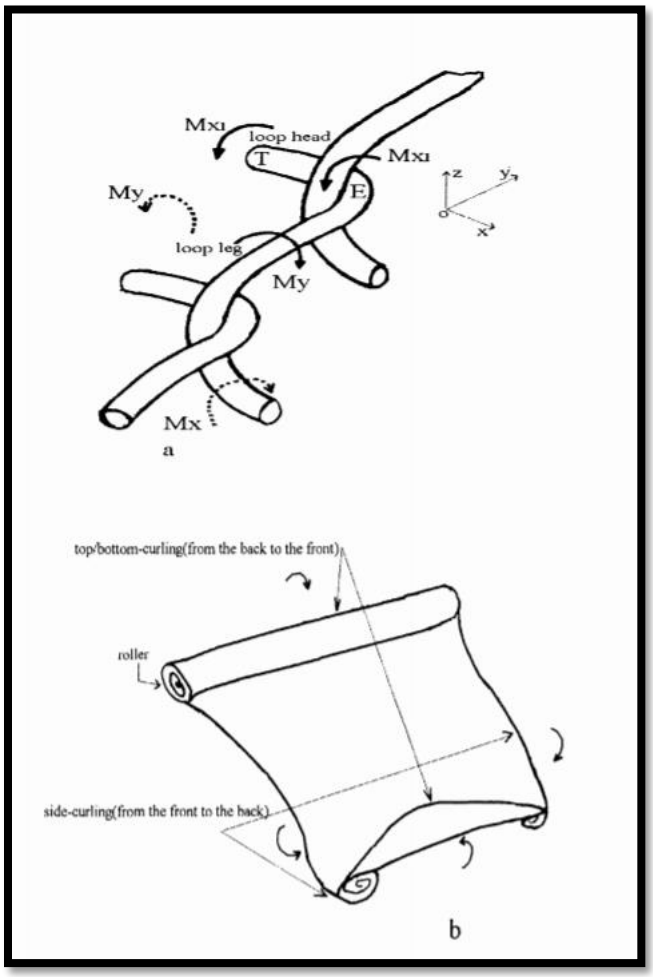

Figure 43: Curling behaviour, (a) the effects of moments, (b) curling of fabric (Ucar, 2000b)

Ucar (2000b) concluded his research by determining the fabric's loop bending and torsion moments which influence the fabric, employing Castigliano's theorem. Ucar (2000b) identified the moments using simple equations, which are functions of yarn and fabric limits, such as bending stiffness, course-wale distance, and yarn diameter.

Ucar (2000a) presented both the experimental and regression analyses. A novel method was devised during the experimental phase to calculate twist spacing, addressing the gap in previous methods that primarily focused on curling tendency rather than curling distance. In the regression analysis, data from the experimental study and some data calculated using the equations developed in the theoretical study were used.

As outlined in the previous study Ucar (2000b), the theoretical analysis of the moments acting on the loop that induces fabric curling provided insights into the phenomena of edge curling, the investigator Ucar (2000b) identified several parameters that influence curling behaviour, including the moment (M_x, M_y), tightness factor, and mass of the loop. The tightness factor has a significant effect on the values of the forces and moments in the loop.

Another important parameter is the mass of the curled roll (Figure 43, b). During curling, as the mass of the roll increases, the moment of mass inertia of the roll increases, and finally, curling stops. This effect must be included in the regression analysis. The proportion of the moment of mass inertia of an individual loop to the moment of the individual loop ($^{I_m}/_{M}$, where I_m is the mass inertia of a single loop) was also included in the regression analysis.

Another parameter that affects the curling behaviour is the coercive moment which describes the resistance of the fabric to change its curling behaviour, which is influenced by inter-fibre friction and the fabric's bending rigidity. These factors were not included in the regression analysis because they were not known before fabric production.

Ucar (2000a), the experimental study concluded that the three parameters included in the regression analysis (d/L, $^{ML}/_{B}$, and $^{I_m}/_{M}$) make it possible to obtain the twisting spacing before making a sensible estimate.

Ucar (2000a) utilised a manifold regression examination to obtain the twisting spacing of a single jersey-knitted fabric by employing fabric and yarn limits. These limits are the yarn counts used to estimate the yarn diameter, bending stiffness, and loop length.

In plain knitted structures, a geometrical model for width-wise curling was suggested by Kurbak & Ekmen (2008). The principal goal was to generate models of $m \times n$ rib and small-diameter cylindrical fabrics.

The curling edge assumed above can cause difficulties in the generation of plain-knitted dressings. Several strategies have been proposed to overcome the problems of edge curling during dressing production.

(a) Attach a sheet to the back of the fabric.
(b) Place a weightier chemical material on both surfaces of the fabric within the open-width final procedure.
(c) Hang fabric below the separating table before snipping.

In addition to these issues, edge curling can also be intentionally incorporated into the design, such as using top-side edge curling to create the pullover neckline, as was the fashion some time ago.

In Kurbak's (2008) model, the highest and lowest portions of the loop are elliptical in shape, while the loop arms have helical forms, wrapping around elliptical tubes positioned parallel to the wale's direction, with a variable helix angle.

This model concluded that the torsion decreased with crimping, whereas the bend radius increased, particularly at the arm midpoints (see Figure 44, and Figure 44). In addition, the torsional and bending energies decreased with width-wise curling, particularly at the midpoint of the loop arms.

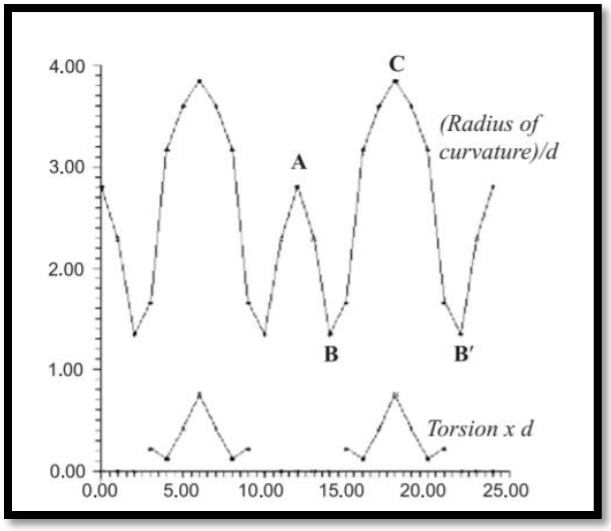

Figure 44: Radius of Kurbak's (2008), plain knit model bends and torsions (d is the active yarn diameter) (Kurbak & Ekmen, 2008)

Using data presented by Ucar (2000) and Kurbak and Ekmen (2008), some of the forces affecting the curling behaviour during the curling phenomena were modelled. Two studies by Ucar were referenced in this analysis.

The approach utilised in my thesis differs significantly from the methodology employed in these studies due to differences in how energy is modelled. As the roll gains mass, the moment of inertia also increases, leading to the cessation of curling. This finding suggests that the samples possess curled edges on both sides, potentially influenced by factors such as the loop length, yarn diameter, bending rigidity, and torsional energies. In my thesis, rather than modelling bending and torsion energies separately, I integrated them into the curling parameters for a more comprehensive understanding.

As the unfinished edges of the fabric sample were left free, they tended to become twisted. A disadvantage of single-knitted fabrics is curling, resulting in snipping, tailoring, and connecting difficulties. Minapoor et al. (2013) investigated the effect of fibre, yarn, and fabric limits such as fabric density, fabric construction, yarn twist and count, blend ratio, fabric density, and relaxation time on the curling phenomenon of single jersey weft-knitted fabrics which exhibit curling in both course and wale trends. Taguchi's empirical determination (Peace, 1993) was employed to estimate the influence of these limits on curling. The ideal fibre, yarn, and fabric limit requirements were determined empirically. Eventually, two neuronal network models were proposed to obtain the curling distance in the course and wale trends.

Taguchi's experimental design (Peace, 1993), is an approach for scheming and presenting tests to explore procedures in which the output is contingent on many components (variables: inputs) without having to run the procedure employing all probable mixtures of those variables, which would be tedious and uneconomical. By methodically choosing mixtures of variables, it is possible to distinguish between their separate influences.

Minapoor et al. (2013) concluded, based on the results of Taguchi technique, that fabric structure and knit density had the most significant impact on fabric curling in both wale and course directions. Specifically, double cross tuck and double cross miss constructions exhibited less curling compared to plain structures. Furthermore, higher knit density was associated with reduced curling. Other components also influenced curling to varying degrees in the wale and course directions. The study highlighted fabric structure and knit density as key parameters for evaluating and controlling fabric curling, which can be incorporated into my thesis.

The curling behaviour of single-jersey-weft knitted fabrics was studied by Hasani, (2014), who investigated the effect of the tuck and miss stitches and yarn curl trends on the twisting of single-jersey knitted fabrics under twisting conditions around the course and wale direction. The tuck-and-miss stitches illustrated in Figure 45.

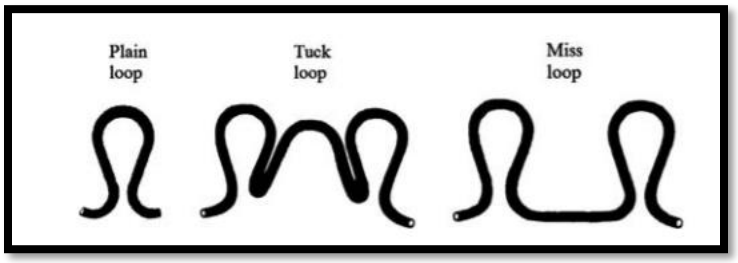

Figure 45: The form construction of plain, tuck, and miss loops (Minapoor et al., 2013b)

For the three knitted structures, during the miss or tuck loop formation, the float yarn expanded from the base of one knitted or tucked loop to the next. In the case of an insert loop, the researchers noted that the convened loop expands into the course until a knitted loop is shaped in the wale.) suggested that, upon examination, an insert stitch is shaped when the needle is convening a loop, with an additional loop. A knitted loop would need to be individually withdrawn. A missed stitch would invariably be floated openly on the functional back, and during the fabric's production, such densities of fabric samples would remain constant. During loop formation, bending and torsion forces were applied to the feeding yarn. These external forces were found to be stored as potential energy; during the curling phenomenon, this potential energy is released, at which point the fabric reaches its lowest energy level. This is more relevant to my project when the energy method is the model that minimises the potential energy because the external forces are sorted during curling.

The researchers concluded the paper by saying that the cross-tuck structure represented a lower curling surface value than the cross-miss structure, either in the course or wale trends, because the lower stitch density of structures includes tuck stitches compared to those involving missed

stitches. In contrast, the double cross tuck gives the structure a higher curling surface in the wale direction compared to those comprising tuck stitches.

This thesis focuses on experimental research totally on plain knitted fabrics for a basis of study. However, the constructed mathematical models are more flexible and permit a diversification of the relative contributions of strain energy and friction. This ability hints that one might use the model for other more complex fabrics, which may also result in different behaviour under varying conditions.

The fabric geometry has a significant effect on performance. To obtain mechanical distortions such as bending stiffness, shear modulus, and initial modulus, it is necessary to study fabric geometry. The construction of warp-knitted fabrics is much more complicated than that of other fabrics. Warp knits are significant because of their unique knitting technique which allows for the production of fabrics. This method is the fastest way to create fabric from yarns, setting it apart from traditional weft knitting, in which each needle loops a single thread. Exploring the conduct of warp knitted construction helps to identify an easy model. Dabiryan and Jeddi, (2011) presented a 3D straight-line model for knitted fabric's two-guide-bar. They ran the weight per unit area of various specimens to verify the suggested model and geometrical parameters.

The study does not include knitted fabrics with a single guide bar. All warp-knitted structures studied in this work have double loops, which means every needle form two linkages. In the simplest case, a two-guide bar tricot fabric is made by using a 1 x 1 lapping movement to form a basic structure alternating the yarn on adjacent needles. As warp-knitted fabric is produced the yarns orient at different angles which facilitates obtaining fabrics with diverse properties. Different views of structures of two-guide-bar warp knitted fabrics (tricot) illustrated in

Figure *46*.

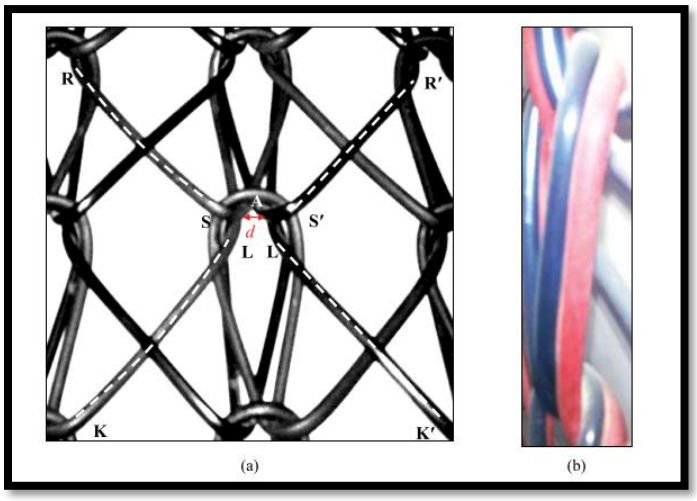

Figure 46: Different views of structures of two-guide-bar warp knitted fabrics(tricot):(a) front view, and (b) side view (Dabiryan & Jeddi, 2011)

Yarn analyses tend to be based on the following assumptions:

- Each loop consists of perfect lines, with the yarn's cross-section forming a ring (Figure 46, a), a single intersection connects one loop to the neighbouring loop in a similar course (RS for the backside rod and R`S` for the frontside rod loops).
- An additional intersection connects to the neighbouring loop in the previous course (KL for backside rod and K`L` for frontside rod loops).
- The initial intersections connect at point A, but the distance between them is equivalent to the diameter of the yarn.

The study's model does not always consider the differences between the backside and frontside rod loops and the backbar loops. A warp-knitted structure model was first reflected along with a theoretical investigation of 3D models.

Experimentally, Dabiryan and Jeddi, (2011) created seven of the two-guide-bar warp knitted fabrics that are more popular (three and four needles satin, three and four needles sharkskin, locknit, tricot, and reverse locknit) were created in this model. All these common fabrics were knitted from polyester yarn.

Dabiryan and Jeddi, (2011) concluded that the differences between the empirical and hypothetical values of various limits demonstrate that the straight-line model is suitable for obtaining the geometric features of two-guide bar warp-knitted fabrics. The research introduced a hypothetical model that is appropriate for estimating the mechanical conduct of warp-knitted fabrics.

Incorporating warp knits into this thesis is crucial as it offers a unique method of knitting that can result in a variety of fabric structures and properties. The current study seeks to establish a comprehensive evaluation of warp knitting and compare it with weft knitting, facilitating the identification of their respective strengths and weaknesses. Ultimately, this information can inform the creation of novel knitted fabrics with specific and desired characteristics.

Recently, use of the applications of warp-knitted fabrics have expanded in different manufacturing like composites making. Therefore, Dabiryan et al. (2012a) attempted to create a mechanical model to obtain the mechanical characteristics like the original modulus of two-rod fabrics of the warp-knitted (satin, tricot, and lock knit) by employing the energy approach. The energy conditions observed in this research were bending, extension, and compression. In addition, the friction energy was reconsidered using the frictional energy term.

Usually, when the model originates from a two-rod tricot fabric, it is feasible to extend it to different constructions. Dabiryan et al. (2012a) assumed that the yarns are incompressible and ideally flexible, and that the yarn had a circular cross-section. The front- and back-side rod loops was also symmetrical. In addition, the influence of yarns on other loops of the unit cell was reflected as strengthening at the midpoint of a connection element. There were two stages of deformation:

- Loop’s shape malformation.
- Change in the element’s loop (structural deformation).

Based on Dabiryan et al.'s (2012a) findings, in the initial stage of deformation, the malformation only occurs for the head of the loop; thus, all the associating connections interact with each other (Figure 47, b), and it seems likely that for the next stage of element change, the deformation will be in the structure (Figure 47, c).

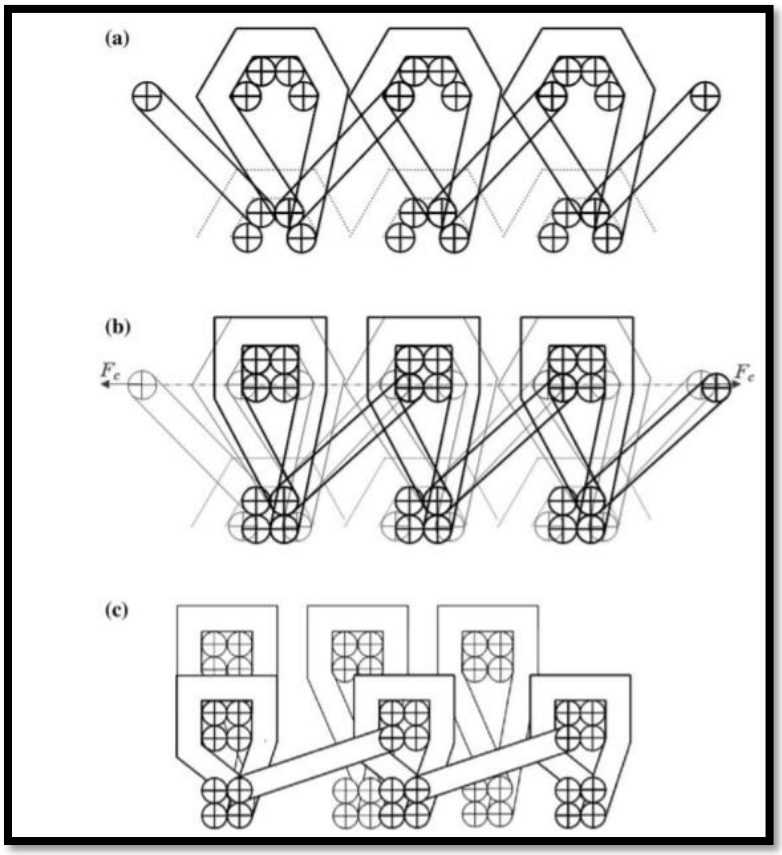

Figure 47: Flexible lamination of the geometry of the fabric under uniaxial tension. (a) moderate geometry, (b) loop lamentation, (c) construction lamentation (Dabiryan et al., 2012a)

Dabirtan et al. (2012a) suggested a geometrical straight-line model, using the weight per unit area and run-in of different samples and the energy method to analyse the tensile features of warp-knitted fabrics. This model is split into mismatched components. From this model, the overall energy of the unit cell was predicted, and the strain and original modulus of the fabric were determined. They displayed perfect concurrence between hypothetical and empirical values.

In Part 3 of this series of papers, Dabiryan et al. (2012b) analysed the tensile properties of the second group of warp-knitted fabrics that have taller overlaps in the backside bar, such as reverse lock knit, three and four, and needle sharkskin. Again, they considered using a model based on energy and Castigliano's theorem to estimate the original modulus of the warp-knitted fabric.

In the stress-strain curve of most fabrics, two primary regions were evident: the first region exhibits low stress, attributed to decrumbing in loop-form fabrics or variations in woven and knitted fabrics, whereas the second region exhibits high stress, which is linked to the extension of the yarn.

Regarding the geometric malformation, the initial part of the expansion was flexible, as can be seen in the photographs of the genuine fabric under uniaxial stress (Figure 48). The construction loops deformed when the warp-knitted fabric was subjected to the exterior force in the course orientation, and then the underlaps were inclined to recline to the employed force orientation.

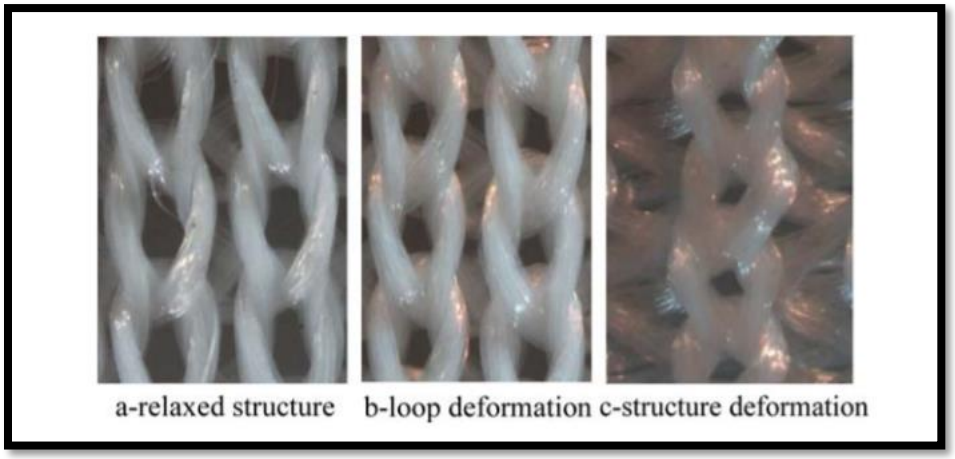

Figure 48: Real photo of the warp-knitted fabric under uniaxial tension in course direction (Dabiryan et al., 2012b)

For the experiment, five samples were examined to estimate the initial modulus. Dabiryan et al. (2012b) accomplished this by comparing the tensile conduct of different warp-knitted fabric constructions and demonstrating the fundamental variation between them. The flexibility of

contractions with taller underlaps on the backside rod is typically lower than the flexibility of those with long underlaps. The authors suggested that the difference between these two groups was related to the friction between the yarn and slipping space of longer underlaps.

Dabiryan et al. (2013) presented a series of experimental models of the actual fabrics to calculate the initial modulus and they used a recent test approach to identify the warp knitted fabric's tensile test. As a result, the initial modulus of the equipped sample was estimated by utilising a tensile tester for comparison with hypothetical values. During the expansion of the fabric, a group of malformations, such as shearing, bending, and extension, were noted according to the interaction between yarns.

Out-of-plane distortion was created by the extension of the fabric, such as curling and buckling (Figure 49). The concept of buckling refers to the dynamic distortion of a fabric weft when incorporated into a populated setting. This distortion can be likened to an uncoordinated movement, as the fabric cannot maintain a straight orientation, making it less precise as a structural element. Buckling can be seen as the unexpected deformation of a material or structure, such as fabrics, when subjected to a load (Dhakal & Maekawa, 2002). A fabric disadvantage matches a defect in the processed superficial fabric, most of which is caused by machine or process malfunctions. Most of these disadvantages result from the impairment of the machine and procedure, and some of the defects are precipitated by malfunctioning yarns or damage to the machine (OCS Team, 2019).

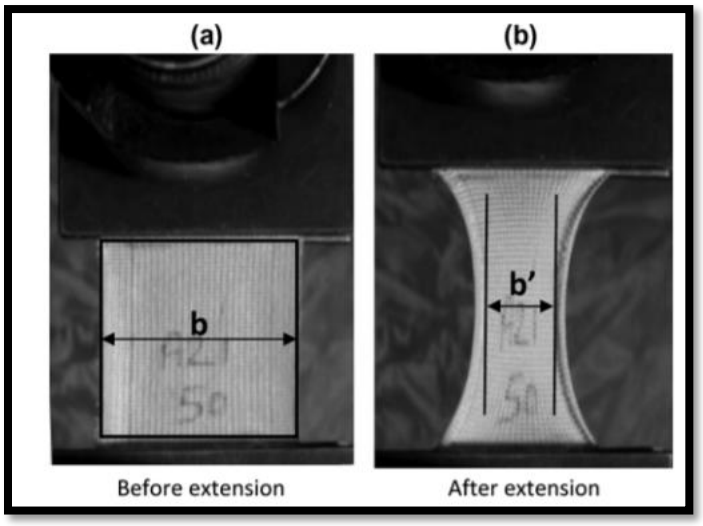

Figure 49: Curling of samples during extension (Dabiryan et al., 2013)

This study demonstrated that the density and construction of warp-knitted fabrics influence their elastic functioning. The elasticity of the fabric was reduced by increasing the density and number of underlaps in each set. In general, the hypothetical and experimental values have good tolerance. The initial modulus of the warp-knitted fabric can be measured with good resolution by utilising the submitted models in the diagram below (Figure 50 and Figure 51).

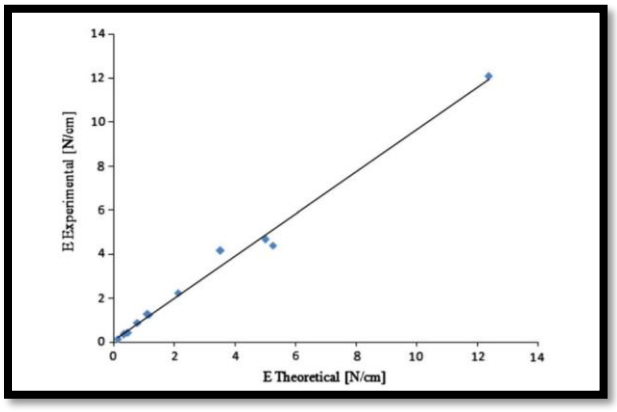

Figure 50: This diagram shows the first set of fabric's initial modulus experimental and theoretical values relationship (Dabiryan et al., 2013)

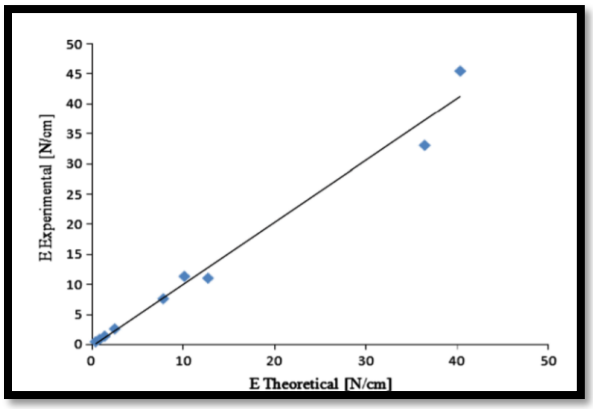

Figure 51: This diagram shows the second set of fabric's initial modulus experimental and theoretical values relationship (Dabiryan et al., 2013)

In this part of the series, Dabiryan and Jeddi's (2012) attempted to model the initial Poisson's ratio of two guide bar warp knitted fabrics in the flexible malformation area by employing geometric associations. In this study, elastic deformation indicated the greatest geometrical malformation among the various formations.

If the warp-knitted fabric is compromised owing to the surface force along the course orientation, the fabric will extend in the course orientation, but it is constricted in the wale orientation, as illustrated in Figure 52. Thus, Poisson's ratio of the warp-knitted fabric is identified as the ratio of the minimisation rate in the wale orientation to the maximisation rate in the course orientation.

Theoretically, the investigators calculated the Poisson's ratio of the warp knitted fabric for the two groups, as mentioned in the preceding sections of this series, by applying force in the course direction for all fabrics depending on the fabric structure. Experimentally, for every sample configuration, five were examined, and all the samples were knitted from the same filament polyester yarn (50 denier/24). The specimens were expanded using INSTRON-5566 equipment. As the hypothetical exploration was affected by fabric expansion in the course direction, the samples were experimentally expanded in the course direction.

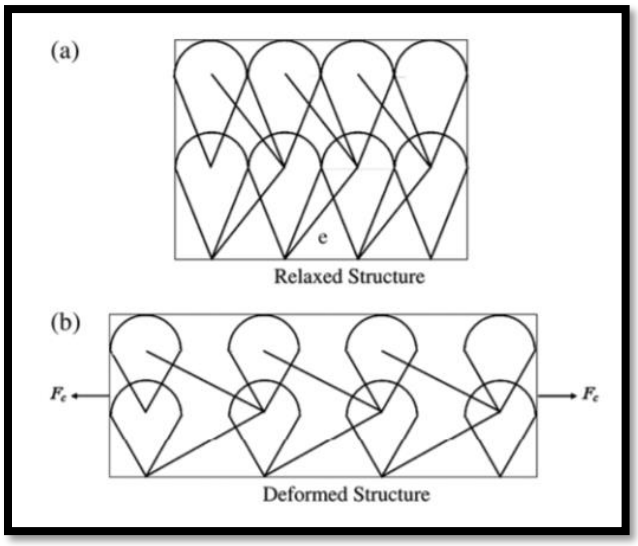

Figure 52: Distortion of wrap knitted constructions, (a) relaxed construction, (b) distort construction (Dabiryan & Jeddi, 2012)

Dabiryan and Jeddi concluded their study by saying that geometrical limits such as fabric density, length of underlaps, and course spacing affect the results of the experimental and theoretical model. Thus, this model could not precisely predict the Poisson's ratio, but the results showed that the produced models provide a probable guideline for the Poisson's ratio of warp-knitted fabrics.

This series of studies by the same investigators included a 5-part examination of the analysis of warp-knitted constructions for both simple and complex structures of fabrics. From these studies, we can summarise the affected parameters of the knitted fabric as the initial modulus, Poisson's ratio, friction between yarns, density, and construction of warp-knitted fabrics that affect their elastic behaviour. All these parameters identified by the researchers were very useful to the current project, as mechanical parameters affect the behaviour of the fabric under extension.

2.8 Energy Method

The energy method which is used in developing mechanical models is based on equations representing the strain or stress, of the material or the strain or displacement or deformation of the way stresses, material properties, and external loads in terms of energy done by external forces.

These associations offer a proper and alternate approach to derive the determining formulas for deformed bodies in solid mechanics due to energy being a scalar quantity. For complex systems, energy methods can obtain approximate solutions while exceeding the challenging function of resolving the sets of partial differential formulas. For these reasons, in the current project, the energy method was chosen to model the fabric's behaviours mathematically by using an equation relating different kinds of energies, such as strain, gravity, bending, torsion, and friction energy. The basic underlying principle is that a system will try to configure itself to minimise its potential energy at any equilibrium state.

This section presents other works based on the principles of this method for different fabric structures.

2.8.1 Energy Model for a Fabric Loop and Structure

A new mathematical model created by K. F. Choi and Lo (2003) describes a plain knitted fabric focusing on the loop energy. Knitted cotton fabrics are common and are extremely fundamental for textile manufacturing. Because of the way knitted fabrics were produced, the yarn was under elevated extension and stress. After washing and drying, the fabric may undergo increased extension and stress owing to shrinkage. This is the result of fabric contraction and reduction in size during cycling. Hence, when the fabric is stretched or put under tension, it may experience heightened extension and stress owing to residual shrinkage effects. A theoretical model can be used to guide the success of the relaxation procedure.

Depending on the focus of the energy investigation, the energy method can be used to examine specific aspects of the mechanical features of plain knitted fabric, such as low stress and measurements. An important property of this model is the natural curvature of the yarn

(the logical curvature is explained as a curvature of a course for yarn when taken out from the knitted fabric without establishing any distortion to the yarn). The approach can furthermore account for the nonlinear mechanical properties of the plain knit. This model can also be utilised to determine the biaxial tensile behaviour of the plain knitted fabric.

To define the loop geometry of a recent model, it is critical to research the features of knit fabrics. In this model, K. F. Choi and Lo (2003) considered that the loop geometry must have satisfactory degrees of freedom to permit the fabric to be configured with a near estimation of the real loop form. The right-hand orthogonal axes (xyz) are adapted,$x-axis$ in the course orientation,$y-axis$ $z-axis$ perpendicular to the fabric plane, as illustrated in Figure 53. A polynomial was used to explain the yarn form.

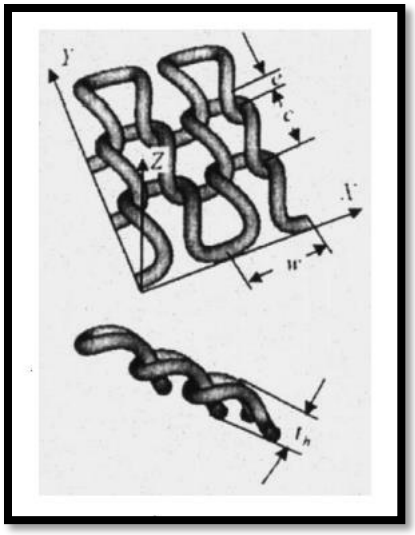

Figure 53: Geometry of the plain-knitted model (K. F. Choi & Lo, 2003)

K. F. Choi and Lo's (2003) model is based on the realisation that the degree of the knitted fabric yarn's set has a substantial effect on the fabric's dimensional stability and, therefore, on the reference situation. The yarn torsion and normal curvature can be represented as functions of the curve length.

The overall mechanical energy was estimated based on the dissimilarity in the yarn torsion strain and bending strain with respect to the torsion and natural curvature. In addition, the authors noted that the fact that the fabric yarn is partly grouped must not be neglected, and only when this parameter is considered can the measurement behaviour of a plain knit construction be comprehended.

The bending stiffness of the fabric is one of the most fundamental factors affecting the relaxation and handling of garments. Ajeli et al. (2009) explained the warp knitted fabric's bending stiffness as an outcome of density (wale and course distance), the knit construction (underlaps length), and yarn bending features. Their research considered seven standard warp-knitted fabrics produced with three different densities (three & four needles satin, reverse locknit, tricot, three and four needles sharkskin, and locknit). The organisational model for the bending characteristics of the warp-knitted fabric's complete interlacing set, including two guide rods, was validated in the study. The results suggest that the method was unsuccessfully implemented using empirical data.

The course-wise and wale-wise bending stiffness of the fabrics were measured using a Kawabata evaluation system (KES-FB-2), as mentioned in the papers above (NC State University, 2021), and an Automatic Cyclic Bending Tester (ACBT). In the Kawabata approach, the sample curves to a particular bend (the bending can change constantly), and the association between the curvature and bending moment is predicted.

In the second approach, the Automatic Cyclic Bending Tester (ACBT) progressively applies a bending moment to the fabric sample while measuring its curvature. the results demonstrated a strong correlation between the two empirical methods used in Ajeli et al.'s (2009) study, (KES-FB-2 and ACBT) validating their effectiveness in evaluating the bending properties of fabrics, the (KES-FB-2 and ACBT), wale-wise and course-wise relationship illustrated in

Figure *54* and Figure 55.

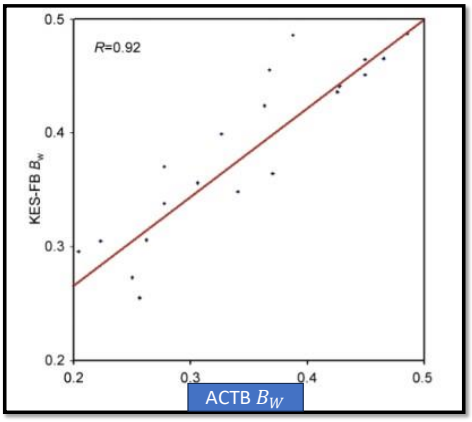

Figure 54: Wale-wise relationship of ACBT and KES variable (Ajeli, Jeddi, Rastgo, et al., 2009)

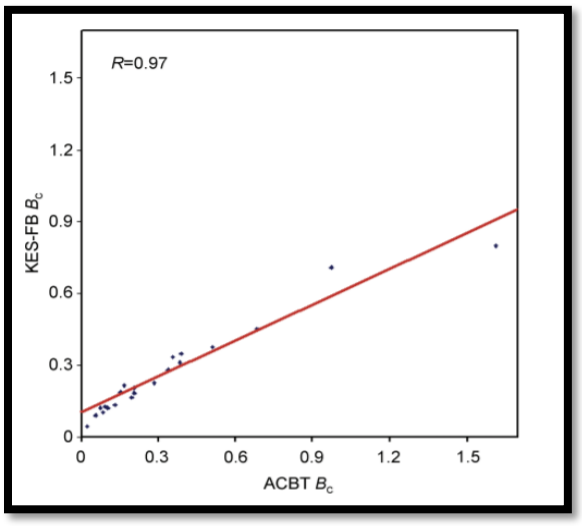

Figure 55: Course-wise relationship of ACBT and KES variable (Ajeli, Jeddi, Rastgo, et al., 2009)

In the theoretical analysis, the warp-knitted loop is supposed to contain a sequence of straight elastic lines and inclined yarns in a plane. The bending stiffness of the warp-knitted fabric is the total amount of bending impedance of the restricted yarn along the bending direction.

Ajeli et al. (2009) concluded the research by demonstrating the experimental modelling result that showed that the influence of the fabric construction on the bending stiffness in the course orientation is much more critical than that in the wale orientation, but it is identified by the density of the fabric in both the course and wale orientations. Theoretically, the model accurately predicts and evaluates the bending rigidity and densities for every structure in the wale orientation.

2.8.2 Energy Method for Fabric Unit Cell

The energy method was developed to determine a method which can be employed uniformly for a variety of fabric constructions and types of deformation. Hearle and Shanahan (1978) introduced the energy approach as a straightforward method to study fabric construction. They described it as a load-bearing system, where changes in internal energy due to deformation are negligible compared to changes in potential energy caused by externally applied stress. Then, they extended the method to include the influence of strain energy in the yarns and fibres that constitute the fabric. This method is particularly suitable for knitted, woven, and other fabrics with repeated unit cells (RUC) and can also applied to informal nonwoven fabrics, where the entire sample acts as the unit cell.

The method predicts the fabric's behaviour under forces significant enough to overcome bending resistance, allowing the yarns to follow shorter, constrained paths with nearly linear slack lengths and adjacent interactions. It assumes that the forces are sufficient to render yarn extension negligible.

The investigators concluded this part of their research by presenting a method designed for ideal fabrics, where energy changes associated with yarn or fibre distortion are negligible. This method predicts the fabric's behaviour under forces substantial enough to overcome bending resistance but small enough that yarn extension can be discharged. As a result, this approach associates any geometrical model of the fabric, which has been suggested to be the ratio of the

established moment and forces. Next, this approach is expanded to more applicable issues involving the strain energy where the yarn and fibres deform.

In the following section of this series by Shanahan and Hearle (1978), the technique of energy is applied to woven fabrics, especially to different plain-weave fabric models subjected to tension. Some woven-fabric construction models are utilised to investigate how the energy approach allows for the incorporation of multiple mechanical effects.

The effects considered in this model are as follows:

- The construction acts exactly as a load-behaviour technique, which means no material deformation.
- Distortion occurs by curling when completely unstretched flexible yarn is used in the process.
- Yarn extension is permitted as a deformation technique.
- Yarn impedance to bending was examined.

The researchers concluded the study by showing how the energy approach can be employed to address issues of load-deformation behaviour for woven fabric construction. According to these geometric models, the energy approach can be applied routinely to different fabric structures and distortion procedures. The automatic methods utilised to back the energy approach take over more of the encumbrance of habitual processing and computation and allow the user of arithmetic methods a more realistic and flexible approach to devising and modifying complexity. The yarn cross-section allows for noncircular shapes by incorporating flattening factors (the ratio of major/minor yarn diameter) kept constant, as shown in Figure 56. A more realistic model is necessary to balance bending and flattening energies. In this model, the

curling decreases according to the yarn and surfacing process reduction in the yarn curvature and bending energy.

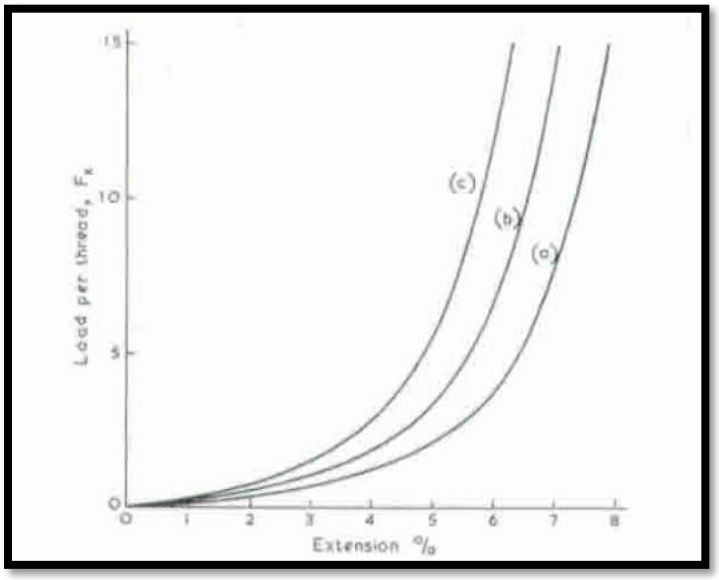

Figure 56: Yarn cross-section as an oval or fattened shape for the plain-weave fabric, showing the different fixed fattening factors that influence uniaxial load-extension curves (Shanahan & Hearle, 1978)

The mechanical features of yarns have a significant influence on the procedure behaviour and functional characteristics of fabrics and yarns. The yarn characteristics, especially the torsional and tensile yarn features, instantly affect their buckled distribution, inclination to snarl, strength, knittability, and yarn buckling variability. In a study by Liu et al. (2007), a comprehensive model was developed using bulky wool single yarns (single strands of yarn) to obtain the torsional and tensile behaviour of a single yarn. The energy approach was employed to estimate the employed force on the yarn, and the tension of the fibre was calculated and compared with the collaboration of the employed force according to the bending and tension

of the fibre. By conserving the fibre's nonlinear behaviour on the significant strain, the entire force deformation bend of an individual yarn can be expected on the minor strain.

Some assumptions for single yarns were made to predict the mechanical response:

- The yarn was cylindrical and had a well-specified surface.
- All fibres have a perfect geometrical (central, helical) shape and are uniform along their length.
- The fibres were assumed to distort without modifying their size.
- The stress-strain features of the fibre in the yarn were assumed to be similar when they were examined individually. The effects of time were discarded.
- The length of the examined scale is short; thus, fibre relocation and fibre sliding can be disregarded.

Prior tension must be applied to the yarn to prevent buckling. The yarn is attributed to two independent freedoms, one of which is elongation freedom, and the other is rotational freedom. The reorientation of fibres during deformation and their ultimate positions post-deformation are governed by the imperative to minimise tensile strain, which is known as the shortest path hypothesis. The fibres can shift readily in the lateral direction to prevent expansion until they are restricted by other fibres. The fibres that cannot shift further horizontally are termed jammed (Figure 57).

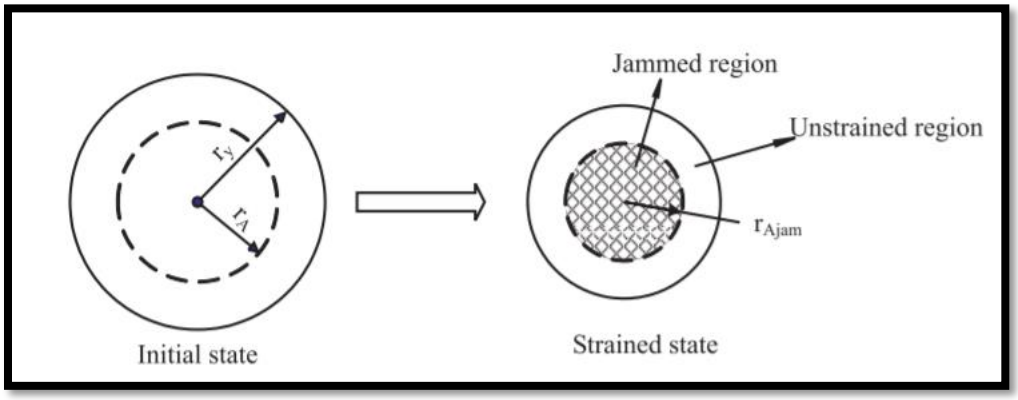

Figure 57: Before and after deformation of yarn and its effect on its cross section (T. Liu et al., 2007)

The energy method relevance of the outer force applied to the yarn is the buffered yarn energy. If the yarn is not all jammed and the distorted yarn can be split into two sections: the jammed area, its position at the centre and the unstrained area, and its position outside the jammed area. This part should be regarded individually in the yarn-energy computation.

In the experimental setup, a series of fibres extracted from both wool and woollen-weave mat yarns were employed to assess the proposed theory. The yarn and fibre dimensions were determined using projection microscopy, while the curvature of the yarn was scrutinised using a bend examiner.

As a result, the combination of yarn and fibre tension was demonstrated to be higher than the summation of the combinations of fibre bending and torsion in the study (T. Liu et al., 2007). All three combinations were fundamental to the torsional model when the prior tension was slightly proportional. The investigators concluded the study by showing that the combinations of fibre torsion and bending to the moment of yarn were discarded, and the prediction agreed satisfactorily with the experimental value.

Generally, the expectations of tensile and torsion were determined to establish appropriately, with empirical values predicted from the yarns of bulky wool, where the original fibre-wrapping density is asymmetrical (Figure 58).

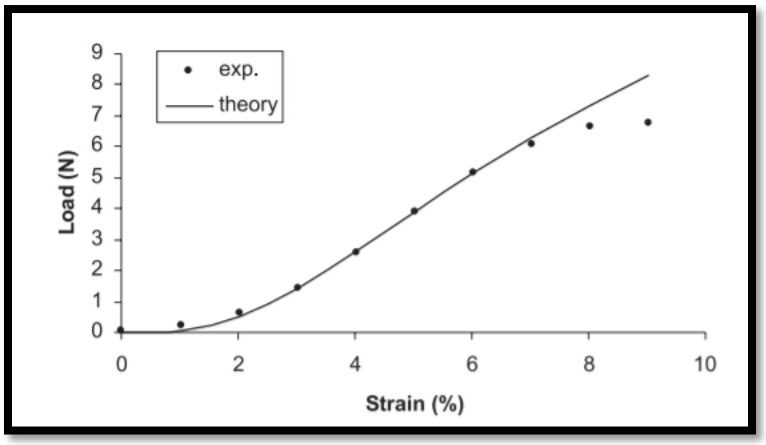

Figure 58: Load-strain curves of individual yarns (T. Liu et al., 2007)

A different yarn's bending energy model was described by K. F. Choi and Tandon (2006). A clear yarn-bending model was established with the initiation of two stages of freedom: fibre self-de-twisting and speed variation of the rotating vector. The torsion and bending energies of the fibres were considered.

One convenient way to identify the fibre geometry in a distorted yarn is to utilise the rotating vector (Figure 59). Theoretically, torsion is more complicated to handle than bending when the bend is zero at specific points, and torsion becomes unrecognised at these points.

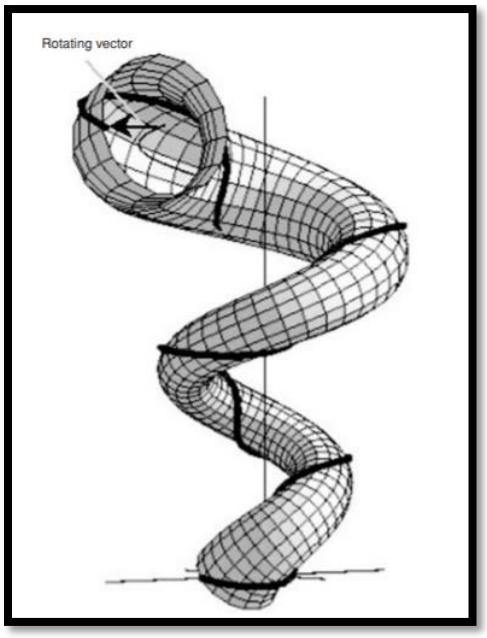

Figure 59: Path of fibre (K. F. Choi & Tandon, 2006)

The assumptions considered in this model are as follows:

- The fibre torsional and bending stiffnesses were linear.
- The fibre was unstretched.
- Fibre paths are space curves on the surface of a circular torus at any bending state of the yarn.
- The inter-fibre friction was zero.

Experiments were conducted using a KES-F bending tester. During the test, all 64 yarns were placed parallel to one another. In this model, the bending hysteresis curve was plotted as an input, with the bending curve of the yarn as a model output. The experimental data for the bending moment were larger than the hypothetical data. It was thought that this was because the model assumed that all the fibre helices could set their fibre ways openly and self-de-twist openly.

The investigators finished the study by considering that the model precisely obtained a linear correlation between the curvature and bending moment of the yarn. A reasonable

correspondence was identified between the experiment and the hypothesis. The bending features of a single yarn are dissimilar from those of the woven fabric because the friction feature of the yarn varies fundamentally after being woven into the fabric. The state is very complicated for knitted fabrics because the yarn in a knitted fabric does not curve as it would in a free, individual state outside of the fabric.

Choi & Lo (2006) proposed a mechanical model for knitted fabric, suggesting that the loop shape changes based on the yarn's twist 'liveliness.' This model accounted for loop curving, resulting in an asymmetrical loop configuration as observed on the fabric's front side. When viewing the loop from the topside, the fabric construction's minimal energy condition also involves the loop's freedom to curve out of the fabric, resulting in rippled loops.

The geometry of the loop should have adequate degrees of freedom to permit the fabric to be distorted approximately near the form of the knitted fabric loops (Figure 60). The right-hand orthogonal (xyz) axis was adopted with the $x\ axis$ in the orientation of the course, the $y\ axis$ in the orientation of the wale and the $z\ axis$ in the orientation perpendicular to the central plane of the fabric. The loops moved freely in the moveable fabric. They can twist in both the orientations of $z\ axis$ and the $y\ axis$ and twisting in the z orientation is the generally known phenomenon of fabric spirality. The twisting of the loop in the y orientation did not influence the total fabric measurements.

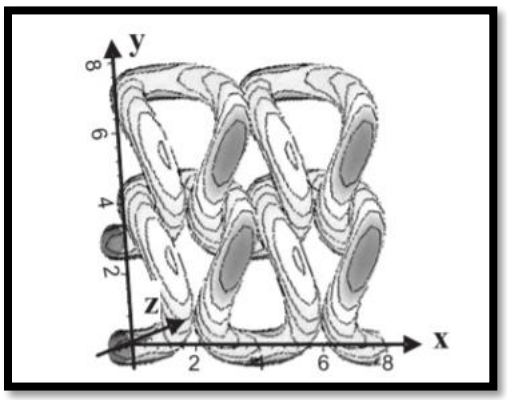

Figure 60: Wavy loop (K. F. Choi & Lo, 2006)

The mechanical energy of the loop incorporates the bending, torsional, and tensile energies. The yarn characteristics requested by the hypothetical fabric model included torsional stiffness, bending stiffness, initial tensile modulus, yarn diameter, and residual torsional strain. For the experimental model of the fabric, a set of plain knitted fabrics of wool yarn was manufactured using a machine with a small-diameter cylinder called Lawson Hemphill Fak. The validity of the experimental model was illustrated by three basic fabric requirements: wale distance, course distance, and wale spirality. The experimental data were split into two groups: one in a wet-relaxed or fully relaxed situation and the other in a dry-relaxed situation.

Choi & Lo (2006) distinguished their model from others in the following ways.:

- The structure energy computation and original configuration of the yarn are nonlinear.

- Instead of assuming loop symmetry, the model considers the inherent spiral nature that results from the variable and irregular shapes of the fabric loops.
- The loop motion of the third dimension located outside the plane was defined as a significant relaxation technique.
- Wale circularity is a result of yarn bending, torsional stiffness, and twisting energy.

The investigators concluded the hypothetical exploration by demonstrating that wale circularity can be influenced by the tightness of the fabric as well as the loop form key, and experimental observations reinforced this conclusion. Fabric measurements can be obtained using this mechanical model, and the length of the fabric in a completely relaxed situation can be computed with perfect accuracy. The precision of the predictions is specified by keys involving the measurement of the yarn's mechanical features, such as the bending, torsion, and tensile models which are neither straight nor associated with each other. The empirical outcomes demonstrated perfect agreement between the theoretical and experimental data for circularity and course distance.

2.9 Particle image velocimetry (PIV)

Particle image velocimetry determines the speed of images (pictures and movies). Usually, this method is used to calculate the velocities of the fluids. However, there are many other

applications. In this thesis, PIV was used to process and analyse textile images to calculate the velocity and strain.

2.9.1 Applications of PIV in Textile Research

Few studies have investigated the use of the PIV method to analyze images in the textile field. The most relevant are geo-textiles.

Plastic polymer materials, also called "geosynthetics", are employed in a variety of geotechnical implementations. An experimental method based on image analysis was applied to identify the strain distribution in different geosynthetics across a range of tensile tests. Guler Murat (2004) presented a technique that utilised a block-based identical algorithm employing LABVIEW. The estimated overall values of the strain were compared with those obtained from the scales of the strain and extensometers. Strain data found by these techniques were competitive with image-based data, and the ultimate value of the variance was lower than 10% of the geosynthetics examined. Guler Murat (2004) concluded the study by showing that new scientific progress in the investigation of images has introduced substantial possibilities for more precise and contactless techniques to identify strains. The PIVLab software was employed for image processing during the tensile test. PIVLab enables to visualization of strain and velocity fields, represented through converging and diverging arrows, providing valuable insights into the material's deformation behaviour

Jones (2000) processed numeric images of three geo-textiles in wide-width tensile tests and exploited them to determine the displacement. This method, called video extensometer, estimates the strain by following two contradictory paths laid on the sample. To identify the lens, a calibration procedure was required to calculate the view of the visual field. The geotextiles were examined with this instrument and cross-instrument directions and exclusions were estimated using a traditional straight contact extensometer and contactless image-based video extensometer methods. The results demonstrated that the image-based system for estimating displacement had an accuracy in the range of 86%-100% respective to the extensometer.

S.R. Mishra, et al. (2016) demonstrated the use of the particle image velocimetry (PIV) method to imagine the localized strains advanced within the wide-width tensile testing of non-woven geotextiles.

A wide-width tensile test was performed on a 200 mm × 200 mm polypropylene nonwoven geotextile. The plain white fabric did not generate sufficient variation to follow the strain; therefore, black plastic paint was sprayed randomly to accomplish the requested spot pattern important for the image procedure. The sample was held between the two jaws of the hydraulic clamps (Figure 61), with a length of scale of 100 mm and clamp pressure of 150 kg/cm^2. . The average strain of 10 mm per minute was applied to the sample. Images were processed using a still numeric camera at 3-second intervals. In this investigation, an individual lens reflex numeric camera was used, where the field of view was separated into a maximum of 6000 pixels for the horizontal field and 4000 pixels for the vertical field.

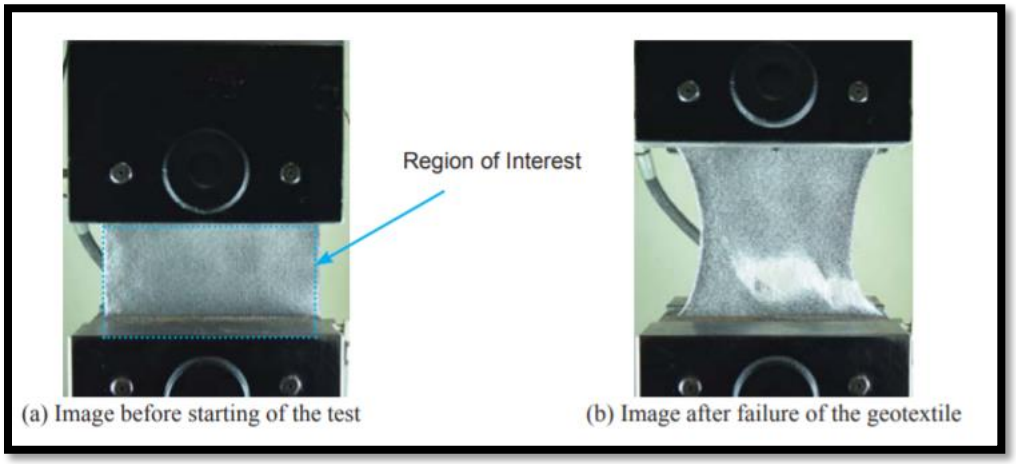

Figure 61: Non-woven geotextile clamped in the hydraulic grip (S.R. Mishra, et al, 2016)

Figure 62 shows a plot of the strain and stress of the sample from the wide-width tensile testing. Although the sample fails at a strain level of approximately 60% (measured from the movement of the crosshead), this number fails to consider the localised strains advanced in the sample.

The conclusion is that the longitudinal strain predicted from the crosshead movement within a tensile test does not represent the real strain advance in the sample. The localized strain can be determined through image procedure methods involving open-source analysis software and cost-effective hardware.

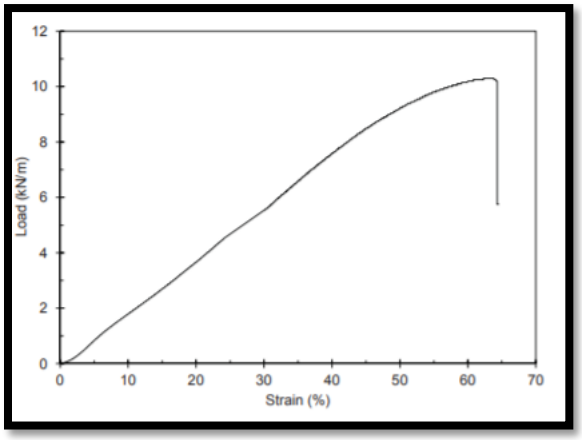

Figure 62: Wide width tensile exam, load with strain sketch (S.R. Mishra, et al, 2016)

In the research presented in this thesis, PIV was used to analyze videos of testing textiles to show local strains in the textile.

2.10 Summary

Several major methods have been employed in mechanical testing to obtain the mechanical behavior of knitted fabrics. These issues were discussed in detail in this review. Nocent et al. (2001) introduced a new method of testing the mechanical behavior of knitted fabrics that consisted of the reduction of knitted cloth parameter numbers, which led to a mechanical level of detail suitable for dynamic animation. A different approach instead sought to understand the contact areas in the knitted structures of different yarn types and focused on the knitted fabric

under tensile and shearing loading by presenting a numerical structure model (Chen et al., 2013). The other mechanical modelling discussed is the finite element method (FEM) that was designed to simulate the stress-strain bend digitally in the wale and course trends (Sharma & Sutcliffe, 2004) and an examination of the fabric testing of both biaxial tension and in-plane shear parameters (Vassiliadis & Savvas, 2007). The final approach introduced in this chapter was the Kawabata Evaluation System of Fabric (KES-F), which is a technique used to measure the properties of textile materials. Kawabata tools identify the position played by shear stiffness (drape), bending rigidity, compression, tensile (stretch), flexing, softness, roughness (close to the skin), surface friction, and thickness.

The review further discussed how the mathematical and mechanical modelling represented by the energy method were reported by some papers that describe plain knitted fabrics with a focus on the energy model of a loop (Ajeli et al., 2009;Choi & Tandon, 2006). Studies that have developed the energy method for variations in potential energy due to the external load and the effect of strain energy in the component yarn fibres in the unit cell were also presented (Hearle & Shanahan, 1978).

This chapter discussed the phenomena that occur in textiles during tensile testing, such as curling (Go & Shinohara, 1959; Kurbak & Ekmen, 2008a; Ucar, 2000a; and bending rigidity (Phukan & Subramaniam, 1995). The discussion highlighted the fabric's ability to recover from bending. It referred to the studies included here to examine textile behaviors such as textile and curling distance, how to prevent curling, curling a couple of moments, and relaxation time of curling. In addition, the buckling phenomenon, which is a weft dynamic malformation within stuffing placement, was modelled as an uncoordinated dynamic deformation (Dabiryan et al., 2013).

Knitted fabrics get their unique qualities from how the yarns are arranged. In weft knitting, the loops are created in a zigzag pattern, allowing each needle to work with its yarn independently. This method gives the fabric a stretchy quality. On the other hand, warp knitting creates loops in the length of the fabric, leading to a different structure and performance. Warp-knitted fabrics are generally more stable and less likely to unravel than weft-knitted ones.

Concerning the energy method, some mechanical properties of textiles have been described theoretically and experimentally (Dabiryan & Jeddi, 2012; Dabiryan et al., 2012a, 2012b) for warp-knitted fabrics. Understanding the differences between warp and weft knitted textiles is essential to improve their mechanical properties and overall effectiveness. By understanding the effects of the type of yarn, fabric variables, and fabric formation on the initial modulus and flexibility of knitted fabrics, manufacturers and designers can make informed decisions when selecting materials and creating product designs. This understanding could lead to the development of textiles with enhanced durability, comfort, and functionality. Additionally, using the energy approach to analyze and model the mechanical properties of textiles can provide valuable insights for optimizing the performance of knitted fabrics.

Finally, this chapter discussed PIV (particle image velocimetry). The use of PIV in analysing textiles is still relatively limited, but there is potential for its application in various textile-related fields. The study of geo-textiles can provide valuable insights and methodologies that can be adapted to other textile materials. It would be beneficial to explore the potential applications of PIV in analysing the behaviour of different types of textiles under various conditions and loads. This could lead to advancements in the understanding and optimising textile performance in different applications. Further research in this area could be valuable for the textile industry.

Chapter 3 Experimental Testing

3.1 Introduction

The third chapter of this thesis describes the techniques used for the experimental investigation of tensile strain effects on different yarns and textile samples. The data collected from these experiments was then compared with the predictions of the proposed theoretical model for each sample to assess the accuracy of the theoretical model.

This section describes the testing of three different knitted fabric samples (silver, stainless steel, and polyester) and, for comparison, a rubber sheet. The behavior of each fabric sample was measured under the same conditions using a texture analyzer. Each sample was stretched between two clamps on the top and bottom edges. The texture analyser machine recorded the force, axial strain, and test speed for each sample. In some cases, the video information was further processed using PIV to obtain data on the local strain and velocity.

The chapter outline consists of the following sections:

Equipment and Setup

- Description of texture analyser machine and its specifications.
- Explanation of the clamp arrangement and sample placement.

Sample Preparation

- Details on how the knitted fabric samples and rubber sheet were prepared.
- Dimensions, material specification of the testing protocol for all samples.

Testing Procedure

- Step by step explanation of the testing protocol for all samples.
- Parameters recorded: axial strain, and test speed.
- Application of controlled strain and measurement protocols.

Particle Image Velocimetry (PIV) Analysis

- Explanation of how PIV used to obtain local strain and velocity data.
- Video processing and image analysis techniques to capture dynamic behaviour.

Results and Observations

- Comparative analysis of the mechanical properties (strain-force relationship) across materials.
- Behaviour of different materials under low and high strain conditions.
- Key findings from PIV analysis, highlighting unique deformation patterns.

Summery

- Recap of key findings from experiments.
- Insights gained regarding the suitability of the materials from smart textile applications.

3.2 Equipment

Tensile tests were performed using a texture analyser (T.A.XT. PLUS, Stable Micro Systems, Texture Analyser, Serial No. 42123, Godalming), an example of which is shown in Figure 63. A texture analyser is commonly employed to measure and quantify compression and tension by applying force and measuring the displacement. The texture analyser has an operating range suitable for these tests (force capacity: 500 N, force accuracy: 0.1 g, speed

range: 0.1-400 mm/s). The system provides full control of the speed range and applied strain and can save the result to a computer for further analysis.

The texture analyser was enhanced by the inclusion of a video capture and synchronisation system. This innovative addition meant that the testing process could be video-recorded. By incorporating this system, it is possible to perform a meticulous analysis of the optical response on a frame-by-frame basis. This feature allows for the mapping of visual recordings to their corresponding force-strain-time readings in real-time. The data gathered through the system were addressed using the Exponent Connect Software provided with the texture analyser.

As the device begins gathering data, the video-capture function is activated. The camera is typically mounted on the side for most applications, offering a side view. the mounting points for the texture analyser's camera are positioned at the base, as illustrated in Figure 63 below.

Figure 63: Texture analyser machine with camera (Scanco, 2018)

3.3 The Sample Collection

Various samples were tested in the present study. The samples varied by choice of conductive and non-conductive yarn used, tubular or flat geometry, method of construction, size of the patch in terms of the number of courses and wales, and surrounding base fabric. All knitted samples in this project were constructed using a Shima Seiki Digital Knitting Machine.

3.3.1 Process of Making the Samples

Shima Seiki's digital programming and knitting allowed for control over the knitted fabric through the adaption of stitch length, stitch structure, the gauge of the machine, and yarn density. These textile structures were programmed and drawn on the Apex 3 Design System using Knit Paint before being knitted using a SIG 123SV intarsia machine. This machine was used to knit both flat and tubular structures.

The plain flat knit structure was produced using a 14-gauge machine, which creates a relatively fine and detailed knit. This level of precision makes it ideal for applications requiring smoothness and accuracy, such as smart textiles or lightweight garments. In knitting, gauge refers to some needles per inch on the needle bed of the knitted machine as can be seen in Figure 64 (A).

The cylindrical knit structure is known as a tubular knit fabric, which is a unique way of constructing a fabric that creates a circular tube shape rather than a traditional rectangular shape. This technique is ideal for creating seamless clothing items, such as socks, leggings, and sleeves. Not only does it provide a sleek and seamless appearance, but it also allows for stretching and comfort in figure-hugging garments.

The tubular knit fabric was also produced using a 14-gauge knitting machine. The machine features two needle beds: a front bed and a rear bed, arranged in a “V” configuration. Figure 64 (B) shows flat and tubular knitted samples made for this research.

In circular knitting machines, the fabric is formed continuously in a ring-shaped layout using a single needle bed. In contrast, flat knitting machines create tubular structures by alternately

knitting courses across the front and rear needle beds. This process also produces a continuous tubular fabric but with the orientations of the fabric differing between the two beds. Specifically, the stitches formed on one bed face the opposite direction to those formed on the other, resulting in a reversed orientation between the beds.

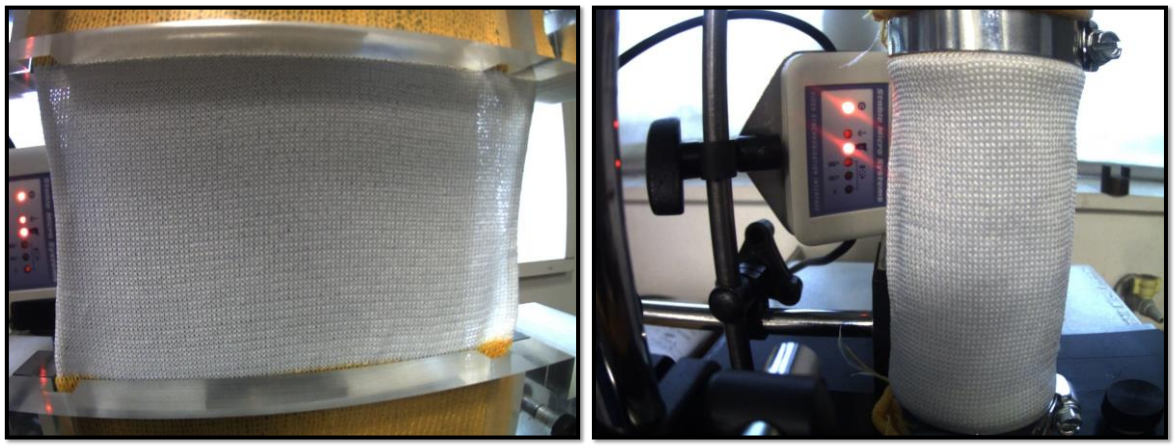

(A) Flat knit structure

(B)Tubular knit structure

Figure 64: Actual fabric sample used in this study

Figure 65, shows a digital rendering of the tubular knit fabric created for this project in the university laboratory using the Shima Seiki SIG123SV knitting machine. While not a photograph of the physical fabric, the image illustrates the programmed knitting pattern as set up on the machine.

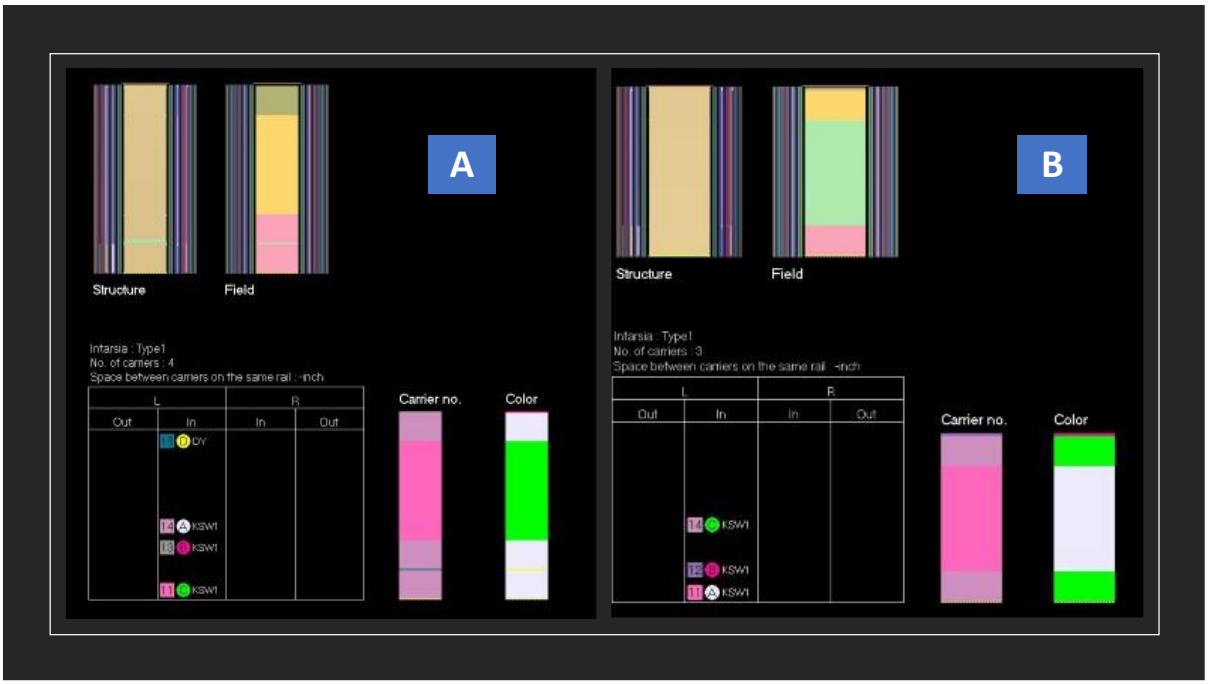

Figure 65: (A, and B) Digital knitting programming for the flat samples

The following steps were taken to prepare the fabrics for testing: First, a machine was used to remove the silicon wax that had been applied during the knitting process. After that, the fabrics were steamed to make sure they were in the best possible condition for testing. Then, the samples were allowed to relax for 3 or 4 days before the tests were conducted.

It is interesting to note that there was not a marked difference in the test results for fabrics before and after resting. This suggests that the relaxation process did not have a marked impact on how the fabric behaved during testing. This could mean that the fabric's mechanical properties were not greatly influenced by the relaxation treatment. This behavior was not anticipated and as such raises questions about how the fabric responds to different treatments that warrant further exploration.

3.3.2 Yarns

The textile samples for this project were knitted using silver-coated nylon, 80/20 polyester /stainless steel, and polyester yarns with or without Lycra®. Lycra is elastane, or spandex, which is an artificial fibre noted for its extraordinary stretchability and recovery. For this project, I chose different yarn materials because material features such as stainless steel have high tensile strength, are easy to format and fabricate, and are temperature resistant. Silver material stands out as a superior choice, boasting impeccable properties such as ease of fabrication, easy machinability, and environmental resistance; when a load is applied to silver, it can be stretched without failure or plastic deformation. For the polyester material, the properties are represented by showing that the polyester fibre has good elasticity and wrinkle resistance and easily returns to its original shape after removing the load. Table 1 lists the yarn properties.

These materials were chosen to represent a variety of conductive and non-conductive options, allowing for a comprehensive examination of how different yarns influence the mechanical characteristics of knitted fabrics.

Table 1: Yarn properties.

Yarn material	**Linear density**	**Manufacturer**
80/20 polyester/Stainless Steel	400 dtex	Schoeller

Silver coated nylon (Shieldex)	303 dtex	Statex
Polyester without Lycra	165 dtex	Polyester unknown
Polyester with Lycra	248 dtex	Polyester unknown. Marulon from Marulontex

The linear density was related to the length and mass of the yarn. To determine the yarn length from the linear density of individual fibres and the weight of the fibres, the equation is as follows:

$$L_0 = \frac{wS}{d}$$	(1)

where L_0 is the yarn length (in meters), w is the fibre weight (in grams), S is the scaling factor listed in

Table 2, and d is the linear density of the fabric given in the corresponding units. Common units for linear density include Denier, tex (weight, in grams, per 1000 m length), and dtex, which stands for "decitex" (1 g per 10000 m) and is a smaller unit than tex that is usually used for fibres and filament yarns. The linear density, which is a measurement of the mass to the fibre's unit length, is employed by fibre manufacturers as a measure of fineness.

Table 2: Scaling factors for Denier, dtex, and tex systems

System	**Scaling factor (m/gram)**
Denier	9,000
dtex	10,000
Tex	1000

3.3.3 Test Samples

Table 3 lists all samples used in this project. Using a precision weigh scale (1219 MP, Sartorius Scale), the readability of the scale between ($1g$ and $0.1mg$), The mass of each knitted sample was measured, and the mass per stitch was calculated. Sample dimensions are given as the number of stitches in the course direction multiplied by the number of stitches in the wale direction. An additional margin of 20 courses of polyester was added to the top and bottom of each sample to be clamped by the texture analyser, as shown Figure 66 and Figure 67.

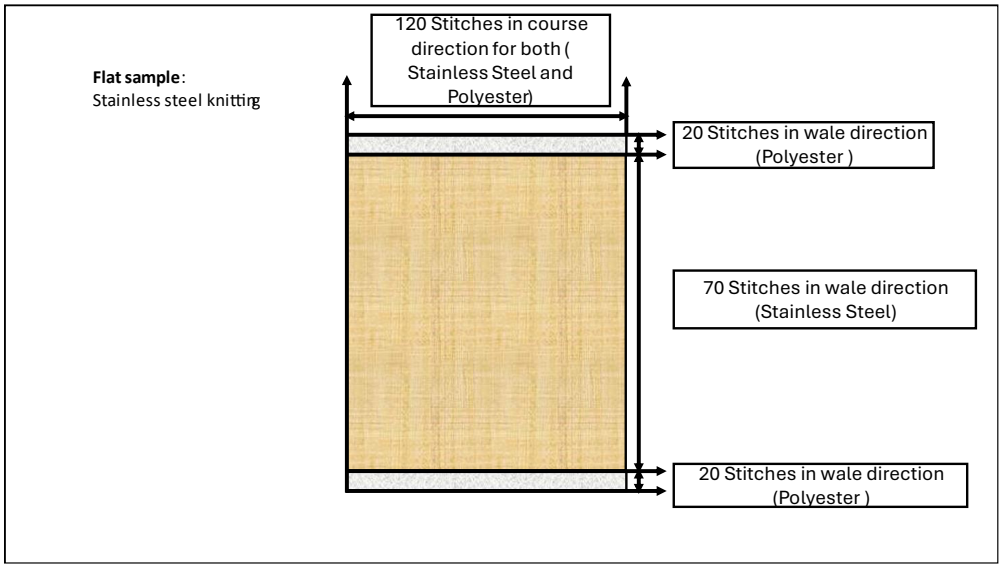

Figure 66: Diagram of sample SSNF4

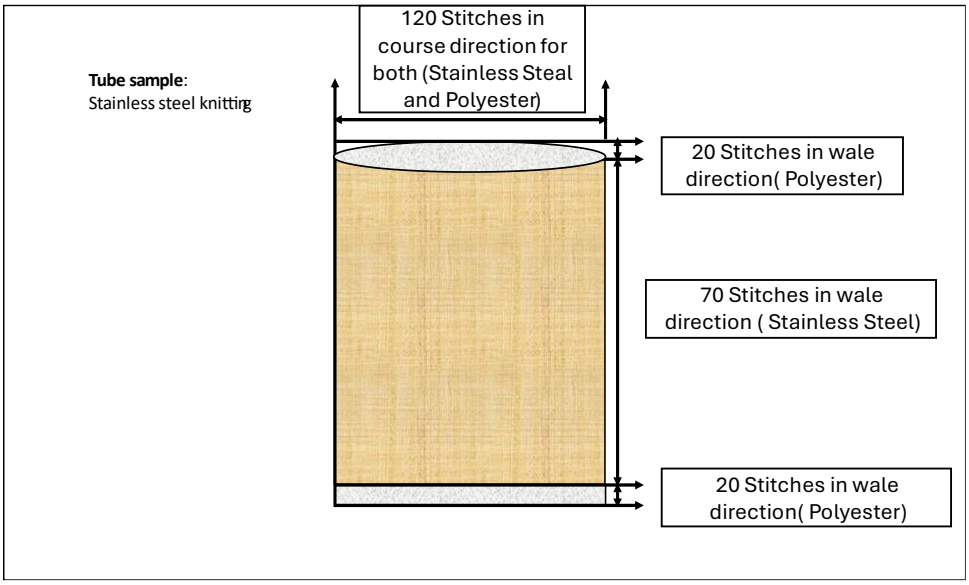

Figure 67: Diagram of sample SST1

Table 3: Sample materials and dimensions

ID	Knitted sample material	Dimensions (stitches) (wale X course)	Nominal dimensions (length X width) (mm)	Mass (gram)	Mass per stitch (grams)	Yarn length (m)	Fabric area density(g/m^2)
AGNF1	Silver coated nylon without wax	60 X 20	81.42 X 27.14	1.04	0.000867	42.4	470.59
AGNF2	Silver coated nylon without wax	70 X 20	94.99 X 27.14	1.88	0.00134	56.96	728.68
AGNF3	Silver coated nylon without wax	80 X 20	108.56 X 27.14	2.02	0.001263	61.21	684.75
AGNF4	Silver coated nylon without wax	60 X 30	81.42 X 40.71	1.20	0.000667	36.36	361.99
AGNF5	Silver coated nylon without wax	70 X 30	94.99 X 40.71	1.96	0.000933	59.39	506.46
AGNF6	Silver coated nylon without wax	80 X 30	108.56 X 40.71	2.10	0.000875	63.63	501.193
AGNF7	Silver coated nylon without wax	60 X 40	81.42 X 54.28	1.33	0.000813	40.30	270.88

AGNF8	Silver coated nylon without wax	70 X 40	94.99 X 54.28	2.09	0.00075	63.33	405.039
AGNF9	Silver coated nylon without wax	80 X 40	108.56 X 54.28	2.15	0.000672	65.15	833.33
AGWF1	Silver coated nylon with wax	60 X 40	81.42 X 54.28	1.45	0.0006	43.94	656.12
AGWF2	Silver coated nylon with wax	70 X 40	94.99 X 54.28	2.14	0.00076	64.84	414.73
AGWF3	Silver coated nylon with wax	80 X 40	108.56 X 54.28	2.30	0.000719	69.69	390.294
SSNF1	80/20 polyester/Stainless steel without wax	60 X 40	81.42 X 54.28	1.61	0.000671	64.40	364.253
SSNF2	80/20 polyester/ Stainless steel without wax	70 X 40	94.99 X 54.28	1.75	0.000625	70.0	339.15
SSNF3	80/20 polyester /Stainless steel without wax	80 X 40	108.56 X 54.28	1.91	0.0005969	76.40	324.113
SSLF4	80/20 polyester /Stainless steel flat sample with Lycra	120 X 70	162.84 X 94.99	5.25	0.000625	210	338.71
SSNF4	80/20 polyester /Stainless steel flat sample without Lycra	120 X 70	162.84 X 94.99	5.15	0.0006131	206	332.26
SSLT1	80/20 polyester /Stainless steel tube sample with Lycra	120 X 70	162.84 X 94.99	4.939	0.000588	197.56	318.65
SSNT1	80/20 polyester /Stainless steel tube sample without Lycra	120 X 70	162.84 X 94.99	4.820	0.000574	192.8	310.97
PELF1	Polyester flat sample with Lycra	120 X 70	162.84 X 94.99	5.26	0.000626	130.45	339.355
PENF1	Polyester flat sample without Lycra	120 X 70	162.84 X 94.99	5.20	0.000619	85.8	335.484
PELT1	Polyester tube sample with Lycra	120X70	162.84 X 94.99	4.94	0.0005881	122.512	159.355
PENT1	Polyester tube sample without Lycra	120X70	162.84 X 94.99	4.71	0.000561	77.72	151.935
PENF2	Polyester 160 mm	120 X 70	160 X 94.99	5.514	0.000656	90.981	362.77
PENF3	Polyester 150 mm	120 X 70	150 X 94.99	5.33	0.000635	87.95	374.04
PENF4	Polyester 140 mm	120 X 70	140 X 94.99	5.19	0.0006179	85.64	396.18
PENF5	Polyester flat 163 stitch	163 X 70	163 X 70	5.20	0.0004557 4	85.80	456.14
PENT2	Polyester tube	120 X 70	162.84 X 94.99	6.24	0.0007428 6	102.96	201.29
RUBF1	Rubber sample	N/A	163 X 70	13.17	N/A	N/A	1155.26

• *ID: Refers to the name of the sample, for example, AABCN where* the *first two letters are a shortening of the material, the third letter captures whether wax or Lycra was used (L= Lycra; W=Wax; N=No have Lycra and Wax). The fourth letter indicates whether the sample was flat (F) or tubular (T). Finally, the number indicates the version number of the same sample type.* • *Fabric area densiy (g/m^2): measures the weight of fabric over a one-square-meter area. It helps compare the heaviness and thickness of different fabrics, with higher values indicating thicker materials and lower values suggesting lighter ones. This standard is useful for selecting materials based on weight and properties in fashion and textiles.*		

In terms of knit structures, the study incorporated various stitch counts and knitting shapes, as listed in Table 3, to evaluate their impact on the overall behaviour of the textiles. Different stitch patterns and structures were utilised to create samples with exact features, such as flat and tubular configurations. The inclusion of Lycra in some samples aimed to introduce different mechanical properties, adding another dimension to the study of mechanical responses under strain.

Based on the findings from Wang et al. (2014a, 2014b) regarding the development of effective models for various samples, a configuration of 40 horizontal stitches and 70 vertical stitches was chosen as the optimal design. This specification was selected due to its superior performance, particularly in reducing the contact resistance of the interwoven conductive yarn under increasing tensile strain. This behaviour sets it apart from the other samples tested, making it the most suitable choice.

3.3.3.1 Silver Sample

Various silver samples were crafted with different stitch configurations and subsequently subjected to testing using a texture analyser. The silver yarn used in these samples was composed of silver-coated nylon, as shown in Table 1 above. Samples with configurations such as (40 × 70) AGNF8, (30 × 70) AGNF5, and (20 × 70) AGNF2 were knitted with conductive sliver yarn and included an additional 20 stitches at the top and bottom, made from polyester, to clamp the sample in place. Two types of silver yarns were tested, one with silicon wax and one without. Among these, the configuration with 40 stitches in the course direction and 70 stitches in the wale direction stood out as the most optimal.

3.3.3.2 Wax and Non-Wax Samples

Incorporating wax into pure fibres serves as a protective agent against biological and atmospheric factors. However, during the manufacturing process, this wax is often removed either intentionally or as a byproduct of treatments like scouring, bleaching, or mechanical processing. This removal can be deliberate to improve dye absorption, enhance fibre adhesion, or achieve a standardised texture. In other cases, it occurs unintentionally due to heat or mechanical stress. While this step is necessary for certain applications, it alters the absorbency and frictional properties of the fibres, leading to a loss of pliability, elasticity, and smoothness.

This modification, specifically the removal of wax, is imperative to meet the specific end-use requirements. Although artificial fibres are crucial for high-speed processes, the presence of silicone wax can affect the mechanical behaviour of knitted fabrics. Therefore, careful consideration is essential to balance the advantages of artificial fibres with the effects of silicon wax on the overall performance of the textile. Two distinct types of yarns were used in this study: silver yarn, composed of silver-coated nylon, and stainless-steel yarn, consisting of 80% polyester and 20% stainless steel, as outlined in Table 1. Each yarn type is further categorised into two types: one treated with silicon wax and the other without.

3.3.3.3 Flat and Tube Samples

To evaluate the impact of the free edges during the tensile testing, two distinct sample shapes were prepared: a flat sample, illustrated in Figure 67, and a tubular sample, depicted in Figure 70.

3.3.3.4 Samples with and without Lycra

Lycra®, a trademarked name for elastic or polyurethane fibre, originally emerged as a polymer-based graft. Typically constituting 5-10% of fabric blends, Lycra® is commonly combined with other fibres to create stretchable fabrics, as garments made entirely of 100% Lycra® are relatively uncommon. The unique properties of Lycra include exceptional extensibility, reaching up to 400%, albeit at a higher cost compared to alternative fibres; notably, Lycra® exhibits a remarkable ability to stretch from to 5-8 times its original length and reverts to its initial state (Ray, 2012).

In general, Spandex is created using a polyurethane polymer containing polymer chains with microfiber grafts woven through it. These polymer grafts act as crosslinks connecting the polyurethane polymer chains. This grafted structure gives spandex its unique flexibility, stretch and recovery, shape retention, and fit characteristics that Lycra fibres are famous for (Kiron, 2014b).

In this project, I deliberately selected samples that incorporated Lycra for various reasons. Some of these choices were driven by commercial considerations, such as the desire for enhanced stretchability, freedom of movement, excellent recovery, elastic qualities, a broad range of motion, and reliable shape retention. Lycra, which has a smooth texture, exhibits high resistance to wrinkles and low moisture absorbency. The inclusion of Lycra in this project was specifically chosen to endow the specimens with superior recovery from mechanical deformation.

During the experimental phase of this study, a notable issue emerged with the initial reading of the texture analyser machine. this problem was characterised by a consistent discrepancy observed across multiple samples, especially during the comparison between the first and second reading in the test. The testing procedure involved applying a load to each sample and

repeating the test five times to ensure the reliability of the results. Strikingly, it was consistently observed that the curve of the first test was lower than that of the second and subsequent tests for materials both with and without Lycra. This deviation from the expected pattern is unusual, and a comprehensive search of existing research papers did not provide an explanation for this issue.

Conventionally, when applying strain to an object, the initial test is expected to demand the highest force, resulting in a relatively higher curve compared to subsequent tests. This fundamental principle was not observed in the experimental results. This observation became a crucial focal point in the experimental test, serving as a basis for comparing the behaviour of the two types of materials under the influence of tensile strain.

For the experimental model, two types of conductive yarns were used: stainless steel and silver. I decided to change the test from using silver to stainless steel because when I did the test, the first and second tests still showed the same trend; hence, I chose another conductive yarn to explore this problem.

The figures below show a flat sample made from stainless steel as the conductive knitting yarn, the former with Lycra Figure 68 and the other without in Figure 69. The subsequent two figures show the stainless steel tube samples represented by Figure 70 for the sample with Lycra and by Figure 71 for the sample without Lycra.

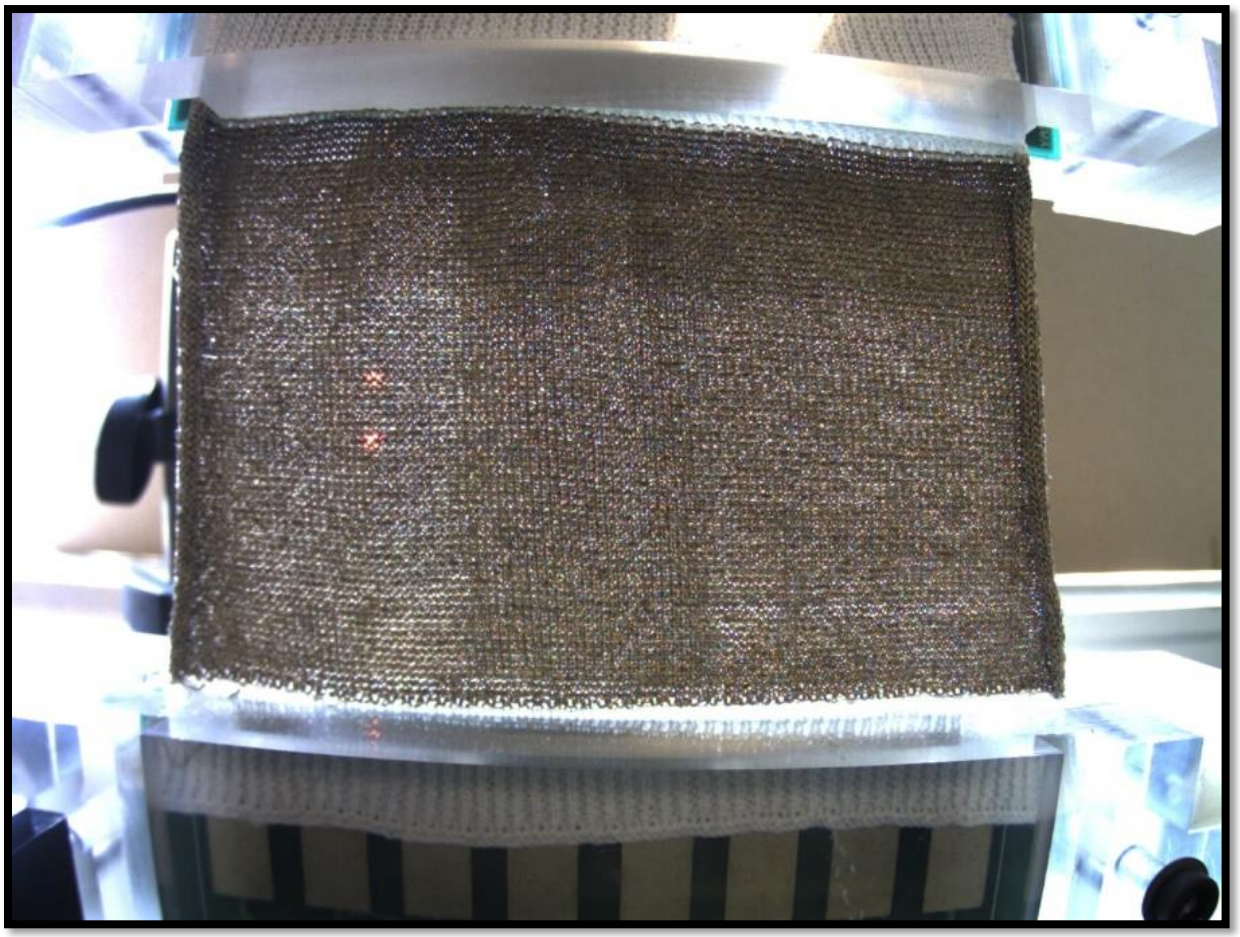

Figure 68: Stainless steel flat sample with Lycra in stretched case (SSLF4)

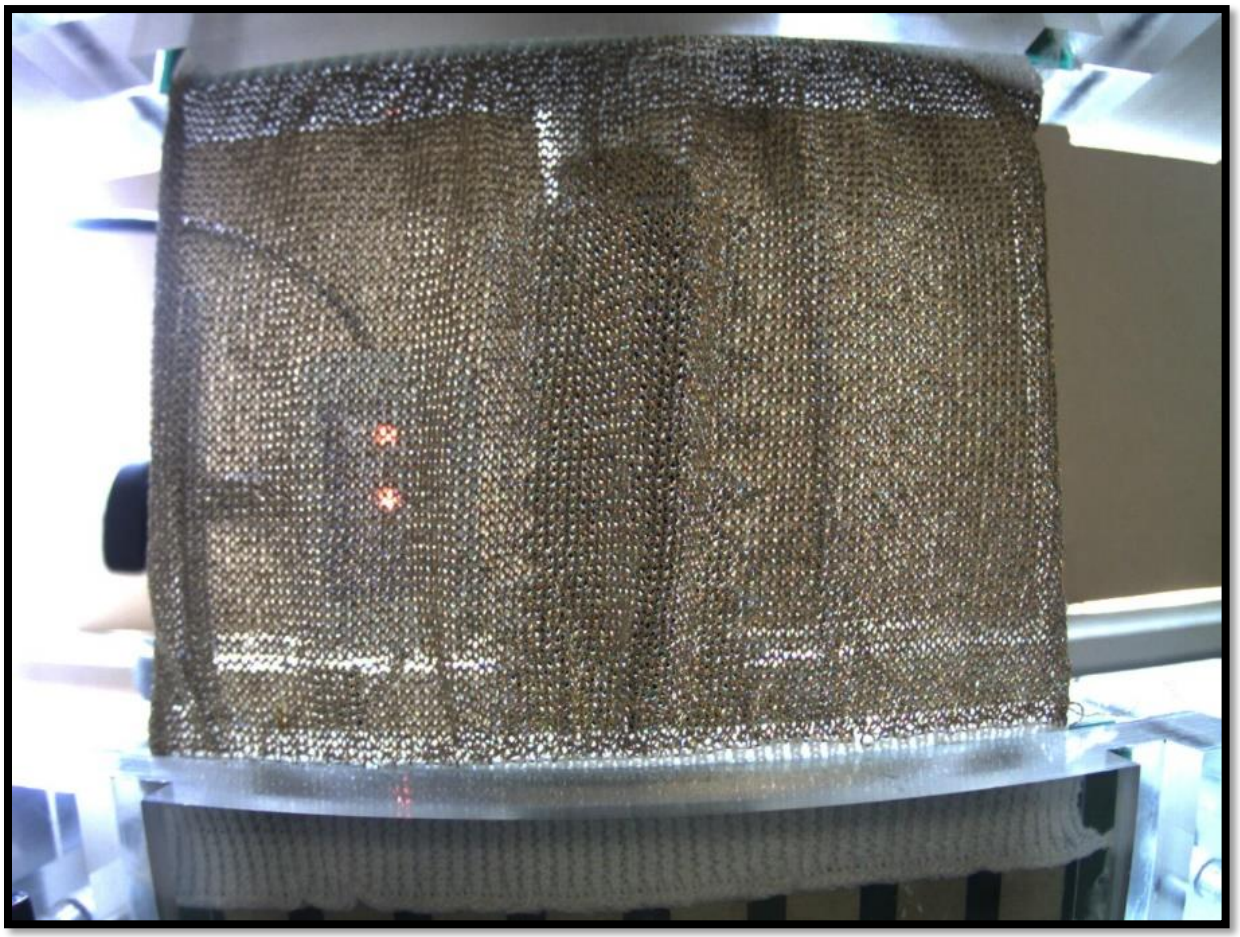

Figure 69: Stainless steel flat sample without Lycra in stretched case (SSNF4)

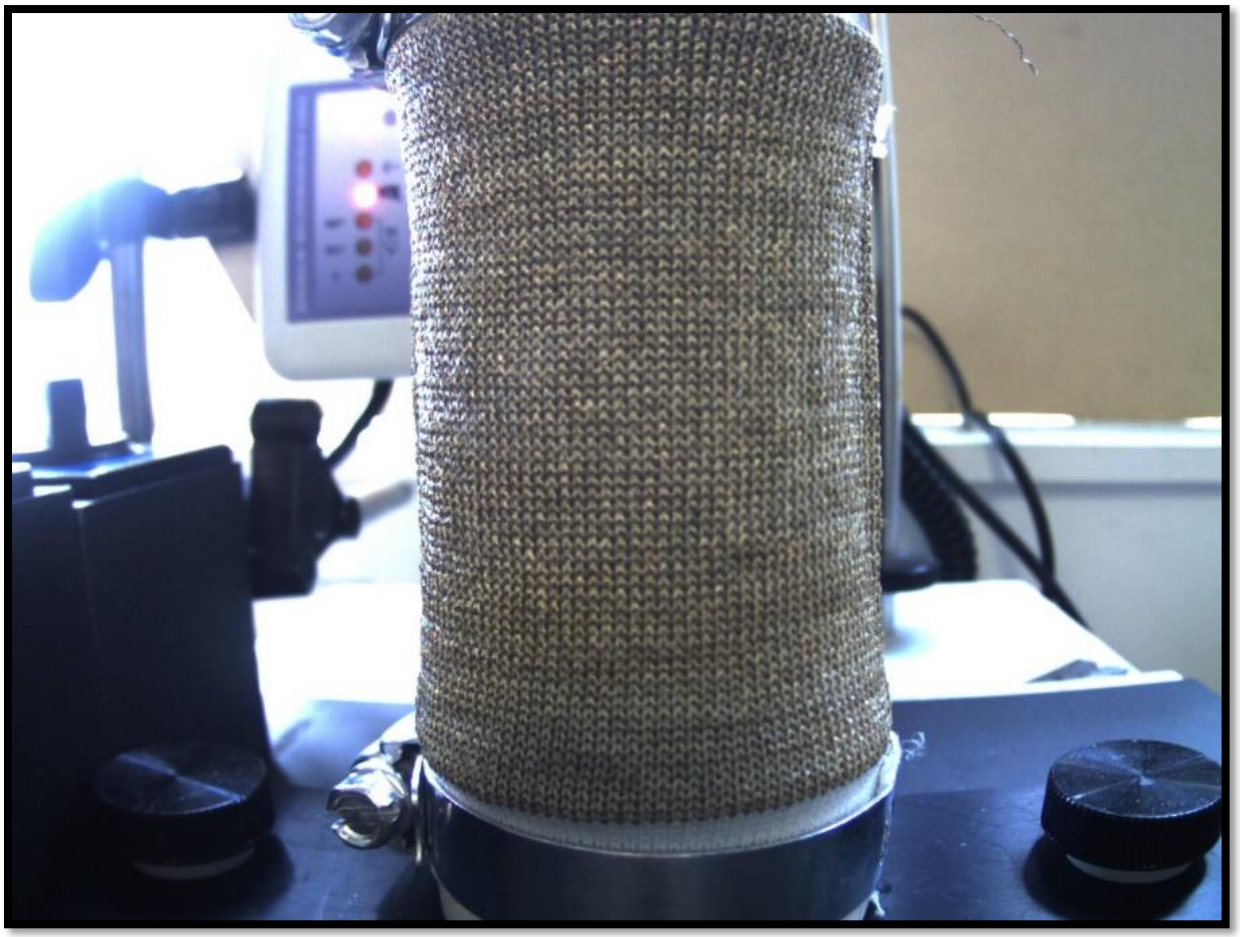

Figure 70: Stainless steel tube sample with Lycra in stretched case (SSLT1)

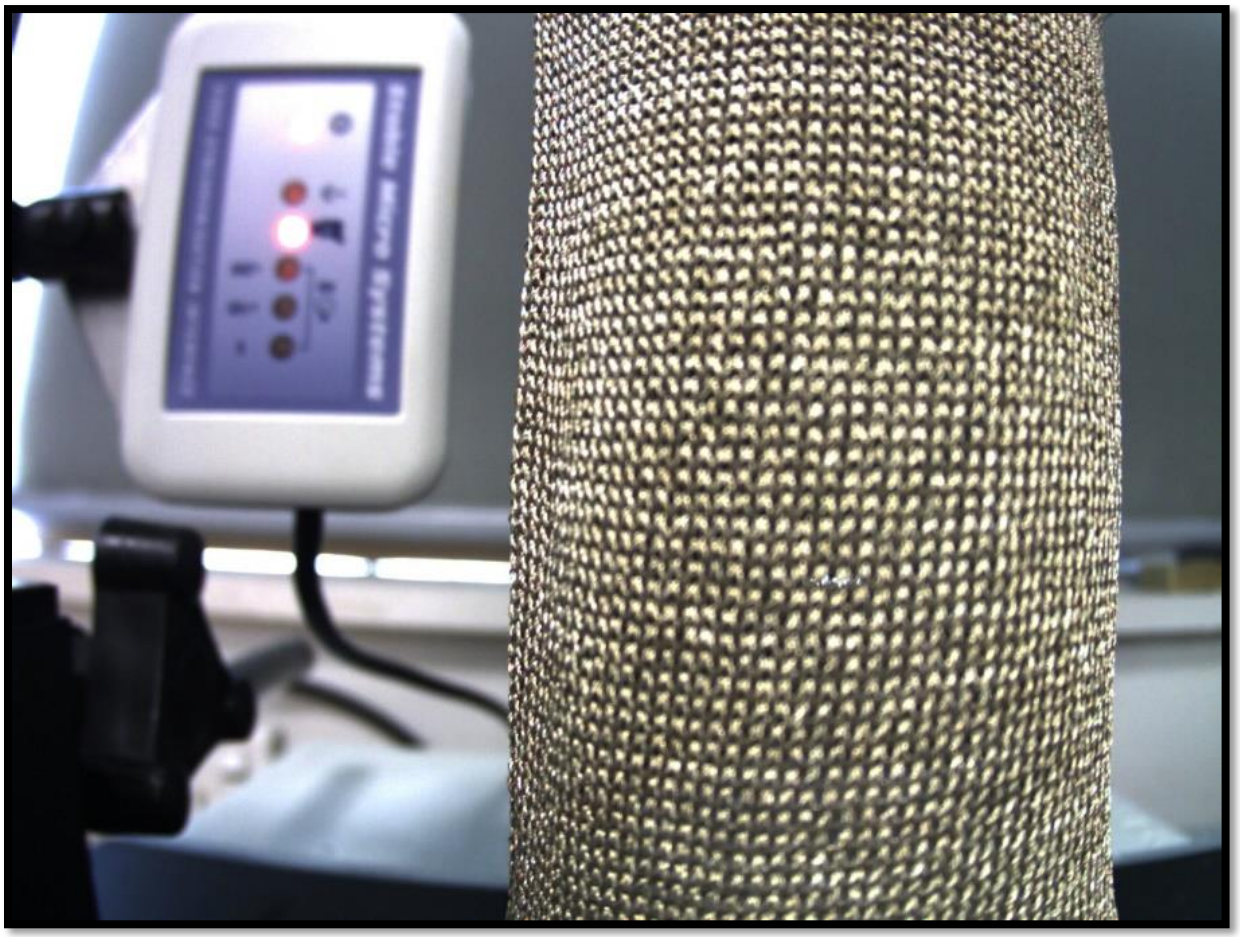

Figure 71: Stainless steel tube sample without Lycra in stretched case (SSNT1)

3.3.3.5 Flat Sample Dimensions

In this study, the tests were designed to apply a specific ratio of 1 gram of force per stitch in the course direction. For instance, if a sample contains 70 wales (stitches in the wale direction) and 40 courses (stitches in the course direction), the trigger force is set at 40 grams. This weight served as the trigger force in the texture analyser machine, signifying the initial force at which the testing sample began to react after the application of a certain amount of strain.

By employing a ruler to measure the width of the sample, one can ascertain the dimensions of the stitches, and the results indicate that the sample with 40 stitches in the course direction has a width of 54.28 mm, as shown in Figure 72.

With a width of 54.28 mm for every 40 stitches, the dimensions of each stitch in millimetres can be determined using the following relationship:

$$1\ stitch = \frac{54.28 \frac{mm}{stitches}}{40\ stitches}$$

$$\therefore 1\ stitch = 1.357\ mm$$

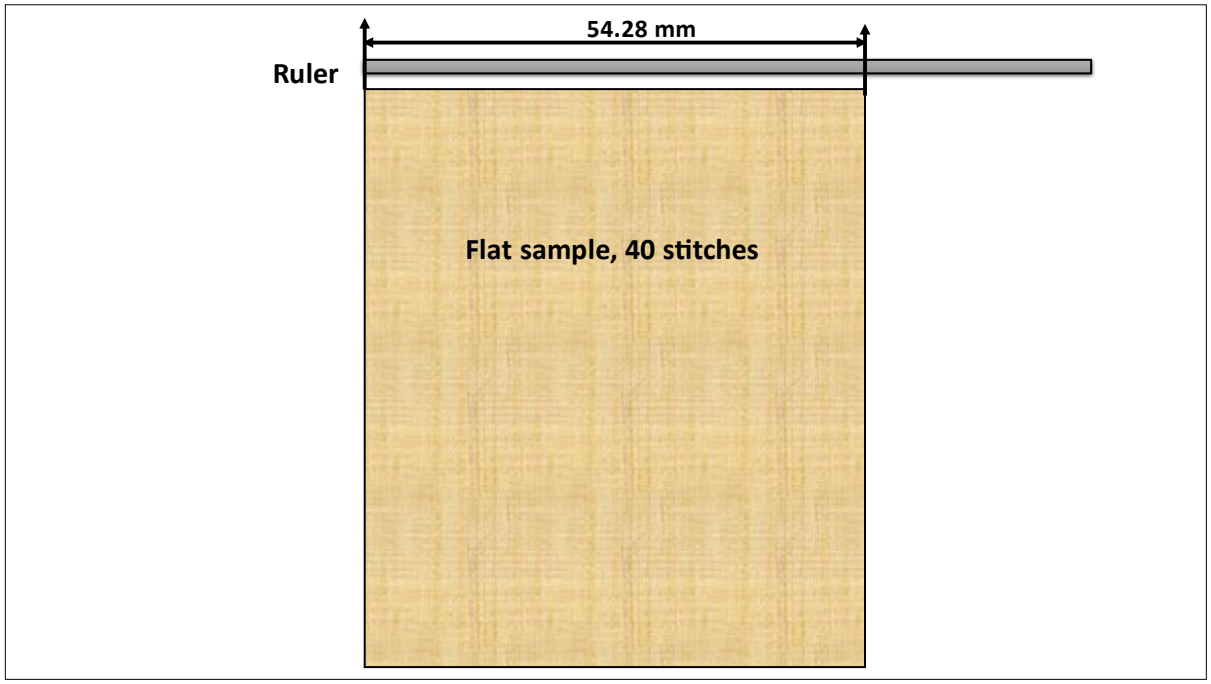

Figure 72: Measurement process for a flat sample

Then, the dimensions of the flat sample 40 x70 are:

40 x 1.357= 54.28 mm as a width and, 70 x 1.357 =94.99 mm as a length.

3.3.3.6 Tube Sample Dimensions

Producing a tube sample with 40 stitches in the course direction and 70 stitches in the wale direction would be excessively tight and impractical for fitting into the designated texture analyser machine. Consequently, the decision was made to treat the actual size of the tube sample as a sum of three flat samples (40+40+40) or knitted three flat samples together to form one tube sample while maintaining the stitch count in the wale direction equivalent to that of the flat sample with 70 stitches.

The calculation for the dimensions and diameter of the tube is as follows:

- Stitch Count in the Course Direction: $40 + 40 + 40 = 120\ stitch$.
- Width of the Tube: $120\ stitches\ x\ 1.357\ mm\ per\ stitch = 162.84\ mm$.
- Length of Tube: $70\ stitches\ x\ 1.357\ mm\ per\ stitch = 94.99\ mm$.

The diameter of the tube (D) is calculated using the formula for the circumference of the circle:

$$Circumference = 2\pi R = \pi D$$

Given the circumference is $120\ x\ 1.375 = 162.84\ mm$:

$$\pi D = 162.84 \Rightarrow D = \frac{162.84}{\pi} \approx 52$$

3.3.3.7 Polyester Samples

In this study, I conducted various testing attempts to achieve optimal results for the selected silver and stainless-steel conductive yarn samples. Through my experiments, the most promising outcome was obtained with the sample featuring the (40 × 70) stitch configuration. Building on this, I modified the yarn top to a nonconductive polyester fabric for comparative analysis with other samples (silver and stainless steel). I categorised the polyester samples into two groups: flat and tubular. For each group, I tested two types of yarn, one knitted with Lycra

and one without. The Lycra-inclusive samples were designed to maintain the same stitch count (40 x 70) and dimensions, as outlined in in Table 3.

For tube specimen testing, various clamp shapes, specifically cylindrical clamps, were used to ensure secure and uniform gripping of the samples. The setup included two cylindrical clamps, each directly fastened to ensure stability and precise alignment with the texture analyser. The top clamp was mounted on the upper part of the texture analyser using a screw, while the bottom clamp was secured into a metal base with a screw and then attached to the lower part of the machine using two additional screws (Figure 72). The tube specimen was firmly attached to the fixed cylindrical clamp with the aid of a hose clamp, providing additional grip and preventing slippage during testing (Figure 74). These cylindrical clamps were machined from Acetal, a durable and highly machinable thermoplastic known for its excellent mechanical properties and dimensional stability, making it an ideal material for such applications.

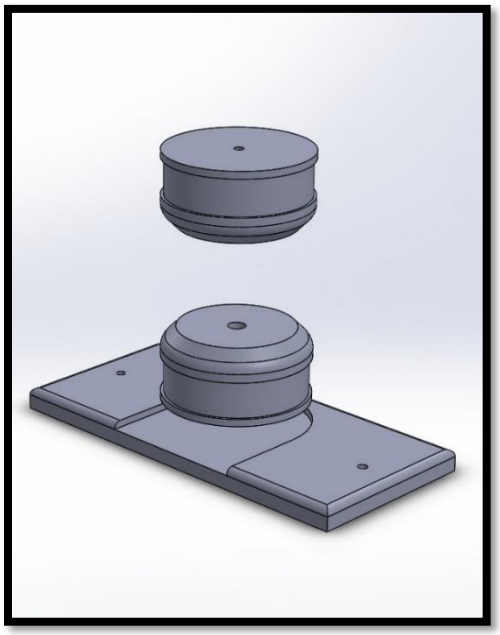

Figure 73: Cylindrical Clamp Assembly for Tube Specimen Testing

Figure 74: Hose clamp (Tridon Hose Clamps - Perforated Band - Regular Clamp 2022)

The test of the samples began by fixing each sample into the flat clamp directly to the machine (see Figure 75 and Figure 76 for the flat sample and Figure 77 and Figure 78 for the tube sample), and the strain was tested by documenting the relationship between the time (s) and the force (g) with a camera capturing a video recording of the testing while the sample was moving into tension and then returning to the starting point after stretching to the specified strain range (2.5, 5, 7.5, and 10%) for five repeated sequences (5 tests/strain). After obtaining the video for each test, image processing was performed to obtain the image data to calculate the strain and velocity for each test.

Figure 75: Flat polyester with Lycra stretched case (PELF1)

Figure 76: Flat polyester without Lycra stretched case (PENF1)

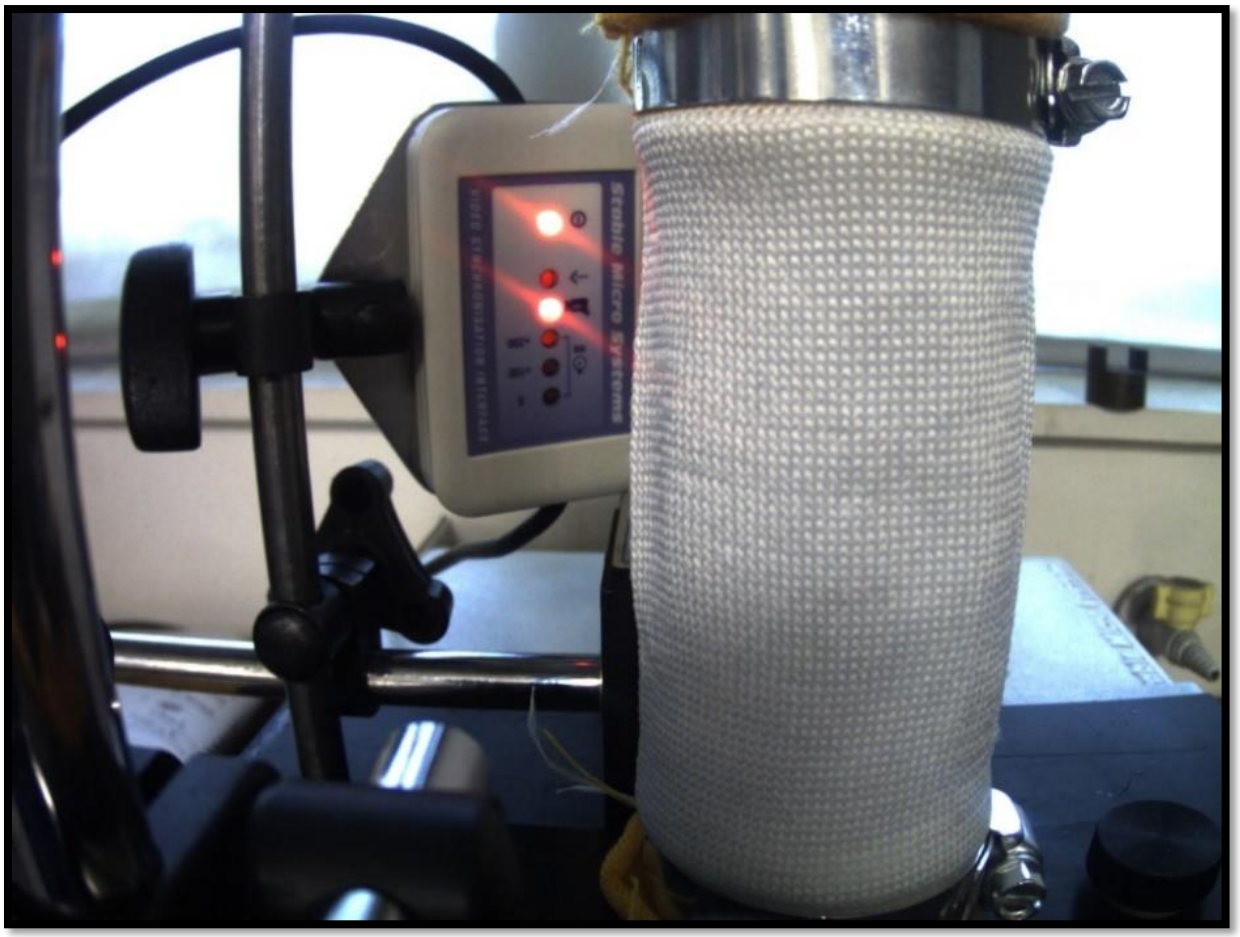

Figure 77: Tube polyester with Lycra stretched case (PELT1)

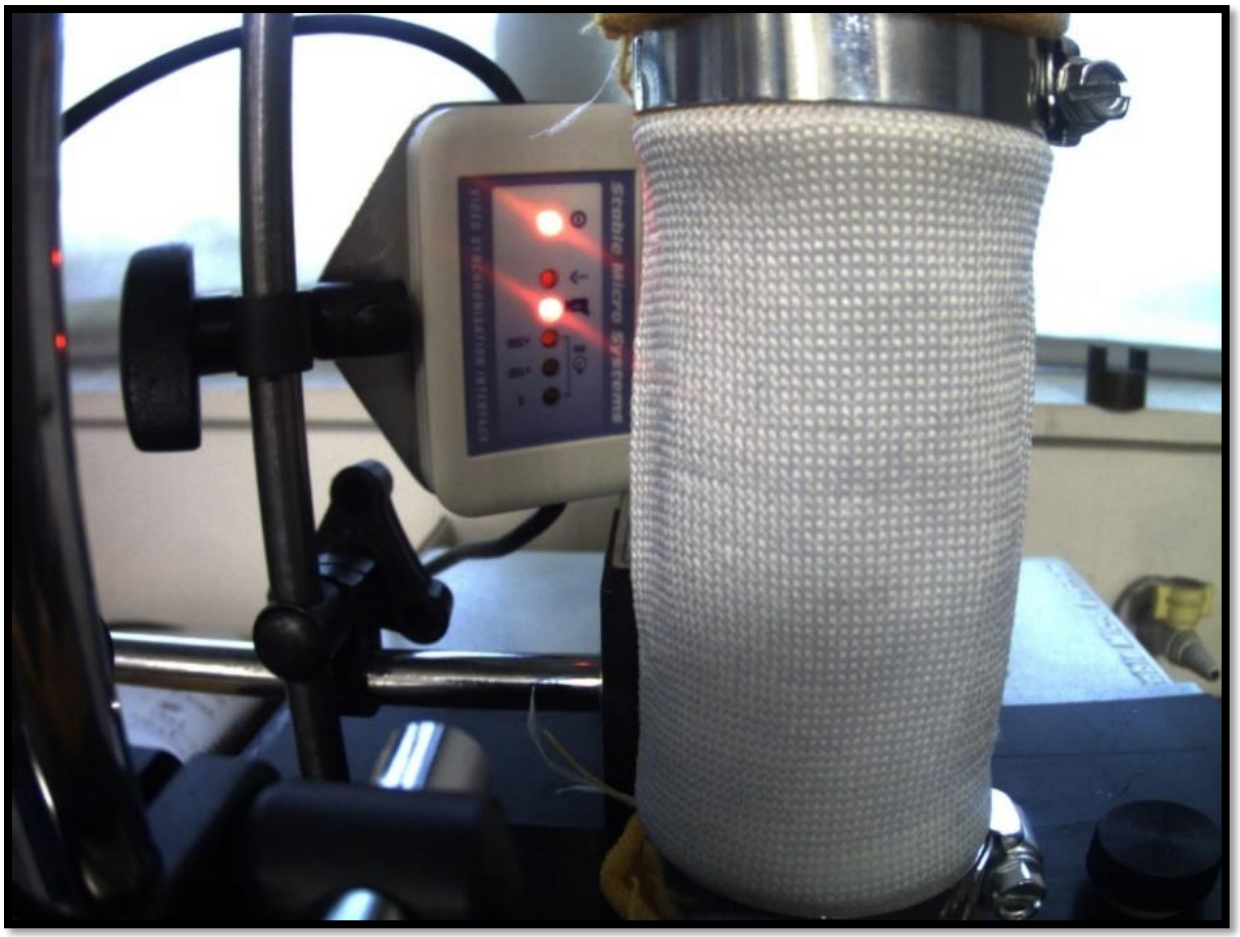

Figure 78: Tube polyester without Lycra stretched case (PENT1)

After all these testing attempts, the dimensions of the samples were adjusted to achieve the best results and to analyse the effect of stitch size on textile behaviour during testing in the texture analyser. From the previously tested specimens, three samples were selected for further analysis. Among these, one sample featured the smallest stitch size, with dimensions corresponding to 120 x 70 stitches, demonstrating how finer stitching influences the textile's performance under testing conditions.

If each stitch measures 1.357 mm, the overall size of the sample would be calculated as

163 mm × 95 mm, based on the dimensions of 120 stitches by 70 stitches.

The dimensions of the new samples were as follows:

- **140 mm x 95 mm**: The stitch size was calculated as
  $140\ mm/120\ stitches = 1.66\ mm\ per\ stitch$ (Figure 80)
- **150 mm x 95 mm**: The stitch size was calculated as
  $15\ mm/120\ stitches = 1.25\ mm\ per\ stitch$ (Figure 81)
- **160 mm x 95 mm**: The stitch size was calculated as
  $160\ mm/120\ stitches = 1.33\ mm\ per\ stitch$ (Figure 82)

The stitch width refers to the sideways distance between two stitches in the same row. In knitting or when sewing knit fabrics, the stitch width, also known as pitch, impacts the stretchiness and density of the finished fabric as see in Figure 79. Controlling the pitch can have a significant impact on the tightness or stretching of knits and looped fabrics (Tamanna et al., 2017).

The dimensions of the polyester sample and their stitch sizes are presented in Table 4.

Table 4: Polyester samples measurement

Size of the sample(mm) in width	**Size of the stitch (mm)** **Stitch width**
140	*1.166*

150	*1.25*
160	*1.33*

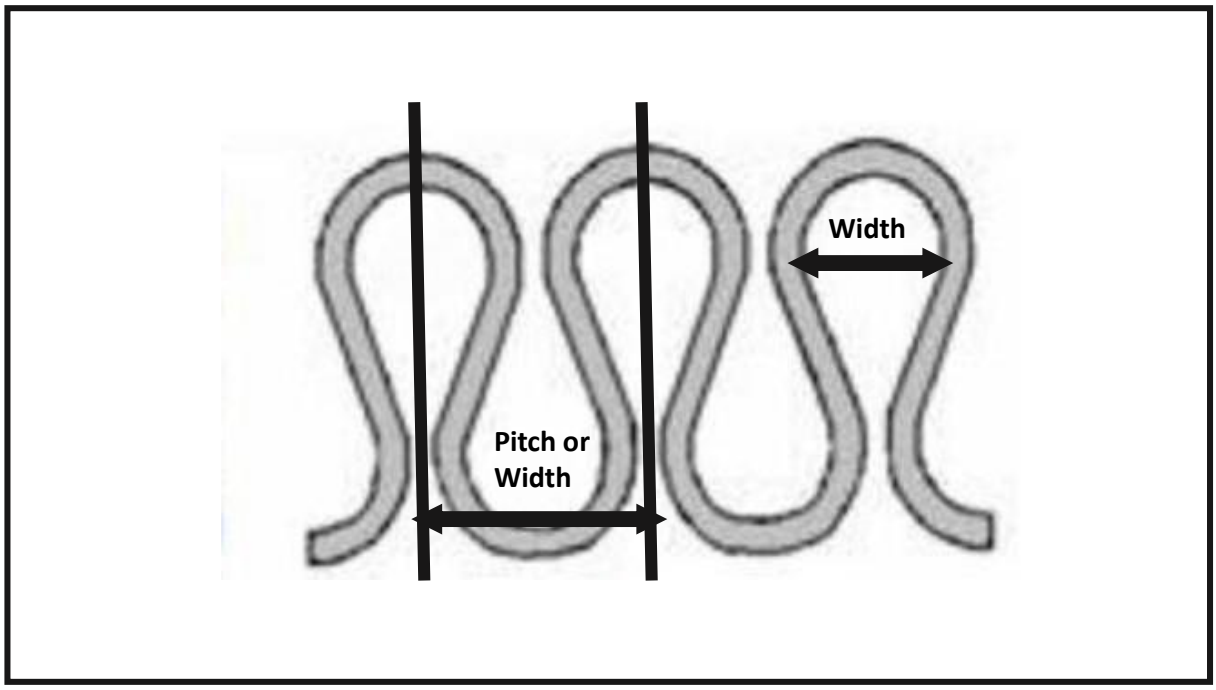

Figure 79: Single-course loop showing the width of the loop (Repon et al., 2018)

Figure 80: Polyester flat sample with 140 mm (PLNF2)

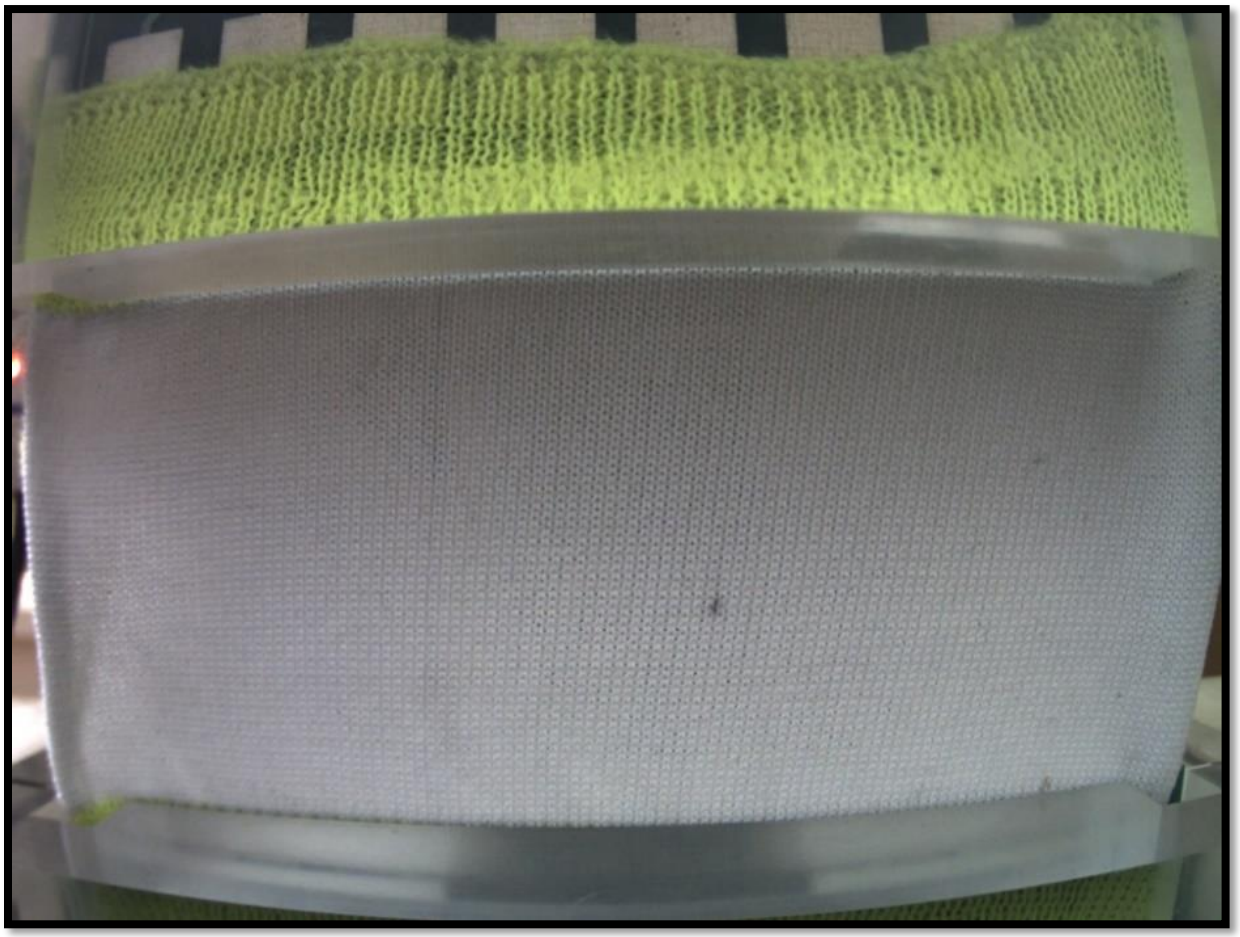

Figure 81: Polyester flat sample with 150 mm (PENF3)

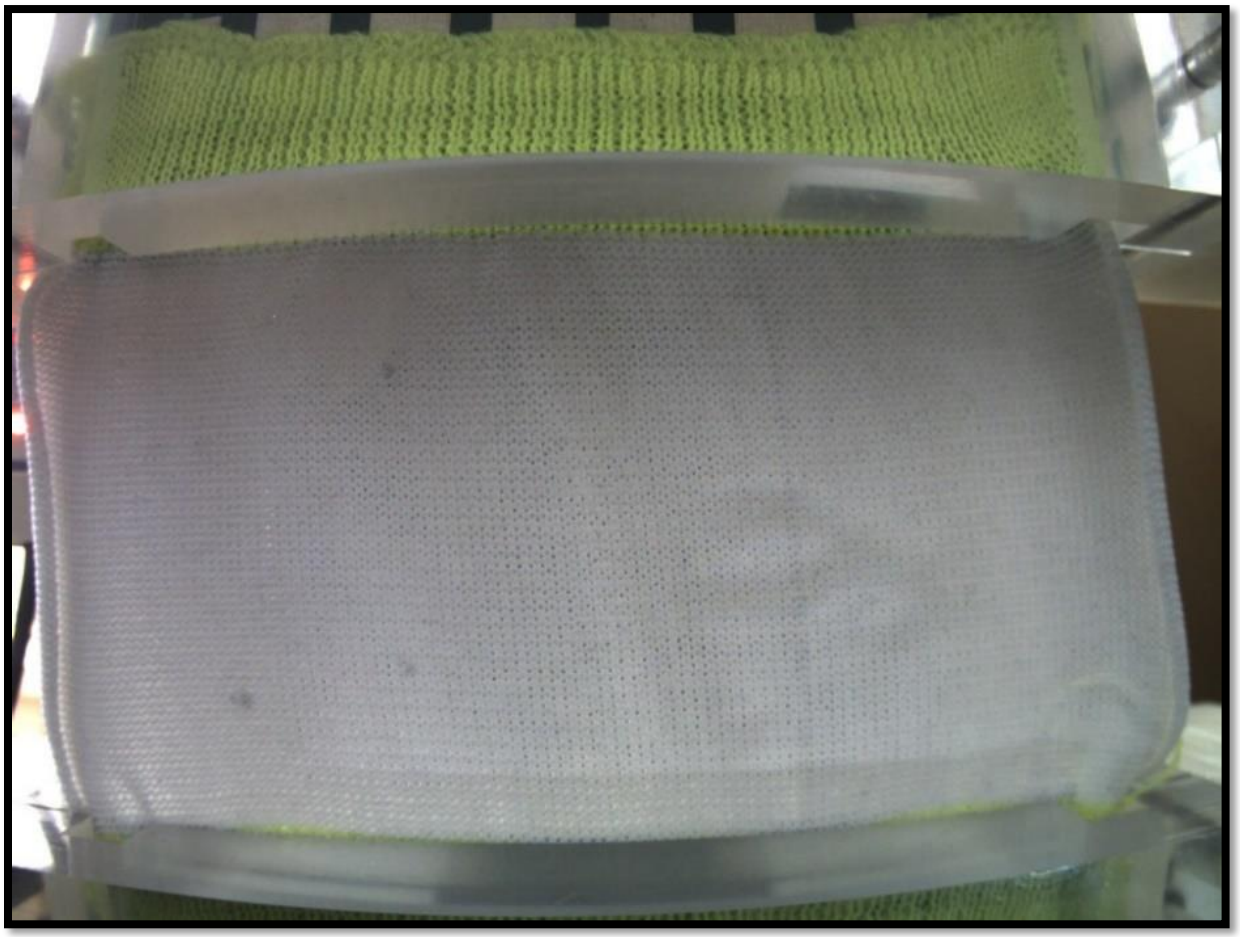

Figure 82: Polyester flat sample with 160 mm (PENF4)

Using the same procedure used previously for the samples, the testing started with strain rates of the strain = (2.5, 5, 7.5, and 10) %.

As previously explained, the fourth sample had a distinct stitch count, where each stitch was equal to 1 mm. The new sample dimensions were 163 × 70 stitches. A picture of this new sample is presented in Figure 83.

Figure 83: Polyester flat sample with 163 stitches (PENF5)

3.3.3.8 Rubber Sample

to compare the strain behaviour of knitted samples, testing was conducted with a rubber sample as a reference material. Rubber was chosen for its simplicity, serving as a clear model when comparing to fabrics that have more complex structures.

Rubber exhibits distinct mechanical properties such as high tensile strength, significant elongation, the ability to return to its original shape, and resistance to cuts and tears. These attributes provide a straightforward contrast to fabrics like polyesters, which are nonconductive and display more intricate mechanical behaviours.

The PIV Lab program was used to analyse the strain and velocity of the materials, helping to determine the mechanical properties of the new material being tested. This insightful comparison highlights how different materials react under stress, deepening the understanding of their performance.

The rubber sample measured 163 mm in width and 95 mm in length, matching the physical dimensions of the polyester sample. However, the polyester achieved these dimensions with a stitch-based structure consisting of 120 stitches in width and 70 stitches in length, while both samples shared the same overall measurements, their structural compositions differed significantly, with the rubber being a continuous material and the polyester relying on a network of stitches. To ensure accurate results, the sample was divided into squares, each measuring 2.5 mm x 2.5 mm. The same testing procedures were applied to the rubber sample using the texture analyser machine. The test began at a speed of 1 mm/s, with the strain gradually increased in increments of 2.5%, 5%, 7.5%, and 10%, as shown in Figure 84.

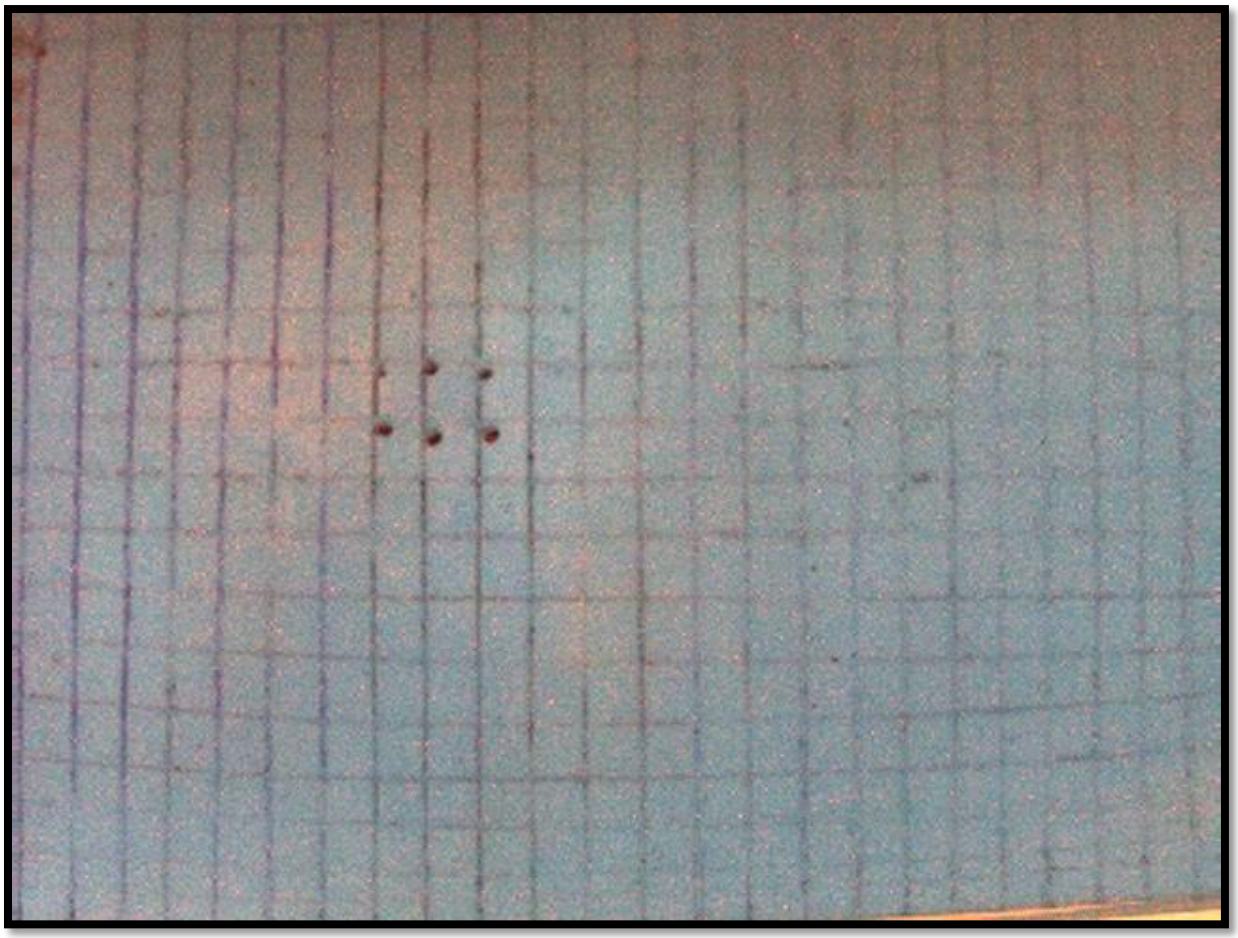

Figure 84: Rubber sample under 2.5% strain (RUBF1)

3.4 Testing Procedure

The texture analyser was calibrated before each measurement session to ensure accurate results. Force calibration was performed using a 50 g weight, while height calibration involved a 10 mm displacement, ensuring the device returned to its starting position. Using left alignment for these measurements also ensured that the units were consistently positioned close to their corresponding values for clarity.

The parameters of the tensile tests included the following:

- **Test mode**: The test mode (tension or compression) is chosen based on the nature of the sample. Some materials are designed to resist tensile (pulling) forces, while others are designed to resist compressive (pushing) forces.
- **Pre-test speed**: The pre-test speed is crucial in determining how fast the probe moves down to make initial gentle contact with the sample that is being tested. A slow speed is used, ideally between 0.5 mm/s and 3 mm/s. This ensures accurate alignment and smooth, gentle contact with the sample, minimising the impact of external factors such as force, movement, and environmental effects.
- **Test speed**: The speed during tensile testing is critical as it can affect the deformation characteristics of the material. It is the rate at which the probe stretches the sample during the measurement phase to assess the material's resistance to pulling force. Speeds can range from 1 mm/s to 20 mm/s, depending on the characteristics of the material being tested.
- **Post-test speed**: The post-test speed is the speed at which the test ends. This is usually slower to prevent any damage to the testing equipment or the sample itself after the test is completed.
- **Target mode**: The target of this test is to determine the strain, time, and force. These are important properties in material science and can provide valuable information about the material's mechanical behaviour.
- **Strain**: Different levels of strain (2.5, 5, 7.5, 10%) are chosen to observe how the material behaves under different levels of deformation.
- **Trigger force**: The trigger force is chosen based on the number of stitches in the course direction. This is a unique parameter for textile materials. The idea is that the force at which the test begins does not start from zero, which reflects the real-world conditions more accurately where the material is already under some initial tension due to the stitches. For instance, if the sample has 70 stitches in the wale direction and 40 stitches in the course direction, the trigger force starts at 40 g.

These parameters are carefully chosen to ensure that the tensile tests provide accurate and meaningful data about the material's mechanical properties. They can be adjusted based on the specific requirements of the material or the application it is intended for.

Unless otherwise noted, the test parameters were set as given, as summarised in Table 5 .

Table 5: Texture analyser settings for tensile test

Parameter	**Value with units**
Test mode	Tension
Pre-Test Speed	1 mm/s
Test Speed	1 mm/s
Post-Test Speed	1 mm/s
Target Mode	Strain
Strain	2.5, 5.0,7.5, or 10%
Trigger Type	Force
Trigger Force	20, 30, or 40 g

The parameters selected for my study were well-suited for assessing the tensile properties of materials, particularly samples with relatively low strength or stiffness, such as textiles. This was especially relevant for vertically aligned samples, as their orientation can influence the results, below the rationale for the parameter selection is presented:

- Test Mode: Tension

Choosing the tension mode is suitable for describing the material's behaviour when subjected to stretching or pulling forces. In this setup, the samples are tested under tensile strain by pulling the sample vertically between the two clamps in the tensile test machine.

- Pre-Test, Test, and Post-Test Speeds

The reliable speed of 1 mm/s for all three stages (pre-test, test, and post-test) ensures a slow and controlled loading rate, which is fundamental for accurate measurement of material properties under stable conditions. This low speed minimises the impact of dynamic effects and allows for a more precise determination of the material's response to tensile strain.
I have discovered that the optimal speed for accurate outcomes is 1 mm/s. A slow speed allows for more controlled and progressive deformation of the sample, reducing dynamic changes in the textile's behaviour during testing. Additionally, a slower speed provides higher resolution data, offering more detailed insights into the mechanical characteristics of the knitted fabric. By identifying 1 mm/s as the optimal speed for texture analyser tests, I have likely found a balance between controlled deformation, data quality, and consistency, leading to more accurate and reliable outcomes in my experiments.

- Target Mode: Strain

Choosing strain as the target mode is a common method in tensile testing as it allows for direct measurement of the material's deformation under applied forces. This is particularly helpful for characterising the material's behaviour and properties.

- Strain Levels: 2.5%, 5.0%, 7.5%, and 10%.

The selected strain levels cover a range of deformation magnitudes, enabling a comprehensive estimation of the material's behaviour from small strains (2.5%) to larger strains (10%). This range can provide understanding into the material's deformation characteristics.

- Trigger Type: Force

Choosing force as the trigger type is suitable when treated with materials that exhibit an initial resistance or preload before the actual tensile strain begins. This is often the case for textiles.

- Trigger Force: 20, 30, or 40 g

The trigger force is an interesting parameter. By not starting from zero, it considers the initial tension in the material due to the stitches. This makes the test more representative of real-world conditions where the material is already under some tension. The different trigger forces allow you to study the effect of this initial tension on the material's behaviour.

The trigger force in a texture analyser acts as the starting point for the test. It is the predetermined force level that signals the machine to begin the measurement process. Once the applied force on the sample reaches this trigger force, the texture analyser starts collecting data on the sample's response. This feature is essential for ensuring tests are conducted using a controlled and consistent method, simplifying accurate and dependable force measurement during texture analysis.

The tests were set up to generate a particular ratio of 1 gram of force for each stitch in the course direction. For example, if a sample has 70 wales (stitches in the wale direction) and 40 courses (stitches in the course direction), the trigger force will be set at 40 grams. This approach

allows me to maintain consistency and control in my project, ensuring reliable and standardized testing conditions.

These parameters provide a comprehensive understanding of the material's tensile properties, which can be crucial for its intended application. It is always important to choose test parameters that best reflect the conditions that the material will face in real-world use.

Each sample was tested over five cycles to evaluate the repeatability of the tests.
As previously established, the optimal speed for achieving accurate results with the texture analyzer is 1 mm/sec. This speed allows for more controlled and progressive deformation of the sample, minimizing fluctuations in textile behavior during testing. Furthermore, it provides higher-resolution data, which enables a more detailed analysis of the knitted fabric's mechanical characteristics such as elasticity and strength.

3.4.1 Test Effect of Initial Gauge Length

In addition to tensile testing as described above, sample AGWF2 was also tested for different initial gauge lengths of the specimens (74, 76, 78, 80, 82, and 84 mm) at a starting speed of 1 mm/s, starting force of 40 g, and strain of 5%. This test was performed to investigate the first-second test problem and to determine whether the starting test height had any effect on the reading test for the first or second readings by applying the same strain for each case.

3.4.2 Test Effect of Relaxation

Sample AGWF2 was also subjected to a set of repeated tests. This sample was subjected to multiple tests in quick succession with a one minute long time delay between every two tests to give the sample time for rest and to return the stitches to their original positions. The gauge length H was set to 74 mm (length of the sample between the clamps), the test speed was 1 mm/s, the strain started from the smallest value of 1%, followed by 2%, 3%, and 4%, and the test ended with a 5% strain test. The trigger force = 40 gm depends on the number of stitches in the course direction, and for each strain, three sets of tests were performed.

3.5 Image processing

In this project, particle image velocimetry (PIV) was performed using the PIVlab - Digital Particle Image Velocimetry Tool for MATLAB (2021). PIVlab is a powerful tool for calculating velocity fields from image data (movies, pictures), as developed by Thielicke and Stamhuis (2014, 2015). It allows users to import a sequence of images, analyse the data, and export the results in a format or alignment tailored to meet the requirements of the examiner or research objectives. PIVlab utilizes individual display images along with the window deformation method to analyse fluid dynamics across sequential frames a crucial aspect of Particle Image Velocimetry (PIV). This technique requires two initial images to set a reference frame. Once the video is segmented into individual frames, PIVlab processes these frames to evaluate the motion and characteristics of the flow in subsequent images.

3.5.1 Image Processing Using PIVlab

All formats of PIV exploration using PIVlab should commence with an imported sequence of images. To extract images from the videos of the experiments, a separate program called Free Video to J Converter (DVDVideoSoft, 2017) was employed, as shown in Figure 85. The software was used to efficiently extract relevant frames from the video and assign each frame a label containing the sample name, experiment number, and frame number. For the textile tests, one frame was extracted for every three video frames due to the way the tensile test software, Exponent, recorded the video.

Figure 85: Free video to PJN converter software

Within PIVlab, the image processing was started by opening the "new session" window using a sequencing style of 1-2 2-3 3-4 (i.e., pairs of consecutive frames). Depending on how the images were imported, they were directly aggregated into suitable couples, Figure 86.

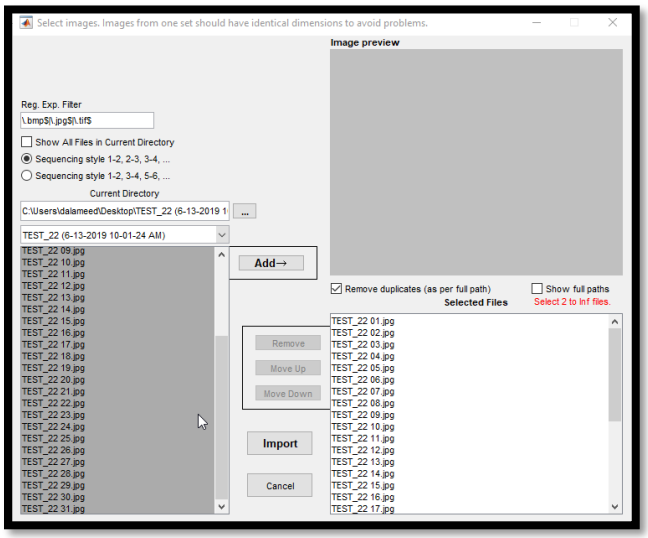

Figure 86: Importing images (MATLAB, 2023)

1. Under the “Analyses Setting” tab, there is an option to define regions of interest (ROI) and apply exclusion masks to the images being analysed. ROIs (illustrated in Figure 86) allow the user to specify a particular area of the image to focus on during analysis while excluding other areas that might introduce errors or distortions. In this case, a region in the middle of the textile was selected as the ROI to minimize distortions caused by the wide-angle lens, which are more pronounced at the edge of the image.

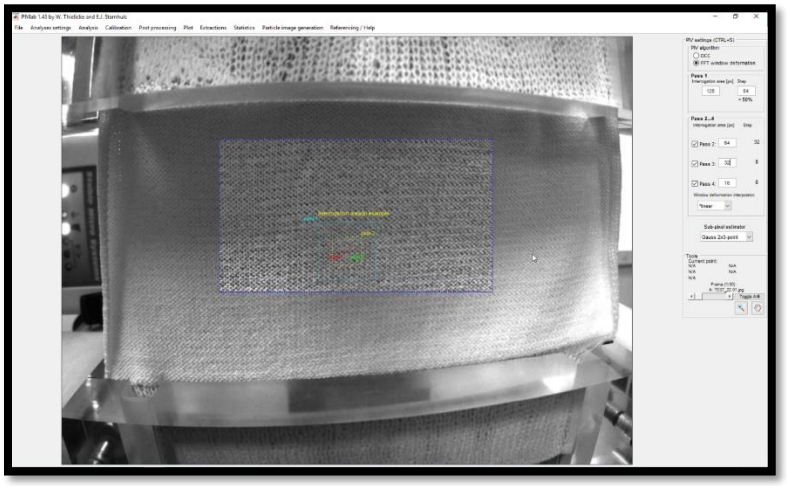

Figure 87: Regions of interest (MATLAB, 2023)

2. Calibration tells PIVlab how many pixels are in one meter and the time link between the images of a single format. The calibration process is shown in Figure 88 (the length of the sample in the image represents the size of the stitches in the course direction, which was 120 stitches or 163 mm) before validating the data.

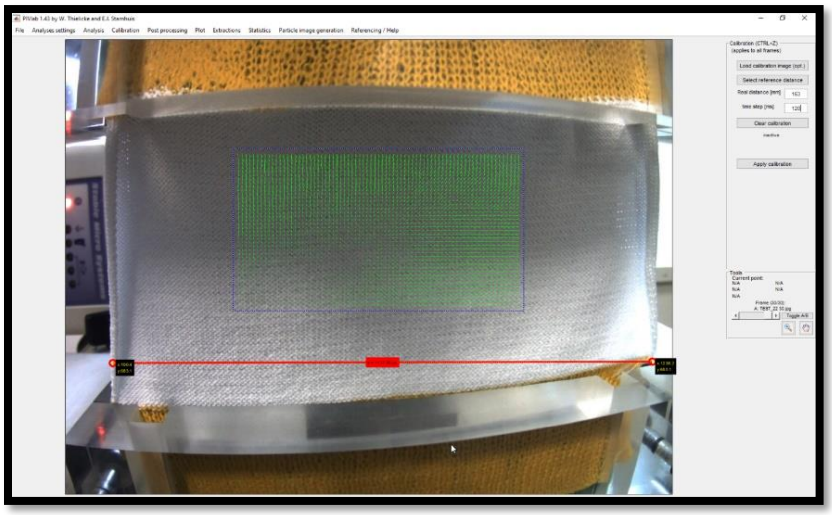

Figure 88: Calibration process (MATLAB, 2023)

3. PIVlab provides various options for controlling how the velocity field is introduced. Figure 89 and Figure 90 show an example of the velocity magnitude (m/s) and higher speeds of textile extension at the top and to the right.

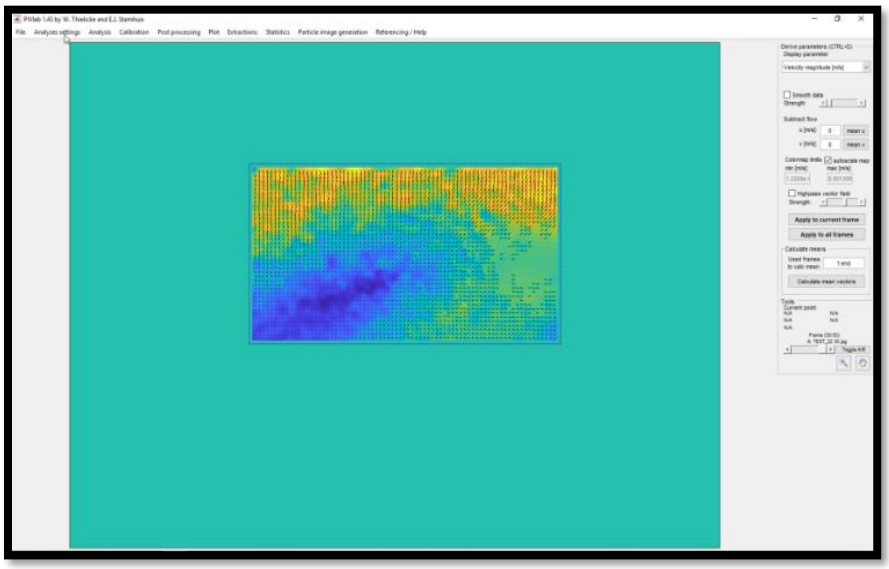

Figure 89: Velocity magnitude (m/s) (MATLAB, 2023)

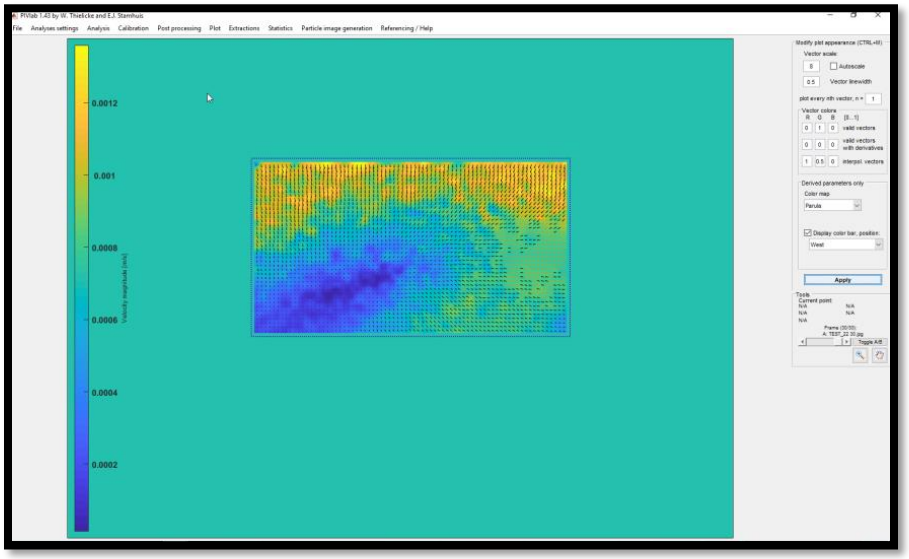

Figure 90: The test's velocity magnitude bar (MATLAB, 2023)

Finally, PIVlab was used to calculate and save the data as a MATLAB file to be imported into a MATLAB program to complete the processing.

3.5.2 Image Processing Using MATLAB.

When using the MATLAB software program to process the test images, the initial step involves creating MATLAB calculation scripts A, B, C, and D, as illustrated in Figure 91. After processing the images using PIVlab, the scripts compute strain along the X- and Y-axes. These calculations are illustrated in Figure 128, Figure 129, and Figure 131.

- Figure 128 shows the V component of velocity (in m/sec), representing movement from left to right.
- Figure 129 illustrates the U component of velocity indicating movement from top to bottom.
- Figure 131 presents the strain in both X and Y directions, along the vectors depicting their respective directions.

These figures collectively illustrate the behaviour of the textile during the tensile test. The diverging and converging arrows in the visualizations represent the direction of strain and velocity, providing insights into the textile response under stress.

Calculations_Script.m

```
%dirs=dir('C:\Users\dalameed\Downloads\image processing group 1\image *');
dirs=dir('E:\RUBBER SAMPLE\2.5%\T1\image processing\PIVlab*');
%dirs=dir('C:\Users\dalameed\Desktop\IMAGE PROCESSING H\PIVlab*');

EX={};
EY={};
for n=1:length(dirs)
    importfile([dirs(n).folder '\' dirs(n).name]);
    [ex,ey]=calculatestrain(x,y,u,v,3);
    div=divergence(x,y,ex,ey);

    figure(1)
    pcolor(x,-y,div);%,'EdgeColor','none');
    shading interp
%     caxis([-60 60])
    colorbar
    view(0,90);
    hold on
    quiver(x,-y,ex,ey,5,'r');
    hold off
    title([dirs(n).name ' Strain'])
%    set(gca,'XLim',[0.08 0.1],'YLim',[0.03 0.04])
%    set(gca,'XTick',0:0.0014:0.12,'YTick',0:0.0014:0.07)
```

A

```
    grid on
    daspect([1 1 1])

    figure(2)
    div=divergence(x,y,u,v);

    pcolor(x,-y,div);%,'EdgeColor','none');
    shading interp
    % caxis([-20 20])
    colorbar
    view(0,90);
    hold on

    quiver(x,-y,u,-v,5);
    hold off
    title([dirs(n).name ' Velocity'])
    daspect([1 1 1])
%    set(gca,'XLim',[0.08 0.1],'YLim',[0.03 0.04])
%    set(gca,'XTick',0:0.0014:0.12,'YTick',0:0.0014:0.07)

    EX{n}=ex;
    EY{n}=ey;
    pause
```

B

```
48
49  end
50
51
52
53
54
55
56
57
58
59
60
61
62  %% Matrix Calculation
63  function [strainx, strainy]=calculatestrain(x,y,u,v,n)
64  strainx = (u(:,(n+1):end)-u(:,1:end-n))./(x(:,(n+1):end)-x(:,1:end-n));
65  strainx=[strainx NaN*ones([size(strainx,1), n])];
66
67  strainy = (v((n+1):end,:)-v(1:end-n,:))./(y((n+1):end,:)-y(1:end-n,:));
68  strainy=[strainy; NaN*ones([n, size(strainy,2)])];
69
70  end
71
```

C

```
70  end
71
72  %% import file
73  function importfile(fileToRead1)
74  %IMPORTFILE(FILETOREAD1)
75  %  Imports data from the specified file
76  %  FILETOREAD1:  file to read
77
78  %  Auto-generated by MATLAB on 18-Oct-2018 11:16:38
79
80  % Import the file
81  newData1 = load('-mat', fileToRead1);
82
83  % Create new variables in the base workspace from those fields.
84  vars = fieldnames(newData1);
85  for i = 1:length(vars)
86      assignin('base', vars{i}, newData1.(vars{i}));
87  end
88
89
90
91
92  end
93
```

D

Figure 91: A, B, C, and D MATLAB calculation scripts (MATLAB, 2023)

3.6 Results and Discussion

A typical result of a tensile test is presented here using sample AGWF2, as shown under the test in Figure 92. In this case, the starting force was 40 g and the test speed was 1 mm/s. The response shows that the first reading always had the lowest reading test curve because of the unpredictable behaviour of the stitches under the initial stretching conditions.

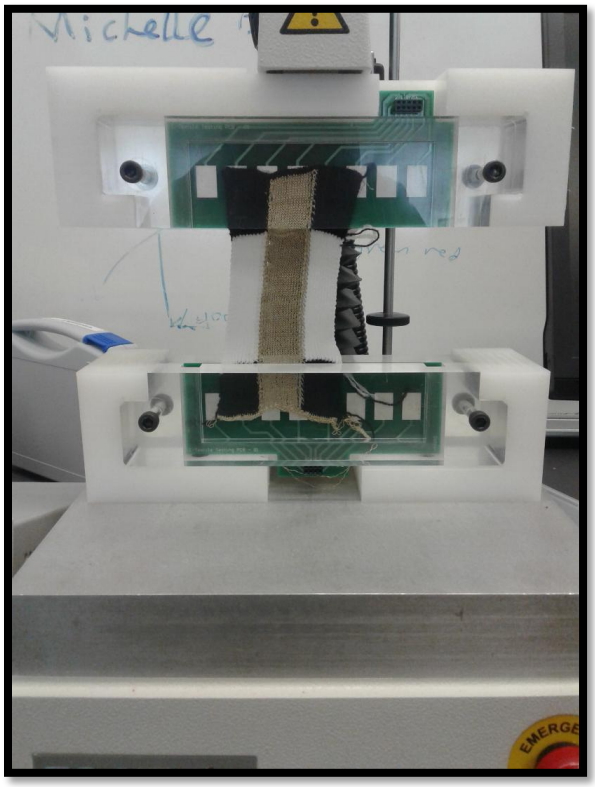

Figure 92: AGWF2 sample clamped in a texture analyser machine

3.6.1 Differing First-Cycle Behaviour

The first-cycle test involved five groups, with each group undergoing five cycles, as illustrated in Figure 93 and Figure 94. The analysis of the relationship between the forces generated by the sample over time shows that the first cycle consistently produces less force compared to subsequent cycles. However, the forces in the second, third, fourth, and fifth cycles exhibit

much greater similarity. This behaviour remained consistent even when the test parameters were modified, such as:

- Using a different starting speed (1mm/s, 5mm/s and 10 mm/s)

  When different starting speeds (1 mm/s, 5 mm/s, and 10 mm/s) are used in texture analyser tests on knitted textiles, the mechanical behaviour observed may vary. By experimenting with different starting speeds, a more comprehensive understanding of how knitted textiles perform under various conditions can be gained.

- **1 mm/s:**

  Controlled and Gradual Deformation: When using this slower speed, the sample's deformation occurs in a more gradual and controlled manner, enabling precise observations of the material's response to stress and strain.
  Accurate Measurement of Mechanical Properties: The slower speed facilitates more precise measurements of stiffness and elasticity, as the material has additional time to react to the applied force. This is especially beneficial for conducting detailed analyses of the material's essential mechanical properties without the interference of dynamic effects.

- **5 mm/s:**

  Moderate Deformation Speed: At 5 mm/s, deformation happens more quickly compared to 1 mm/s, yet it is still controlled. This speed strikes a balance between capturing dynamic reactions and ensuring precision in measurements.
  Dynamic Responses: Tests at this speed may introduce the material's performance under moderately dynamic circumstances, which is crucial for situations where the textile experiences moderate forces. This speed can capture passing behaviours that may not be as apparent at slower speeds.

- **10 mm/s:**

Quick Deformation: When using a speed of 10 mm/s, the sample undergoes rapid deformation, possibly leading to increased stresses and changes in force and strain.
Insights into Rapid Loading Conditions: This speed offers insights into the material's behaviour in fast-loading states, helping in understanding its performance when subjected to quick stretching or compression. However, the results may be less accurate due to the fast deformation, with the data showing more of the material's dynamic response rather than its fundamental mechanical properties.

By utilising different starting speeds in the texture analyser tests you can obtain diverse insights into the mechanical behaviour of knitted textiles. The slower speed of 1 mm/s enables more precise and dependable measurements, making it the preferred option for in-depth analysis. This methodology guarantees a thorough characterisation of the mechanical properties, resulting in stronger and more relevant outcomes for smart textile research.

- Using different trigger forces (20 g, 30 g, and 40 g) or starting the test recording from a Trigger Force=0

  When you use different trigger forces (20 g, 30 g, and 40 g) or start the test recording from a trigger force of 0 when conducting texture analyser tests, the results can differ in terms of the initial deformation and the sensitivity of the measurements. Here are some potential outcomes based on these different triggers:

- **Trigger Force = 20 g**

  Initial Sensitivity: Using a lower trigger force of 20 g increases sensitivity to initial deformation, detecting the material's response right when a small force is applied.

  Potential Noise: Despite being more sensitive, this lower force may also capture additional noise or minor fluctuations, which could add complexity to the data analysis.

- **Trigger Force = 30 g**

Balanced Sensitivity and Noise: With a trigger force of 30 g, you achieve a balance between sensitivity and noise reduction. This level of force is sufficient to detect early deformation while keeping minor fluctuations or noise in check.

Early Mechanical Behaviour**:** This setup is valuable for examining the material's early mechanical behaviour, including the turn from initial deformation to more noticeable mechanical responses.

- **Trigger Force = 40 g**

Reduced Sensitivity: Using a higher trigger force of 40 g decreases sensitivity to very early-stage deformation, highlighting the material's response under slightly higher stress levels.

Minimised Noise: This setup helps to reduce noise and minor variations, resulting in clearer data on the material's mechanical properties when subjected to a more significant force.

Less Detailed Initial Data: However, this choice leads to less detailed information about the initial deformation stages, which could be crucial for specific analyses.

- **Trigger force of 0**

This approach captures the material's immediate response to force application, which can provide valuable insights into its initial behaviour. However, it is essential to be aware of the potential challenges introduced by increased data complexity, such as minor fluctuations and positioning effects.

- **Using different sample sizes (40X70, 30X70 and 20X70)**

The decision to vary the stitch count in different sample sizes offers valuable insights into how the material behaves under different conditions. By testing each sample size

under consistent conditions, researchers ensure that the results are comparable and reliable.

- **The 40x70 sample size:** With a larger number of stitches, the 40 x 70 sample size provides a comprehensive understanding of the textile's mechanical behaviour under stress and strain. This size allows for a detailed analysis of the material's response to external forces.

- **In contrast, the 30x70 sample size**, with a reduced stitch count, helps in identifying any subtle differences in mechanical properties compared to the larger sample. This variation sheds light on how minor changes in stitch count can affect the material's behaviour.

- **The smallest sample size, 20x70** presents a unique perspective by determining the minimum sample size that can still provide reliable data. Testing this size highlights the importance of sample size selection in ensuring accurate and consistent results for texture analyser tests.

Overall, the results emphasise the significance of selecting an appropriate sample size for obtaining precise and reliable data on the mechanical properties of textiles. By understanding how sample size influences the outcomes, informed decisions when conducting texture analyser tests can be made.

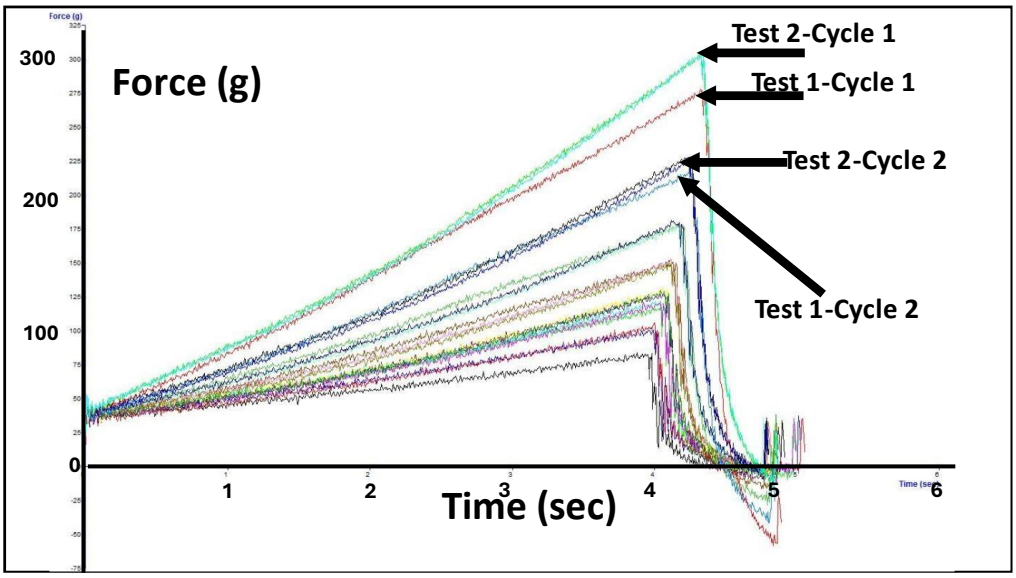

Figure 93: Repeated tests for the sample; the red curve is the first reading test, and the green curve is the second reading test

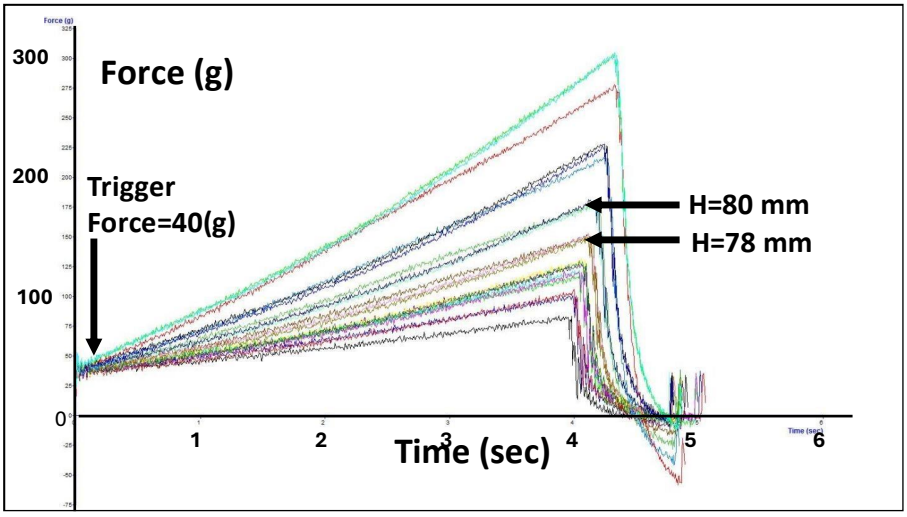

Figure 94: Results of repeated tests at gauge lengths of 78 mm and 80 mm with the application of trigger force.

To further investigate this, the initial gauge length or the length of the sample before stretching was varied. H, between clamps of 74, 76, 78, 80, 82, and 84 mm, were tested for

the sample AGWF2. The test speed was 1 mm/s, starting force was 40 g, and maximum strain was 5%. The results of the tests were as follows:

- When H=74 mm, the problem remained the same; the first test generated the lowest force.
- At H=76 mm, the difference in the forces was small.
- At H=78 mm, all the five tests exhibited the same generated forces.
- When H=80 mm the result was also similar.
- For H=82–84 mm, the problem started again, and the first test generated a lower force.

The data presented in Table 6 show the range of the sample gauge length and the tensile test results. From the data noted in the table, we conclude that the first and second problems fluctuated when using a different starting height for the setting sample between two clamps in the texture analyser. For the lowest and highest heights (74, 76, 82, 84, and 86 mm), the first test was always lower than the second test, even if the height range was different, but for the medium heights (78 and 80 mm), a more suitable result was obtained because the tensile test curves were much closer to each other for the first-second test.

Table 6: AGWF2 sample different high tensile test result

Sample gauge length (mm)	**T1(g)**	**T2(g)**
74	83.22	100.56
76	105.9	121.92
78	127.7	130.4
80	152.01	153.13
82	149.66	179.4
84	218	227.96
86	278.411	303.92

Another set of tests was performed using a time delay between every two tests of approximately one minute to give the sample time for rest and to return stitches to their original positions. These tests were performed using the AGWF2 with H= 74 mm (length of the sample between

the clamps), Test Speed =1 mm/s, Strain from 1 to 5%, Time Delay = 1 min/ test, Trigger Force = 40 g, number of tests = 3 times.

Table 7: AGWF2 sample with different tensile test range

Tensile Strain %	**T1 (g)**	**T2 (g)**
1%	50.44	54.7
2%	62.1	62
3%	76.28	73.49
4%	92.1	95.4
5%	116.9	117.8

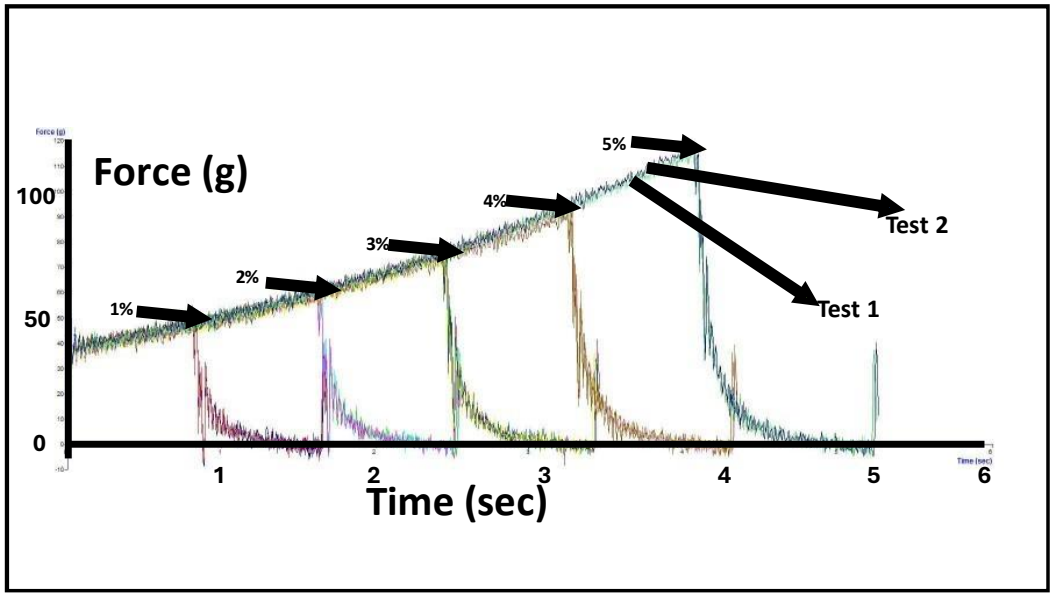

Figure 95: Repeated tests with relaxation time

The results showed that the force was lower for the first cycle when using 1%, 2%, and 4% strains. For 3% strain, the second cycle force was lower than the cycle force in the first test. For 5% strain, the forces were approximately equal for all three tests. The results are presented in

Figure 95 and Table 7. Similar tests were performed for SSNF2 with the measurements illustrated in Figure 96: SSNF2 sample testing with a different strain, and the data are shown in Table 8. The tensile test was performed using H= 90 mm, initial force of 40 = g, test speed of 1 mm/s, and strains of 1, 4, 7, and 10%. The tests indicated that the first-cycle force was lower. However, the difference was smaller when yarn was used without silicone wax.

Table 8: SSNF2 sample without silicone wax, with different tensile test ranges.

Tensile Strain %	T1(g)	T2(g)
1%	59.3	70.01
4%	96.27	151.1
7%	286.12	303.77
10%	531.04	550.5

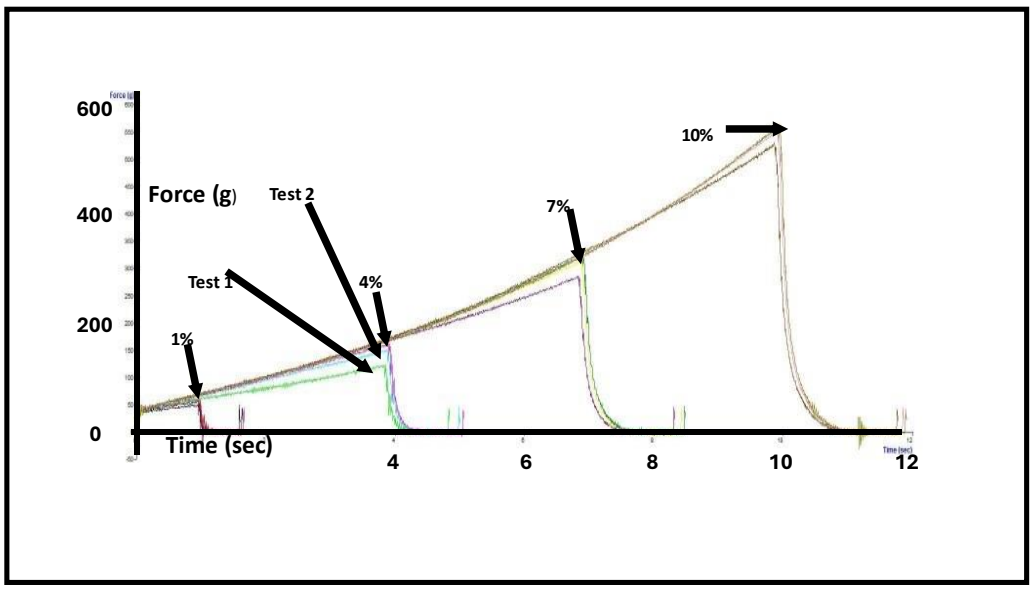

Figure 96: SSNF2 sample testing with a different strain

The anomalous first-cycle behaviour was also noted when testing both flat and tube samples knitted from stainless steel with and without Lycra.

This phenomenon has not been adequately discussed in the literature. The anomalous behaviour of the first cycle can be explained by referring to Figure 97. Initially, the sample begins in an untested state (Position A), characterized by randomness in the stitches' arrangement. As the test progresses, this randomness is reduced as the material stretched, reaching the maximum tensile strain represented by (Position AB). After the test, the sample did not return to its original state (Position A) but instead settles into a new configuration (Position B). subsequent cycles then start from (Position B) and proceed to (Position C).

The initial randomness implies that less force is required to extend and specimen for the first cycle. The material behaviour varied depending on factors such as of yarn quality, the number of stitches in the course direction, and the wale direction.

For textiles containing Lycra, the behaviour is generally more consistent. Lycra's elasticity means that while the first cycle may still produce the lowest force reading, it typically requires greater tensile strain to achieve vertical stretch. Lycra also reduced the maximum force- to -mass ratio compared to samples without Lycra because of its high elasticity.

If the applied strain during the initial stretch is low, the first reading is expected to be lowest. However, with a gradual increase in strain, the first cycle may produce a force equal to or slightly higher than that of the second cycle, depending on the yarn composition of the simple.

In summary, the explanation provided is an observation based on test results, with hypotheses incorporated to account for the anomalous behaviour of the first cycle and its dependence on material properties and initial randomness in the textile structure.

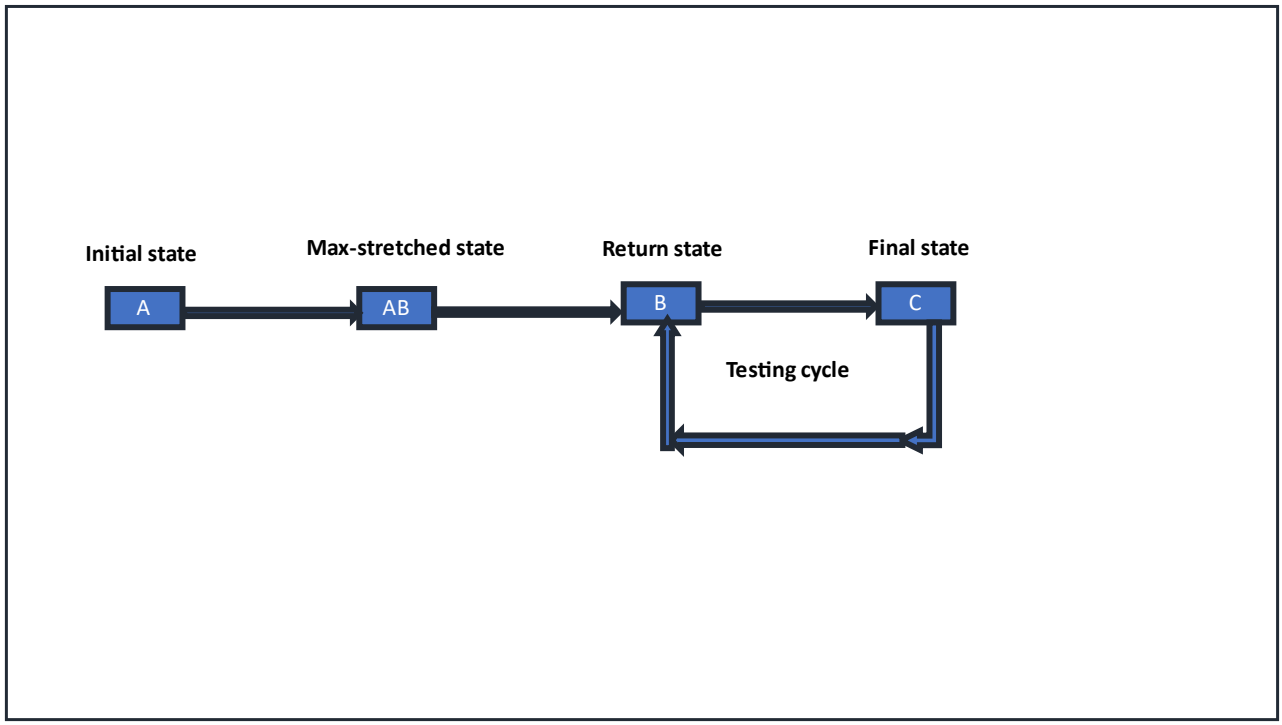

Figure 97: Random first test behaviour

Further evidence for this random "pre-strain" is observed in the first test, where the forces recorded after the sample returned to its initial displacement were smaller compared to those in subsequent cycles.

The anomalous behaviour of the stitches for the AGWF2 sample under a 5% tensile strain could be observed with the initial gauge length of the sample before being stretched at 74 mm (Figure 79). The blue line in Figure 79 represents the first reading of the test with the initial state (A) and the peak of the test where the tensile test is at the maximum state (AB), and the final test is represented as state B. The second reading of the test is represented by the orange line, where state C identifies where the next test starts, as well as where the rest of the test series begins (tests 3, 4, and 5). The unit force/ mass in (gram) refers to the trigger force which assumed to be as the same amount as the weight of the testing sample in grams.

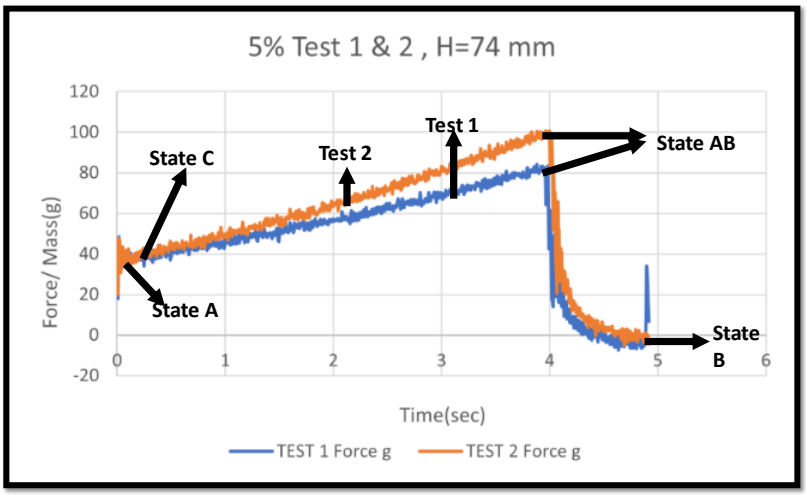

Figure 98: AGWF2 sample stitches the anomalous behaviour states. The force/mass (g) is the force in weight units

3.6.2 Comparison between Flat Stainless Steel with and without Lycra

The responses of stainless steel flat samples without Lycra (SSNF4) under 2.5% strain are displayed in Figure 99, and Figure 100 shows the corresponding outcomes for a sample without Lycra (SSNF4) under 10% strain. Several noticeable differences can be observed in Table 9.

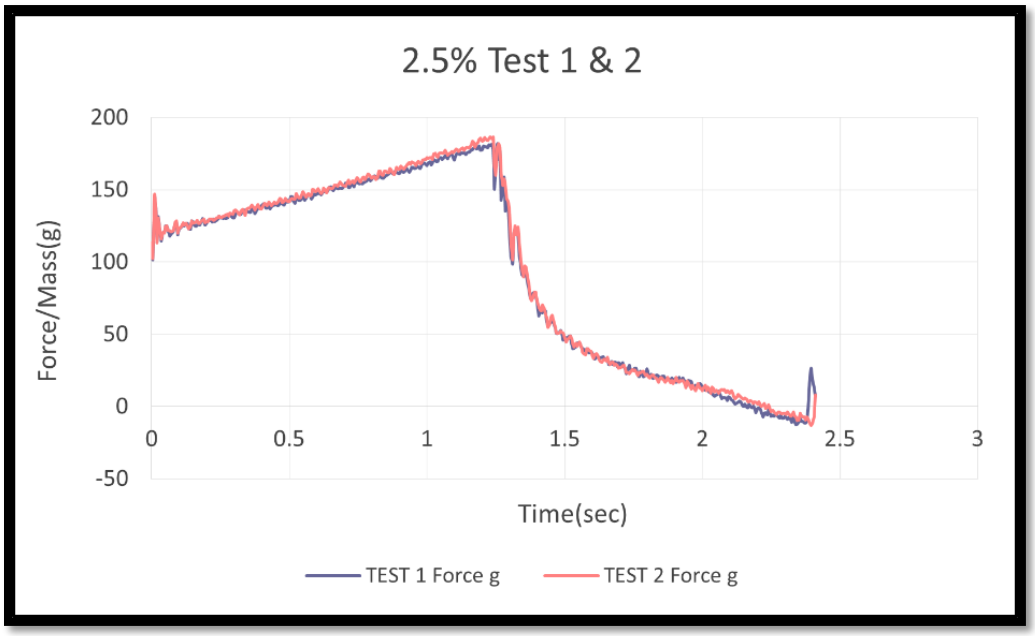

Figure 99: Stainless steel flat sample without Lycra (2.5%) (SSNF4)

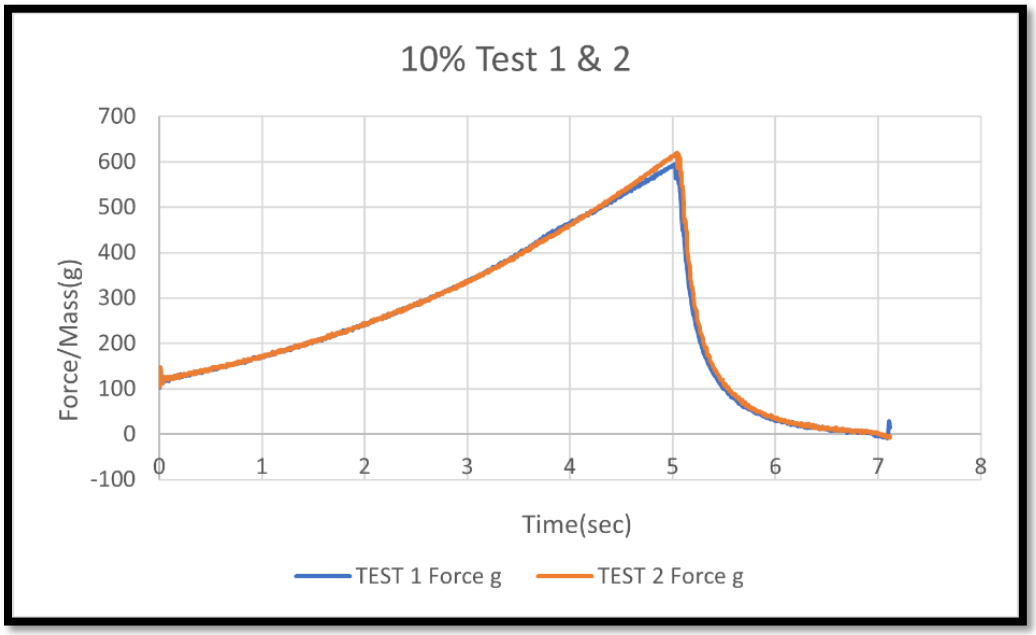

Figure 100: Stainless steel flat sample without Lycra (10%) (SSNF4)

Table 9: Stainless steel flat sample without Lycra (SSNF4) testing data

Strain%	**Max Force/Mass (g) T1**	**Max Force/Mass (g) T2**	**Test Max Time (s) T1**	**Test Max Time (s) T2**
2.5%	181.1	186.5	2.41	2.435
10%	589.8	620	7.12	7.18

For the stainless steel flat sample with Lycra (SSLF4), the maximum force/mass value shown in Table 10 and illustrated in Figure 101 is 2.5%, and 10% in Figure 102.

Table 10: Stainless steel flat sample with Lycra (SSLF4) testing data

Strain %	**Max Force/Mass (g) T1**	**Max Force/Mass (g) T2**	**Test Max Time (s) T1**	**Test Max Time (s) T2**
2.5%	148.5	149.26	2.015	1.94
10%	259.7	262.4	5.805	5.81

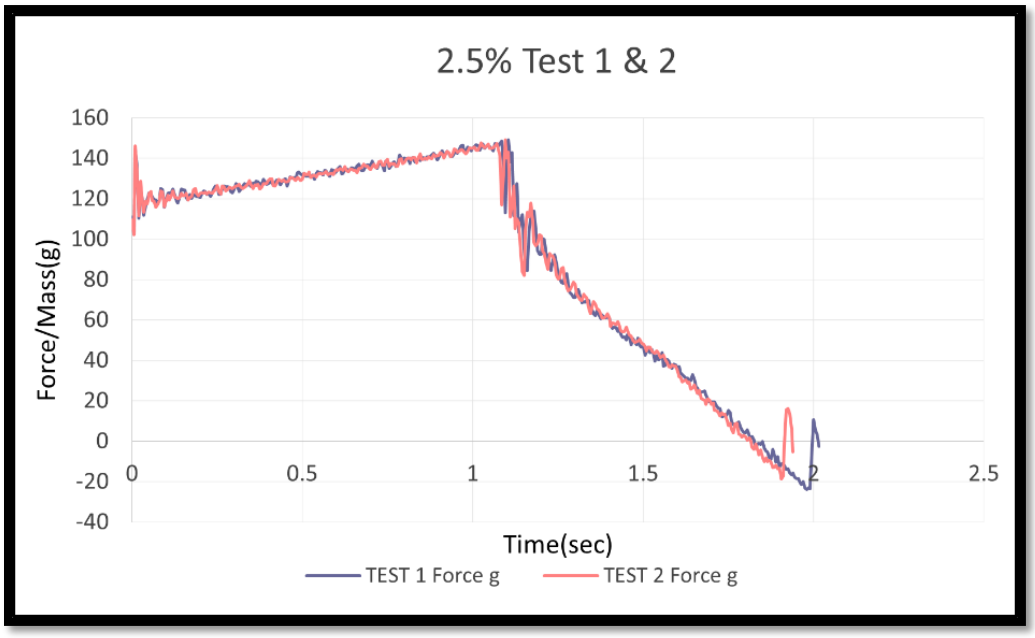

Figure 101: Stainless steel flat sample with Lycra (SSLF4) (2.5%)

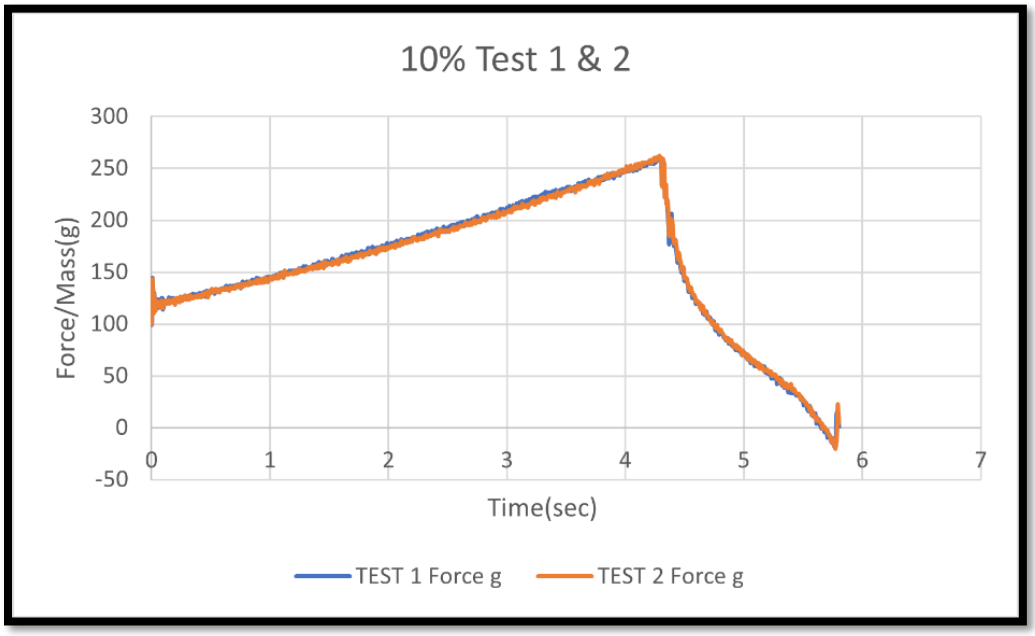

Figure 102: Stainless steel flat sample with Lycra (SSLF4) (10%)

The plots above suggest that the stainless-steel sample with Lycra seems to require much lower forces for the same strain. As can be seen in Figure 103, the first test seems more linear than

the second test because the first test needs to stretch forcibly and return to a point different from the initial point while the second test starts from the returning point, as explained previously. For the knitted fabric containing Lycra, the overall elasticity increases, requiring more force to stretch the fabric. This is because the loop length is shorter than that of the stitches in samples without Lycra.

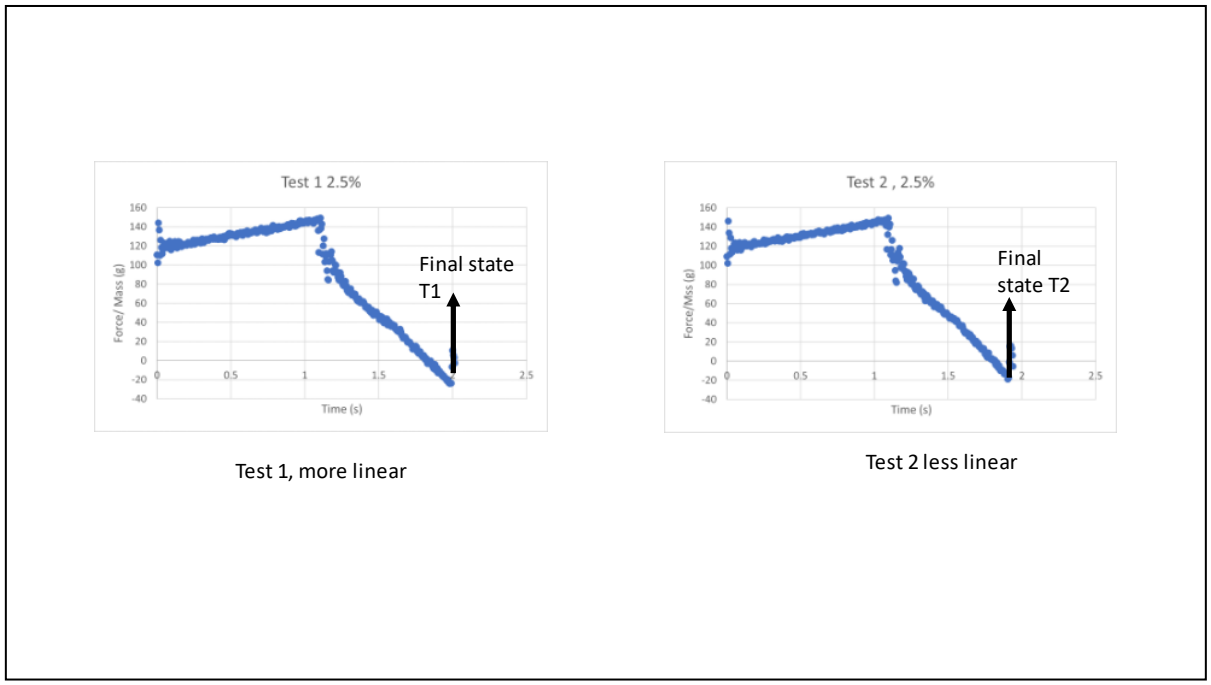

Figure 103: SSLF4 test 1 and test 2

For the stainless-steel sample, the first cycle always produced the lowest test force, with or without Lycra, because for this material, the difference was very small, even at low strain. The testing curves were very similar at a high strain (10%).

Table 9 and Table 10 show the stretching times of the two samples (SSNF4 and SSLF4). The data show that the stainless-steel sample with Lycra stretched for less time than the sample without Lycra, even when the tensile strain applied to the samples was high or low. This is because the sample with Lycra did not stretch easily because the stitches were closer to each other. Therefore, the time required for stretching was shorter than that required for the sample that does not consist of Lycra.

3.6.3 Comparison between Tube and Flat Stainless-Steel Samples

Stainless steel tube samples with and without Lycra were also tested. The data are presented in Table 11 for a 2.5% strain in Figure 104 and for a 10% strain in Figure 105.

Table 11: Stainless steel tube sample with Lycra (SSLT1) testing data

Strain %	**Max Force/Mass (g) T1**	**Max Force/Mass (g) T2**	**Test Max Time (s) T1**	**Test Max Time (s) T2**
2.5%	140.4	139.5	1.47	1.4
10%	220.3	221.5	3.495	3.51

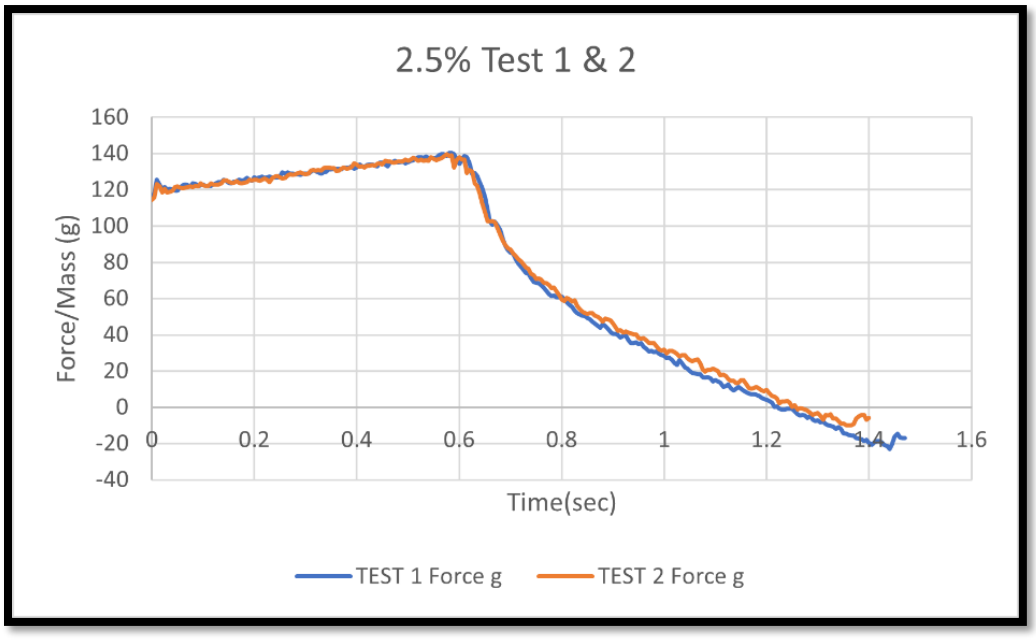

Figure 104: Stainless steel tube sample with Lycra (SSLT1) (2.5%)

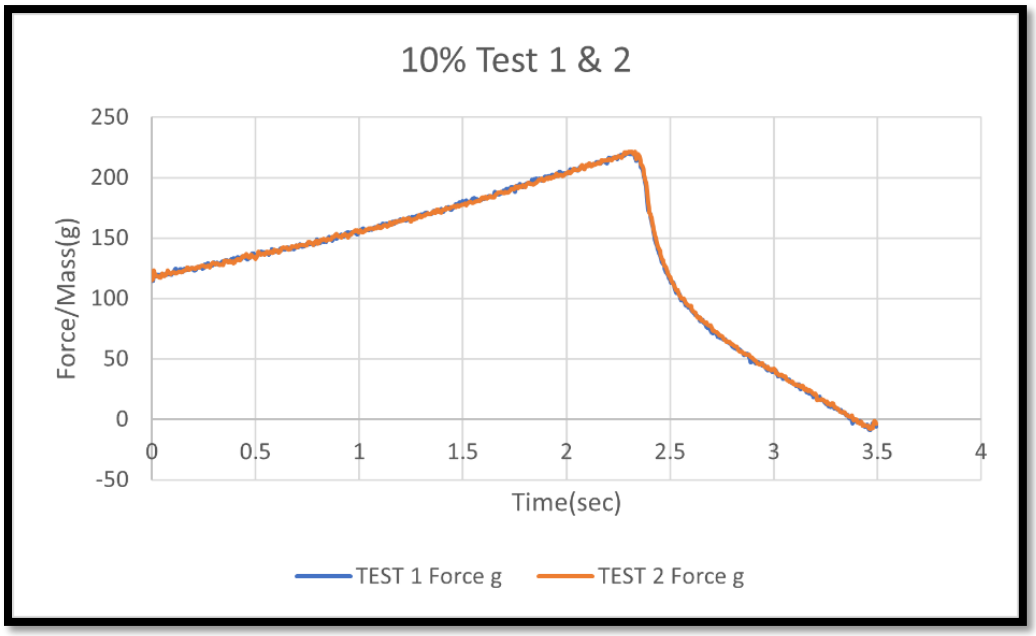

Figure 105: Stainless steel tube sample with Lycra (SSLT1) (10%)

For the stainless steel tube sample without Lycra (SSNT1), data are shown in Table 12 and the testing cycle is illustrated in Figure 106 and Figure 107 below.

Table 12: Stainless steel tube sample without Lycra (SSNT1) testing data

Strain %	**Max Force/Mass (g) T1**	**Max Force/Mass (g) T2**	**Test Max Time (s) T1**	**Test Max Time (s) T2**
2.5%	208.98	208.4	1.185	1.185
10%	822.8	820	3.61	3.615

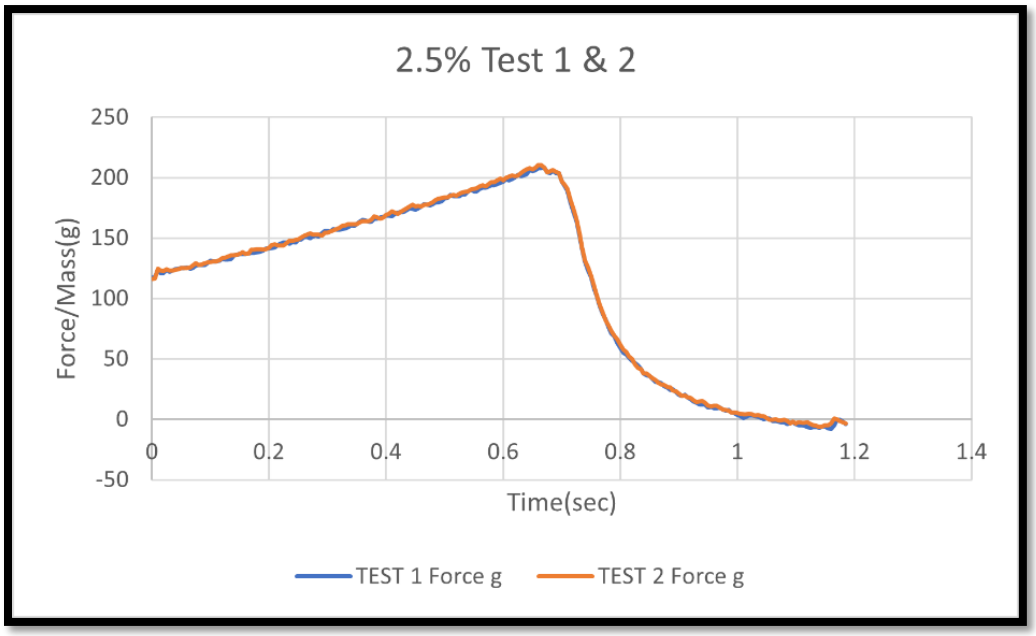

Figure 106: Stainless steel tube sample without Lycra (SSNT1) (2.5%)

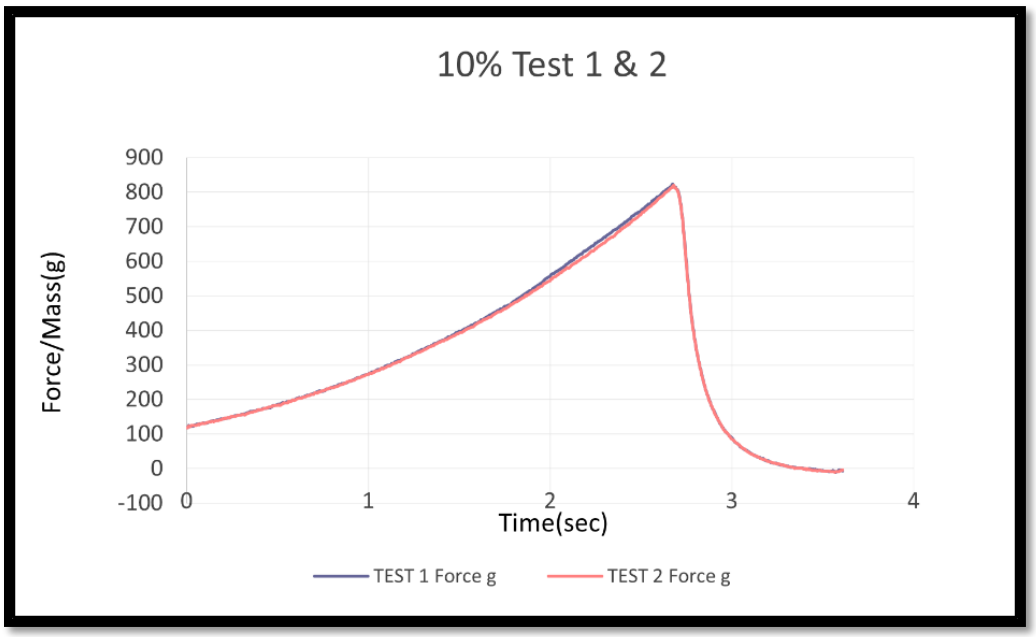

Figure 107: Stainless steel tube sample without Lycra (SSNT1) (10%)

The analysis of the tensile test for the stainless-steel tube samples with and without Lycra highlighted some fundamental features as noted below:

- At both tensile strains (2.5% and 10%), the first test reading is very close to the second test reading in Table 11 and Table 12 compared with the previous samples represented as stainless-steel flat-knitted fabric with and without Lycra. This is because the tube sample was thinner than that of the flat sample. The tube-knitted fabric in this study was observed to be more elastic and less thick to touch. In addition, it exhibited considerable movement owing to its lower stiffness. In comparison, the flat knit showed higher stiffness, with its stitches being more compressed. All these properties made the stretching of the tube sample more flexible, and as a result, the test curve was very close for all testing attempts.
- Because of the high elasticity of the tube knit, the stretching time for the samples with and without Lycra was less than the stretching time for the flat sample. They stretched more easily and faster than the flat-knit samples.
- When the tube knit sample trigger force was very high (120 g), after the sample stretching, the curve reached a very high value of force/mass and then returned to the original position again, returning to zero. However, when stretched, the flat sample reached a peak, and when the sample returned to the original position, it had a negative value of force/mass.

It also appears that the tube knit sample without Lycra had more freedom to stretch than the flat knit sample without Lycra and the value of the maximum force in both low and high tensile strain was higher than that of the flat knit sample without Lycra because the round shape of the tube sample made it easier to stretch. With the flat knit sample without Lycra, the value of the maximum mass was very close to the value of the maximum mass for the tube knit sample without Lycra. Both flat and tube-knitted samples with Lycra were less elastic. The Lycra samples were less elastic because of the specific properties of the Lycra, such as the high elasticity, high tenacity, excellent recovery to the original shape, lightweight, and being very soft as well as its effect on the dimensions of the stitches.

3.6.4 Polyester Samples with and without Lycra

Testing was then performed using different nonconductive materials to investigate the differences in behaviour between these materials for lengthwise stretching. Polyesters are

widely used in producing non-conductive knitted fabrics, primarily due to the versatility and durability of polyester yarns and fibres. Polyester is created through a polymerization process involving Ethylene glycol and terephthalic acid, which serve as its primary precursors.

Polyester is renowned for its numerous beneficial properties, making preferred material in textile manufacturing (Jaffe et al., 2020)

- Durability: Polyester fibres are highly resistant to shrinking, stretching, wrinkling and abrasion, ensuring long-lasting performance.
- Mechanical strength: They exhibit exceptional tensile and tear strength, enabling the fabric to withstand significant stress and wear.
- Low Moisture Absorbency: Polyester fibres absorb minimal moisture, making them quick-drying and resistant to mould or mildew.
- Lightweight Yet Strong: Despite being lightweight, polyester is remarkably strong, offering a balance of comfort and resilience.
- Shape Retention: Polyester fabrics maintain their shape exceptionally well, resisting deformation even under strain.
- Chemical Resistance: The fibres can endure exposure to various chemicals, enhancing their adaptability in different environments.

These properties collectively make polyester an excellent choice for applications ranging from everyday clothing to technical and industrial textiles.

The experimental test for this knitted fabric was divided into four groups: flat polyester with Lycra, flat polyester without Lycra, tube polyester with Lycra and tube polyester without Lycra (as shown in Table 13) Each was tested with strains of 2.5% and 10%. The results for the polyester flat knit with Lycra are shown in Figures 107 and 108.

Table 13: Polyester flat sample with Lycra (PELF1) testing data

Strain %	**Max Force/Mass (g) T1**	**Max Force/Mass (g) T2**	**Test Max Time (s) T1**	**Test Max Time (s) T2**
2.5%	359.1	479.1	3.625	3.625
10%	1137.02	1134	14.345	14.365

A clear difference was observed between the first and second tests under a low strain (2.5%), although both test results were very close to each other under a high strain (10%).

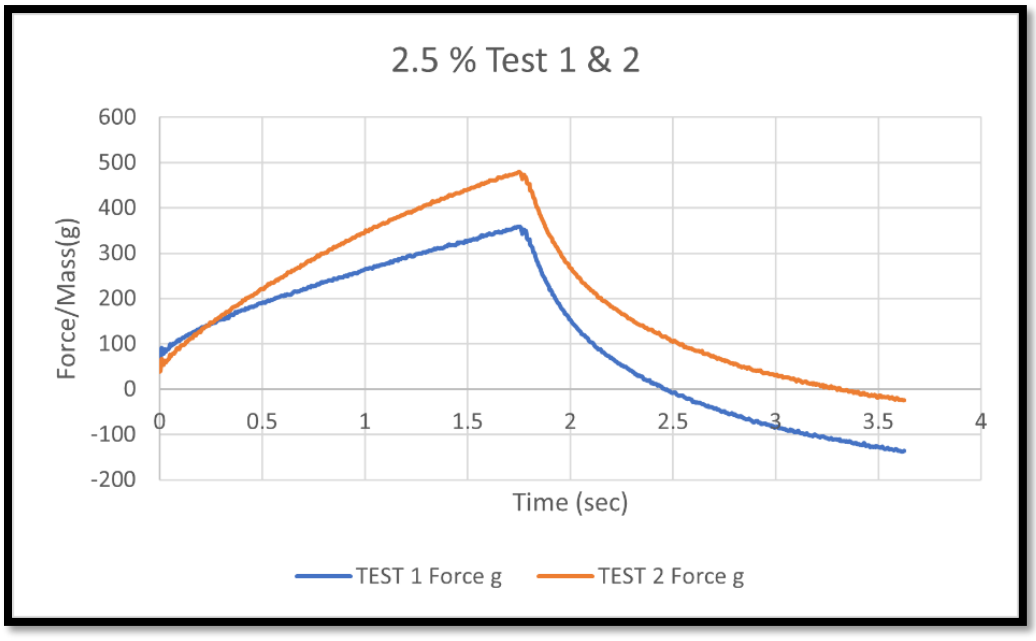

Figure 108: Polyester flat sample with Lycra (PELF1) (2.5%)

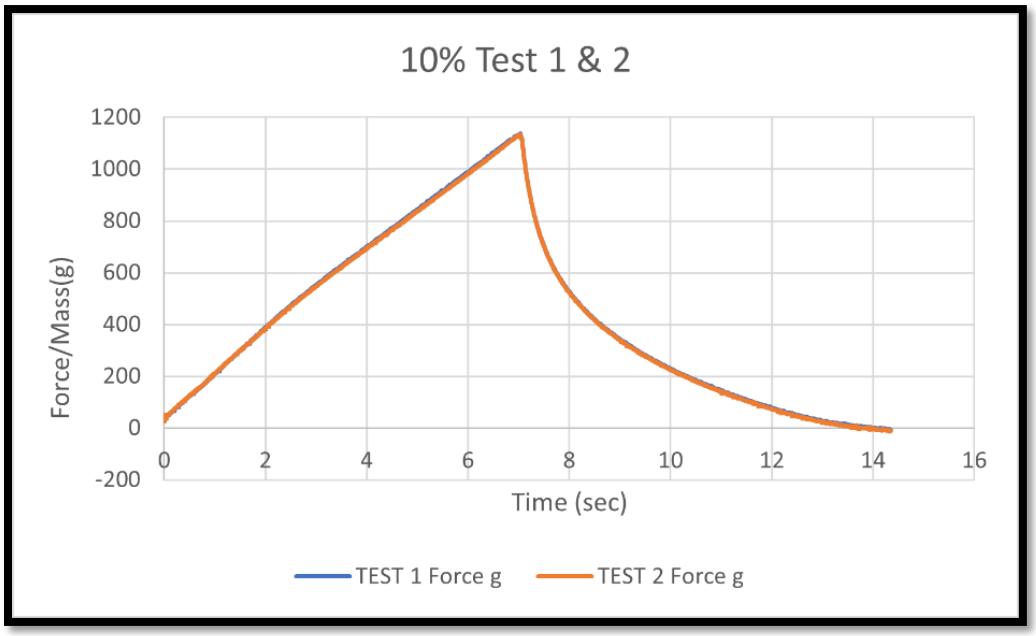

Figure 109: Polyester flat sample with Lycra (PELF1) (10%)

For the polyester flat knitted fabric without Lycra, the testing data are presented in Table 14, and the testing results are shown in Figure 110 and Figure 111.

Table 14: Polyester flat sample without Lycra (PENF1) testing data

Strain %	**Max Force/Mass (g) T1**	**Max Force/Mass (g) T2**	**Test Max Time (s) T1**	**Test Max Time (s) T2**
2.5%	501	620.1	4.35	4.375
10%	1617	1654	17.57	18.06

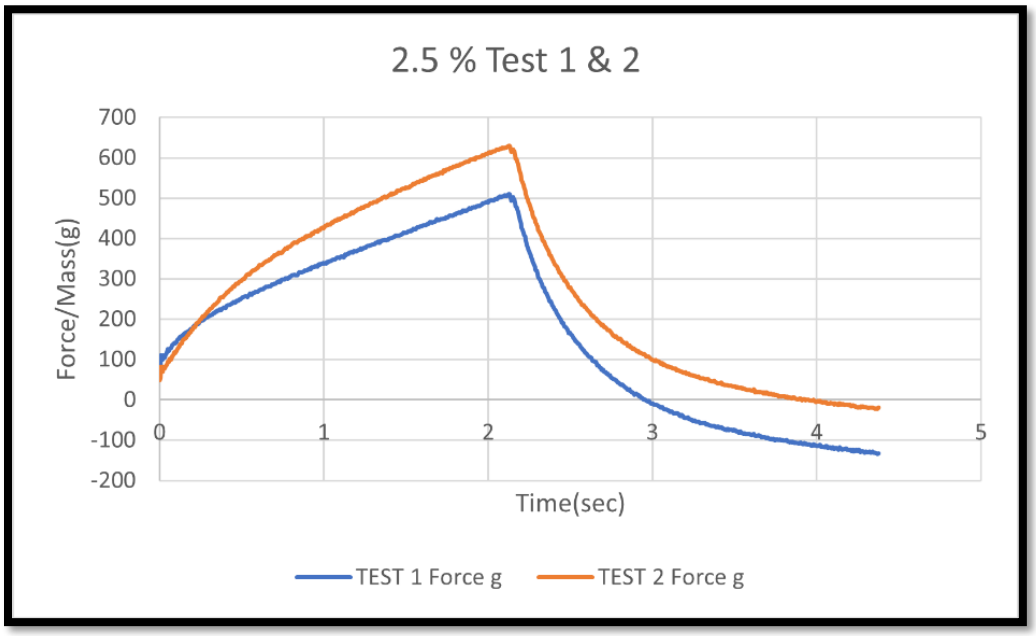

Figure 110: Polyester flat sample without Lycra (PENF1) (2.5%)

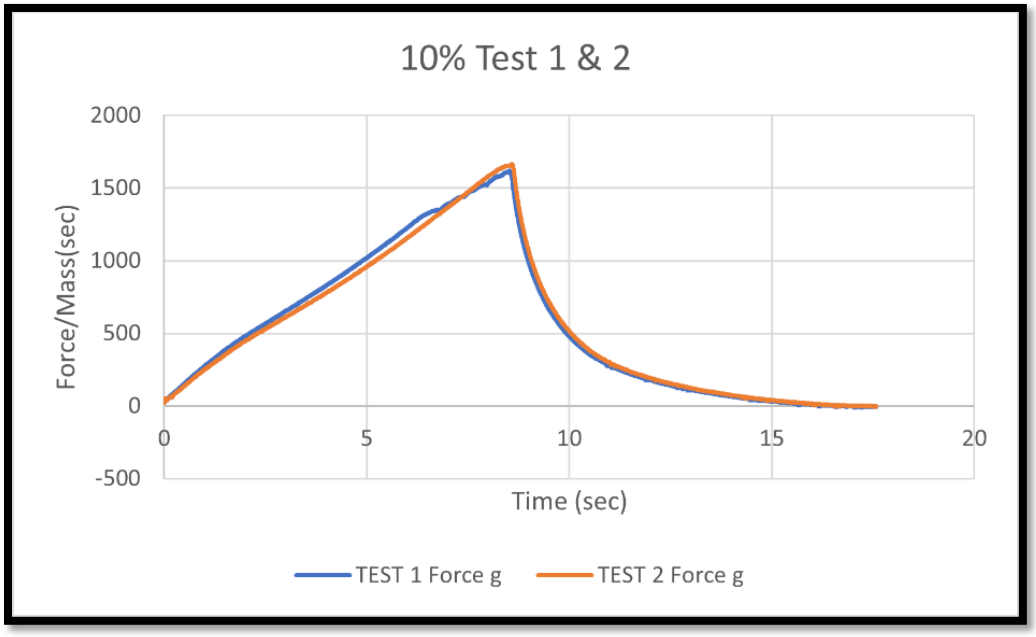

Figure 111: Polyester flat sample without Lycra (PENF1) (10%)

The results of these tests demonstrate the distinctive features of the polyester samples with and without Lycra. When the fabric contained Lycra, the sample extended with lower forces than the fabric without Lycra. Lycra is more extensible (requires a lower force to extend) than polyester, which is known to return to its original state and is highly strain-resistant (that is, stiff). When polyester was mixed with Lycra, it extended with a lower force.

With polyester under high strain, the fabric test shows a negligible difference between the first and subsequent test cycles (the test trend curves start and return to zero). In contrast, at low strains, the first measurement cycle returns to a much more negative force than the subsequent testing cycles. This behaviour was not observed in the stainless-steel fabric.

The testing data for the polyester tube sample with Lycra are shown in Table 15 and illustrated in Figure 112 and Figure 113.

Table 15: Polyester tube sample with Lycra (PELT1) testing data

Strain %	**Max Force/Mass (g) T1**	**Max Force/Mass (g) T2**	**Test Max Time (s) T1**	**Test Max Time (s) T2**
2.5%	204.45	398	2.625	2.625
10%	793	785	10.135	10.135

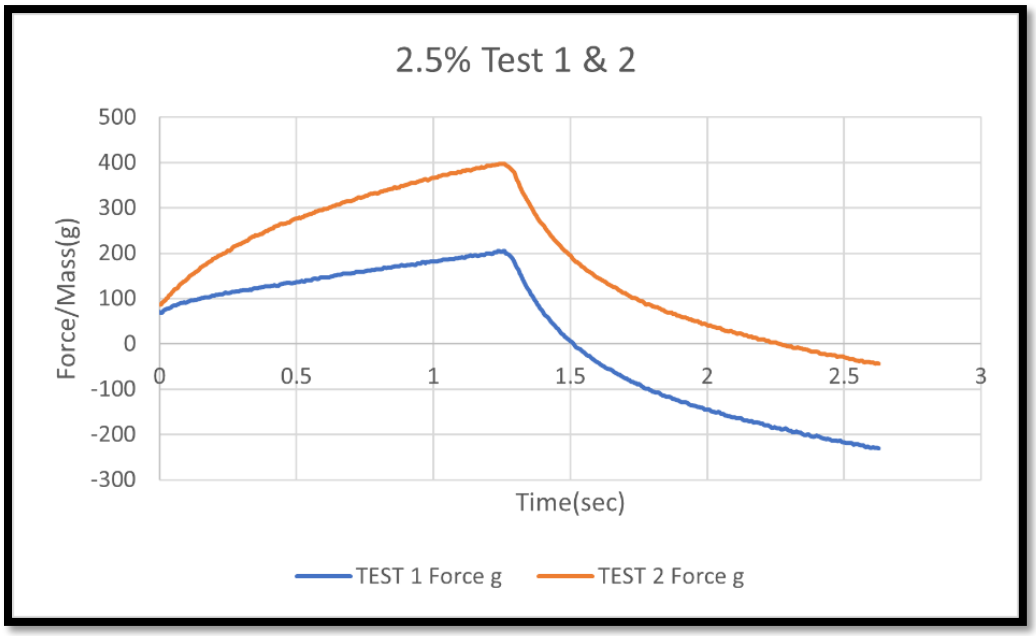

Figure 112: Polyester tube sample with Lycra (PELT1) (2.5%)

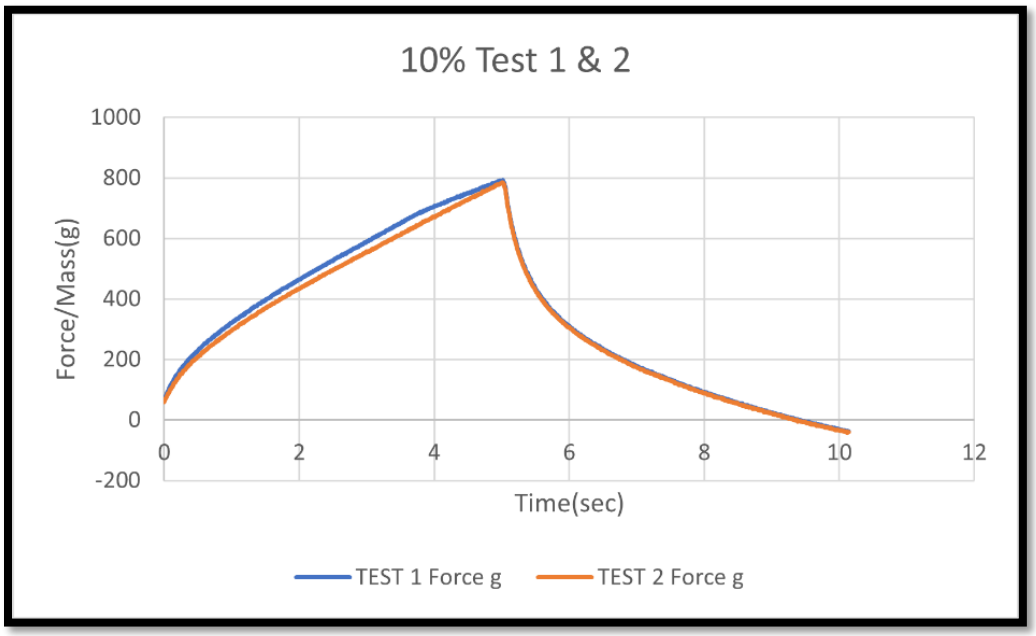

Figure 113: Polyester tube sample with Lycra (PENT1) (10%)

The data for the polyester tube without Lycra are shown in Table 16 and illustrated in Figure 114 and Figure 115.

Table 16: Polyester tube sample without Lycra (PENT1) testing data

Strain %	**Max Force/Mass (g) T1**	**Max Force/Mass (g) T2**	**Test Max Time (s) T1**	**Test Max Time (s) T2**
2.5%	316	365	3.39	2.39
10%	794	787	13.32	13.345

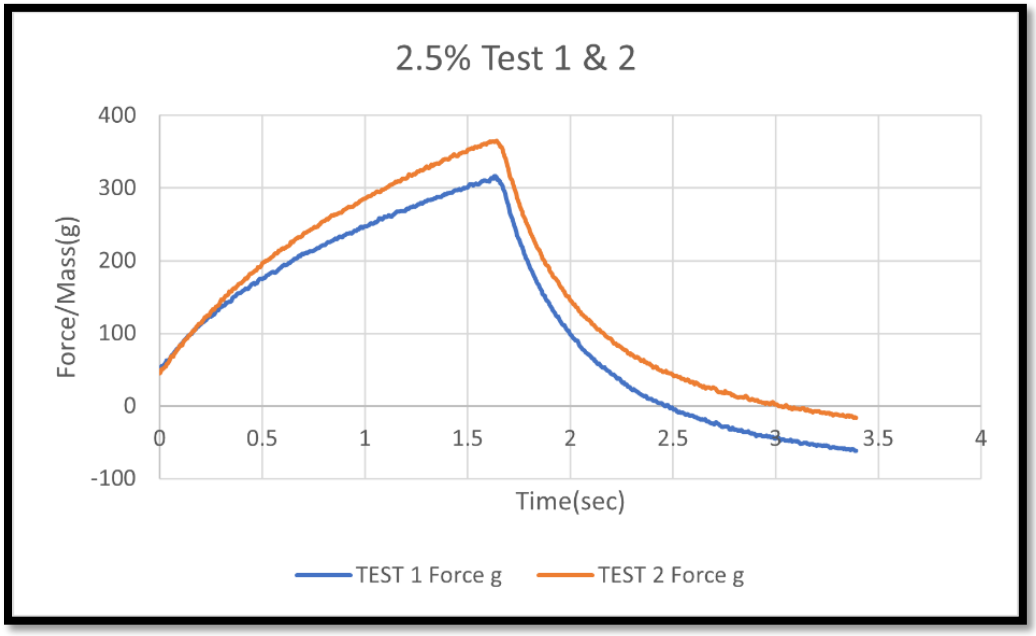

Figure 114: Polyester tube sample without Lycra (PENT1) (2.5%)

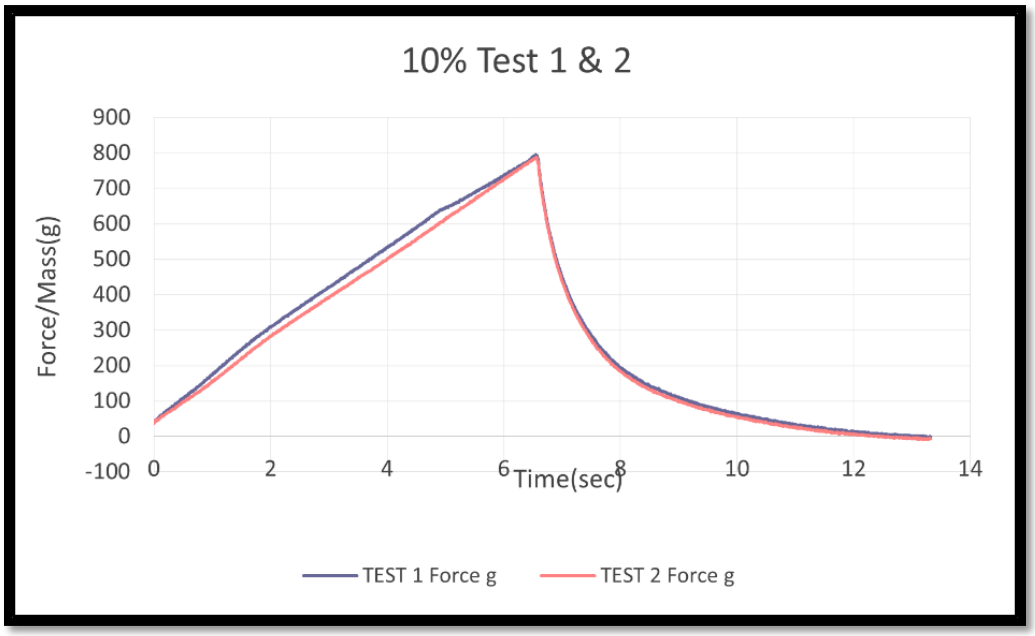

Figure 115: Polyester tube sample without Lycra (PENT1) (10%)

3.6.5 Comparison of Polyester Tubes with and without Lycra

When we compare the tube sample with and without Lycra, it can be seen the starting time for the sample with Lycra is less than the time for the sample without Lycra. This is because the tests started at a particular force; then, the strain was measured from the original length for the subsequent testing attempts.

3.6.6 Comparison between Polyester Flat and Tube Samples

The results show that flat polyester samples with Lycra at low strain or high strain required more force to stretch than the tube sample with Lycra. However, in general, the flat samples with and without Lycra required a higher force than the tube samples with and without Lycra. As explained previously, the tube knit is thinner than the flat knit and more flexible, requiring less force to be stretched under the given strain.

The tube sample without Lycra required more force than the tube sample with Lycra under low and high tensile strains.

Notably, the behaviour of the polyester knit fabric differed from that of the stainless steel knit fabric. The stainless-steel flat samples with and without Lycra required less force than the tube samples with and without Lycra.

The outcomes of the testing were notably influenced by the distinctive properties of polyester fibre, such as its exceptional resistance to shrinkage, abrasion, and stretching, as well as its high strength, lightweight nature, and remarkable ability to revert to its original shape.

3.6.7 Comparison between Polyester Samples with Different Stitch Densities

Experiments were performed to explore the influence of the stitch length on the fabric reaction. Three polyester samples without Lycra were prepared. Each had the same number of stitches (120), but the length of the stitches of the samples varied (1.166 mm, 1.25 mm, and 1.33 mm), resulting in overall dimensions of 140, 150, and 160 mm in width and 95 mm in height. For comparison, the samples for which the results were previously presented had stitch dimensions of 1.357 mm.

The results are presented in Table 17 and illustrated in Figure 116 and Figure 117.

Table 17: Polyester flat 140 mm sample without Lycra (PENF4) testing data

Strain %	**Max Force/Mass (g) T1**	**Max Force/Mass (g) T2**	**Test Max Time (s) T1**	**Test Max Time (s) T2**
2.5%	231.96	271.3	4.235	3.995
10%	791.18	841	13.18	13.42

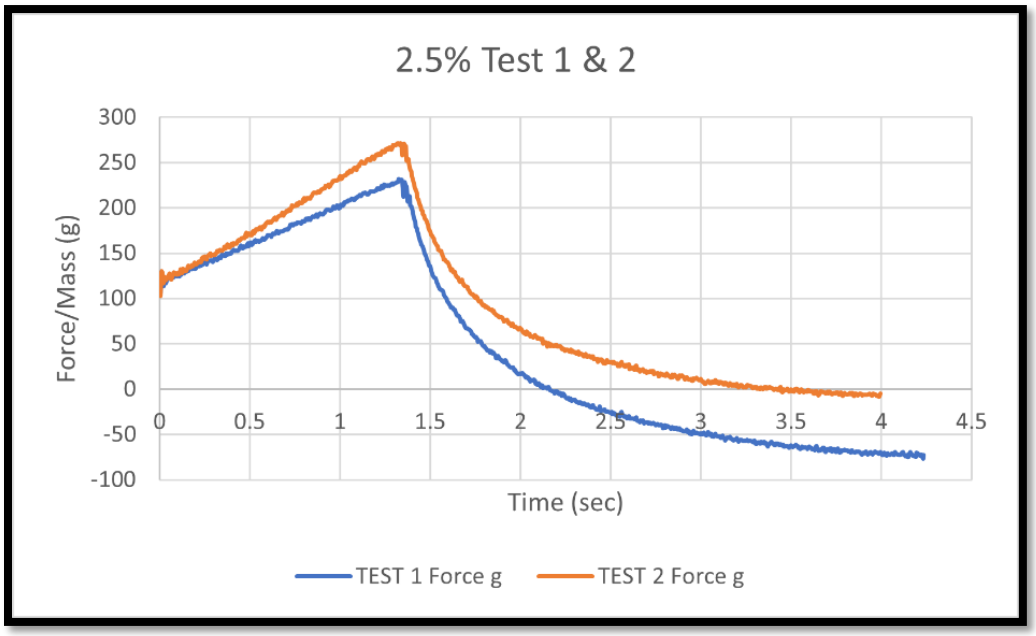

Figure 116: Polyester flat sample 140 mm (PENF4) (2.5%)

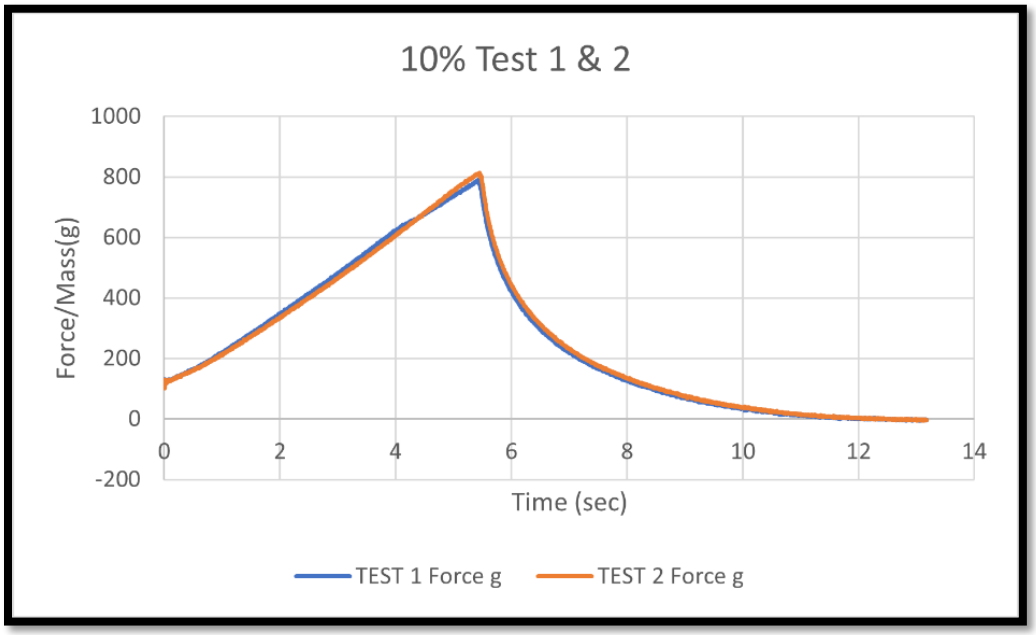

Figure 117: Figure 18: polyester flat sample 140mm (PENF4) (10%)

The 150 mm sample data are presented in Table 18 and illustrated in Figure 118 and Figure 119.

Table 18: Polyester flat 150 mm sample without Lycra (PENF3) testing data

Strain %	**Max Force/Mass (g) T1**	**Max Force/Mass (g) T2**	**Test Max Time (s) T1**	**Test Max Time (s) T2**
2.5%	255.6	347.5	3.3	3.125
10%	832	842	11.665	11.735

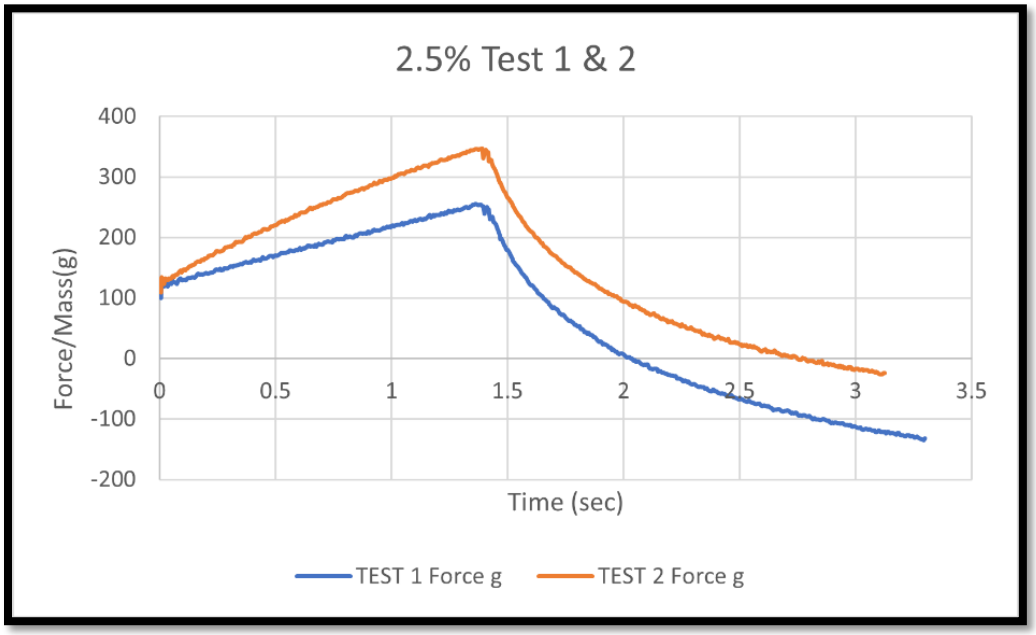

Figure 118: Polyester flat sample 150mm (PENF3) (2.5%)

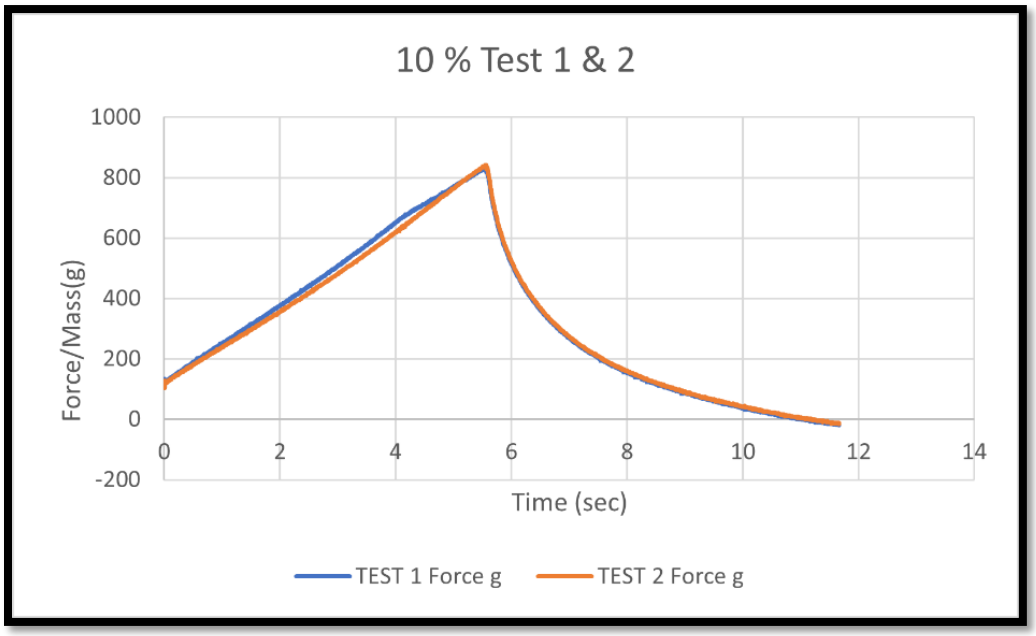

Figure 119: Polyester flat sample 150mm (PENF3) (10%)

For the 160 mm polyester flat sample, the resulting data are presented in Table 19 and Figure 120 with Figure 121 below.

Table 19: polyester flat 160 mm sample without Lycra (PENF2) testing data

Strain %	**Max Force/Mass (g) T1**	**Max Force/Mass (g) T2**	**Test Max Time (s) T1**	**Test Max Time (s) T2**
2.5%	243	256	4.525	4.275
10%	622.5	629	15.19	15.29

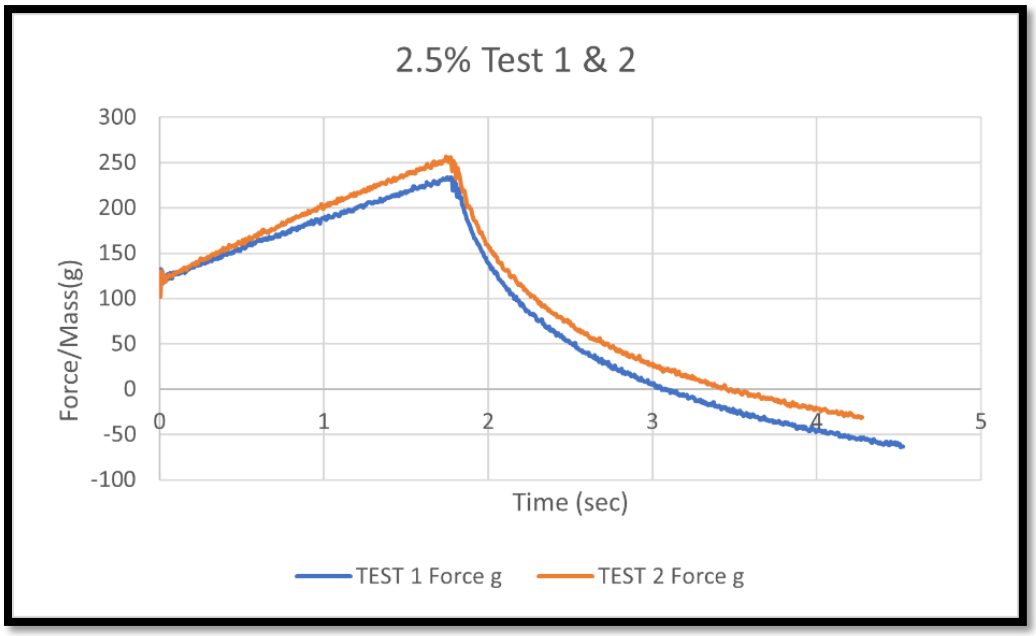

Figure 120: Polyester flat sample 160 mm (PENF2) (2.5%)

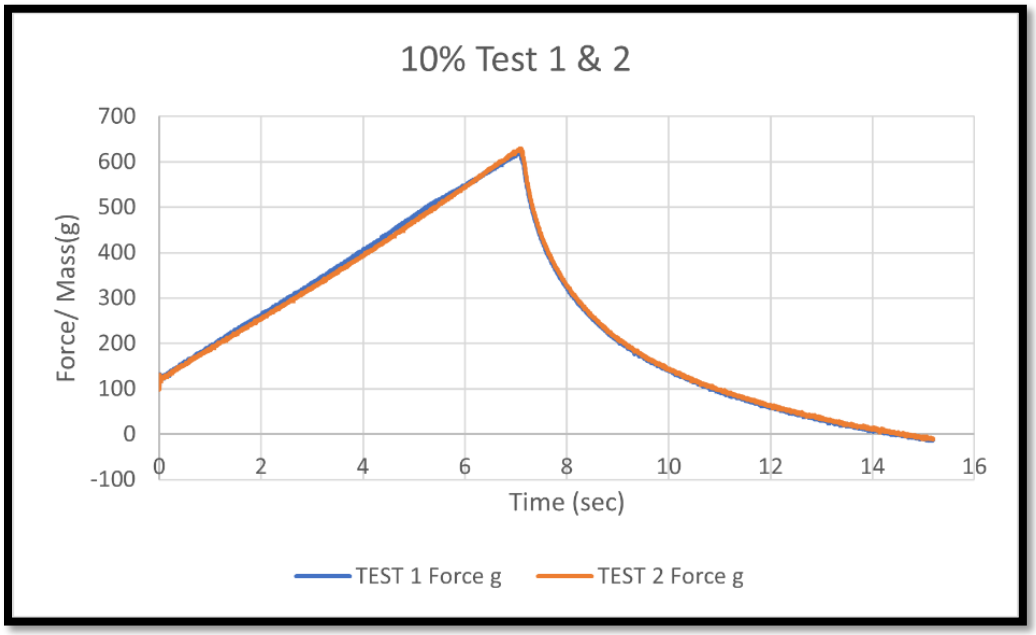

Figure 121: Polyester flat sample 160 mm (PENF2) (10%)

3.6.8 Comparison with Polyester Sample with High Stitch Density

Tensile tests were conducted with another sample made of polyester but with a different stitch density. The new sample had 163 stitches but was the same size (163 mm in width) as the previous samples with 120 stitches. This corresponded to a stitch size of 1 mm. The results are presented in Table 20 and Figure 122 Figure 123.

Table 20: Polyester flat 163 stitches sample without Lycra (PENF5) testing data

Strain %	**Max Force/Mass (g) T1**	**Max Force/Mass (g) T2**	**Test Max Time (s) T1**	**Test Max Time (s) T2**
2.5%	415.5	615.6	3.01	2.975
10%	1345.4	1378.3	11.41	11.47

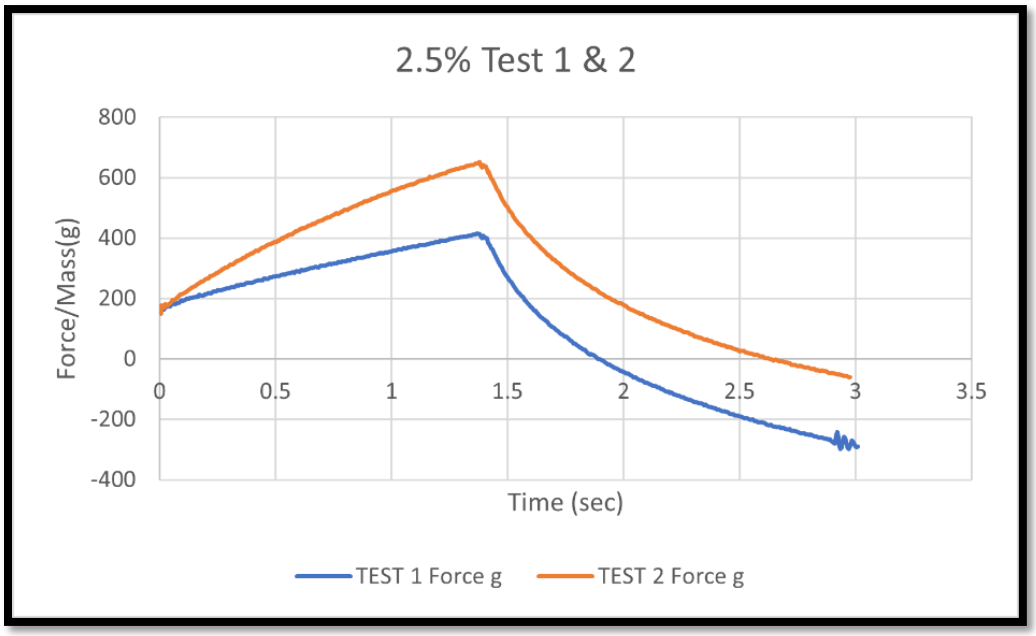

Figure 122: Polyester flat sample 163 stitches (PENF5) (2.5%)

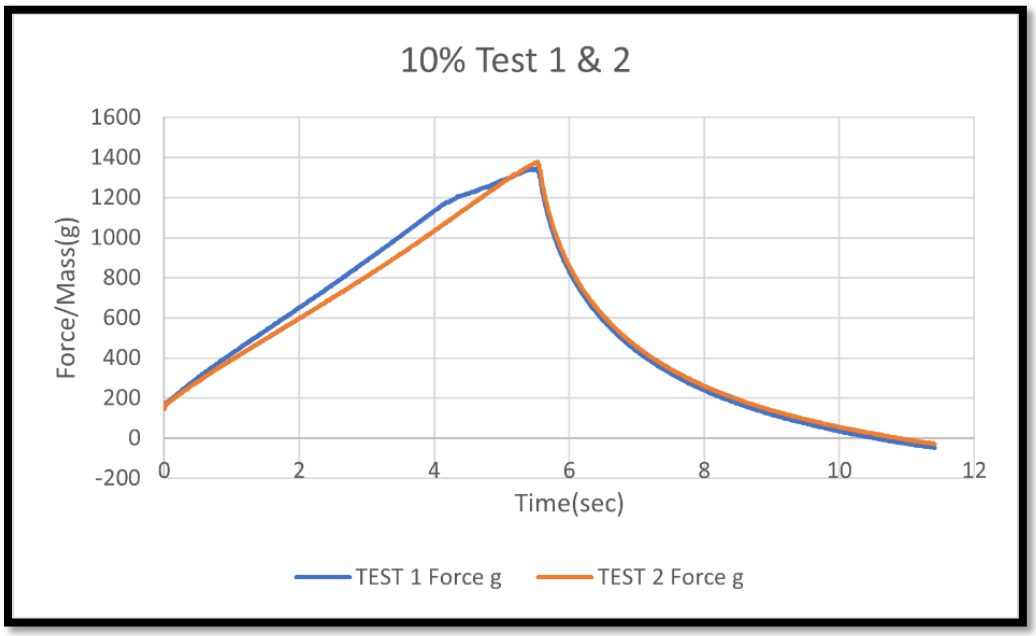

Figure 123: Polyester flat sample 163 stitches (PENF5) (10%)

A comparison between PENF5 and PENF1 revealed distinct patterns. At a low tensile strain (2.5%), PENF5 required less force for the initial extension, mirroring the trend observed at a high tensile strain (10%). Additionally, the maximum time required to stretch PENF5 was

notably shorter than that of PENF1. These findings suggest a correlation: smaller stitches seem to facilitate a quicker and easier stretching process based on the observed results.

3.6.9 Rubber Sample Testing Result

Rubber is a unique material characterised by its remarkable elasticity and viscosity. It possessed a low modulus of elasticity, allowing it to undergo deformation of as up to 1000 % (J. Schaefer, 2018). Once the deforming force is removed, the rubber quickly returns to its original dimensions, demonstrating its high elasticity and resilience.

Rubber features a low modulus of elasticity, allowing for softness and easy deformation, while also having high elasticity to return to its original shape. This unique property comes from its long, coiled polymer chains that uncoil under stress and cross-links in the polymer network that provide "memory." This combination makes rubber highly stretchable, flexible, and resilient, making it ideal for applications requiring both flexibility and durability.

In this thesis, experiments were conducted on rubber to compare its behaviour with that of knitted fabrics, providing insights into their respective mechanical and elastic properties.

The test results for the rubber sample are presented in Table 21 and illustrated in Figure 124 and Figure 125.

Table 21: Rubber sample (RUBF1) testing data

Strain %	**Max Force/Mass (g) T1**	**Max Force/Mass (g) T2**	**Test Max Time (s) T1**	**Test Max Time (s) T2**
2.5%	245.1	251.9	5.38	5.43

10%	783.9	787.7	20.475	20.505

Figure 124 and Figure 125 show that the behaviour of the rubber material sample is different from that of the other tested materials under the same conditions. Although the rubber sample generated forces of similar magnitude to the textile samples, for the low strain (2.5%), test one and test two were very close to each other, while under high strain (10%), the curves of the two tests were congruent. The shape of the test curve was also significantly different, presenting a triangular shape. The triangular shape of the test curve indicates the material exhibits elastic behaviour, with a proportional relationship between stress and strain during loading and unloading. Its return to near-zero force demonstrates high elasticity and minimal residual stress, allowing it to recover almost fully without permanent deformation.

Rubber demonstrates more linear behaviour compared to textiles, although some randomness in the initial configuration is evident in both low-strain and high-strain tests. This variability may be attributed to the margin of error in the test equipment.

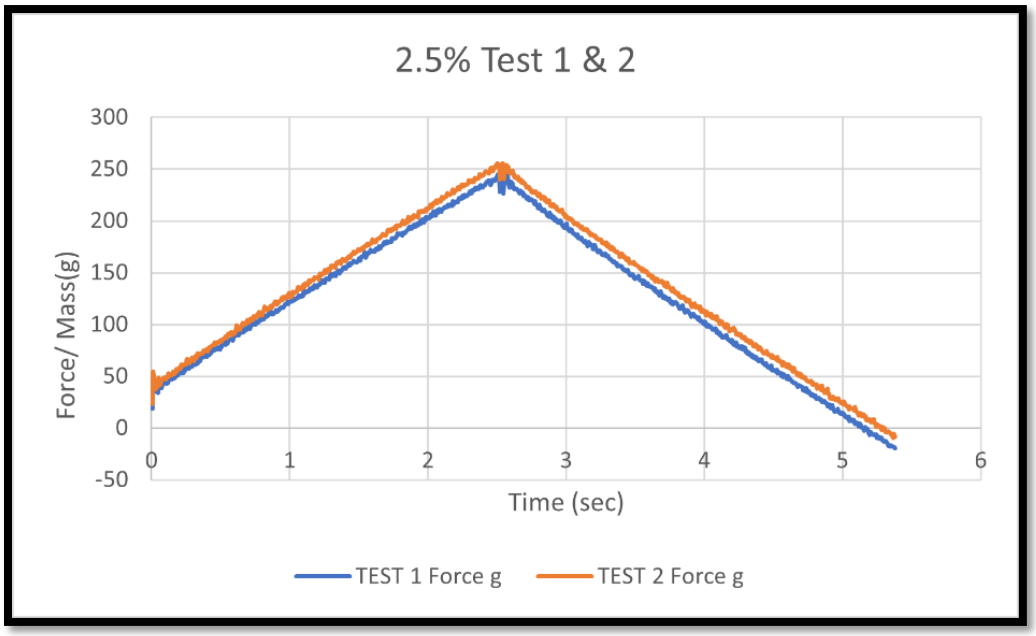

Figure 124: Rubber sample (RUBF1) (2.5%)

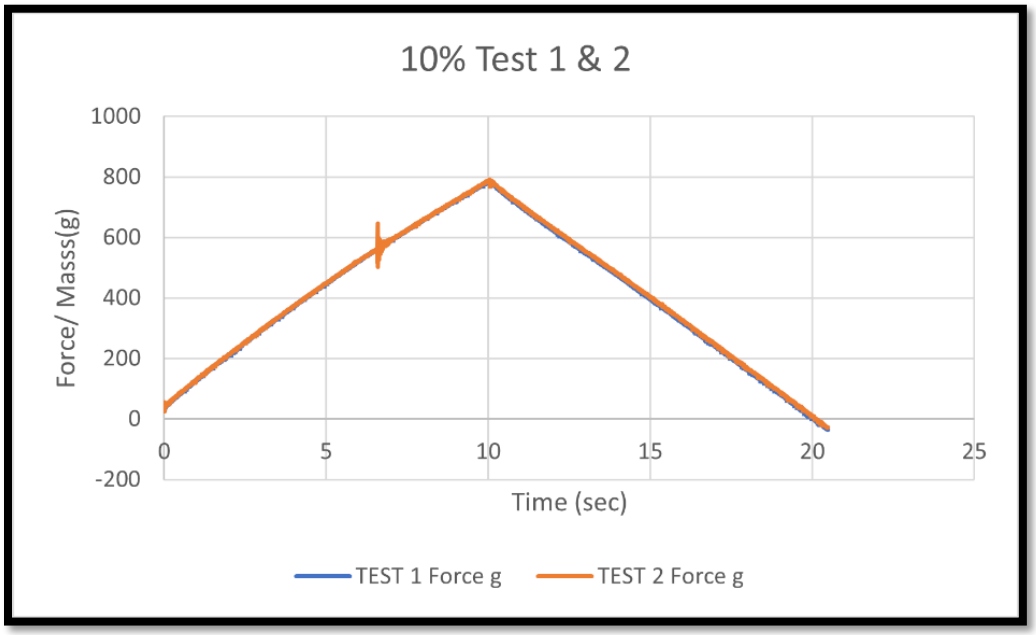

Figure 125: Rubber sample (RUBF1) (10%)

3.7 PIV Results

The outcomes generated by PIVlab complemented the experimental investigation into the behaviour of the samples under strain by providing a detailed analysis. Using image processing, the software tracked the movement of fibres from point to point, as indicated by the directional arrows, offering valuable insights into the material response to stain. For instance, in the case of the silver sample (AGWF2), which had 70 stitches in the wale direction and 40 stitches in the course direction as depicted in Figure 126, the sample was secured between the clamps of the texture analyser. Notably, owing to the camera settings, only one clamp was visible in the recording.

The post-image analysis shown in Figure 127, demonstrates velocity magnitude of the sample obtained from the test results. This analysis was conducted on processed images captured during the testing, providing valuable insights into the sample's behaviour.

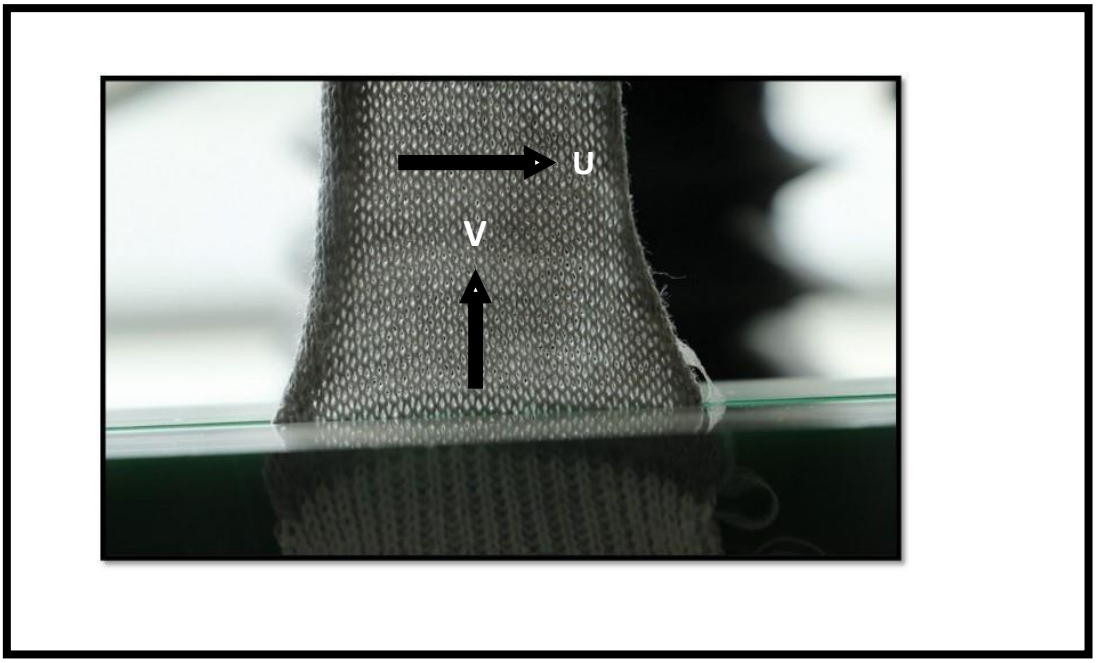

Figure 126: Silver sample with wax (AGWF2)

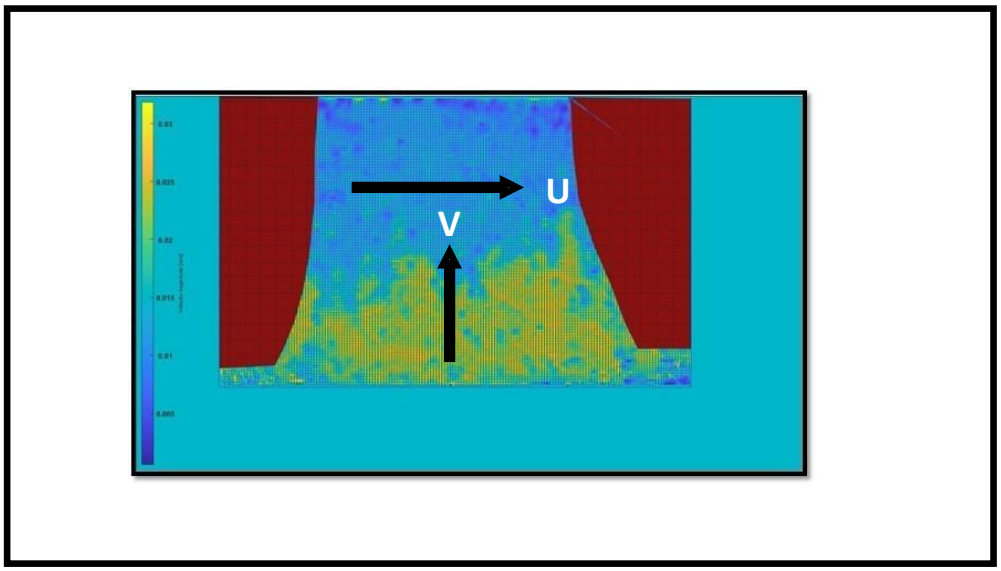

Figure 127: Velocity magnitude of the silver sample (m/s) (AGWF2) (MATLAB, 2023)

The results for the velocity magnitude at a strain of 5% are shown in the V component (m/s) and U component(m/s) in Figure 128 and Figure 129, respectively.

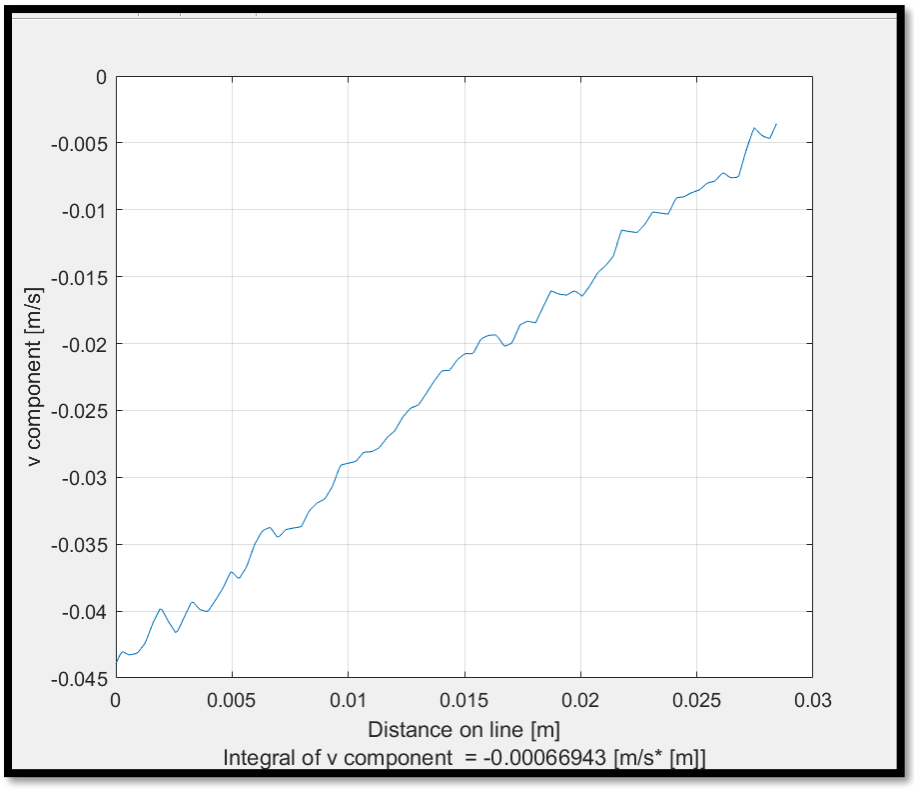

Figure 128: V component (m/s) (MATLAB, 2023)

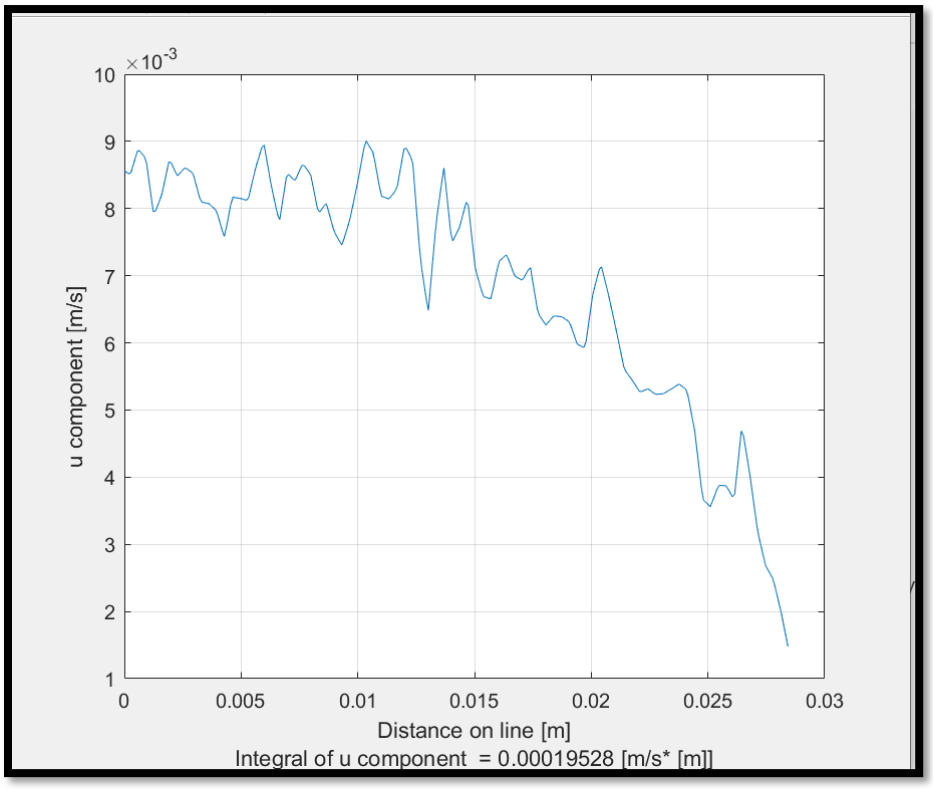

Figure 129: U component (m/s) (MATLAB, 2023)

The V and U components both represent the velocity of the same test, but there are marked differences between the V and U components. Thus, the U component represents the horizontal velocity component, typically from left to right (or right to left). It is associated with movement along the x-axis of the image. The V component, on the other hand, represents the vertical velocity component, typically from top to bottom (or bottom to top). It is associated with movement along the y-axis of the image. This means that the negative sign of the velocity refers to the flow of the velocity from right to left in Case U and from bottom to top in Case V. As shown in the figure above, the U component value is negative, indicating that the flow velocity for the sample is from right to left, whereas the V component has a positive sign that shows the flow of the velocity from top to bottom.

In addition, we can represent the velocity as arrows in Figure 130, Figure 131, and Figure 132.

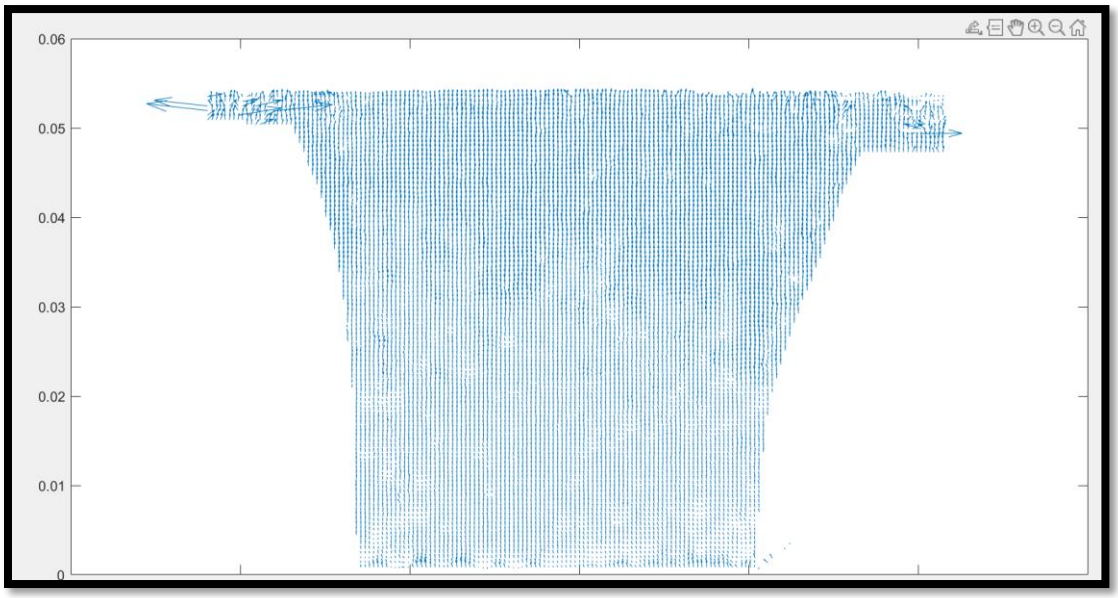

Figure 130: Velocity magnitude as arrows (MATLAB, 2023)

The close-up arrows of the magnitude velocity show the direction of the U-component from the bottom to the top.

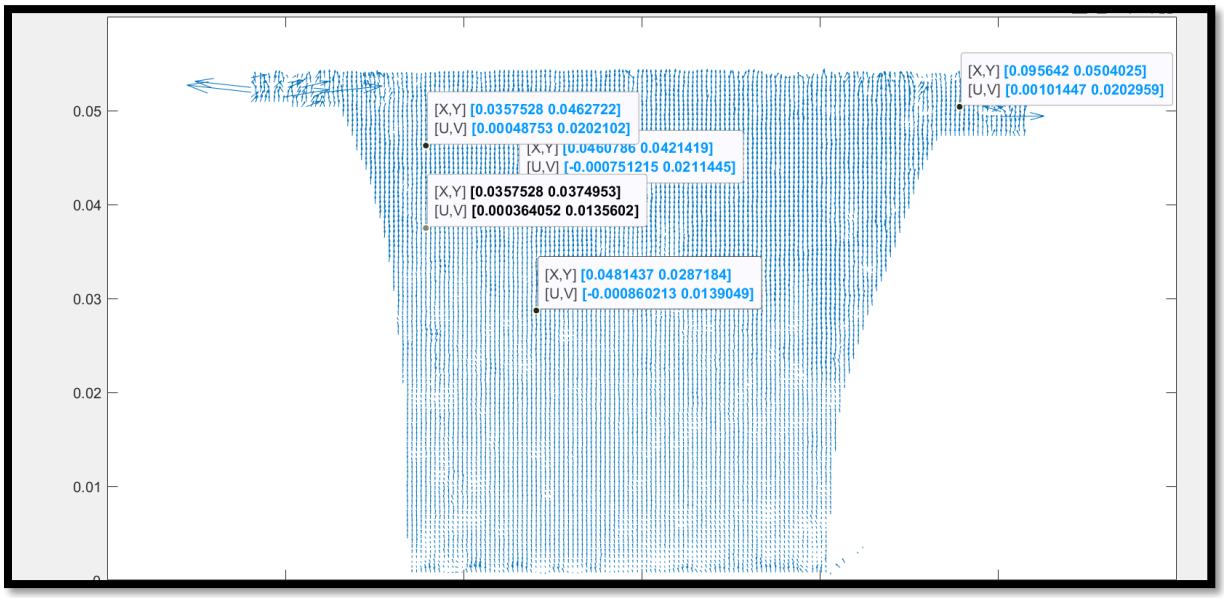

Figure 131: (X, Y) and (U, V) component points(MATLAB, 2023)

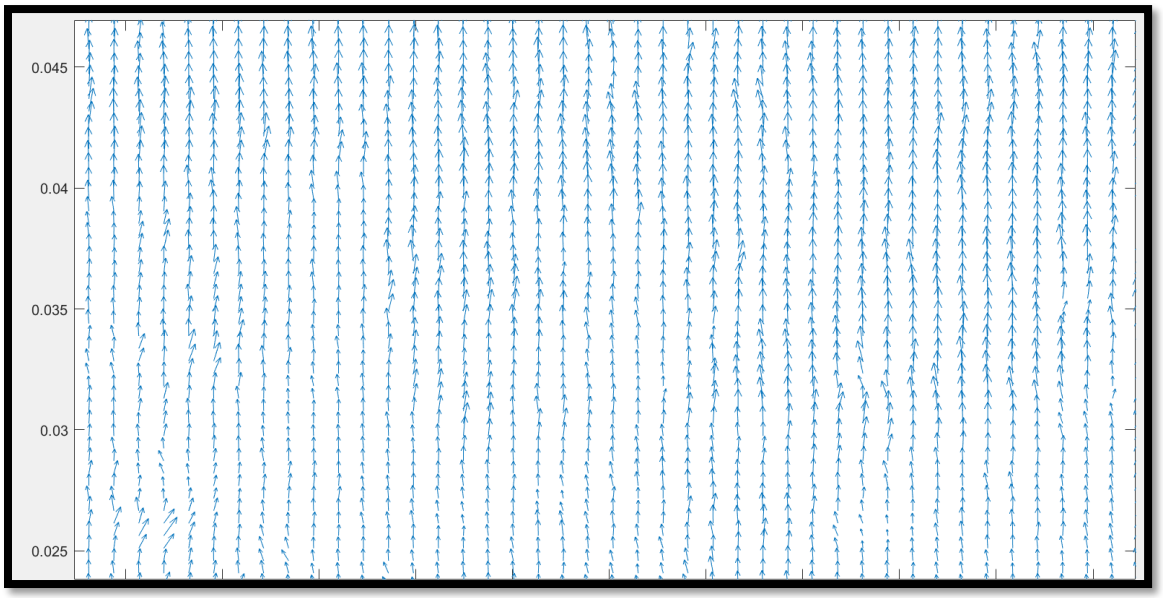

Figure 132: Close-up arrows of the velocity magnitude (MATLAB, 2023)

3.7.1 PIV Velocity Test for Stainless Steel Knit Fabric with Lycra

Adding Lycra to stainless steel knitted fabrics brings the following benefits:

- The tensile strength is improved up to almost 50% if Lycra is incorporated into the material (Sadek et al., 2012).
- Improved flexibility: It gives a characteristic of flexibility, which ensures the easy shape of the material without undermining its rigidity.
- Better deform resistance: The combination of stainless-steel and Lycra gives very good resistance to deformation by a substantial level of strain of 2.5 and above.
- Higher bursting strength: The bursting strength of elastane (Lycra) containing fabrics increases with an increased amount and extension per cent of elastane.
- Reduced fabric spirality: A higher percentage of elastane and at a bigger extension per cent decreases the spirality values of knitted fabrics.

All these elements added together make this alloy a perfect choice of material when the application demands durability while needing flexibility at the same time (Eryuruk & Kalaoglu, 2016).

PIVlab (Thielicke & Stamhuis, 2014, 2015) is well-suited for analysing the motion of particles or fibres in textiles under strain through quantitative image analysis. In this study, PIVlab was used to visualize and measure the effects of strain on Lycra and stainless-steel materials. Notable changes in the motion fields within Lycra were observed at strain of 2.5% and higher, indicating a significant interaction between strain and fibre behaviour. These analyses provide precise measurements and visualizations of how the textile structure adapts under mechanical stress, offering insights into the dynamic features of material deformation.

3.7.1.1 PIV velocity test for Stainless-Steel flat knit fabric with Lycra under low strain.

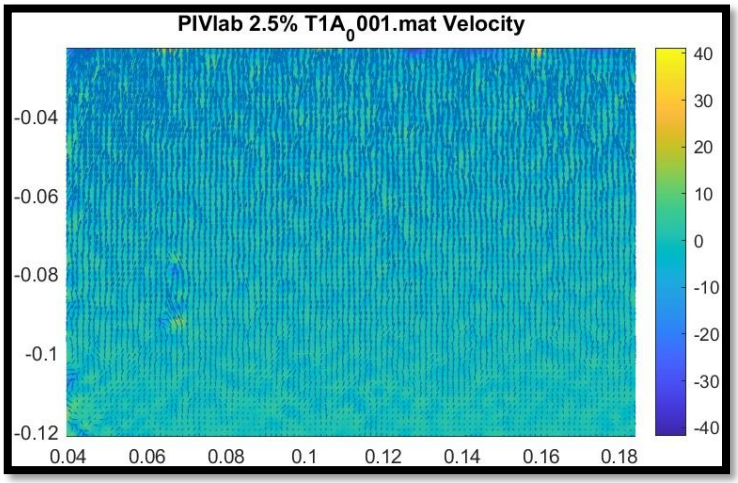

Figure 133: Velocity Test NO.1, for stainless steel flat knit fabric with Lycra (2.5% strain) (MATLAB, *2023)*

A graph of the textile velocity measurement is represented by Figure 133, and the processing was done using the software applications of PIVlab. This software does particle image velocimetry analysis, which can be used to investigate particle behaviour or movement on a surface or medium. Much can be learned from a textile velocity measurement graph by scientists as to how the textile is behaving over a given time. The graph, which is presented in Figure 133 above, presents nothing more than the deformation of a certain surface. PIVlab goes beyond merely capturing deformation by transforming that information into a graph like that of participle image velocimetry, which is an interpretation of particles within the surface as to their velocity.

The image that is generated by the PIVlab software consists of small arrows in various colours that indicate the speed and direction of movement. Longer arrows represent faster movement, with colours ranging from dark purple for slow movement to yellow for faster speeds. This visualisation method communicates textile characteristics by indicating the speed and direction of the deformation.

So, colour and length mark speed, and the way the arrows are pointing marks the direction.

Moreover, the motion of particles of fibres within textile materials can be studied using PIV to analyse their structural and mechanical properties. This technology offers insights into the internal behaviour of textiles under various conditions, such as deformation, stress or environmental changes (Licina & Nazaroff, 2018; Mac Namara et al., 2012). For instance, PIV can reveal how fibres or yarns within the textile shift, stretch, or compress relative to each other under strain. The numbers displayed along the sides of the images represent the physical size of the analysed region, and after calibration, units like millimetres (mm) or millimetres per second (mm/s) provide precise measurements of displacement or motion.

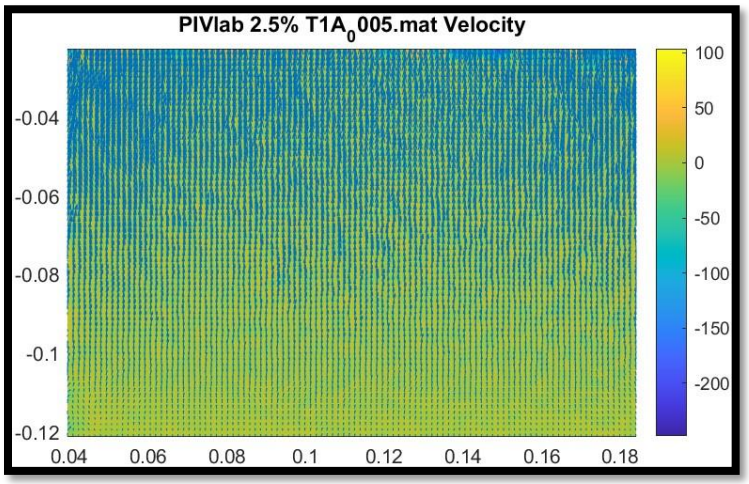

*Figure 134: Velocity Test NO.5, for stainless steel flat knit fabric with Lycra (2.5% strain) (*MATLAB, *2023)*

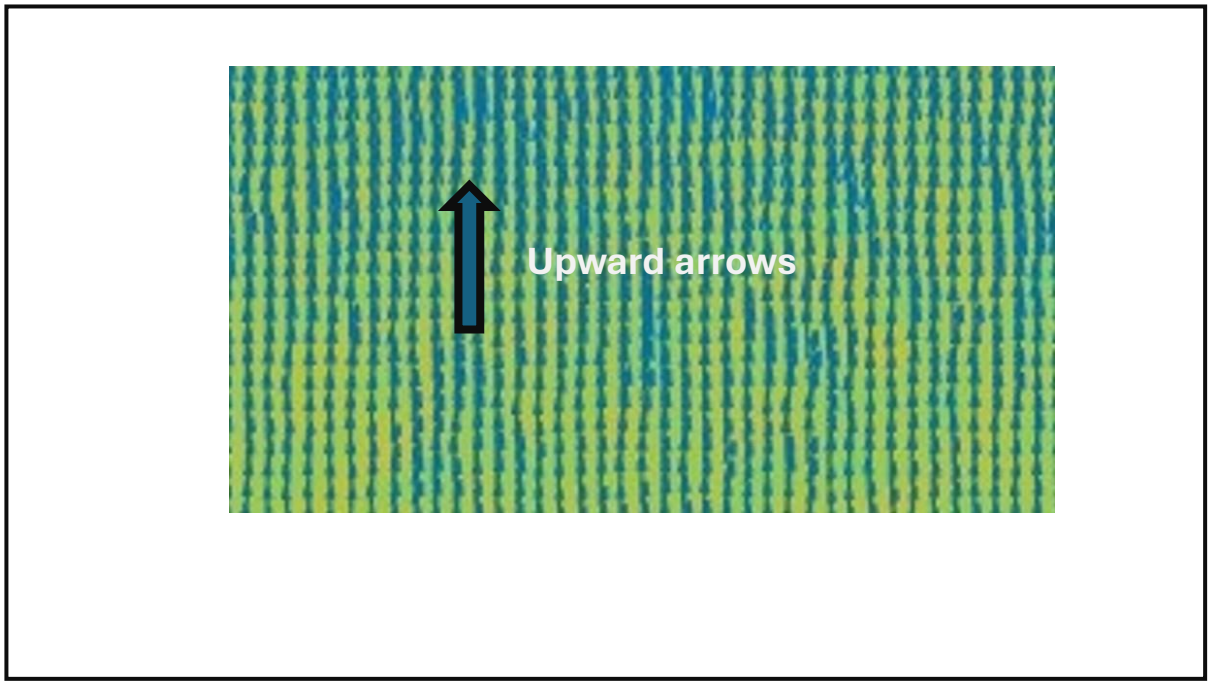

*Figure 135: Velocity Test No. 5, Close-up view of arrow directions for a stainless steel flat-knit fabric with Lycra at 2.5% strain. (*MATLAB*, 2023)*

In the velocity field shown in Figure 134, the arrows represent the speed and direction of motion at various points within the analysed area. Each arrow's orientation indicates the flow direction (for example, upward for upward movement), while its length corresponds to the speed of motion, with longer arrows for faster movement, and shorter arrows for slower movement. In this figure, most arrows point upward, indicating a prevailing upward motion, but their varied lengths highlight uneven flow speeds. The image is composed of a grid of arrows, each representing the velocity at specific points. This variability in arrow length and direction reflects differences in flow characteristics, influenced by factors such as textile properties.

As shown in Figure 135, the image consists of numerous tiny arrows arranged in a grid, forming a velocity field.

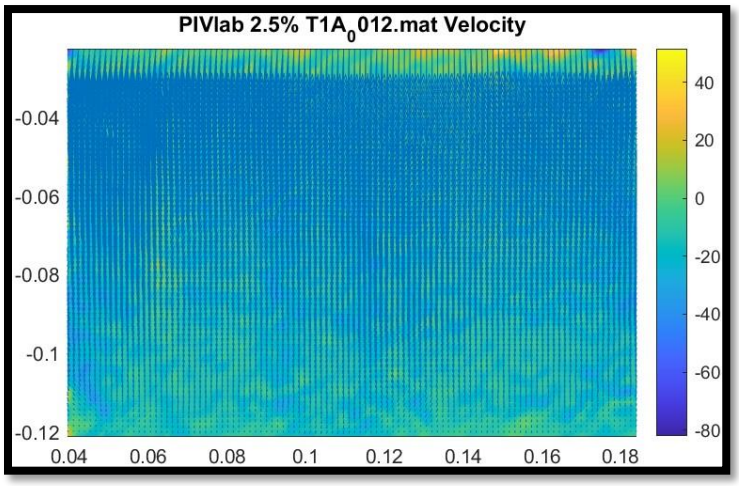

*Figure 136: PIV velocity test NO.12, for stainless steel flat knit fabric with Lycra (2.5% strain). (*MATLAB, *2023)*

In Figure 136, an analysis of the colours in the plot reveals insights into velocity distribution within the field. Blue and green shades dominate, indicating moderate velocity values. Patches of yellow and light green represent higher velocity areas that are of interest for further investigation. The colour transition from bottom to top implies increasing velocity in that direction, possibly reflecting a specific motion pattern or phenomenon. Overall, studying plot colours aids in understanding velocity distribution and pinpointing significant field areas.

The visualisations included in this research have offered significant insights into the behaviour of the samples being tested and the data generated from these tests. Using graphical representations, it was possible to discern patterns and trends that might have been overlooked using conventional analytical techniques alone. By considering multiple plots in conjunction, a more holistic understanding of how various variables interact within the dataset was developed. This underscores the importance of leveraging data visualisation tools to enrich our comprehension and analysis of intricate datasets. This highlights how integrating visual aids into our analytical workflow is essential for deriving more informed and precise conclusions (Cohen & Swerdlik, 2009).

3.7.1.2 PIV velocity test for stainless steel flat knit fabric with Lycra under high strain.

The first stage test of the stainless-steel textile with Lycra at a 10% strain rate was conducted using PIVlab, focusing on the movement of velocity from the bottom to the top, as indicated by arrows, Figure 137 illustrates the velocity field through colour-coded arrows and a scale, which provide insights into how the material behaves under varying velocity conditions. This analysis offers valuable information on the performance of the stainless steel and Lycra mixtures, allowing us to observe directional changes and velocity magnitudes visually.

For instance, if the textile shows high velocities, represented by yellow or hot colours, it might mean that it has good motion properties. On the other hand, if that material exhibits low speeds, indicated by blue or cold colours, it may imply some form of resistance to flow within its structure, indicating that it is less mobile than expected. Thus, during velocity tests, these changes in colour together with the readings from the gauge tell us more about how the textile particles move and react under certain flow parameters.

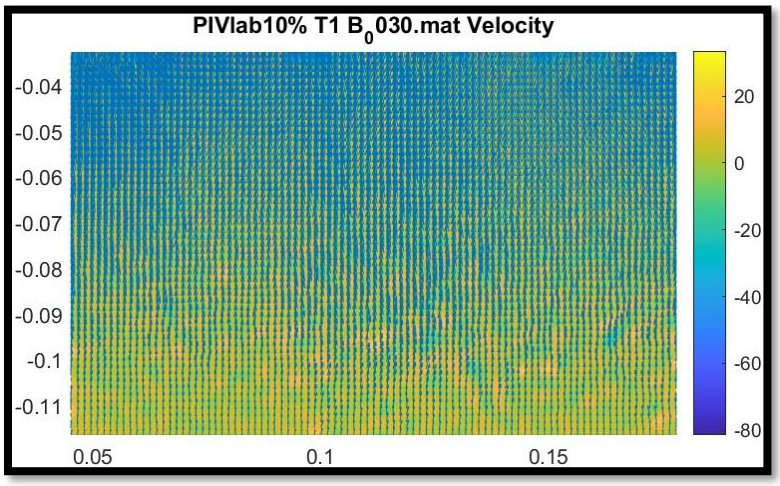

*Figure 137: PIV Velocity test NO 30, for stainless steel flat knit fabric with Lycra (10% strain)(*MATLAB, *2023)*

3.7.1.3 Evaluating stainless steel behaviour at different strain rates:

The velocity indicators detected by the PIV analysis program displayed minimal variation or shift over the fabric sample area, suggesting that there was a little distortion of the material at low-stress levels in the early testing phase.

When the textile material is tested at a higher strain rate (10%), the velocity arrows in the flow field display increased complexity in their movements. These movements involve divergence, where arrows move apart, and convergence, where arrows move closer together. This indicates that, as the strain on the textile increases, the material's surface undergoes non-uniform deformation patterns. Areas of divergence in the motion field likely represent regions where the material is being stretched or thinned out, while areas of convergence suggest compression or bunching of the material.

The varying speed arrow patterns at increased strains show the intricate small-scale changes that happen in the stainless steel-Lycra fabric mix under heavier loads. These diverse deformation areas may be affected by how the rigid stainless-steel fibres interact with the stretch Lycra part in the material structure. Additional factors that could contribute to the shift in arrow orientations in the speed assessment of the stainless steel-Lycra fabric blend when subjected to higher levels of stress might involve:

- The distinct material characteristics of stainless steel and Lycra can cause different deformation behaviours when subjected to strain. The inflexible quality of stainless-steel fibres, in contrast to the flexible Lycra component, may lead to diverse reactions to strain, resulting in complex movements of the arrows.
- The relationship between the stainless-steel fibres and Lycra in the fabric's composition can impact how it deforms. The way these fibres interplay and shift about one another when strained can impact the flow pattern, leading to alterations in the orientation of arrows.
- The way strain is spread out within the fabric sample may not be consistent, causing specific points in the motion field to either come closer together or move apart.

Differences in strain levels can create various deformation shapes and impact how the velocity arrows move.

- The arrangement of fibres and the weave pattern in a stainless steel-Lycra fabric mix influences how the material deforms when under strain. Alterations in the fabric structure can result in variations in flow behaviour and velocity patterns.
- External elements like temperature, moisture, and atmospheric pressure can impact the way fabrics deform. These external factors might combine with the characteristics of the material and levels of strain to alter the flow pattern and orientation of velocity indicators.

Researchers can enhance their understanding of how the stainless steel-Lycra fabric blend responds to varying motion conditions and strain levels, which will aid in improving the fabric's effectiveness across a range of applications (Miao et al., 2020) and (Kikuta, 2003).

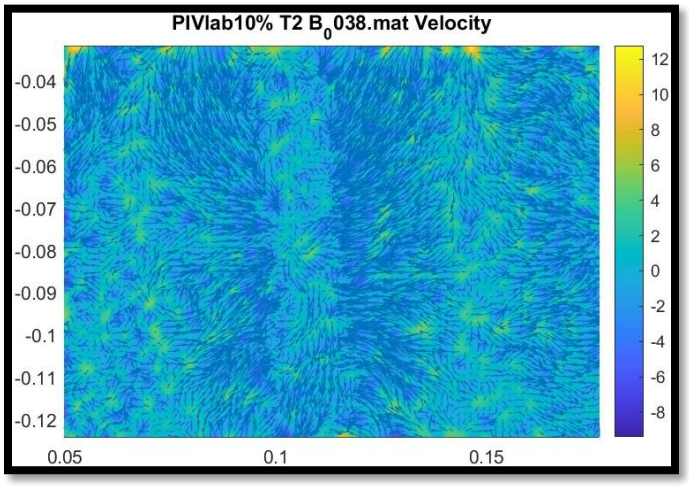

Figure 138: PIV velocity test NO.38, for stainless steel flat knit fabric with Lycra (10% strain)(MATLAB, 2023)

Concerning Figure 138, it can be observed that the blue background brightens in areas where the vectors converge. This change in brightness indicates variations in velocity, suggesting that the motion speed is higher in these regions. The concentration of vectors in these areas further highlights shifts in the material's movement, providing an important understanding of the flow behaviour.

3.7.2 PIV Velocity Test for Polyester Flat Knit Fabric with Lycra

Polyester textiles blended with Lycra, a trademarked elastic fibre, have improved stretch and recovery capabilities compared to regular polyester fabrics. Recent particle image velocimetry (PIV) laboratory tests have provided quantitative evidence of the performance benefits imparted by the addition of Lycra (Schröder & Willert, 2008). The PIV data for polyester/Lycra blends revealed higher elastic strain limits and more uniform strain fields than 100% polyester controls. The Lycra component allowed the fabrics to stretch farther without rupturing while still fully recovering their original dimensions after the tensile force was removed (Sheikh et al., 2022).

3.7.2.1 PIV Velocity Test for Polyester Flat Knit Fabric with Lycra under Low Strain

This section describes the performance of the polyester flat knit fabric with Lycra under minimal stress levels, where the material experiences little stretching. The analysis focuses on how the fabric behaves mechanically under such conditions, including its deformation patterns, elasticity, and ability to recover.

Polyester fibres are recognised for their ability to resist stretching and changes in dimensions. The polyester element of the material helps uphold its overall shape and size, particularly at low levels of strain. Additionally, the inclusion of Lycra yarns in the fabric enhances its elasticity and recovery attributes. Even with minimal strain, Lycra fibres assist in restoring the fabric's original form and dimensions following any deformation. Lycra fibres are recognised for their capacity to return a fabric to its initial shape and size after being deformed.

To confirm this assertion, various tests can be carried out. For instance, fabric swatches containing Lycra fibres could be exposed to varying degrees of deformation by stretching or compressing them using mechanical equipment, which would allow for an analysis of the alterations of the fabric’s shape and size before and after the deformation process. By contrasting the initial dimensions with those post-deformation, it can be determined if Lycra fibres effectively aid in restoring the fabric's original form and measurements.

In my experiment, the initial test on the sample under minimal strain extended the material until it reached a strain of 2.5%, replicating a moderate level of stretching commonly encountered during regular use. This specific strain was selected to evaluate the fabric's initial flexibility and ability to bounce back. The outcomes indicated that the Lycra-polyester blend could stretch and change shape under low strain but showed significant recovery once the strain was released. Moreover, there was no notable damage or distortion observed as the fabric returned to its original form, highlighting the effectiveness of Lycra in providing elasticity and maintaining shape.

The subsequent test involved stretching the fabric to a slightly higher strain, like what might occur during more intense activities. This assessment aimed to determine the material's maximum stretch capacity and its resilience against higher strains. Results from this test demonstrated that the Lycra-polyester fabric could stretch further without enduring permanent damage or deformation, showcasing its impressive elasticity and ability to withstand greater strains while preserving structural integrity. In summary, the experimental evaluation illustrated that the Lycra-polyester fabric possesses outstanding stretch characteristics.

How knitted patterns are constructed, such as the type of stitches used, the tightness of the stitches, and how yarn is placed, is crucial in determining how a fabric responds to slight stretching. Various stitch patterns like ribbing or stockinette can alter the fabric's elasticity and draping qualities (Pavlović & Vrljičak, 2020), and the tightness of the stitches influences how much the fabric can stretch and its overall durability. Additionally, where yarn is positioned - either horizontally or vertically - affects how well the fabric stretches and stays stable. These elements impact the fabric's ability to maintain its shape, endure strain and pressure, and offer comfort and utility to the wearer. In general, the arrangement of knitted components significantly affects the performance and features of knitwear. The properties are essential for comprehending the performance and mechanical properties of the polyester flat sample blended with Lycra when subjected to minimal stress and velocity tests with PIVlab.

Based on these considerations, it can be expected that the fabric with Lycra shows elastic deformation and reverts to its original shape after the strain. Localised strain variations may occur due to the knitted structure and Lycra distribution. PIV analysis can reveal strain distribution, with polyester likely having lower strains than Lycra due to its lower extensibility.

The PIV analysis provides velocity fields showing the movement of regions within the fabric sample under applied deformation. Polyester and Lycra in the knitted fabric are likely to create a balance between stability and elasticity. The fabric should recover well at low strains, returning to its original shape.

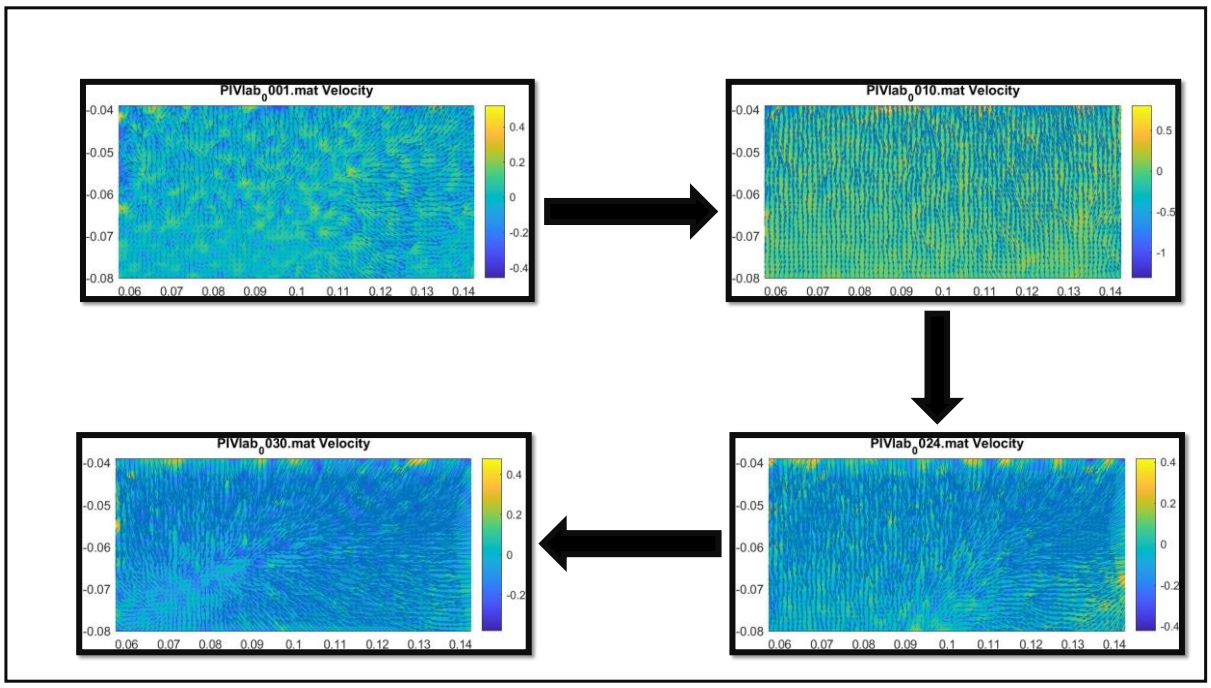

*Figure 139: velocity first tests of the polyester flat knit fabric with Lycra under (2.5% strain) (*MATLAB*, 2023)*

The first velocity test for the polyester knit fabric with Lycra under 2.5% strain resulted in 30 pairs of images that could be used for PIV analysis. The initial velocity test for the polyester with Lycra at low strain showed a random movement of arrows. The intricate textile patterns observed in the velocity field are influenced by various factors such as the interactions between textile fibres, knitting patterns, yarn type, and fabric porosity. These elements impact how strain flows through the textile material, causing variations in velocity and direction that may seem disorderly. For instance, in Figure 139, arrows indicated positive velocity as they moved from bottom to top. The "010" displayed in the image corresponds to the file identifier of the dataset that was utilised to create the graph. This is a component of the file name "T1A0010.mat" situated at the upper left corner of the image. Another example, No. 024, depicts textile particles initially moving right, slowing down, changing direction to the left, and accelerating in a negative direction, before coming to a stop. Most arrows in the scenario

involving image pair No. 030 were oriented towards the right, indicating horizontal flow with varying angles, suggesting complexity rather than straightforward movement. Notably on the left side of the image in Figure 137, a cluster of blue arrows signify slower flow speed compared to other areas. The colour of these arrows represents particle speed with blue denoting lower speeds; hence a concentration of blue arrows indicates slower fluid movement within that region.

The referenced information suggests that the textile material exhibits compositional behaviour characterised by moderate heterogeneity and a combination of non-uniform strain and movement patterns. The following discussion explores interpretations of these observations examining their implications for the fabric's performance and behaviour under the test conditions. Additionally. hypotheses are presented to explain these effects, offering insights into the underlying mechanisms and confirming why such behaviours arise in the textile material:

- Non-Uniform Deformation: The differential in orthogonal strain rates exhibits non-uniform behaviours behaviour across surfaces. Influenced by factors like local stress concentrations and irregularities in the material or fabric properties.
- Anisotropic Behaviour: Diverse conduct is noticed in textile fibres occupying different regions of the textile. This suggests that the material can be regarded as a material that exhibits anisotropic behaviour. This may result from different orientations of fibre or patterns of knit or even the presence of different materials in the fabric.
- Complex Stress Distribution: Continuous changes in strain flow direction and velocity lead to complex stress distribution in textile materials, caused by external forces or internal fibre and yarn interactions.
- Boundary Effects: Blue cones on the left indicate low flow rates, suggesting boundary effects or interactions with nearby materials. These effects can influence the textile's performance, alerting properties like permeability, stress distribution, or wear resistance during testing.
- Material Heterogeneity: Additionally, the changes in velocity and line strain could be the products of differences in the inside structure of the textile that manifests in an unevenness of fibre alignment, density of yarn, or construction of the fabric. Thus, the

heterogeneity would be one of the causes that can explain the chaos recorded at the exams.

For the second velocity test of the polyester knit fabric with Lycra under the low strain of 2.5%, illustrated in Figure 140, it can be observed in image pair No. 001 that the speed of the particle starts at zero and rises to a maximum positive value of around 0.04. It then drops to a minimum negative value of about -0.08 before increasing again to a peak of approximately 0.06. Following this, it decreases to a negative peak of around -0.07 and then rises once more to reach a positive peak of about 0.04. This alternating pattern continues throughout the remaining sections of the graph.

Due to the continuous changes in velocity, it can be inferred that the particle is experiencing acceleration. The direction of this acceleration can be deduced based on the slope of the graph: a positive slope indicates positive acceleration, while a negative slope indicates negative acceleration. In general, the graph illustrates that the object is experiencing regular movement, indicating that its speed is consistently fluctuating repetitively. This happened because the Lycra content contributes to the fabric's ability to stretch and bounce back, the fabric's dimensional stability and elasticity may differ from its initial state. A second velocity test would identify any variations in stretch, expansion, and spirality, the second PIV (Particle Image Velocimetry) test is carried out to investigate any changes in the directions of stretch, expansion and spirality. The reason for this may be that the first test set a benchmark or initial readings, while the second one verifies whether the material or object under investigation remains constant or has changed with time/under different circumstances. It is important to identify these variations because it allows us to understand how the material behaves and thereby learn about its quality as well as performance about its intended use. For the No. 002 image, the graph's rising incline probably shows the textile's velocity rising as it moves from left to right. The peak of the graph shows the highest velocity reached by the textile, while areas with no velocity would suggest times when the textile is not in motion (stationary).

The information in the images provided shows that textiles behave in different ways depending on their velocities during testing. In Image No. 018, a wave pattern is observed where textile velocity changes over time. It reaches its maximum speed, then falls back to zero and repeats this motion several times.

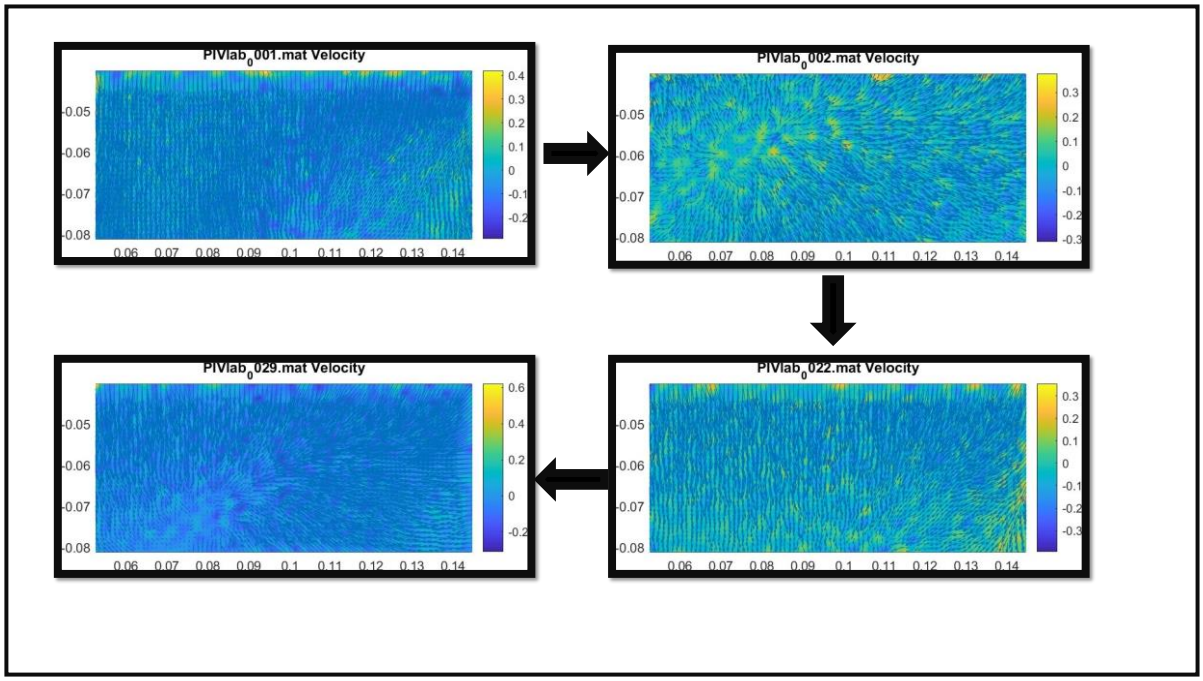

*Figure 140: PIV velocity second tests for polyester knit fabric with Lycra under (2.5% strain)(*MATLAB, *2023)*

The particle shows oscillatory motion, initially moving to the right and oscillating near position 0.1. Its velocity starts at the maximum of approximately -0.6 at 0.08 seconds, gradually decreases to -0.08 by 0.14 seconds, and then comes to a stop, as observed in image 029. This behaviour suggests dynamic changes in motion, possibly influenced by the surrounding conditions or forces acting on the textile.

3.7.2.2 PIV Velocity Polyester Knit Fabric with Lycra under High Strain

The current section explores the PIV velocity of polyester knit fabric:

The data suggests that in the beginning of the tests, the Lycra strands stretched out completely to withstand most of the applied pressure. The polyester stitches in the fabric also lengthened and loosened to adapt to changes in shape.

By utilising PIV imaging during tests that put stress on the material, we can record comprehensive maps showing how strain and displacement are distributed across its surface when undergoing extreme deformation.

The graph exhibits some irregularities, possibly attributed to the data being obtained from an actual experiment as noise is inherent in real-world data collection. Thus, for image 049 in **Error! Reference source not found.**, the particles look like they are moving upwards overall, with some changes. The speed seems to be greater at the lower part of the picture and decreases as it goes up. Some regions show bigger changes in speed and direction, indicating turbulence or intricate flow designs. The particles near the centre exhibit more consistent movement compared to those at the edges, where motion seems more erratic. For image 068, The speed of the particle initially peaks at 0.2 at approximately 0.08 second before dropping to zero around 0.09 seconds. It then decreases further, reaching a minimum of -0.2 by 0.11 seconds, before returning to zero by 0.13 seconds.

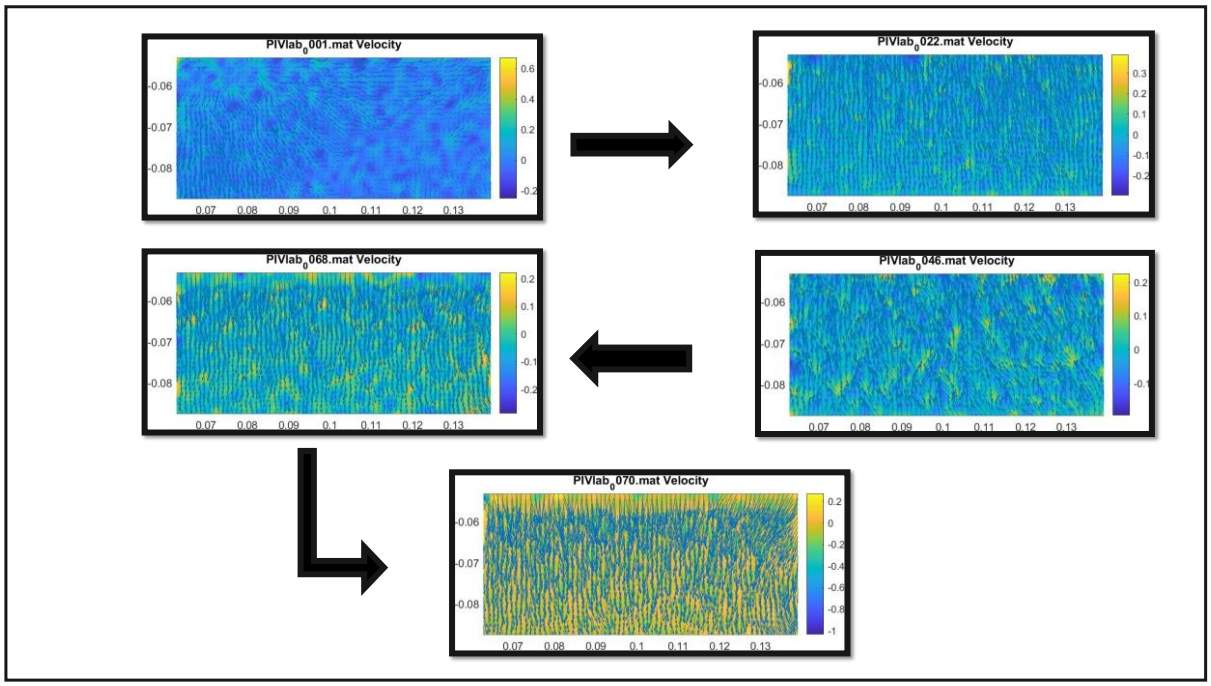

*Figure 141: PIV velocity test of the polyester knit fabric with Lycra under (10% strain) (*MATLAB, *2023)*

This cycle repeats across the graph, indicating a recurring pattern in the textile velocity represented by the movement of the particle. The motion of the particle resembles a textile

velocity with each repetition displaying a balanced sequence of speeding up and slowing down. This regular back-and-forth creates an impression of orderliness and predictability in how the particle moves along the x-axis. The speed transitions smoothly between positive and negative values, suggesting a harmonic motion that recurs consistently over time intervals. This repetitive cycle implies a periodic force or factor influencing the particle's movement steadily and repetitively. In this analysis, the velocity graph shows a consistent pattern of increasing, decreasing, and returning to zero. This suggests that the velocity of the textile goes through the same repetitive motion cycle.

The chart illustrates the velocity reaching zero at distinct intervals. This is important as a velocity of zero indicates a moment when there is no change in the textile velocity position. As the cycle repeats, the velocity hits zero once more, signalling that the wave is coming back to a particular point in its cycle and getting set to start the same sequence of movement again. For image 070, The average speed of the particle is a bit on the positive side, suggesting that it tends to move more toward the right than the left. This corresponds with its overall displacement in a positive direction. The image shows arrows pointing downwards, suggesting that the particle's speed is reducing. This indicates a slowdown but doesn't guarantee a complete halt. It might just be decelerating before switching course or picking up speed once more until the test stops.

The results from the second PIV velocity test, which involved subjecting the polyester knit sample with Lycra to high strain, closely mirrored those of the initial test. The velocity test also demonstrated similar dynamics to the first trial. These findings highlight a uniform performance throughout both experiments, underscoring the trustworthiness of the collected data. It can be inferred from these outcomes that even under extensive strain, the polyester knit sample with Lycra retains its essential characteristics. Moreover, the resilience of this material was reaffirmed by the consistent results obtained from the velocity assessment.

3.7.3 Comparison of the PIV Velocity Test between the Stainless Steel Flat Knit Fabric and Polyester Flat Knit Fabric with Lycra

This section offers a preliminary comparison of stainless steel-Lycra and polyester-Lycra fabric combinations, examining their characteristics and behaviour under different strain levels using Particle Image Velocimetry (PIV). The aim is to elucidate how these fabric combinations respond to both low and high-strain conditions, providing insights into their performance and potential applications. By correlating the PIV results with the unique characteristics of each fabric, this analysis enhances our understanding of the dynamic behaviours of textile materials when subjected to stress.

The comparison suggests that the textiles' performance at lower stress and pressure levels is characterised by a relaxed state, experiencing little or no strain. This indicates that the mechanical forces acting on the fabric under these conditions do not generate significant stress. If this observation applies to both textile types, it highlights a shared behaviour under minimal force. However, if the observation is specific to one type. It underscores a distinct difference in how these materials respond in low-stress conditions

During the PIV velocity test under small stresses, the textiles may have behaved smoothly and uniformly so that they offered low resistance to mechanical forces as well as showing minimum distortion or stretching. Therefore, this sense of ease and calmness indicates that the cloth was not maximally stretched to its limits while mechanically performing comfortably within an acceptable limit.

Stainless steel-Lycra fabric is known for its strong tensile strength, corrosion resistance, and long-lasting properties. These characteristics are typically assessed using well-established industry testing protocols. Lycra material is recognised for its elasticity, ease, and adaptability, which can be examined by methods such as tensile testing to assess stretch characteristics and comfort evaluations conducted through wear trials or user input (Senthilkumar et al., 2011). The characteristics of the stainless steel flat knit sample containing Lycra (SSLF4) demonstrate that incorporating Lycra causes a decrease in tensile strength in the fabric's lengthwise orientation. This weakening of strength is associated with the fabric needing less energy to

stretch because of the enhanced elasticity provided by Lycra, resulting in a denser fabric composition. The results of the experiments showed that when subjecting the flat sample with Lycra to minimal strain, the initial test curve was longer than the subsequent one and exhibited greater variation in form compared to trials conducted at higher levels of strain.

The integration of Lycra into stainless steel fibres results in developing a composite material that possesses an exceptional blend of robustness, pliancy, and versatility (O'Brien et al., 2017). Lycra 's elasticity and recovery performance play a fundamental role. Under high tension levels, the material maintains robust stretch capacity, essential for dynamic applications. Additionally, Particle Image Velocimetry (PIV) analysis reveals fluctuations in flow dynamics linked to the interaction of Lycra and stainless steel within the fabric structure, highlighting the cooperative response of the composite material under stress.

A material blend of stainless steel and Lycra offers a unique combination of durability and flexibility. This innovative pairing brings together the strength and resilience of stainless steel with the stretchiness and comfort of Lycra. The integration of these two materials results in a versatile product that can withstand wear and tear while providing a comfortable fit for various applications. The incorporation of Lycra into the stainless-steel composition adds a touch of elasticity, making it an ideal choice for products that require both sturdiness and adaptability. Lycra, known for its elasticity, initially flexes to alleviate pressure while stainless steel stays strong to uphold its structure. The use of Particle Image Velocimetry (PIV) allows for the observation and analysis of deformation patterns and speeds.

Lycra, with its stretching capabilities, enhances flexibility and recovery at low strain levels, while polyester offers stability and support. Through Particle Image Velocimetry (PIV), researchers can visualise velocity and flow patterns to evaluate the performance of these fabric compositions. When subjected to high strain, Lycra absorbs pressure through its stretching ability, while polyester maintains the integrity of the material's structure. This combination allows the fabric to respond dynamically to tension. By utilising PIV analysis, we gain a deeper understanding of how these textile blends behave under different levels of strain, shedding light on the contributions of each fibre to the overall functionality and resilience of the fabric. While Lycra offers elasticity and flexibility, polyester provides strength and durability, making the blend highly versatile for various applications.

3.7.4 PIV Velocity Test for Stainless Steel Tubular Structure without Lycra.

The current investigation aims to examine the structural strength of stainless-steel tubular knit when exposed to different strain rates through PIV lab velocity testing. By studying the velocity field of a stainless-steel cylindrical knit at varying strain rates, researchers seek to comprehend how the material reacts and potentially changes its shape. These data are crucial for designing and evaluating the safety of such elements as they shed light on the time-dependent ratcheting behaviours and cyclic deformation traits of the material. Understanding how a stainless-steel cylindrical knit behaves under different strain rates is vital for ensuring its structural durability and thus for developing secure components. This study intends to enhance the current knowledge on the time-dependent ratcheting behaviours and cyclic deformation characteristics of stainless steel cylindrical knits (G. Kang et al., 2006). The primary method employed was PIV velocity testing to assess the structural integrity of the stainless-steel cylindrical knit. Additionally, factors such as strain or stress rate, peak and/or valley strain or stress hold, and multiaxial loading paths are considered when examining the strain cyclic characteristics and ratcheting behaviour of the material. Through PIV velocity testing on stainless steel cylindrical knits under various strain rates, this section of the research aims to offer valuable insights into how the material responds and may deform, thereby influencing component design and safety evaluation.

3.7.4.1 PIV Velocity Test for Stainless Steel Tube Knit Fabric without Lycra under Low Strain

The focus of the image from the first velocity test of the stainless steel textile, captured in image pair No.001 shown in Figure 142, appears to be on illustrating the velocity vectors, including both their direction and magnitude. As can be seen in the picture, these vectors mostly point in an upward direction, indicating a general upward movement at different speeds, as shown by the variation in colours. The downward-pointing arrows in the diagram symbolise the prevailing movement from the upper to lower regions. The diverse sizes and angles of these arrows represent not only the speed but also the specific direction of the flow at various locations within the system. This visual representation shows how velocity varies throughout, providing valuable insights into the dynamics and behaviour of this process. For image pair

No. 004, the directional indicators depicted in the image predominantly show a downward trend, implying a dominant flow in that specific direction. Nevertheless, it is important to recognise that arrows exhibit diversity in orientation and length. This diversity implies the existence of distinct velocities and flow configurations dispersed across different locations within the area. Essentially, while an overarching downward motion is observed, the intricacies of speed and flow structures are evident across the illustrated expanse. The test was stopped at image pair No. 006, likely due to the specific characteristics of the material being tested. The absence of Lycra and its cylindrical shape of the material may have influenced the test duration and the result. A more detailed comparison, as discussed in section 3.7.4.2, will explore how these factors might have impacted the outcomes.

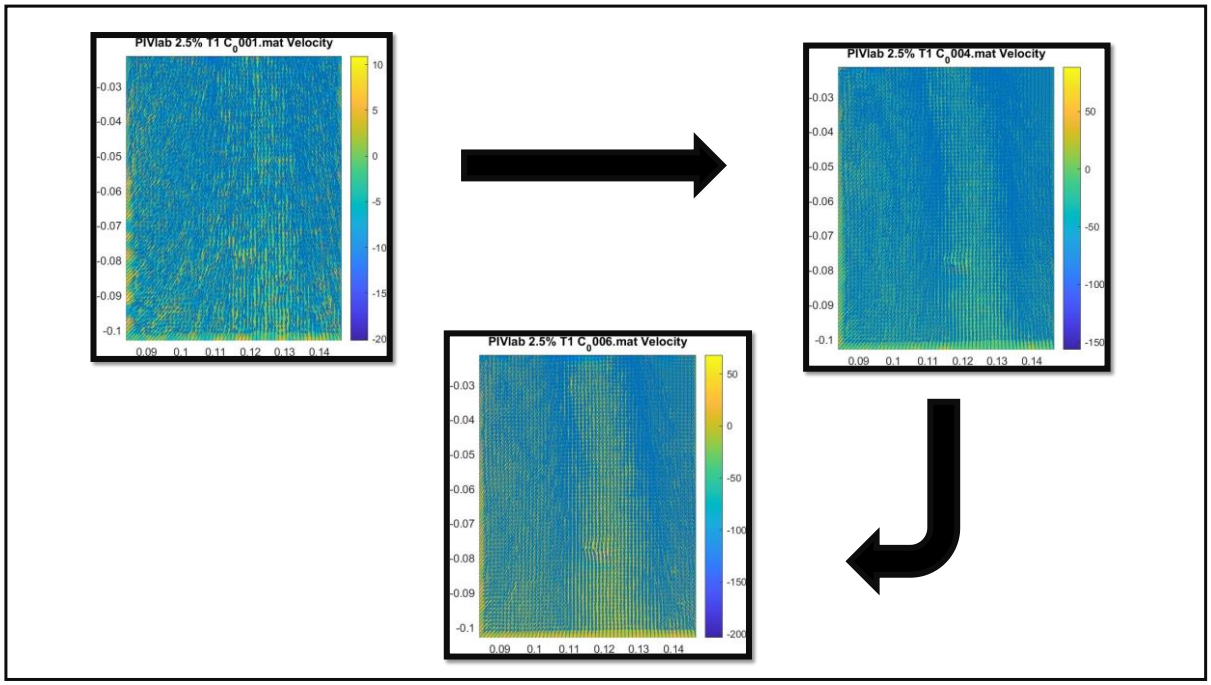

*Figure 142: PIV first velocity test of stainless-steel tube knit fabric without Lycra under low strain (2.5%)(*MATLAB*, 2023)*

For the second test, the central part of image pair No. 001 in Figure 143 depicts a collection of vectors or flow lines shown on a blue backdrop. These lines appear evenly spaced and point upward, suggesting a consistent flow in that specific direction. The varying intensity of colours throughout the display implies diverse velocity levels and flow features. Brighter blue sections signify faster velocities, whereas darker blue regions suggest slower speeds.

The colour bar indicates that the colours within the motion field correspond to different velocity values, with red representing the highest velocities and purple the lowest (or possibly negative) velocities.

About image pair No. 006, the primary part of the picture displays a rectangle filled with small vectors (arrows) on a background coded with colours. These arrows depict the speed and size of the velocity at various points in the analysis area. The colour-coded backdrop symbolises the numerical value of the velocity magnitude or related aspects.

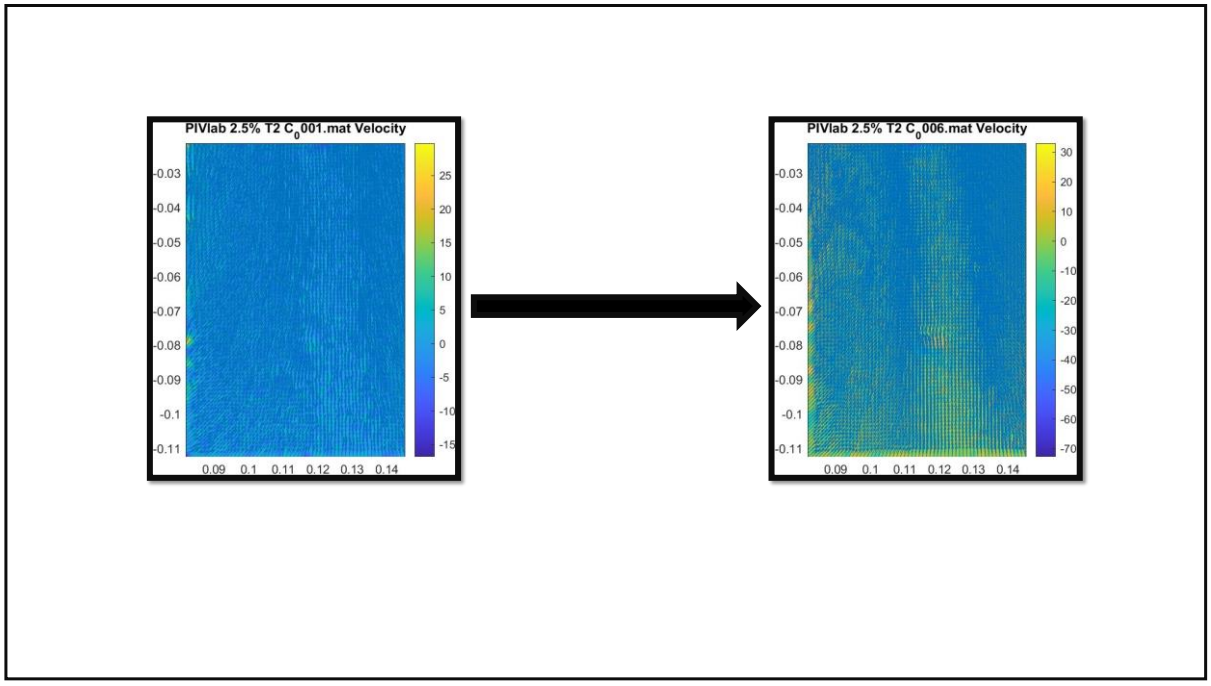

*Figure 143: PIV velocity second test for Stainless steel tube knit fabric without Lycra under low strain (2.5%) (*MATLAB, *2023)*

The initial velocity test for the stainless-steel cylindrical knit without Lycra closely matched the second test at low strain. This consistently can be attributed to the inherent strength and durability of stainless steel, which leads to stable results under different conditions. However, the speed of the test is likely influenced by other factors, which will be explored in more detail later.

The lack of Lycra, a stretchable material, may help achieve more uniform test outcomes. Conducting tests at low strain levels reduces the impact of external influences for more consistent results. PIVlab is recommended for velocity measurements because it provides accurate data, ensuring consistent results between tests. Its precision and capabilities contributed to the close correlation observed in the velocity tests. The material properties, testing conditions, and reliable equipment likely led to the close matching of the first and second velocity tests under low strain.

3.7.4.2 PIV Velocity Test for Stainless Steel Tube Knit Fabric without Lycra under High Strain

For the first velocity test, the legend on the right side of image pair No. 001 in Figure 144 associates colours with velocity measurements ranging from -20 to +15 units. Darker colours represent negative values, green signifies zero, and positive values change from green to yellow. This suggests that negative values are part of the measurement range and may indicate reverse or downward flow, depending on the orientation of the experiment or simulation. For the No. 003 image, the image vectors are mostly shaded in blue, indicating low-velocity levels.

For image pair No. 024, the central component of the visual image is a grid containing arrows or vectors that indicate both the direction and strength of the flow at locations. The alignment implies that the arrows have a general downward movement, with minor disturbances causing a ripple effect throughout the area.

Factors affecting the downward movement pattern in textiles can vary significantly depending on their structural dynamics. A primary factor is the influence of gravity, which exerts a constant downward pull, often determining the direction of flow within the material. The gravitational force tends to drive the movement of particles within the textile in a downward direction, particularly when the textile is oriented vertically or inclined. Additionally, external forces, such as pressure differentials or applied mechanical pressure can markedly influence the movement behaviour. These forces can be deliberately adjusted or controlled to regular or redirect the movement, enabling precise management of the desired movement pattern within the textile.

For the last image pair, No. 026, the picture features a vertical colour strip on the right side that serves as a legend for interpreting the colours used to display various speeds. These numerical values align with the distinct speed measurements, enabling observers to understand the intensity of the speeds illustrated by the colours in the image.

In the images, most of the arrows indicate a downward direction, which implies a prevailing flow going downwards. Nevertheless, there may be variations or shifts in the flow direction within the area. These changes may arise from elements such as turbulence or engagements with other existing flow designs in the setup.

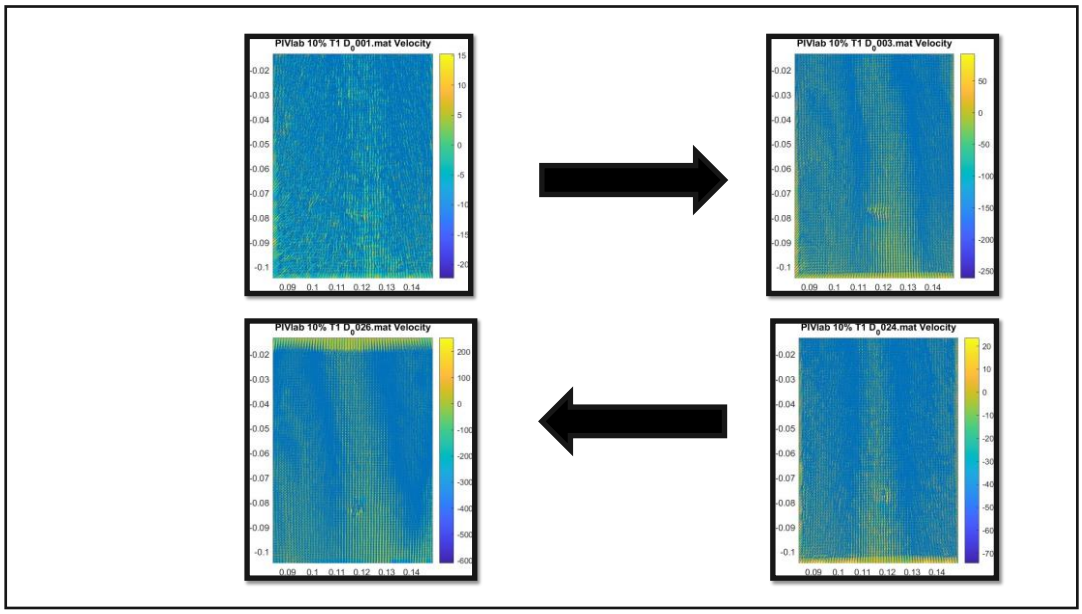

*Figure 144: PIV the first velocity test for stainless steel tube knit fabric without Lycra under high strain (10 %) (*MATLAB*, 2023)*

The second velocity test of the sample showed the number of image pairs with velocity variations. For all the image pairs, 26 images, the middle area of all figures with a blue background, contain many vectors that are small yellow in colour and represent flow characteristics for different regions in the flow field. The arrows are small and close together, pointing downwards, and gradually become more curved from top to bottom. The vector length and direction varying trend suggest a curly or swirling flow pattern with small-scale fluctuations, probably due to both vortices and turbulence.

3.7.5 PIV Velocity Test of the Polyester Tube Knit Fabric without Lycra

The popularity of polyester tube knit fabric in the textile sector has increased owing to its elasticity and unique three-dimensional surface texture. By performing PIV velocity analysis on this material, a deeper understanding of its flow properties and functionality across different uses can be achieved (Yan et al., 2021b). The PIV velocity examination of the polyester tube knit fabric lacking Lycra sheds light on its textile velocity measurement and responses under varying circumstances. This evaluation involves utilising Particle Image Velocimetry to gauge the speed and movement of particles within the fabric's composition. Such data can assist creators and producers in enhancing the performance of materials for applications such as activewear, shapewear, and medical textiles. Employing PIV velocity assessment on polyester tube knit fabric devoid of Lycra offers valuable insights into its textile velocity measurement, aiding in shaping innovative textile designs that merge utility with style. The outcomes of the PIV velocity test can help determine whether the fabric is suitable for specific uses while guiding enhancements to its structure or manufacturing methods. Ultimately, undertaking a PIV velocity test on a polyester tube knit fabric without Lycra is crucial for discerning the motion of textile particle’s effectiveness.

3.7.5.1 PIV Velocity Test of Polyester Tube Fabric without Lycra under Low Strain

The examination involved subjecting a polyester tube textile lacking Lycra to a PIV velocity test at minimal strain to scrutinise its textile particle movement characteristics and potential functions. Upon analysis, it was observed that this fabric displayed enhanced PIV velocity values compared to fabrics containing Lycra. This outcome suggests that more favourable particles are represented by arrows within the fabric structure, hinting at promising applications in various settings.

For the first velocity test by PIV under (2.5%), represented in image pair No. 001 in Figure 145, the arrows predominantly indicate an upward direction, suggesting a prevailing upward movement within the visualised region. It is crucial to emphasise that the length of each arrow correlates with the velocity at that specific location; therefore, longer arrows symbolise higher

speeds. This visualisation not only conveys an overall trend of upward motion but also provides insights into varying speed intensities across different points in the area.

The random arrow movement suggests that the movement of the textile does not adhere to a consistent or organised route. Possible causes for this include turbulence, different pore dimensions or blockages in the fabric, and irregularities in the motion of textile particles.

The elongated form of the arrows might be due to the impact of the textile structure on particle movement. The material could present barriers or form pathways that result in motion extending or distorting in specific areas, resulting in the lengthened appearance of the arrows.

For image pair No. 012, the vectors, which are closely packed and span the entire image, depict the motion of the textile particle orientation at numerous locations. Arrows that are predominantly oriented upward with minor deviations to either side suggest a predominantly vertical with some horizontal motion. The arrow lengths appear to differ, indicating varying flow speeds across different areas. Overall, when the arrows appear longer, it implies a greater velocity or quicker movement of the particles. On the other hand, shorter arrows suggest reduced velocity or slower particle movement. The scale on the right-side ranges from blue to yellow, with blue representing lower speeds (approximately -0.9) and yellow denoting higher speeds (around 0.2). The colours in between (such as green and orange) show the various speeds between the two extremes. This image indicates that the sample reaches a higher strain before returning to its initial shape.

For the last image pair, No 021, the colours in the background span from blue to yellow, matching the key on the right side. This indicates that the colours symbolise the velocity magnitude at various locations, with blue sections representing negative velocities (such as flow in a different direction or downward) that vary between -0.2 and 0.2, indicating the scope of speed values included in this examination.

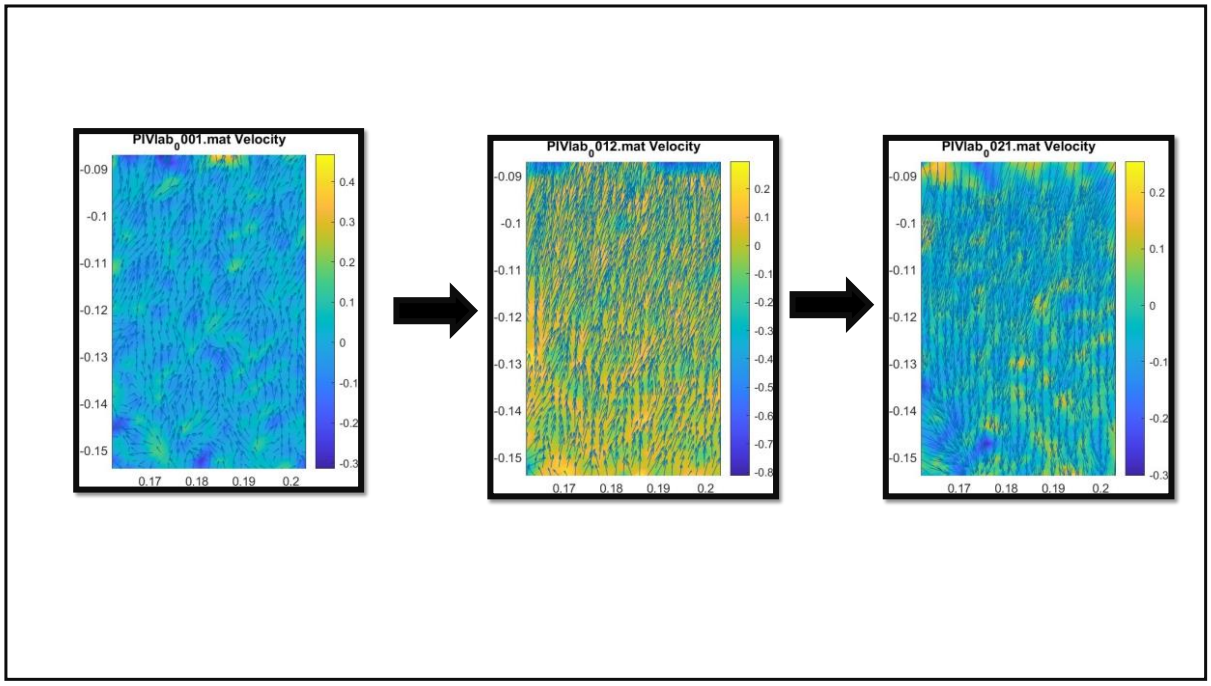

*Figure 145: PIV velocity first tests of the polyester tube knit fabric without Lycra under low strain (2.5%) (*MATLAB*, 2023)*

Two velocity tests were conducted on a polyester tube without Lycra material, and the velocity data from the second test were consistent with those of the first. Furthermore, the images from the second test showed greater correlation, reflecting improved alignment and similarity in the visualization of the textile's particle motion field. This improvement can be attributed to advancements in the experimental setup, better data analysis techniques, noise reduction efforts, fine-tuning of parameters, and enhanced calibration protocols used during the second test. Additionally, the absence of Lycra fabric in the polyester tube might have contributed to minor variations in image alignment observed between the two tests. Overall, the enhanced image correlation in the second test indicated improvements in the accuracy and consistency of the experimental approach.

3.7.5.2 PIV Velocity Test of Polyester Tube Knit Fabric without Lycra under High Strain

High stretching of the knitted polyester fabric can cause structural changes. This can affect how particles move through the fabric, which affects the speed measurements obtained using

Particle Image Velocimetry (PIV). In addition, the knit structure of the fabric, particularly when Lycra is lacking, can lead to anisotropic flow. The motion speeds may differ in various directions within the material because of the arrangement of the knit loops and yarns.

The intense stress on the material can change the boundary layer dynamics close to the material surface, influencing the speed variations and flow patterns near the material, which will be shown in the PIV outcomes. Moreover, analysing PIV data from a fabric under high strain can be challenging owing to the deformations and complex motion patterns. Proper image preprocessing and data interpretation techniques are crucial to extract meaningful velocity information.

By considering these elements and performing the PIV velocity examination in a structured manner, you can acquire important knowledge about how the flow characteristics of the polyester tube knit fabric without Lycra change under significant stretching. This aids in enhancing comprehension of its textile particle motion and mechanical attributes.

In the first velocity test conducted using PIV, the initial set of image pairs No. 001, shown in Figure 146, contains a background with a visible colour gradient. This gradient may reflect variations in the measured motion properties, such as velocity or another relevant parameter. Colours range from dark blue to yellow, with possible intermediate colours such as green or red. Darker colours typically indicate lower values, while brighter colours represent higher values. The arrows in the diagram are closely spaced, demonstrating a thorough examination of velocity data across the field. The distribution of velocities is consistent throughout the entire field, enabling a complete understanding of how the fluid flows and the arrows show the way that things move at each location. The arrows can point in different directions, which tells us that the flow changes orientations as it goes through the area. Observing the patterns made by the arrows can give clues about how the textile parts are moving. Areas where the arrows are all pointing in the same direction mean the flow is smooth and organised (laminar). On the other hand, areas where the arrows point in different directions or cross each other likely mean that the flow is turbulent or unstable.

For the image pair No. 032, the image's background has a colour gradient that changes from yellow to orange to blue and small arrow-like shapes are over the colour gradient background.

These arrows show the direction and strength of speed at different parts of the image. Most of the arrows are blue, which shows the main direction of the flow, this image represents the maximum strain that the textile reached before returning to the original shape. For the image pair No. 064, the image shows a smooth colour shift from deep blue to yellow and then to deep red. This colour gradient visually represents speed variations, with darker colours indicating slower speeds and brighter colours indicating faster ones.

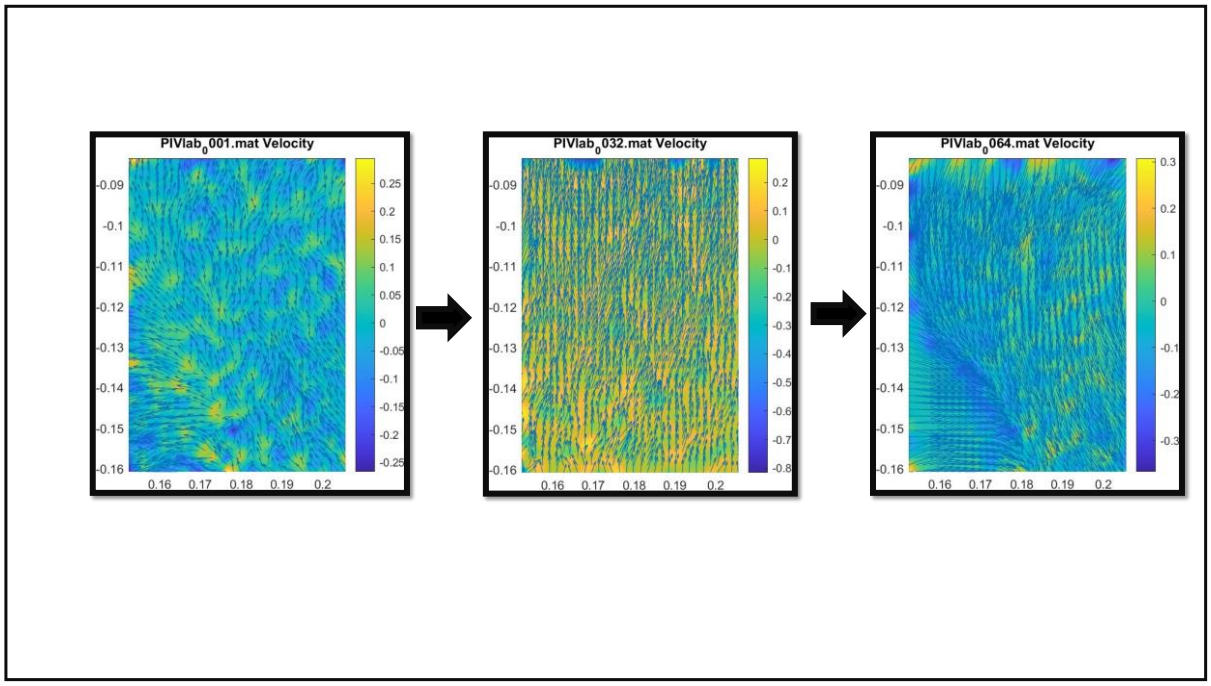

Figure 146: PIV velocity first test for the polyester tube knit without Lycra under high strain (7.5%) MATLAB, *2023)*

The second velocity test for the polyester tube knit fabric without Lycra is very similar to the first one due to several reasons. First, the test is conducted on the same type of fabric, namely polyester tube knit fabric without Lycra. Second, the same test settings and methods are used consistently (e.g., applied force, load rate, and measurement techniques). These consistent conditions enable the comparison of fabric performance and mechanical properties for the polyester knit fabric without Lycra. The resulting similarities in the second velocity test are attributed to the fabric itself and the unchanging test parameters. The second speed test for the polyester tube-knit fabric without Lycra is comparable to the first, as both assessments aim to analyse the fabric's mechanical attributes under similar regulated settings. This similarity

allows for a direct comparison of the fabric's performance. The standardised testing conditions ensure that any variations seen between the two velocity tests are attributed to the fabric's inherent properties, rather than external influences (Lu & Sick, 2013; Peng & Green, 2012).

3.7.6 Comparison of the PIV Velocity Test between the Stainless-Steel Tube Knit Fabric and Polyester Tube Knit Fabric without Lycra

The evaluation of the PIV velocity experiments between the stainless-steel tube woven material and polyester tube knit fabric without Lycra shows various distinctions and resemblances.

- Direction of flow:

Both textiles displayed a primarily upward flow orientation in the early images under minimal strain. At high levels of strain, the stainless-steel material showed downward curving patterns, whereas the polyester fabric displayed colour changes which indicate different velocities along its surface.

- Speed Measurements:

The stainless-steel fabric showed a reduced test time at low strain, potentially because of its natural durability and uniformity during testing without Lycra. The polyester material, conversely, exhibited greater PIV speed measurements in comparison to fabrics containing Lycra.

- Similarities:

The subsequent tests on the two materials closely resembled the initial tests, suggesting uniform material performance and test conditions in the absence of Lycra. Both examinations offered an understanding of how the fabrics behave and their characteristics when subjected to varying rates of strain.

The test results imply that the stainless-steel fabric without Lycra and the polyester fabric without Lycra have distinct flow patterns and velocity traits. These variations stem from the

innate qualities of the materials, strain rate influences, and fabric structural dynamics. The findings are beneficial for fabric manufacturers and designers to enhance fabric designs for specific purposes. Stainless steel is ideal for applications needing robustness (Ding, 2024), while polyester's flexibility is advantageous in activewear where stretchiness is crucial (Hassan et al., 2012).

Analysing strain test images of knit fabrics using Particle Image Velocimetry (PIV) is a complex process that necessitates advanced techniques and high image clarity. Unfortunately, in this specific instance, the image quality was subpar, and the arrow movements were not clearly defined. Consequently, conducting a thorough analysis of the strain test images for all knit fabrics using PIV proved challenging. This limitation underscores the importance of further research to enhance image clarity and arrow movements in strain test analysis for knit fabrics.

It is crucial to recognise that utilising PIV for strain test image analysis can offer valuable insights into the mechanical properties and performance of knit fabrics, benefiting fabric developers and manufacturers. However, the lack of clear image quality and distinct arrow movements hindered the comprehensive analysis in this study. Therefore, this aspect of the research may be deferred for future exploration to devise more effective techniques that can address these challenges and yield precise strain test results for knit fabrics through PIV analysis.

Chapter 4 Mathematical Model

4.1 Introduction

Mathematical modelling is essentially about taking real-world problems from different fields and turning them into manageable math equations. This process helps us uncover insights and solutions that can be directly applied to real-life situations.

These models play a crucial role in many applications, especially when we need precision and the ability to make predictions. By helping us understand how systems behave, mathematical models allow for better designs and more effective control strategies.

With the power of modern computing, we can create these models faster and more accurately, leading to improved design processes. This not only enhances our design capabilities but also encourages innovative approaches to controlling various systems.

In the current study, mathematical models of the energy in a textile under uniaxial strain were developed. The models aim to demonstrate the extent to which the principle of the minimum overall energy within the knitted textile can replicate the experimentally observed behaviour in the samples. These observed behaviours include:

- The changing configuration of the specimen when it stretched from the top edge while the bottom is fixed, particularly the narrowing of the middle (see Figure 147).

- The sideway ripples that were observed during the tensile tests (see Figure 148).
- The curling of the left and right edges of the textile (see Figure 149).
- The sagging due to gravity (see Figure 150).

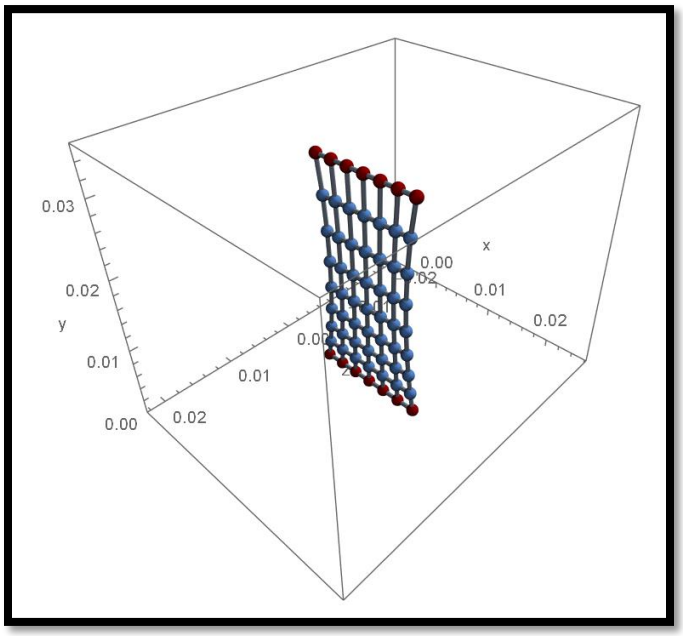

Figure 147: Strain length energy

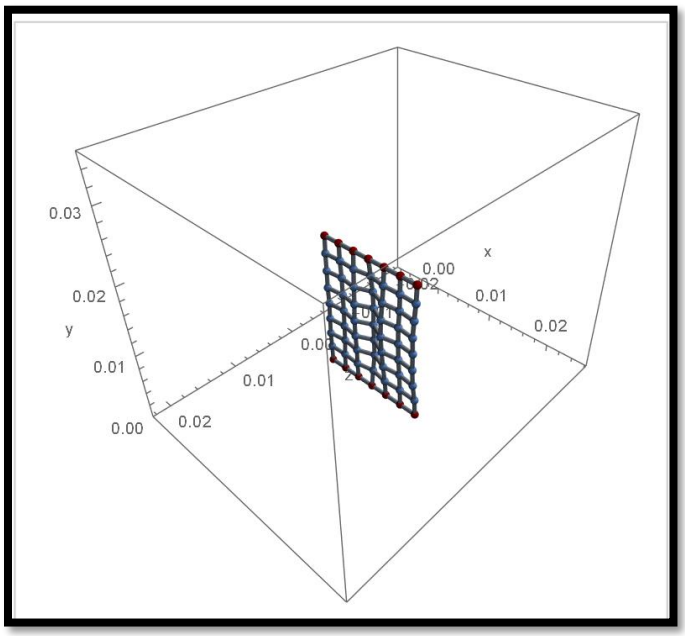

Figure 148: Strain energy-sideways ripples

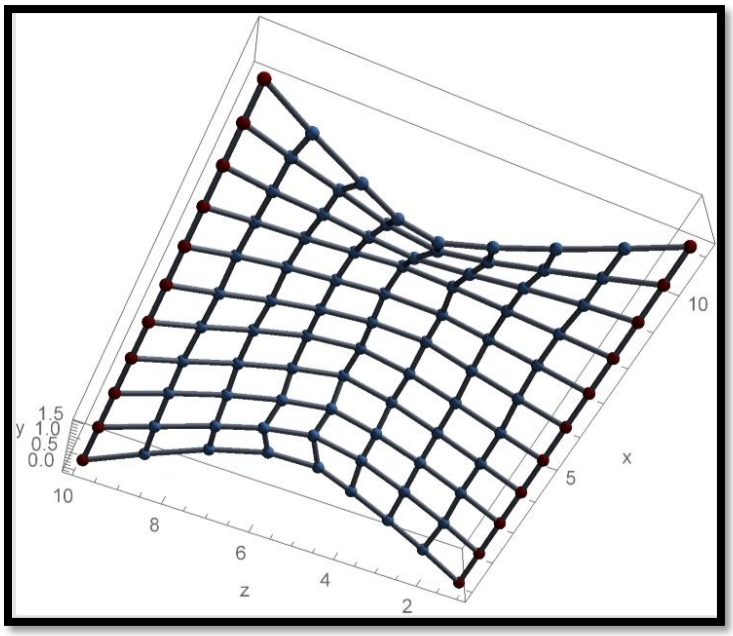

Figure 149: Weft curl energy

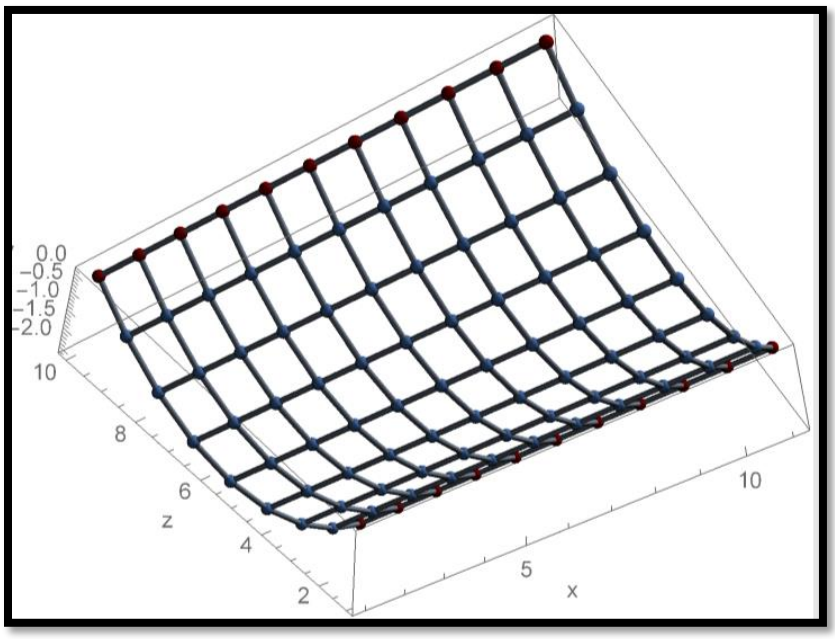

Figure 150:Gravity energy

In the experimental part of this project, samples of different types of yarns (silver, stainless steel, and polyester) were used. Each yarn has a specific density and modulus of elasticity. The flat and tube sample shapes were tested. In this section, the models developed are representative of generic textiles and were not designed to emulate a specific test scenario. However, these models are based on important variables, such as mass, density, modulus of elasticity, and other physical parameters. Equations were derived to relate the available variables, and then a computer mathematics program was employed to resolve the formulas to mimic the behaviour of the generic textile.

Several methods have been developed by other investigators as discussed in the literature review chapter (see Chapter 2), to establish a new mathematical model to calculate the mechanical features of the fabric. These include finite element models developed by Sharma and Carvelli (2001) and Savvas and Din (2018). This Finite Element Method (FEM) tackles force-equilibrium challenges; however, its utilisation has certain drawbacks. As the complexity of the model increases, the construction intricacies and computation time escalate due to extensive input data and the multitude of equations to resolve. This method mandates digital computing and deals with intricate force representations through vectors. Moreover, the output results of this model exhibited considerable variation.

To address the challenges, the current study seeks to solve an energy minimisation problem to effectively simulate the mechanical behaviour.

4.2 Energy Methods

Energy methods provide alternative methods for determining mathematical models. These techniques are based on flexibility behaviour and energy saving, which means that the action performed by exterior forces is equivalent to the energy kept in the construction under load. It is also assumed that a system finds equilibrium in a minimum-energy configuration; that is, the internal energy will decrease and approaches a minimum value at equilibrium. This method restates the laws of thermodynamics.

In this project, the energy method aims to minimise the energy in the textile after stretching (applying strain). In the simple case of the strain energy, the relationship between the change in energy (dU) and the applied force (F) over a small displacement (dx) is given by the following equation:

$$dU = Fdx$$	(2)

where dU is the increment in strain energy, F is the applied force, and dx is the increment in displacement owing to the force integration.

The relationship between force and displacement in a linear elastic system given by Hook's law, the strain energy (U) stored in the system is obtained by integrating the force-displacement relationship

$$F = Kx$$

The strain energy (U) is given by the work done, which is the integral of the force (F) over the displacement (dx) :

$$U = \int_0^X Fdx$$

Substituting $F = Kx$ into the integral:

$$\int_0^X Kxdx$$

Evaluate the integral:

$$U = \frac{1}{2}Kx^2$$

Since $F = Kx$, we can also write Uin terms of force and displacement as:

Therefore, assuming a constant force, the strain energy U would be

$$U = \frac{Fx}{2}$$	(3)

Thus, the strain energy is proportional to the square of the displacement or, equivalently, half the product of force and displacement.

In the experimental part of this project, the textile was under tension from the top edge, as shown in Figure 151. Part A represents the textile in the original configuration and part B shows the textile under the effect of force F. This force stretches the textile by moving the top clamp a distance X. The reaction to the applied force is due to the tension of the fibre, fibre torsion, and fibre bending. The work from stretching the textile itself was equivalent to the overall energy stored in the textile after stretching. The question this study aims to address is how to model the energy distribution within a textile.

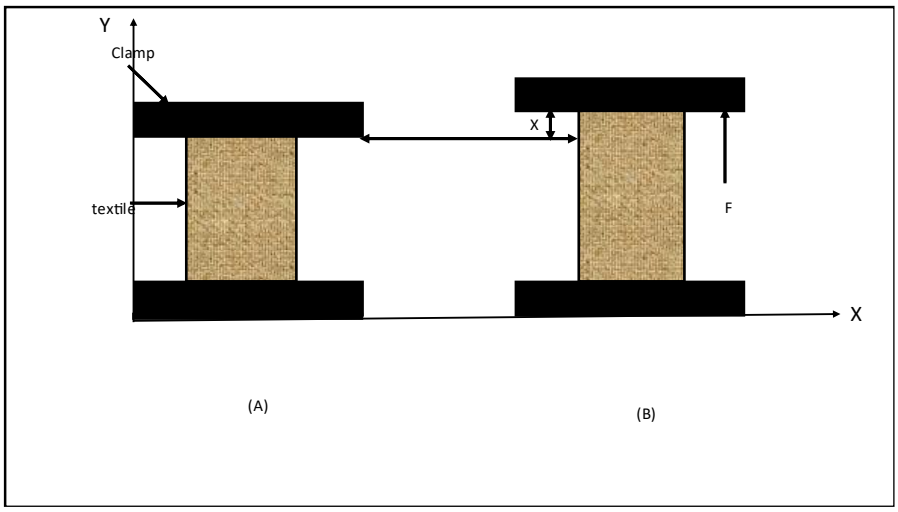

Figure 151: Textile under tension

4.3 Modelling

The structure of the knitted textiles was organised along horizontal and vertical axes. These are referred to as courses and wales, respectively. The course is a horizontal row of stitches. We indexed the courses using $j = 1\ to\ m$. The vertical column of stitches is known as the wale and is indexed by $i = 1\ to\ n$ as shown in Figure 152.

In a typical sample, the number of wales was n =70, and the number of courses was m=120 (plus 20 courses to the top and bottom to clamp the piece of textile in the textile analyser during the tensile test). However, in this mathematical simulation, we did not use the actual number of wales/courses. Each "knot" in our simulation could therefore be considered to represent a patch or cluster of stitches, rather than an individual stitch. However, for simplicity, these patches or clusters are referred to as "stitches" in this chapter.

In the nomenclature used, the Y-axis corresponds to the vertical (top-to-bottom) direction, and the applied stress was extended in the textile by changing the distance between the top and bottom edges.

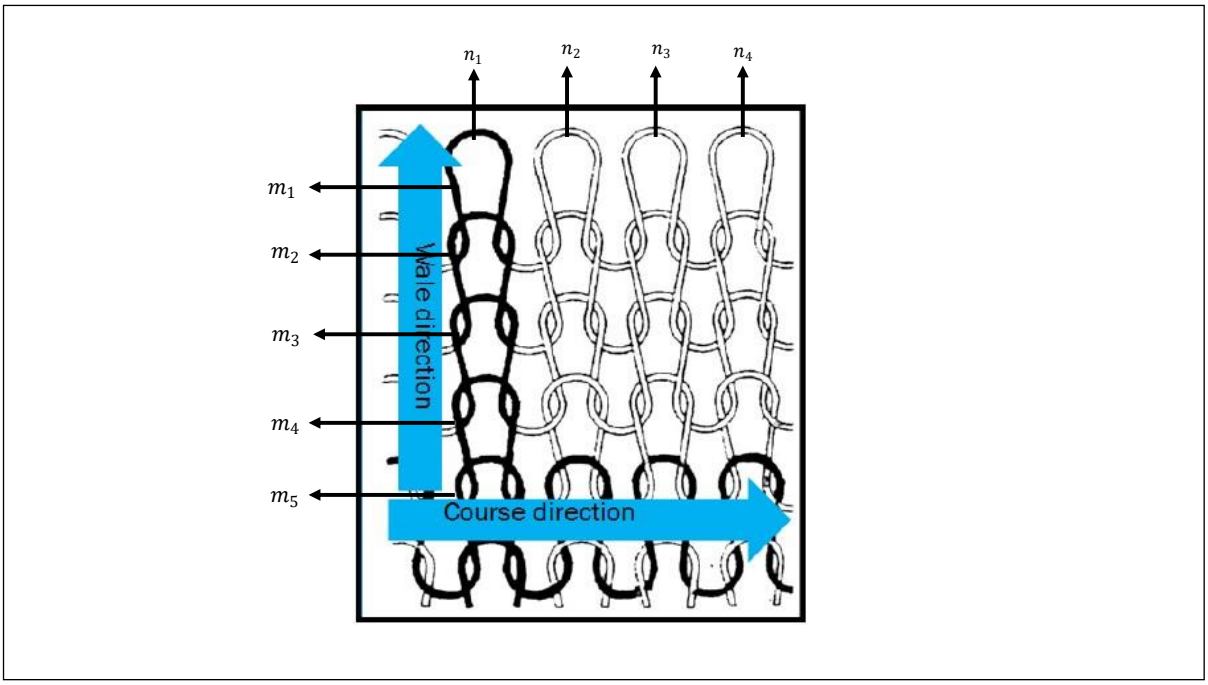

Figure 152: Diagram of wale and course trend of plain knitted fabric with (m_j, n_i) (Ghapanvari et al., 2015b)

To predict the total energy U_{total} under the effect of the force, the following types of energy are calculated and summed:

$$U_{total} = U_{strain} + U_{length} + U_{gravity} + U_{bending} + U_{torsion} + U_{friction} + U_{curl} \quad (4)$$

In this model, the total energy is represented as the sum of contributions from various sources, including strain energy (U_{strain}), energy due to changes in length (U_{length}), gravitational energy ($U_{gravity}$), bending energy ($U_{bending}$), torsional energy ($U_{torsion}$), frictional energy ($U_{friction}$), and the energy associated with curling (U_{curl}).

The individual energy components are discussed in greater detail in the following sections.

4.3.1 Strain Energy, U_{strain}

The energy stored within a material when it is stretched is termed strain energy. Strain energy is a type of energy retained in a structural component due to elastic deformation.

In this project, the strain energy is defined as the energy within a patch upon the deformation work performed by all applied forces. Since the textile sample was clamped from the bottom and top sides of the texture analyser machine, the vertical movement of the top clamp deformed the patches of the textile, as shown in Figure 153 (A). Note that the patch deforms in both the course and wale directions and may also skew. one of our assumptions is that knots and stitches can slip during deformation. In the world of knitting, the interlocking pattern of loops is known as a "stitch" - the fundamental building block of any knitted piece. Each stitch is created by pulling yarn through an existing loop, and the collective arrangement of these stitches gives the fabric its unique texture and design. Using a variety of techniques and arrangements, skilled knitters can produce an array of beautiful patterns and textures through the manipulation of stitches.

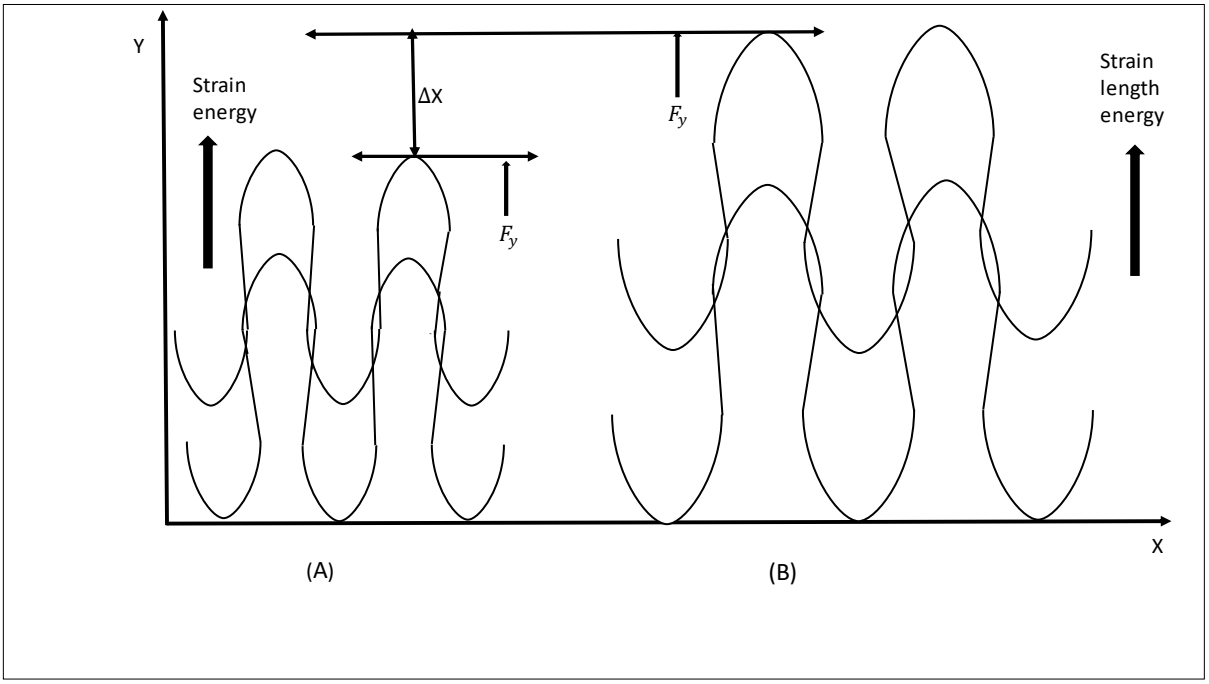

Figure 153: Distinguishing between strain energy and strain length energy

Starting from Equation (3), we assume a relationship between the applied force and stress, σ, involving the cross-sectional area A:

$$\sigma = \frac{F}{A}$$	(5)
$$U_{strain} = \int_0^X A\ \sigma\ dx$$	(6)

For linear elastic behaviour:

$$\frac{\sigma}{\epsilon} = E$$	(7)

where E is an elastic modulus and ϵ is strain, defined as:

$$\epsilon = \frac{\Delta X}{X_0}$$	(8)
$$\Delta X = X - X_0 = x$$	(9)
ΔX represents a change in a characteristic length from $X_0$to X. Substituting in () gives $U_{strain} = \int_0^{\Delta X} A\ E\ \frac{x}{X_0}\ dx$	(10)

$$U_{strain} = \frac{A\,E}{X_0}\frac{\Delta X^2}{2} = w_{strain}\Delta X^2$$	(11)

For a particular textile patch or stitch, the term $\frac{A\,E}{2\,X_0}$ can be considered constant, and U_{strain} is proportional to the factor w_{strain} to the square of the displacement ΔX. In this simple model, the strain energy from the displacements in the course and wale orientations are summed. When the knitted fabric sample underwent vertical stretching, the size of the stitches was altered in both the wale and course orientations by an equal value, despite differing directions.

Referring to Figure 154, which shows the positions (x, y) of the four adjacent stitches $(i, j), (i+1, j), (i, j+1), (i+1, j+1)$, the total strain energy is:

$$U_{strain} = w_{strain}\sum_{i,j}\left(x_{i+1,j} - x_{i,j} - X_0\right)^2 + \left(y_{i,j+1} - y_{i,j} - Y_0\right)^2$$	(12)

Where X_0 and Y_0 are the "relaxed" inter-stitch distances, the model can be extended into three dimensions. As force is applied, the stitches and yarn compress, leading to strain energy, which is represented in the model. Assuming nodes slip, for example, the distance between the two knots is (x_1) after stretching the textile. Moreover, the knots are moving from (x_i) to (x_{i+1}) in a horizontal direction and from (y_i) to (y_{i+1}) in a vertical direction. This compression and yarn force is related to changes in internode distance.

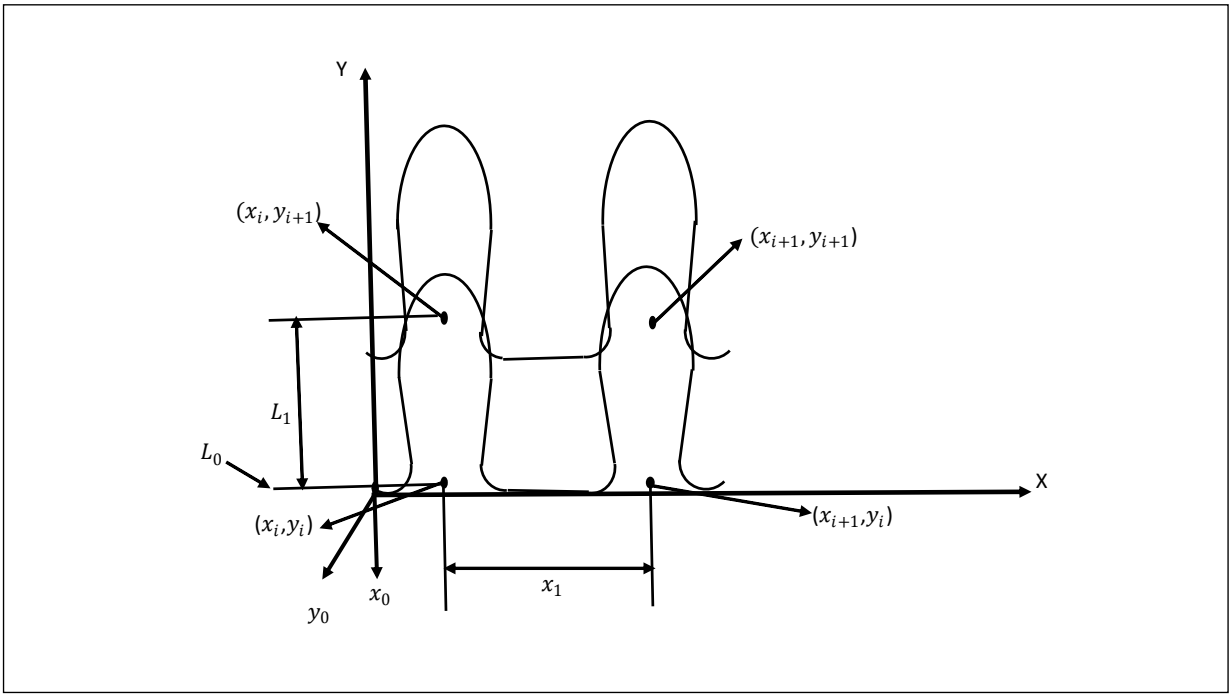

Figure 154: The positions (x, y) of four adjacent stitches $(i, j), (i+1, j), (i, j+1), (i+1, j+1)$

4.3.2 Strain Length Energy, U_{length}

A change in length occurred when a force was applied to the textile. However, for a knitted structure, this change in length can occur because of a change in the shape of the patch, for example, as stitches bend or distort without changing the length of the yarn. The difference between the strain length energy, U_{length}, and the strain energy previously discussed, U_{strain}, is that the latter represents the patch being stretched and changing shape, while the strain length energy is about the elongation of the yarn itself.

Thus, in a similar manner to the previous derivation in Equation (13), we may write:

$$U_{length} = \frac{A\,E}{2L_0}\Delta L^2 = w_{length}\Delta L^2 \qquad (13)$$

Where:

- L_0 : Initial length of the yarn.
- ΔL : Change in length ($L_{strectched} - L_0$)
- A : Cross-sectional area of the yarn.
- E : Young's modulus (elasticity of material).
- w_{length}: A proportionally constant

The original length of the yarn can be referenced to the volume, V, of a textile sample and the yarn's linear density, through the equation (1) in section 3.3.2 Yarns:

$$L_0 = \frac{V}{A} = \frac{wS}{d}$$	(14)

As shown in Figure 154, the overall length of the yarn is related to the positions of the knots, which can slip along the yarn. The yarn length associated with a knot, $l_{i,j}$, is related to the internode distances and modelled using:

$$l_{i,j} = \left(\frac{x_{i+1} - x_i}{2}\right) + 2(y_{i+1} - y_i) + \left(\frac{x_i - x_{i-1}}{2}\right)$$	(15)
$$L = L_0 + \Delta L = \sum_{i,j} l_{i,j}$$	(16)

4.3.3 Gravitational Potential Energy, $U_{gravity}$

Gravitational energy is the potential energy related to elevation on Earth. Each stitch/patch has gravitational potential energy, and the overall gravitational potential energy is the sum of the individual contributions., as shown in the following equation:

$$U_{gravity} = \sum_{i,j} m\, g\, y_{i,j} = w_{gravity} \sum_{i,j} y_{i,j} \quad (17)$$

where m is the stitch mass in kilograms and g is the gravitational acceleration (9.81 m/s^2). These constants define the factor of proportionality, $w_{gravity}$.

4.3.4 Bending Energy, $U_{bending}$

Bending properties describe the behaviour of a thin or elongated structural component, such as beams, fibres, or textile elements that react when a load is applied to them from the side, rather than along their length. When this load is applied, the structure bends, and the amount of bending that occurs depends on several key factors: how stiff the material is, the shape and size of the component, and the strength of the force applied. Grasping these bending properties is essential for accurately predicting how these structures will perform under various loads and for making sure they remain strong and reliable.

In this project, the bending energy arises from changes in the yarn shape, specifically the curvature of the yarns during the fabric expansion caused by interference. As the yarns bend, the fibres within them glide past each other, resulting in very low overall bending rigidity of the yarn.

The bending energy for linear elastic behaviour is given by the following equation:

$$U_{bending} = \frac{l\,M^2}{2B} \propto \frac{l\,\Delta L^2}{2B}$$	(18)

Where:

- l is the unit cell length
- M is the applied bending moment.
- L is the yarn length
- B is flexural rigidity.

In this model, the bending energy is negligible but can also be considered represented in the first strain energy component, U_{strain}, as tighter stitches relate to more bending (that is, bending moments are proportional to changes in the length of the patch, so $U_{bending} \propto U_{strain}$).

4.3.5 Torsional Energy, $U_{torsion}$

Twisting in yarn is a procedure that connects yarns or fibres cooperatively in a continual rope, completed in plaiting or rotation processes. The orientation of the twist may be to the right or left and can result in torsion energy, as shown in Figure 155.

According to Castigliano's second theorem that considers the case of uniaxial tension:

$$U = \frac{F^2 L}{2EA}$$	(19)

Where:

- F is the applied force.
- L is the yarn length.

- E is elastic modulus.
- A is the cross-sectional area.

The displacement through which the force moves can be obtained by differentiating the expression for the force, as can be seen in the following equation:

$$\Delta = \frac{dU}{dF} = \frac{FL}{EA}$$	(20)

Similarly, the torsion of the circular bar was represented in the yarn as follows:

$$U_{torsion} = \frac{T^2 L}{2GJ} = \int_0^L \frac{T^2}{2GJ} d_x$$	(21)

In the equation

- T is the torque.
- L is the length of the yarn
- G is the modulus of rigidity.
- J is the polar second moment of the area of the cross-section which is represented by the equation below (Figure 155).

$$J = \frac{\pi r^4}{2} = \frac{\pi d^4}{32}$$	(22)

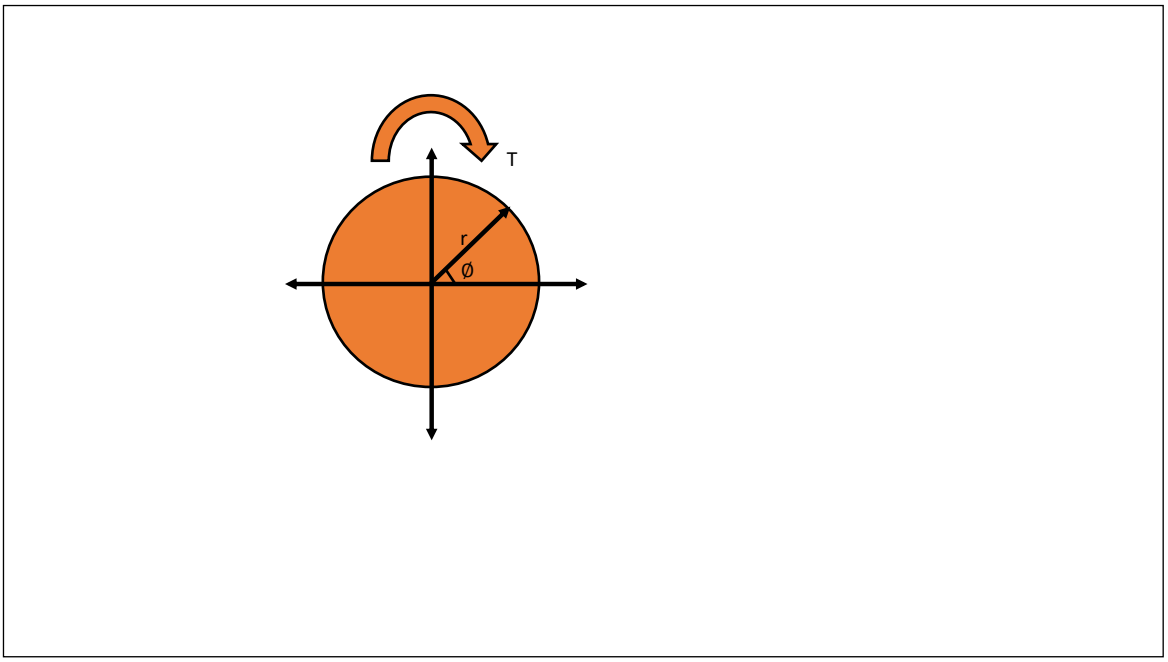

Figure 155: Yarn's cross-sectional area

The last general equation of the torsion energy will be:

$$U_{torsion} = \frac{16\,T^2 L}{\pi G d^4} \quad (23)$$

And the differentiation gives:

$$\emptyset = \frac{dU}{dT} = \frac{TL}{GJ} \quad (24)$$

If the yarn starts to twist, a prior tension must be applied to the yarn before any additional twisting to prevent torsional buckling. The strain energy related to this source of torsion, therefore, corresponds to a component of U_{length} – that is, it contributes to the lengthwise stiffness of the yarn.

Liu et al. (2007) explained that when a textile is stretched, the yarn starts to bend because the force and the yarns start to slip over each other. The fibres will shift openly to prevent being expanded till they are prevented from doing that by fibres that preoccupy the space. The fibres of the yarn that cannot shift horizontally are referred to as jammed. The torque that appears in this region contributes to the torsional energy in the jamming region. If not all the yarn jammed, the distorted yarn can be split up into two sections, the jammed origin, which is placed at the middle point and the unstrained zone which is outside the jammed zone, as can see in Figure 156. In this figure, the initial state refers to the textile yarn before any strain or load is applied; all regions coloured green represents no jamming. However, once jamming occurs, the radius of the yarn in the jammed region will be less than the radius in the initial state, and the yarn will be jammed in the middle region. Other authors, for instance (Tandon et al., 1995) have shown that this component of the torsional energy is negligible, but also represented in the first strain energy component, U_{strain}, as tighter stitches relate to more torsion.

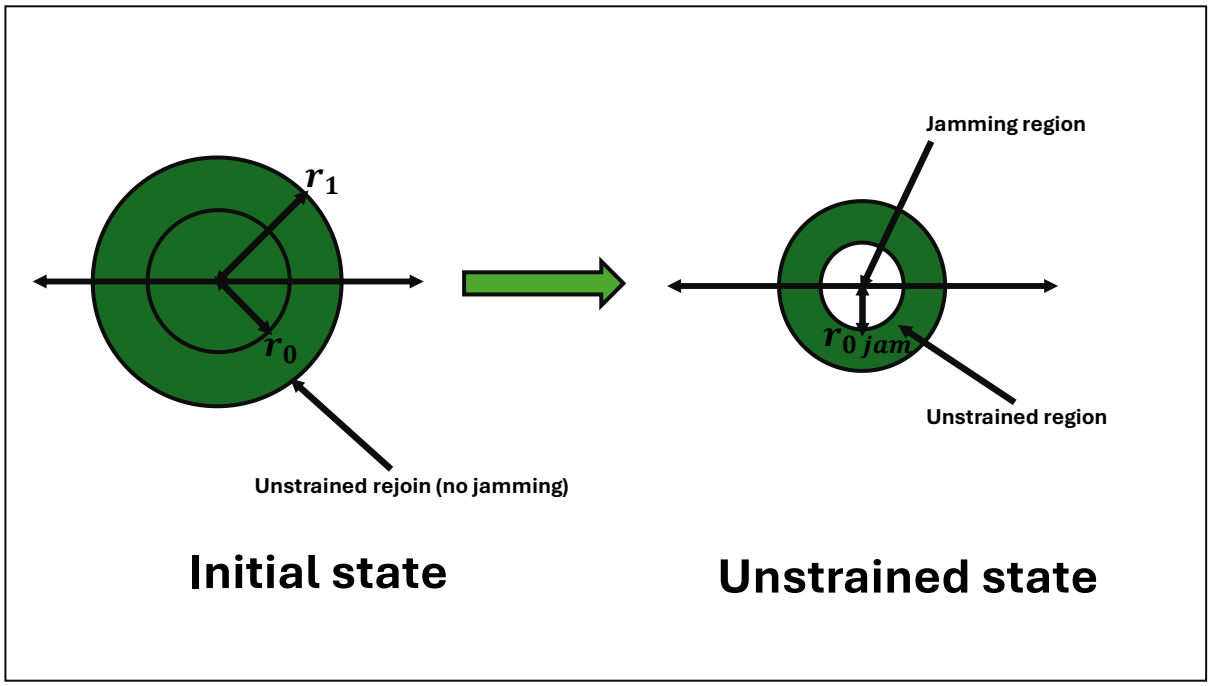

Figure 156: Yarn cross-section before and after deformation

4.3.6 Frictional Energy, $U_{friction}$

Friction is the force that grips fibres jointly in a knitted yarn and the interfacing threads in a fabric. If the friction is too small, the yarn fails, which means the fibres will come apart, and the dimensions of the fabric will be decrease steadily. The friction energy occurs when the loads applied on the yarn are very high. This matter suggests that the friction's role in the textile's mechanical behaviour, but the load in this research is less than it is for friction energy to be formed.

When yarns bend or expand, fibres slide past each other, and yarns slide on each other during the expansion of the fabric. Thus, work done on the textile is partially used to overcome friction in two regions:

i) Between fibres during sliding in yarn construction.

ii) Between yarns at junction points during fabric construction.

It is difficult to capture the frictional energy in a quasi-static energy model, such as the one proposed, because it is path dependent. Friction is the loss of energy from the system that is no longer conservative. This analysis neglected friction because the distances moved were small, and the frictional energy was proportional to the distance moved.

4.3.7 Curl Weft Energy, U_{curl}

Curling of the edges of a knitted fabric is a recognised phenomenon. This is caused by the release of energy saved in the fabric during loop formation (known as curl-weft energy). This phenomenon is complex but can be explained simplistically as follows: the yarn tends to adopt a straight configuration, a form that is influenced and supported by the tension from neighbouring loops. However, at the edges, where there are no neighbouring loops on one side to provide counter-support, curling occurs as the balance of forces is disrupted.

In this project, it was found that after the textile was stretched vertically while clamped in the texture analyser machine, as discussed before, curling became more pronounced. This suggests that higher tension in the knit stitch provides more stored energy, which causes curled edges.

An example of this is shown in Figure 158. The right and left edges have curvatures that occur because of the curl-weft energy.

The curl weft energy is represented in this model as being related to the angle between the three stitches. Essentially, the model tries to make the relaxed (minimum energy) state of a row of stitches not flat, as can be seen in Figure 157.

in the context of this study, the curling energy, U_{curl}, quantifies the energy associated with deviations in the yarn's curvature from its reference state. The reference curvature is defined by the angle θ_0, while the actual curvature at each point is represented by $\theta_{i,j}$. The curling energy is calculated as the weighted sum of the absolute differences between the sine of these angles. Mathematically, it is expressed as follows:

$$U_{curl} = w_{curl} \sum_{i,j} \left| \sin \theta_{i,j} - \sin \theta_0 \right| \quad (25)$$

Where:

- w_{curl} is a constant of proportionality.
- $\theta_{i,j}$ represents the angular orientation of the (i,j) fiber yarn segment, or structural component.
- θ_0 is the reference angle (not flat).

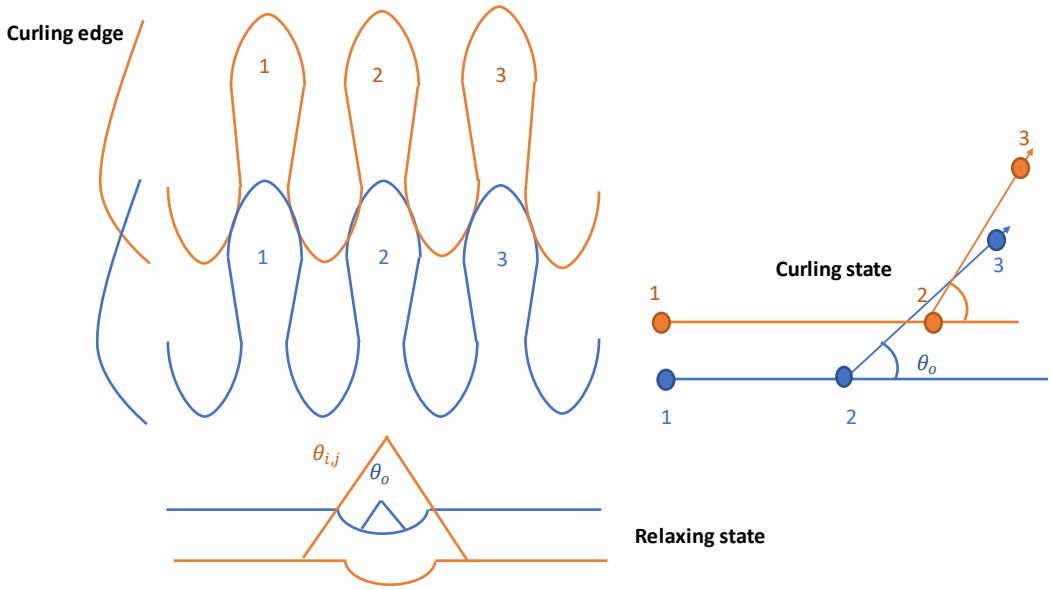

Figure 157: Curling and relaxing state with the angle between the stitches for the knitted fabric

Figure 158: Curl weft energy

4.4 Simulation of Mathematical Model

Based on the discussion and derivations above, the total energy depends on the strain energy, gravity energy, length energy, and curl weft energy. As previously discussed, the torsional and bending energies are also represented in the first and second strain energy components, as the length strain and tighter stitches are related to more torsion and bending. Friction was expected to have an unnoticeable or negligible effect on this project.

The overall energy equation is therefore given by:

$$U_{total} = w_{strain} \sum_{i,j} f_{strain}(x_{i,j}, y_{i,j}, x_{i+1,j}, y_{i,j+1}) + w_{length} \sum_{i,j} f_{length}(x_{i,j}, y_{i,j}, x_{i-1,j}, x_{i+y,j}, y_{i,j+1}) + w_{gravity} \sum_{i,j} y_{i,j} + w_{curl} \sum_{i,j} f_{curl}(\theta_{i,j}) \quad (26)$$

Where:

- f_{strain}, f_{length} and f_{curl} are functions described in the sections above, and all are dependent on the positions $(x_{i,j}, y_{i,j})$ of the stitches/patches.

This equation for the total energy that affects the yarn under the applied displacement was programmed into Mathematica (Wolfram Research, IL, USA). The objective of employing the energy method is to minimise the overall energy within specific boundary conditions, typically set as fixed points akin to those being clamped. Initially, the placement of non-fixed points is arbitrary and not crucial for the initial assignment. Mathematica was then used to optimise the locations of the other points to determine the minimum energy configuration. This algorithm is presented in Figure 159.

Weighting factors are like special numbers that help us understand how important different pieces of information are within a group. In this study, these factors act as set values that affect how much each type of energy contributes to the overall results. They let us see which data points matter more and which ones matter less when we look at the outcome. For example, consider the weighting of 1 for the gravity energy, $w_{gravity}$. Because the gravitational probable energy is commensurate with the mass of the yarn, the effective mass will double if the weighting is set to a value of 2 while keeping other contributions to the strain energy constant. Conversely, if the weighting was zero, there would be no gravitational energy effect.

For other energies, such as tensile strain energy and strain length energy, the weighting is related to elongation, elastic modulus, and other factors. Changing a weighting such as w_{strain} from 1 to 2 changes the effective ratios of these constants.

In the following simulation results, the effect of changing the weighting value for each energy in the system is investigated. The results are presented with different numbers for each energy weighting to demonstrate the changes in textile geometry. In some cases, the weights are set equal to zero, meaning that in this case, there is no effect of the corresponding energy.

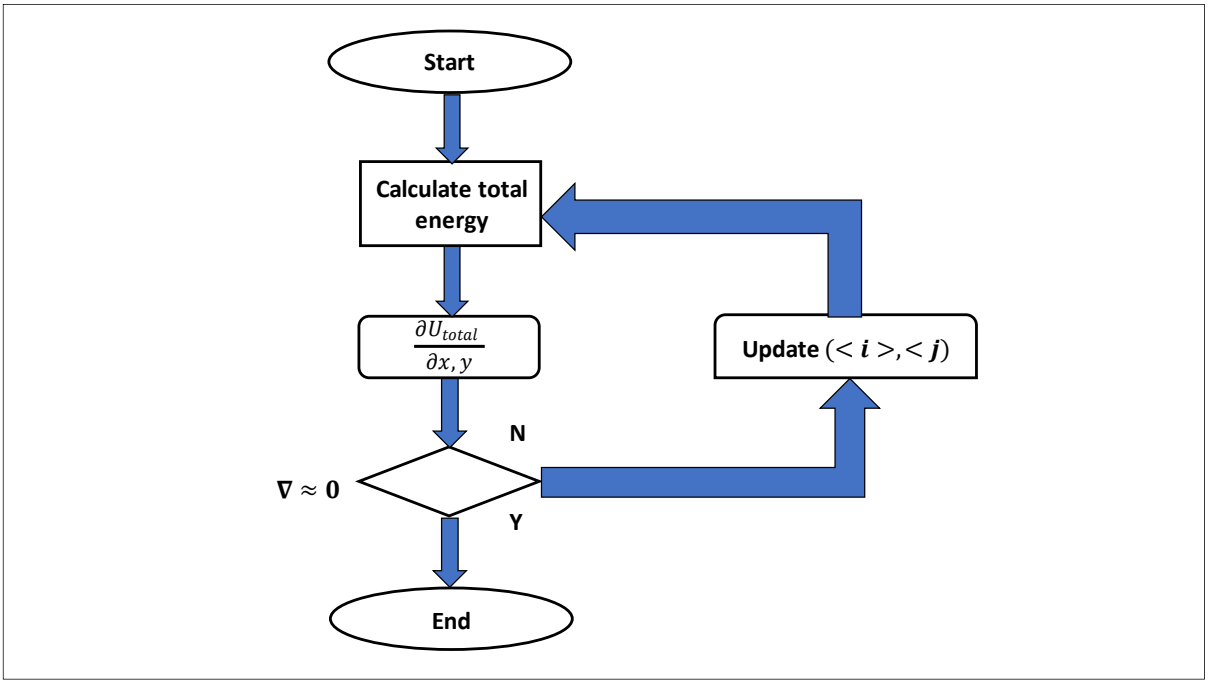

Figure 159: Algorithm flowchart to minimize energy

4.5 Results and Discussion

In this section, changes to the relative weighting of the energies (w_{strain}, w_{length}, $w_{gravity}$ and w_{curl}) are made to examine the predicted effect on textile behaviour and results are discussed. The weightings were varied individually and subsequently in combination.

Figure 160 and Figure 161 show a baseline scenario where all the energy functions are assigned a weighting factor of 1. The textile is modelled as interconnected patches consisting of nine wales and 11 courses. This segment represents a small section taken from the middle portion of a large experimental sample. The first and last courses had fixed positions corresponding to the texture analyser clamps. The textile was stretched in the Z-direction by one unit, resulting in a strain of 5%. The model predicts that under these conditions, the textile would not remain flat. The length of the yarn between any two nodes would become non-uniform, and the edges of the textile would begin to curl and curve due to the influence of curl weft energy

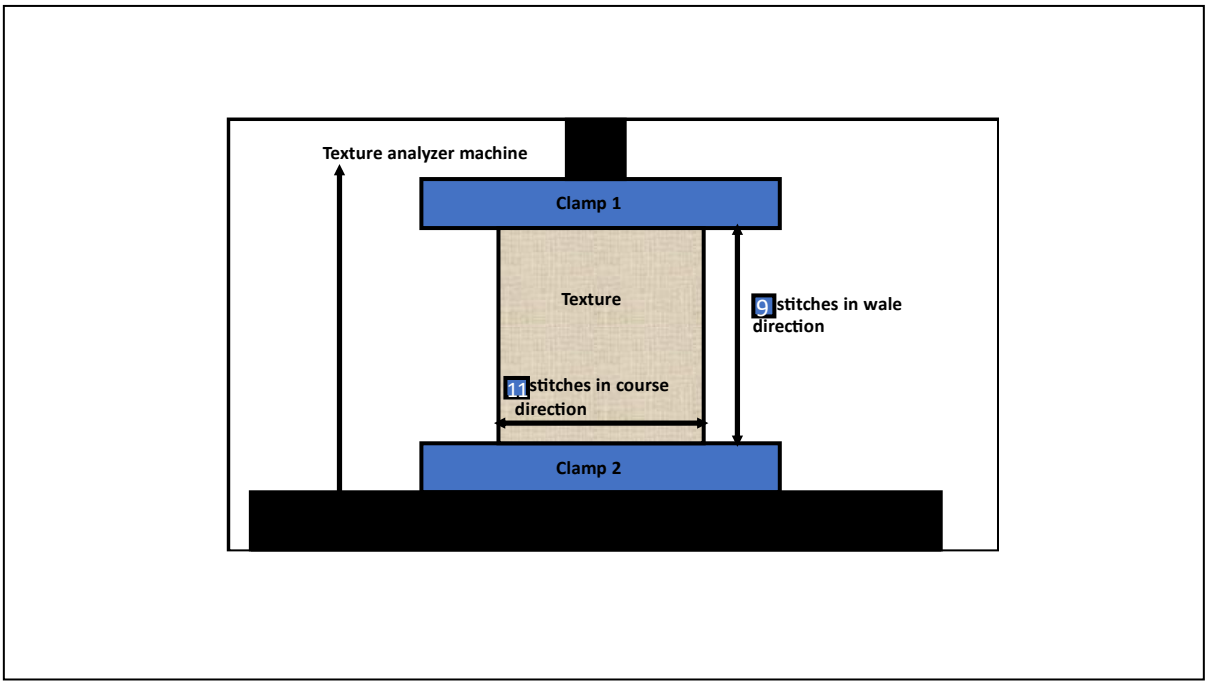

Figure 160: The textile testing diagram

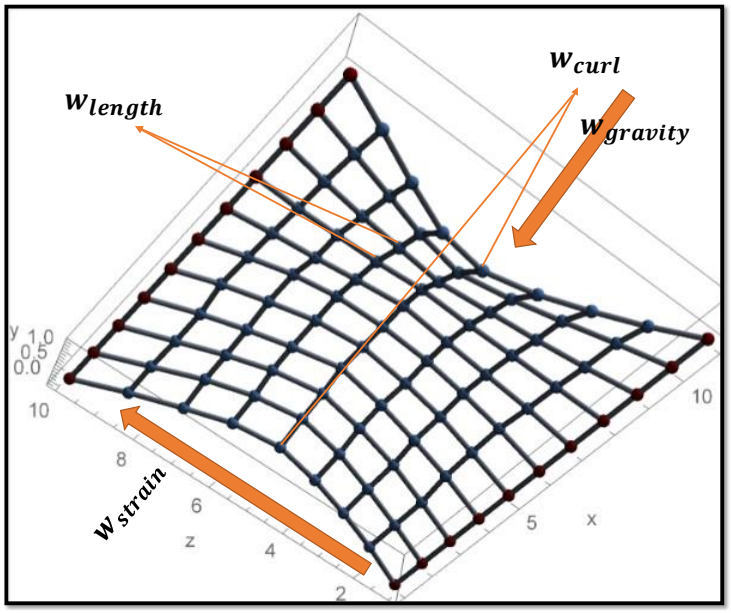

Figure 161: Mathematica software testing result shape with all energies effect

4.5.1 Strain Energy Weighting

Table 22 represents weightings for scenarios where strain energy weighting is varied within the range of 0.1 to 2, with 2 being the highest weighting considered suitable for the test. The corresponding figures are Figure 162–165, respectively.

Table 22: Scenarios changing strain energy weighting.

Energy \ Scenario	**A**	**B**	**C**	**D**	**E**
Strain energy	0.1	0.5	1.5	1.8	2
Strain length energy	1	1	1	1	1
Weft curl energy	1	1	1	1	1
Gravity energy	1	1	1	1	1

A. In case A the strain energy weighting was 0.1 (i.e., low). The resulting shape shows the random behaviour of the textile in the middle area: the space between the nodes is different in length, and there is a dragging and wavy shape.

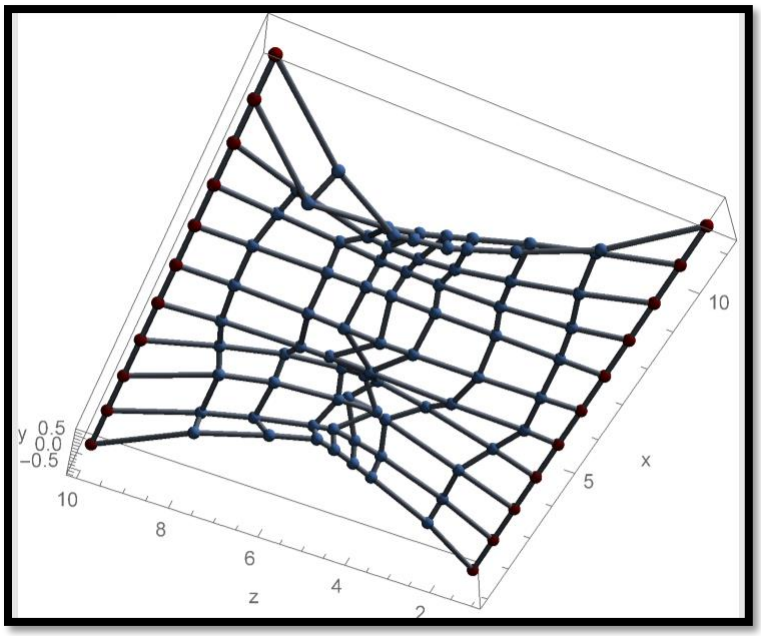

Figure 162: Case A (strain energy weighting =0.1)

B. In case B, the amount of strain energy weighting was increased to 0.5, and, as can be seen in Figure 161, the textile shape starts to behave more uniformly than in case A, with slight interlocking in the middle area. The bottom and top edges of the fabric are wavy in the Z direction. The node spacing is not uniform.

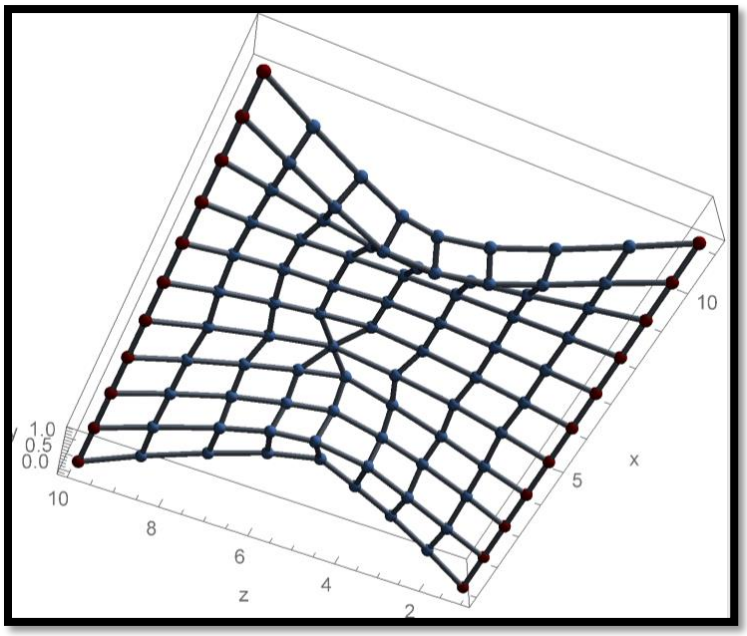

Figure 163: Case B (strain energy weighting= 0.5)

C. In Case C, the strain energy weighting was increased to 1.5. Figure 161 shows how the textile starts to stretch regularly with some curvature. The distances between the nodes were equal, with no interlocking or tangled nodes.

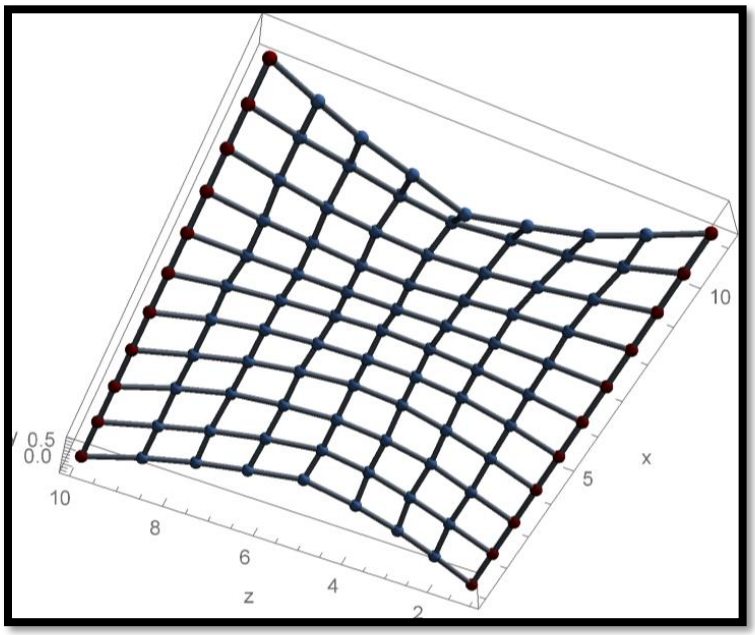

Figure 164: Case C (strain energy weighting= 1.5)

D. In Case D, the strain energy weighting was 1.8. Some waviness is observable in the middle, but the shape, in this case, appears more regular than in the other cases.

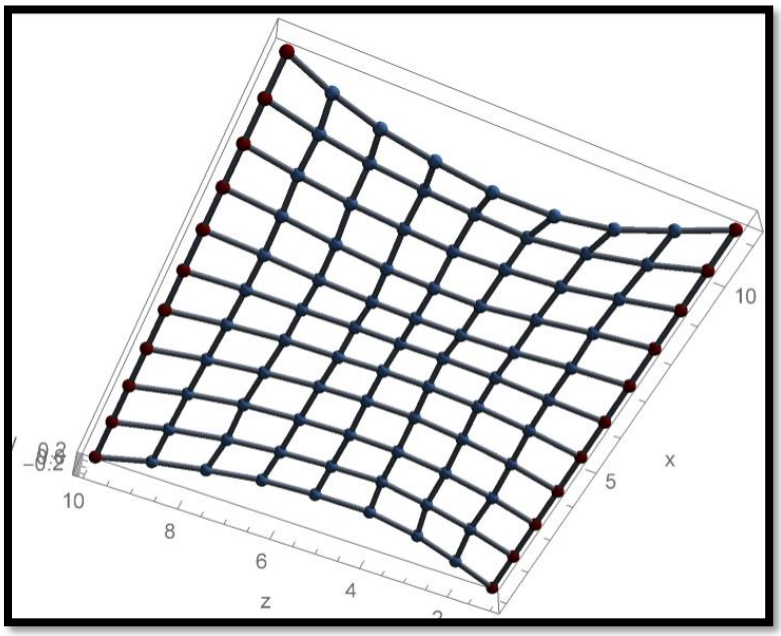

Figure 165: Case D (strain energy weighting= 1.8)

E. In Case E, the weighting was 2, and the shape is similar to that in Case D.

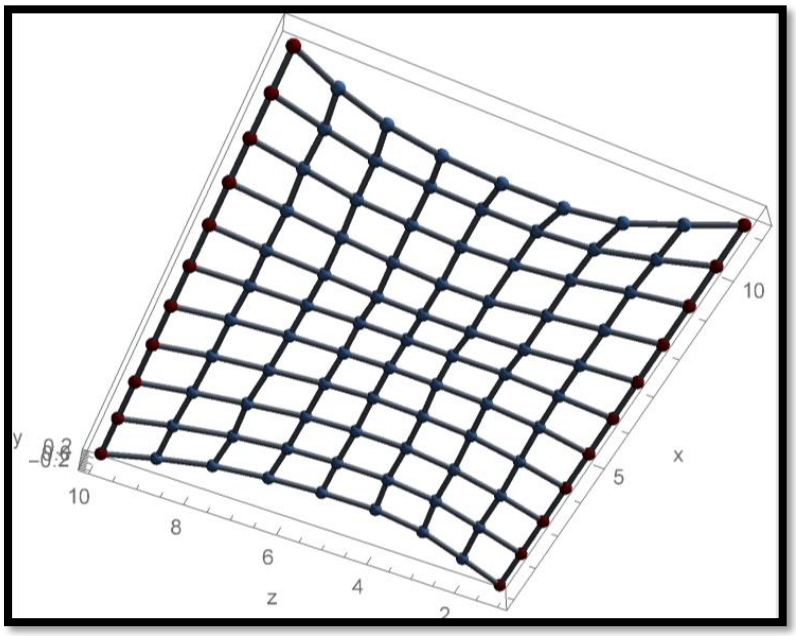

Figure 166: Case E (strain energy weighting= 2)

These results show that if the strain energy has a low weighting, then the textile shape after stretching appears irregular and has a wavy shape, unformed node spacing, and curvature on the edges. However, when the strain energy has a higher weighting than the other energies, its effect on the shape of the textile is to make it more regular in node spacing, with no tangling on the nodes, and the textile shape after stretching will be regular.

4.5.2 Strain Length Energy Weighting

Table 23 shows scenarios that change the straining length energy weighting independently of other weightings. The results are shown in Figure 167 to 170.

Table 23: Scenarios changing strain length energy weighting.

Energy \ Scenario	**A**	**B**	**C**	**D**	**E**
Strain energy	1	1	1	1	1
Strain length energy	0.1	0.5	1.5	1.8	2
Curl weft energy	1	1	1	1	1
Gravity energy	1	1	1	1	1

A. In case A, the straining length energy weighting was set to 0.1, and the other three energies (strain, curl weft, and gravity) were set to a normal weighting of 1. There is no obvious change in the length of the yarn, but the courses zigzag with some curvature in the free lower and upper edges in the direction of the Z axis, and some convergence between the nodes in the central region with increased spacing between nodes in the regions closer to the clamps (z=1 and z=10).

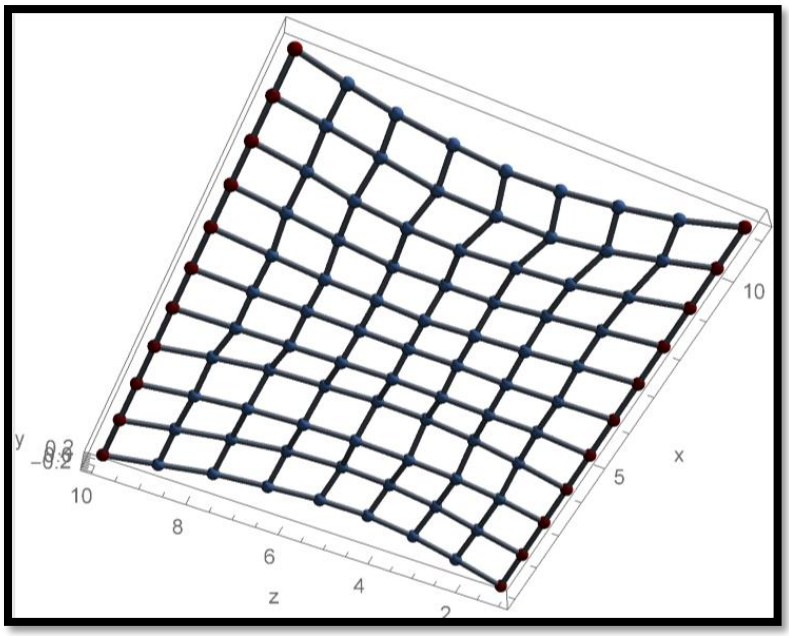

Figure 167: Case A (strain length energy weighting=0.1)

B. Case B shows the results when the weighting of the strain length energy is 0.5. It can be observed that the yarn length is highly variable in the central region, and the yarns start intertwining to become one node in the middle.

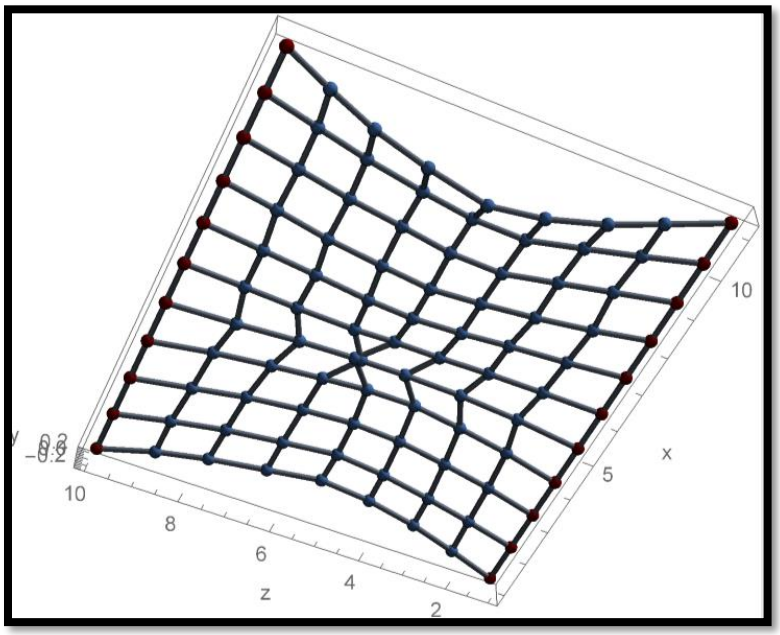

Figure 168: case B (strain length energy weighting=0.5)

C. In Case C, the weighting of the strain length energy was 1.5. Although there is no intertwining, some changes in the inter-node distances are present, and this result shows sharper defined curves on the free edges.

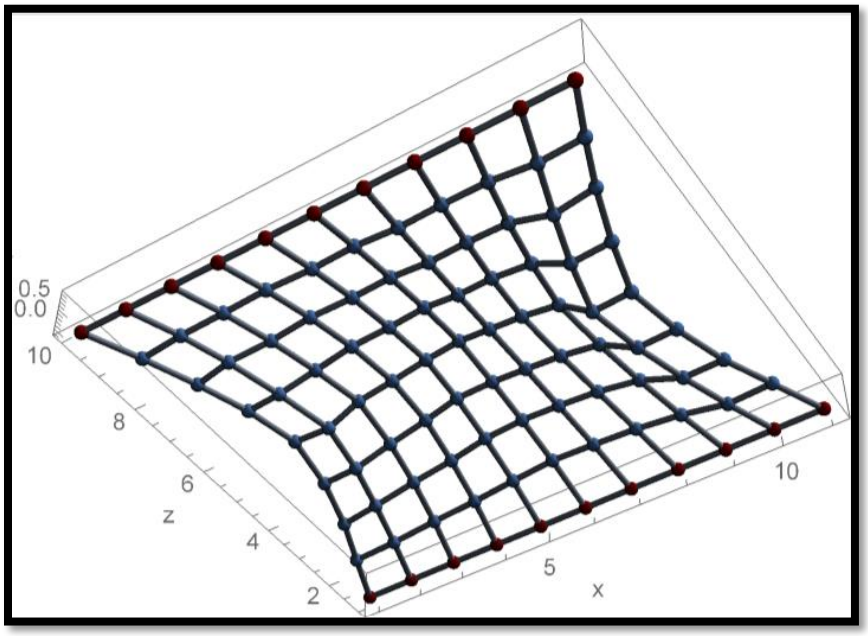

Figure 169: Case C (strain length energy weighting=1.5)

D. In Case D, the energy weighting was 1.8. The shape is irregular with tangled yarns, especially in the middle area, and the distance between the nodes is highly variable.

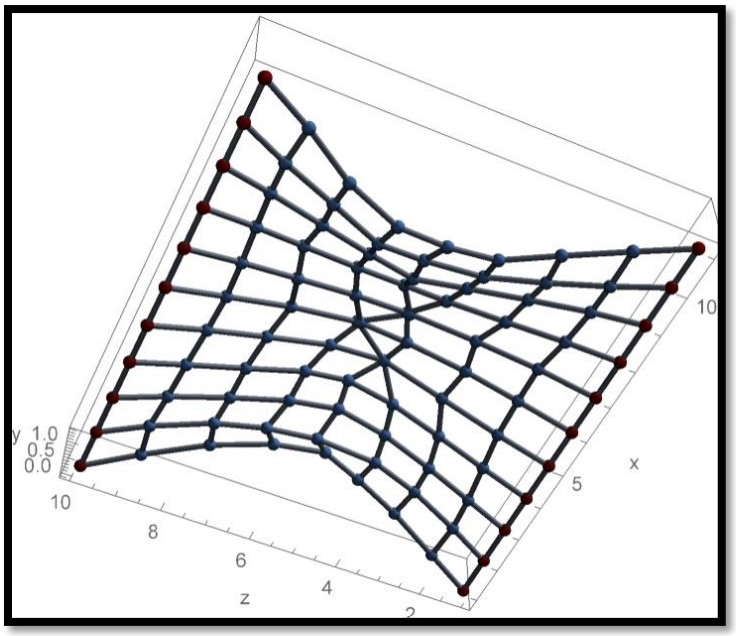

Figure 170: Case D (strain length energy weighting=1.8)

E. In case E, the weighting of the strain length energy was double that of the other energies. Notably, the shape stretches relatively regularly.

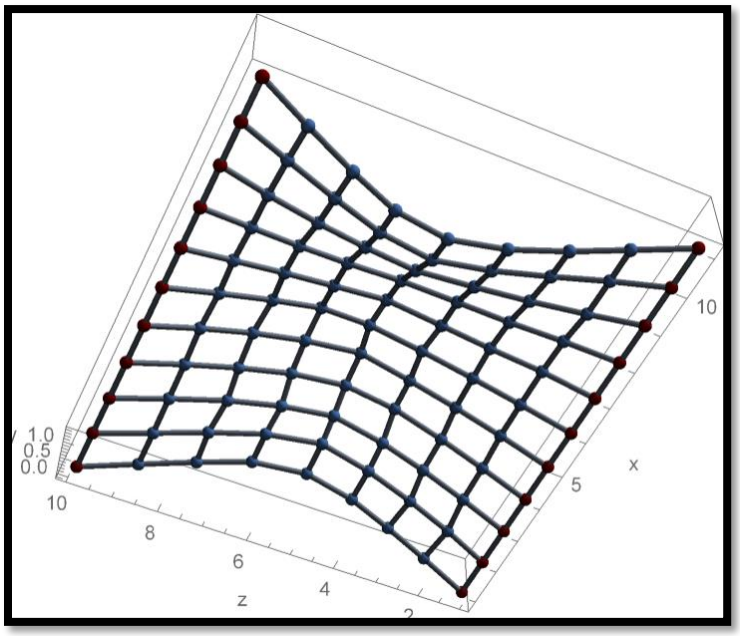

Figure 171: Case E (strain length energy weighting=2)

Strain length energy weighting controls the ability of yarn length to change as the sample is extended during a tensile test. A high weighting for the strain length energy shows a zigzag shape of the textile and curvature in the central region, and the nodes are closer to each other with a sharp curvature on the free edges. Higher weightings for strain length energy noticeably affect the curvature (or narrowing) in the central region with an irregular textile shape until the factor is two or more; then, the shape will be ordered without any tangled nodes.

4.5.3 Gravity Energy Weighting

Scenarios that change the effect of gravity energy with weightings of only 0.1, 0.5, 1.5, 1.8, and 2 with the same value for the other three energies (1) show very little difference in the final shape of the simulated system.

However, when the length strain energy weighting is markedly reduced, gravity has a significant effect. In Figure 172, the value of the weightings is 1, except for the length strain energy weighting, which is halved, which could, for example, correspond to a significantly reduced Young's modulus of the yarn material. This figure shows that the textile node spacing starts to be closer at the bottom of the shape, whereas the spacing between the nodes on the top side of the shape is longer. This implies that gravity energy effects appear when the shape is dragged to the bottom.

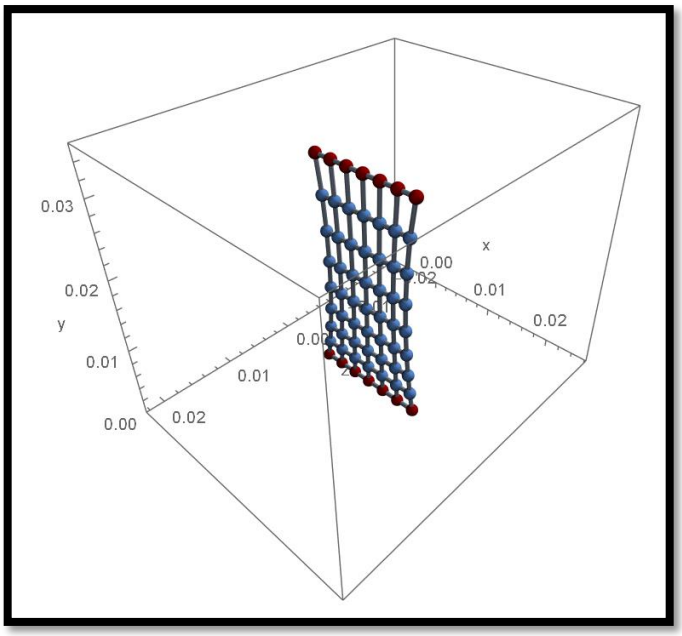

Figure 172: Case 1(strain, weft curl and gravity energy weighting =1 & strain length energy =0.5)

In Figure 173, the function length energy has zero weighting, whereas all other energy functions have a weighting of 1. The textile has been oriented so that it is horizontal instead of vertical. As a result, the fabric is stretched because the gravitational energy drags the fabric downwards from the middle.

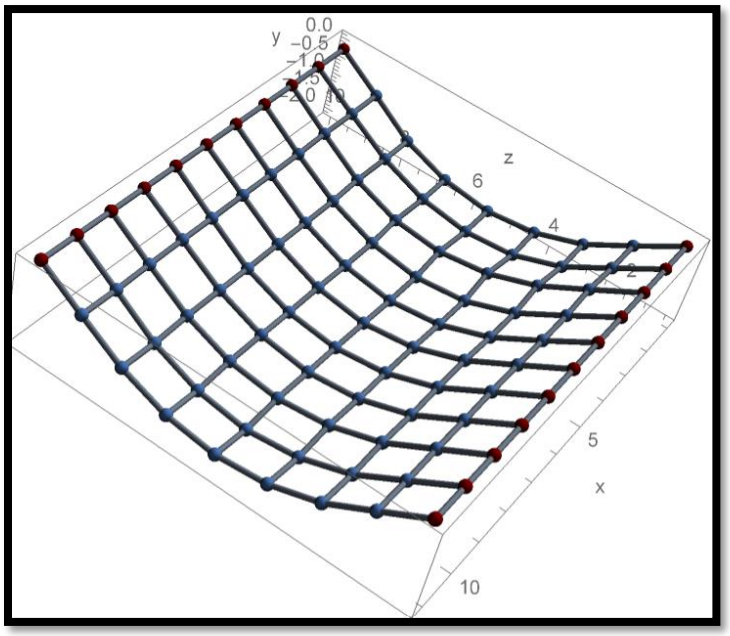

Figure 173: Case 2 (strain, weft curl and gravity energy weighting =1 & strain length energy =zero)

From these results, the gravity energy appears to play a significant role in the textile when it is stretched, because if all the energies have zero weighting, the sample would disappear as the sample would fly off into space according to the weight of the sample. The gravity energy would also drag the textile down and no other energies could influence the textile. In my project, when the sample in the experimental test was between the two clamps and before stretching started, the sample appeared closer to the bottom clamps than after stretching, when some curvature occurred along the left and right edges. However, this curve is closer to the bottom end.

4.5.4 Curl Weft Energy Weighting

Table 24 shows scenarios that change the straining length energy weighting independently of other weightings. The results are shown in Figure 174 to 177.

Table 24: Scenarios changing curl weft energy weighting.

Energy \ Scenario	**A**	**B**	**C**	**D**	**E**

Strain energy	1	1	1	1	1
Strain length energy	1	1	1	1	1
Curl weft energy	0.1	0.5	1.5	1.8	2
Gravity energy	1	1	1	1	1

A. In case A, the curl weft energy had a weighting of 0.1, whereas the other three energies (strain, length strain, and gravity) had a weighting of 1. The figure shows a slight curl along the weft direction. The effect of other energies is apparent in the shape of the textile.

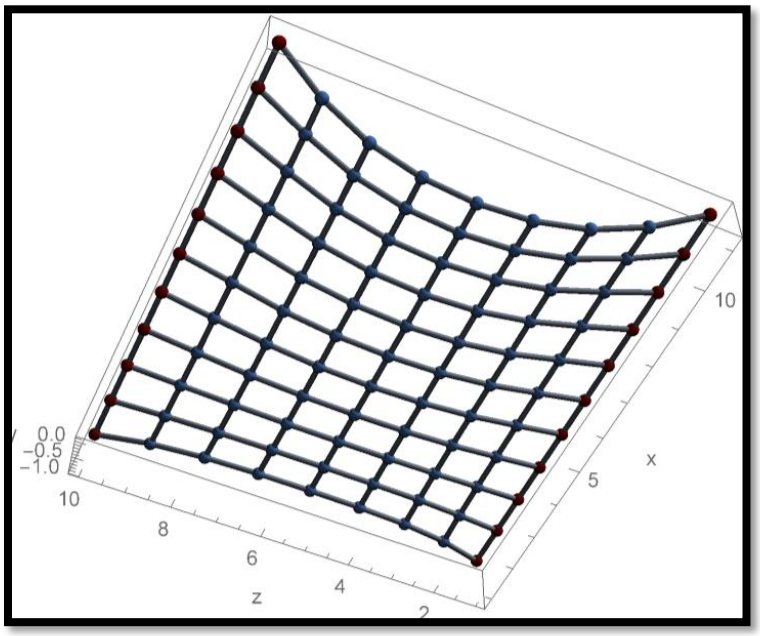

Figure 174: Case A (curl weft energy weighting=0.1)

B. In the case of B, the weighting was 0.5. The textile starts to wave with a ripple in the middle area.

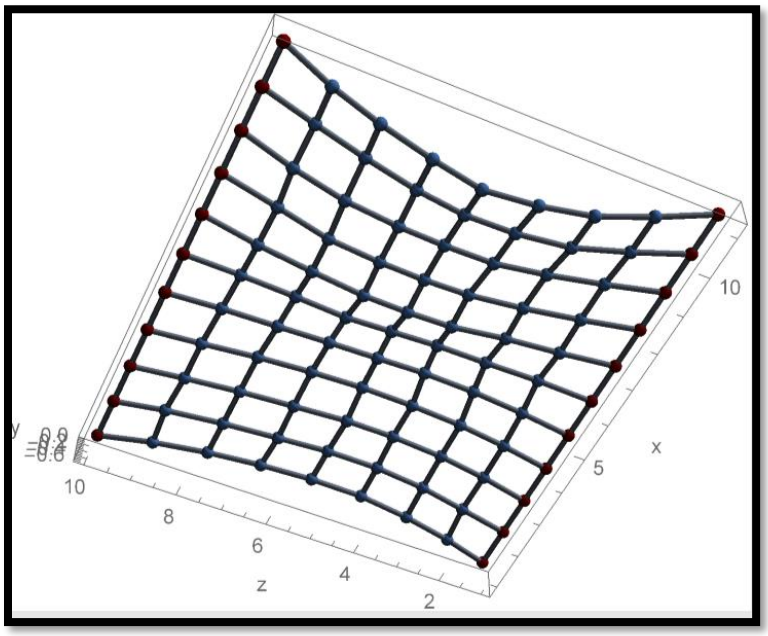

Figure 175: Case B (curl weft energy weighting=0.5)

C. In Case C, the weighting was 1.5. The curl in the weft direction is strongly apparent with tangles in the region of the upper free edge. This causes the other nodes to form a zigzag line for the yarn.

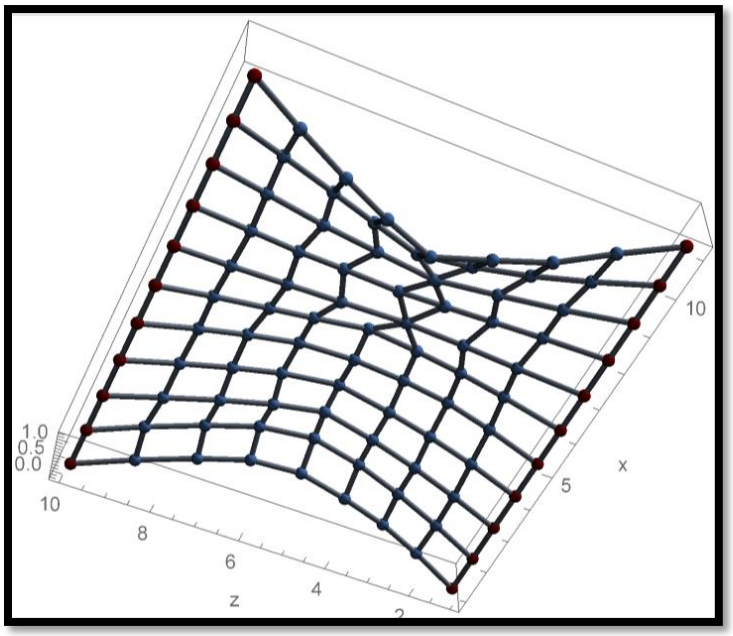

Figure 176: Case C (curl weft energy weighting=1.5)

D. In Case D, the weighting was 1.8. The curl-weft energy affects the upper and lower free edges, and there are some ripples in the middle region.

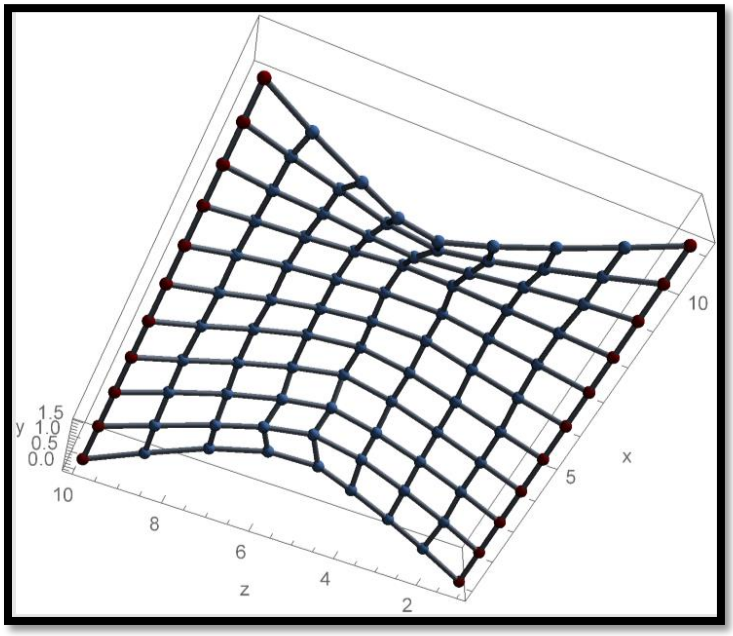

Figure 177: Case D (curl weft energy weighting=1.8)

E. In case E, the weighting for the curl-weft energy was double that of the other energies, with a value of 2. Again, the textile shows convergence in the central area to create one point node with sharp curling of the upper and lower edges.

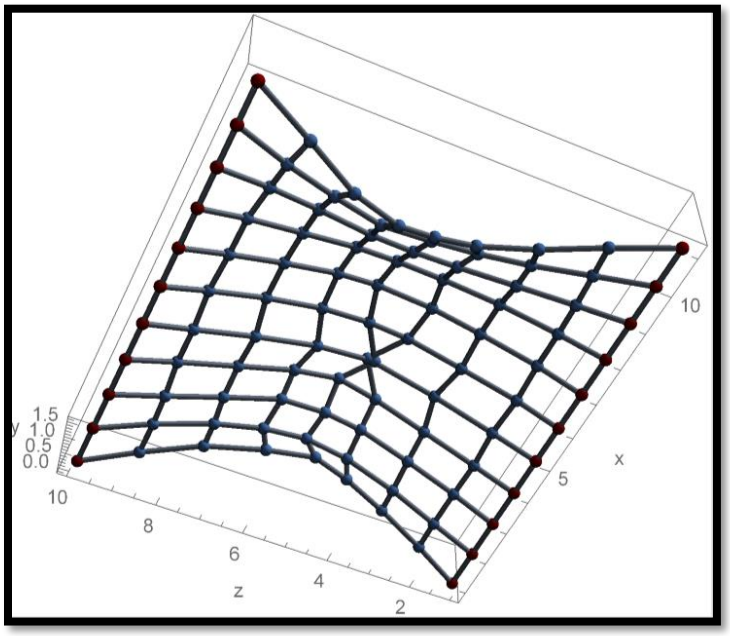

Figure 178: Case E (curl weft energy weighting=2)

These results show that curl introduces waviness in the textile plane and starts to curl the free edges. This does not significantly change the narrowing; however, it is still subject to randomness.

4.5.5 Effects of Individual Energy Functions

Table 25 shows the weightings for scenarios in which the contributions from individual strain energy sources are examined. The corresponding figures are Figure 179 to 185.

Table 25: Scenarios of changing strain energy weighting

Energy \ Scenario	**A**	**B**	**C**	**D**	**E**	**F**	**G**	**H**
Strain energy	0.5	1	0	0	0	0	0.5	1
Strain length energy	0	0	0.5	1	0	0	0	0
Curl weft energy	0	0	0	0	0.5	1	0	0

Gravity energy	0	0	0	0	0	0	0.5	1

These scenarios are not necessarily realistic, but they serve to demonstrate some of the previously discussed effects. In case A, the strain energy weighting was 0.5, whereas all the other energies (strain length, curl weft, and gravity) were given a weighting of 0. In this case, the shape appears realistic and regular. There is an even distance between the nodes, no curl, or warped shapes. In Case B, the weighting of the strain energy was increased to 1, keeping the other energies with no effect (zero weighting). The shapes remain the same.

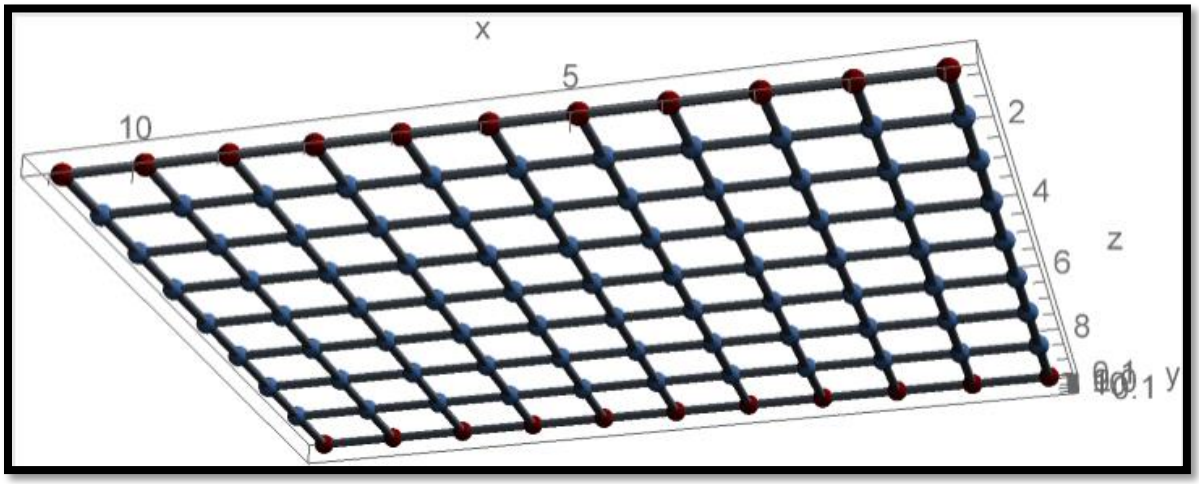

Figure 179: Case A (strain length, weft curl, and gravity energy weighting= zero - strain energy weighting =0.5)

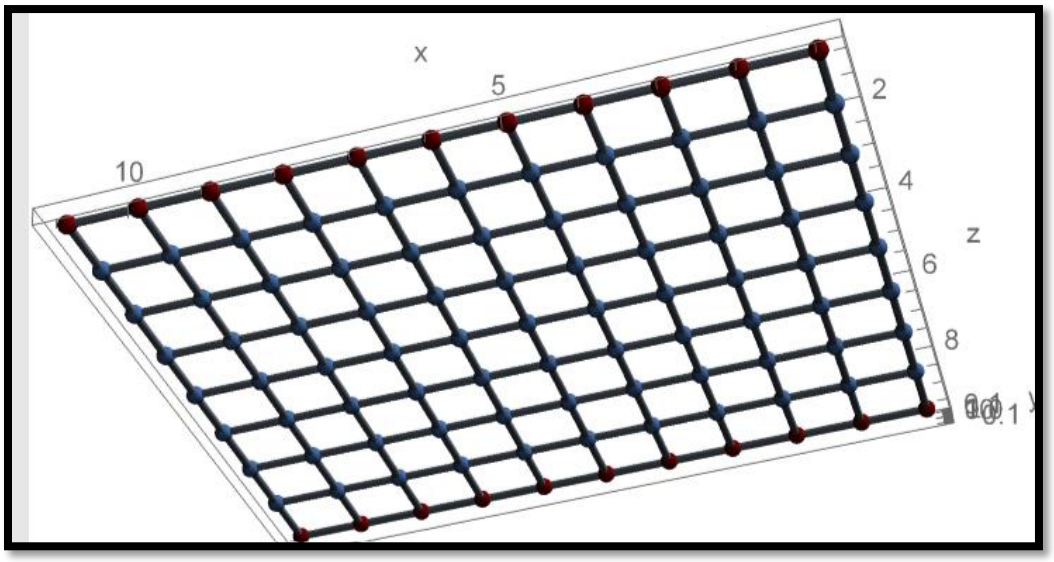

Figure 180: Case B (strain length, weft curl, and gravity energy weighting= zero - strain energy weighting =1)

The strain energy is important for simulating the shape of a textile in a plane and maintaining the overall grid shape.

For cases C and D, the weightings for the strain length energy were given as 0.5 and 1 respectively, while the other three energies (strain, curl weft, and gravity) had zero weightings. In both scenarios, nodes in the centre of the textile are drawn close to each other. There is some curl at the edges because the out-of-plane movement does not significantly affect the variance between the initial length of the yarn and the yarn length after the tensile test. There is no meaningful difference between D and C. This shows that if knots can slip without friction and strain when stretching the yarn, the lowest energy configuration is to minimise the length of the yarn (and is unrealistic). With respect to yarn friction, as the friction force increases, thin places or weak points of the yarn also increase, and the yarn becomes easy to break. Thus, the elongation of yarn decreases. The low friction force between yarns therefore produces uniform and strong textiles.

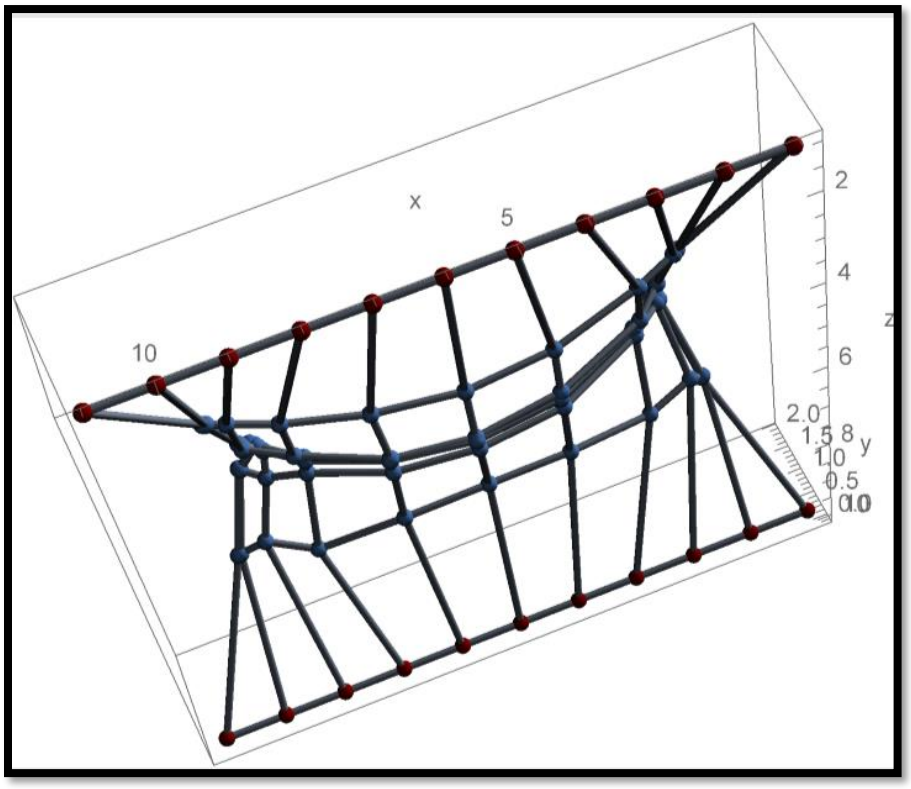

Figure 181: Case C (stain, curl weft, and gravity energy weighting=zero- strain length energy weighting=0.5)

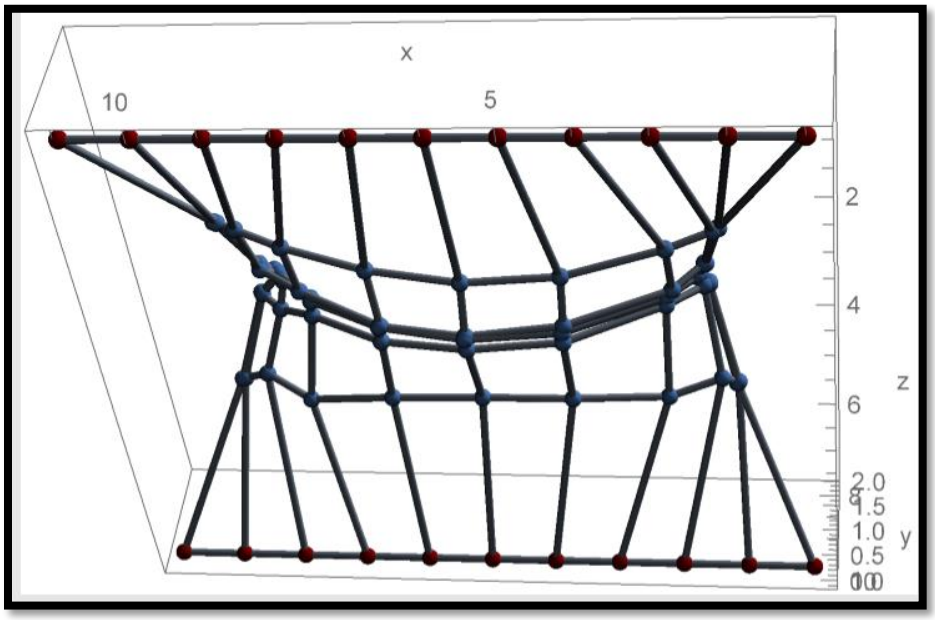

Figure 182: Case D (stain, curl weft, and gravity energy weighting=zero- strain length energy weighting=1)

In cases E and F, the curl weft energy was assigned weights of 0.5, and 1, and the strain, length strain, and gravity energies were given zero values (no effect on the textile). The resulting shape is like a dome in the weft direction because the chosen settings allow the yarn to curl. Because there is no constraint on the yarn length, the dome has longer internode distances. The general appearance is the same for E and F.

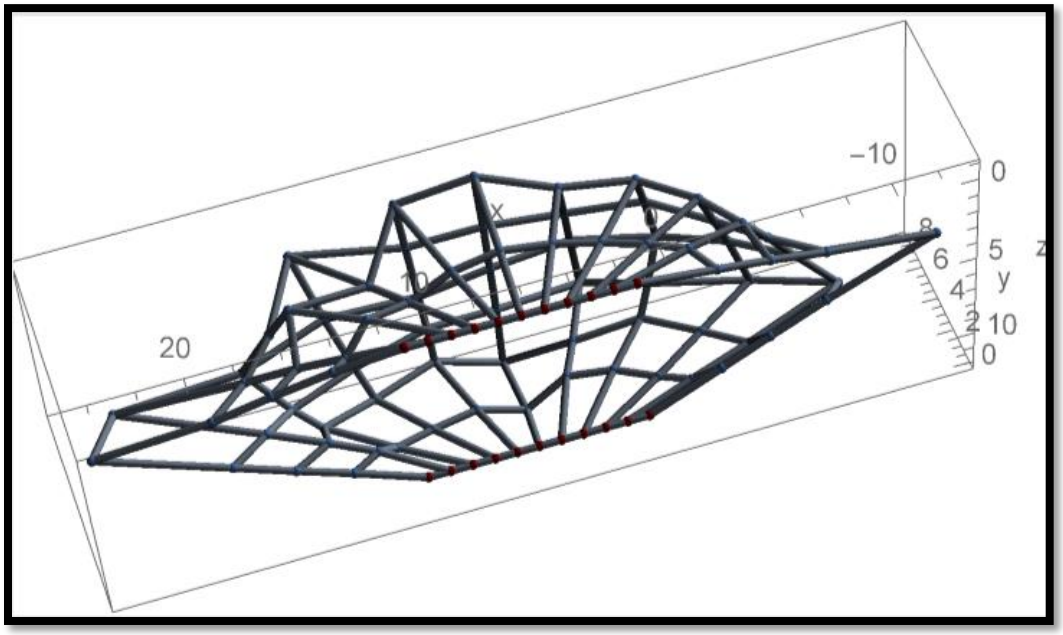

Figure 183: Case E (strain, length strain, and gravity energy weighting = zero- curl weft energy weighting =0.5)

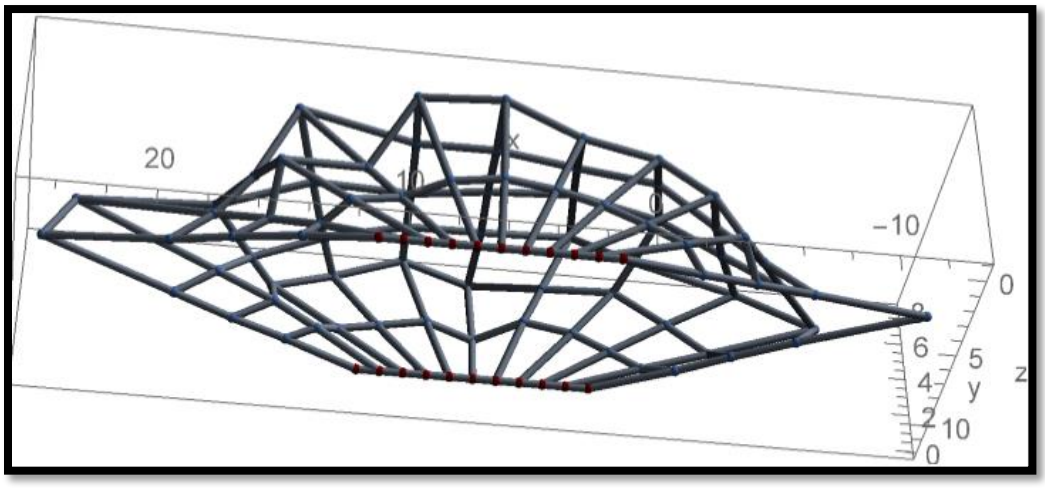

Figure 184: Case F (strain, length strain, and gravity energy weighting = zero- curl weft energy weighting =1)

For the last cases, G and H, weightings were given to two of the energies (gravity and strain) with values of 0.5 and 1, respectively. Strain is included because when only gravity energy is included, the shape will fall without resistance. In this case, acceleration according to gravity is in the Y direction (the effect of gravity acting in the Z direction is described in section 4.5.3.) Both cases show a believable sag owing to gravity.

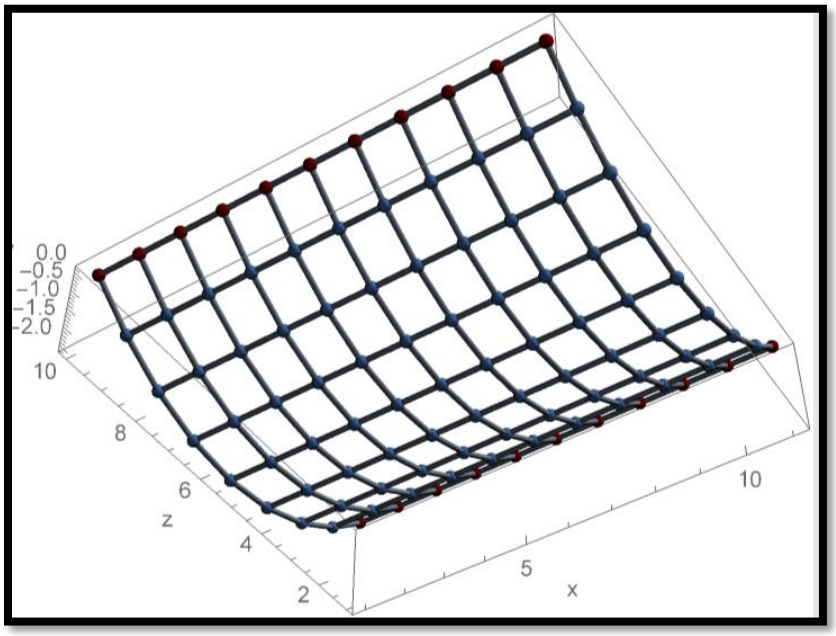

Figure 185: Case G (strain and gravity energy weighting=0.5)

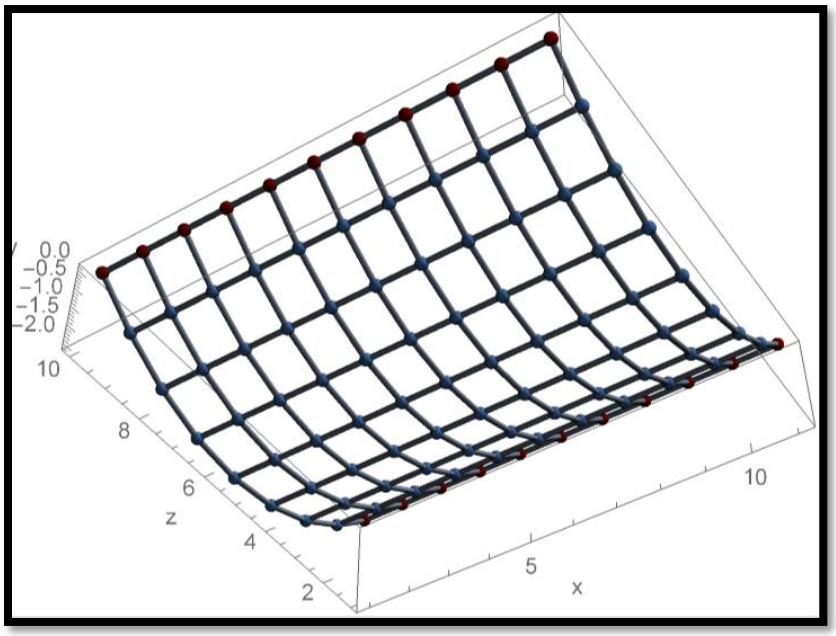

Figure 186: Case H (strain and gravity energy weighting=1)

4.5.6 Combinations of Energy Functions

Upon scrutinising individual weightings, this section unveils the outcomes from various combinations of energy weightings to understand their collective impact on textile behaviour. Specifically, I have chosen to explore combinations that focus on the influence of gravity energy and its effect on the behaviour of the sample, which leads to the disappearance of the sample in space. By comprehensively combining these energies, I aim to elucidate in greater detail how different energy interactions shape the behaviour of the sample. The scenarios are described in Table 26 and Figure 187 to 191.

Table 26: Scenarios with various weighting combinations

Energy \ Scenario	**A**	**B**	**C**	**D**	**E**	**F**
Strain energy	0	1	1	1	1	1
Strain length energy	1	0	1	1	0	1
Curl weft energy	0.1	1	0	1	1	0
Gravity energy	0	1	1	1	0	0

A. In Case A, the energy function length strain had a weighting of 1, and the energy function curl weft had a weighting of 0.1. The results show that the yarns assemble in the middle area. It is also noticeable that the fabric starts to curl.

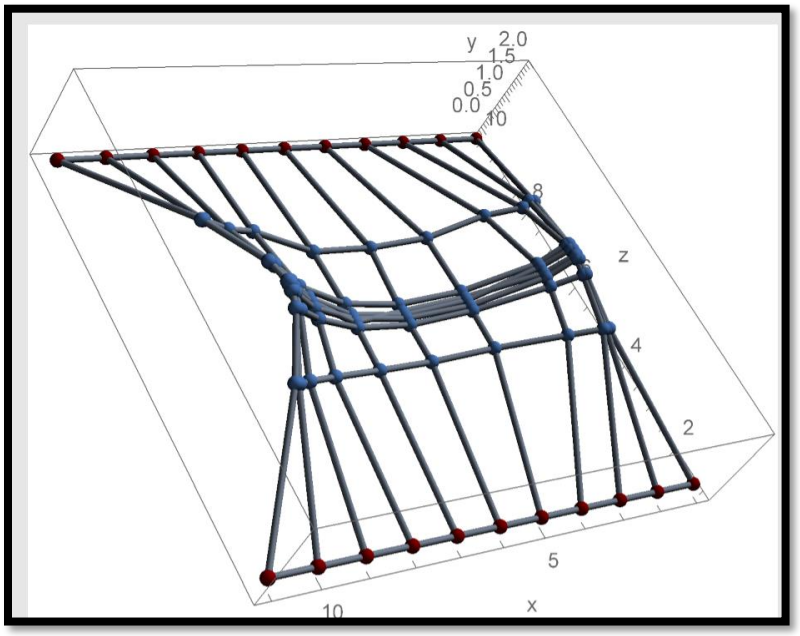

Figure 187: Case A (strain length energy weighting =1 & curl weft energy weighting= 0.1)

B. In Case B, the function length energy had a weighting of 0, whereas all the other energy functions had a weighting of 1. The result is remarkably similar to the previous cases G and H in section 4.5.5 and Figure 185 and Figure 186, but some small ripples are noticeable in the otherwise regular grid pattern (the courses do not completely line up against the Z axis).

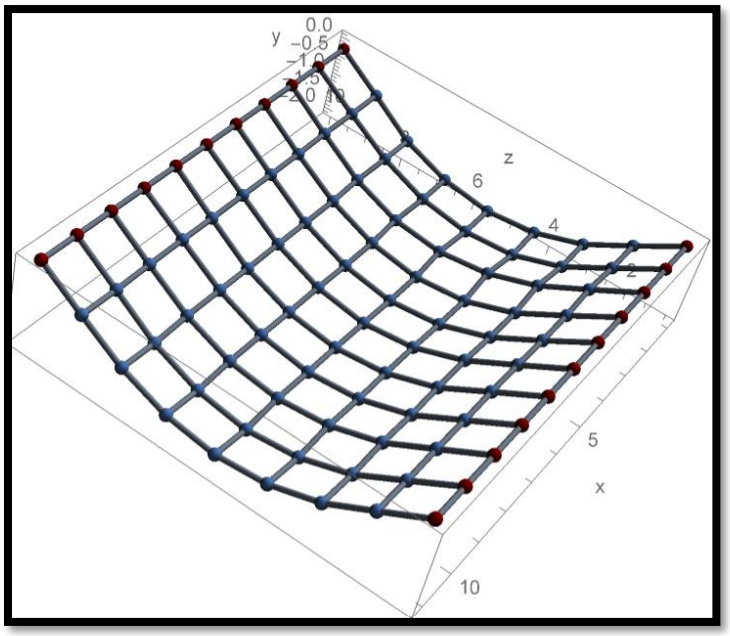

Figure 188: Case B (strain, curl weft, and gravity energy weighting =1- strain length energy weighting =zero)

C. In case C, the curl weft energy had a weighting of 0, and all other energy functions had a weighting of 1. As Figure 189, shows the fabric is stretched with some changes in the yarn length. In the middle, the nodes are closer together. The effect of gravity (acting in the negative Z direction) is apparent in the smaller distances between the nodes when Z is small. There is no tendency for the patch to curl up at the edges or ripples to appear.

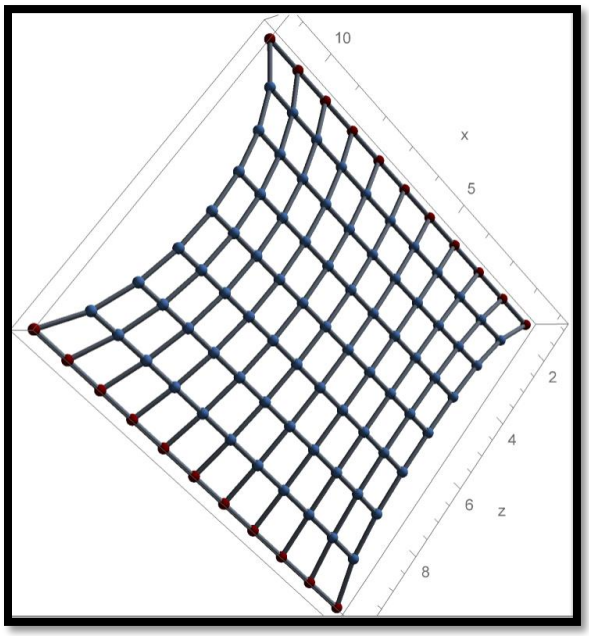

Figure 189: Case C (strain, strain length, and gravity energy weighting= 1- curl weft energy weighting =zero)

D. In case D, all the energy functions had a weighting of 1. The result is like the previous one, except that the textile is starting to curl.

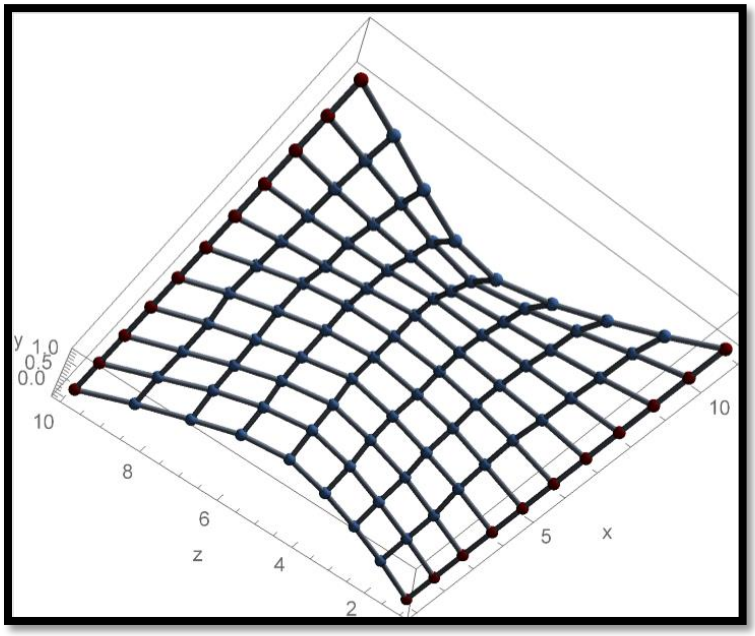

Figure 190: Case D (all the energies weighting=1)

E. In case E, both the energy length strain and gravity had weightings of 0, but the other energies had a weighting of 1. The results in Figure 191, demonstrate that the fabric is stretched with waviness in the middle area, but there is no dragging owing to gravity, and the unit cells are regular in shape.

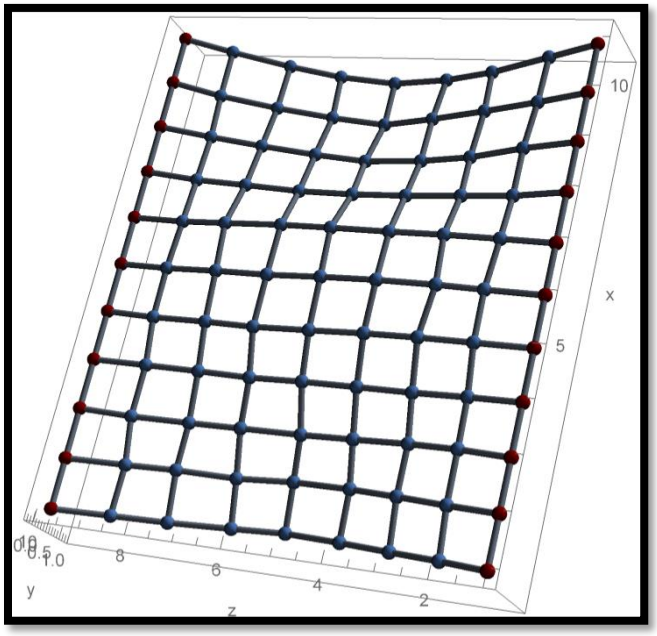

Figure 191: Case E (strain length and gravity energy weighting =zero- strain and curl weft energy weighting=1)

F. In case F, the curl weft and gravity had a weighting of zero, whereas the other energies had a weighting of one. As a result, the textile is stretched evenly in the Z direction, with an obvious narrowing in the middle. No dragging or curling can be observed in the weft direction.

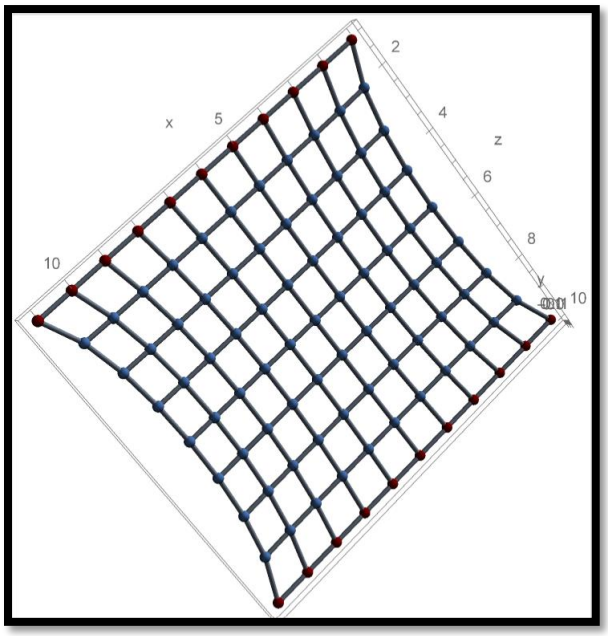

Figure 192: case F (curl weft and gravity energy weighting= zero- strain and strain length energy weighting = 1)

4.5.7 Unstretched and Stretched Configurations

Figure 193 shows an unstretched textile patch in its minimum energy configuration. In this scenario, all energy functions were assigned a weighting of 0.1 except for the strain length energy, which was assigned a higher weighting of 1. As can be seen in Figure 191, the middle has waviness, and the right and left edges have bends because of the effect of the curl weft energies. In addition, because of the impact of gravity energy, the curvature in the central area of the textile is very clear. There is no effect of other energies, such as strain or strain length energy, as this configuration is not stretched.

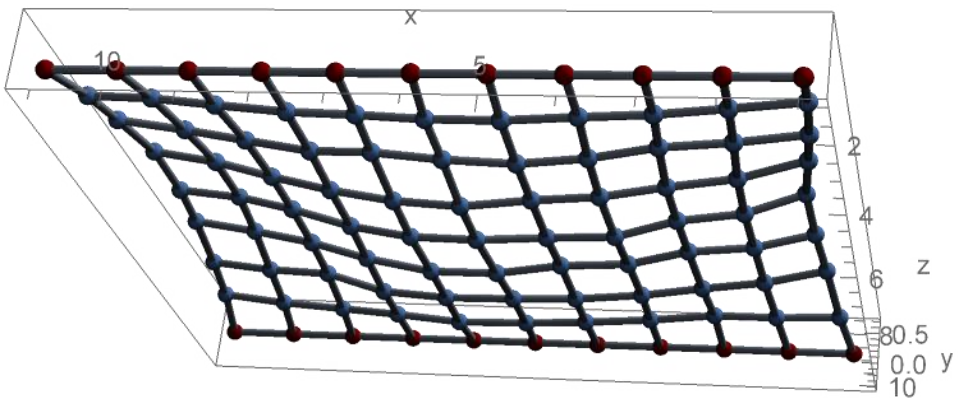

Figure 193: Unstretched textile patch in its minimum energy configuration

There is a strong correspondence between the experimental work on the textile analyser machine and the simulation results. As the sample is stretched vertically between the top and bottom clamps, there is an interplay between the components that extend the sample, and changes in the yarn length contribute to the strain length energy, but some sample elongation occurs without changes to the original length. Owing to the curl weft energy, when the sample is clamped, the left and right sides exhibit a slight curl, which is unavoidable and likely to occur even before the test begins. Figure 194 illustrates this phenomenon, showing how the sample sagged slightly under the effect of gravity when relaxed (before the start of the test). However, once the test commenced, the sagging ceased, and the influence of gravity became negligible.

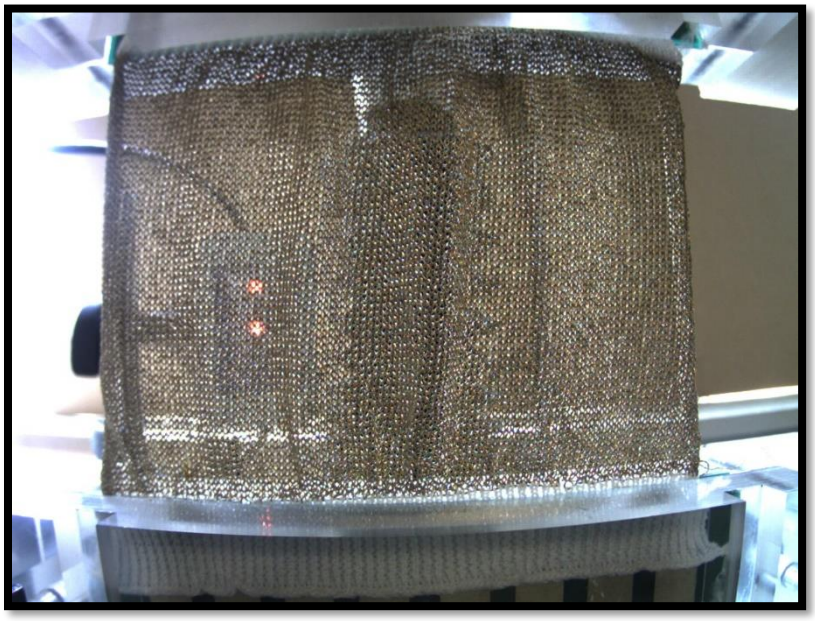

Figure 194: Stainless steel testing sample in a relaxed state

4.6 Summary

In keeping with the original objectives, the phenomena that have been simulated (shown in the figures above) are the effects of four types of energies:

- The phenomenon observed for the strain length energy is the changing shape of the sample when it is stretched from the top edges while the bottom is fixed, as shown in Figure 147, particularly the narrowing of the middle. A higher weighting makes the shape irregular, which means that factor 2 or above would increase the narrowing in the middle area of the shape, which would make the shape unacceptable for the test under energy effects.
- For the tensile strain energy, the effect that was noted is a sideways ripple during the tensile test energy, as demonstrated in Figure 148. In this case, for the low weighting factor, the strain energy has no observed effect on the shape, but when the factor is high (2 or more), the sample shape has a regular shape with no tangle of nodes in the middle area of the shape.
- For the curl weft energy, it was observed that the left and right edges of the sample curve, as shown in Figure 149, and that an increase in the weighting factor increases the curvature at the edges of the shape until the shape is irregular and the nodes are closer to each other.
- In Figure 150, the influence of gravity energy, as evidenced by the sagging effect, remains remarkably pronounced. The force of gravity consistently drags the shape downwards even when the sample is securely clamped within the texture analyser machine. The weight of the sample leads to a slight lowering or sagging of the lower portion, which is particularly noticeable after the tensile test is concluded. This phenomenon, attributed to gravity, highlights the substantial impact it has on the sample positioning within the texture analyser machine.

In my assessment, achieving an acceptable shape for the sample during the tensile test required weighting factors for all energies within the range of 1–1.8. This range seems to

contribute to maintaining a consistent and desirable shape for the sample under testing conditions.

Chapter 5 Discussion and Conclusion

5.1 Introduction

This study represents a novel investigation into the mechanical properties and behaviour of knitted textiles, specifically examining how they respond to different mechanical conditions. The main goal is to explore their potential use in smart textile technologies. Although the focus is on textiles instead of finished garments, the results are significant, providing important insights that could help advance the creation of innovative materials for various future applications.

This project investigated four groups of samples: silver-coated nylon conductive yarn with and without wax, (80/20) % polyester/stainless steel conductive yarn with and without wax, and with and without Lycra. The samples were divided into two groups: plain flat knit samples and plain tubular knit samples. Polyester nonconductive yarns with and without Lycra were also divided into two groups of flat and tube samples, and a rubber sample was tested for comparison. All experimental fabrics used in this study were either plain knit or plain tubular knit structures. For the experimental investigation, these materials were tested using a texture analyser to investigate the relationships between strain, force, and time. Theoretically, a mathematical model based on energy methods was developed using MATLAB to analyse the data generated by PIVlab.

This chapter brings together the findings from various research approaches, discusses them in the context of existing work, highlights the contributions and limitations of the research, and identifies areas for future research.

5.2 Different Behaviour of First and Subsequent Tensile Tests

5.2.1 Findings and Discussion

This study repeatedly confirmed that the first tensile test of the knitted textile behaved differently from the second and subsequent tests. The force generated in the first test was less than that generated in the second test when tested with a fixed strain. This investigation demonstrated that this was true for various yarns, strain rates, and single-jersey-knitted fabric structures. The polyester sample exhibited more consistent behaviour than other knitted fabrics, such as silver or stainless steel. The flat polyester knitted fabric samples, with or without Lycra, required more force to stretch than the tube sample under the same tensile strain, whereas the stainless-steel knitted fabric flat samples, with or without Lycra, required less force to stretch under the same conditions. When comparing the behaviour of knitted fabrics treated with and without silicon wax, particularly with conductive materials such as silver or stainless steel, it becomes evident that the presence of silicon wax mitigates frictional effects and affects absorbency properties. Silicon wax plays a crucial role in lubricating both artificial and natural fibres, especially in high-speed processes, to enhance their performance.

In general, polyester knitted fabrics were found to have good characteristics, such as high resistance to shrinking and stretching, and they returned to their original shape very well. These mechanical properties distinguish polyesters from the other knitted fabrics.

During the investigation of the project challenges and methods to address them, it was discovered that the initial tensile test of a knitted textile differs from the subsequent tests. It was observed that the gauge length, specifically the optimal distance (associated with a greater gauge length), significantly influenced the similarity between the first and subsequent tests.

Another experiment involved testing conductive stainless-steel yarns with and without silicone wax. The silicone wax appeared to ensure that the first test was closer to the second test, as can be seen in Section 3.3.3.2 Wax and Non-Wax Samples above.

Another significant factor that could affect the discrepancy between the first and second tests is the maximum strain applied during the tests. In the data collected, maintaining a maximum

strain below 3% and implementing a 1-minute delay between tests led to higher results in the first test than in the second test. However, when the strain was increased to 5%, the curve of the first test closely aligned with the subsequent tests, as discussed in Section 3.6.1 Differing First-Cycle Behaviour in

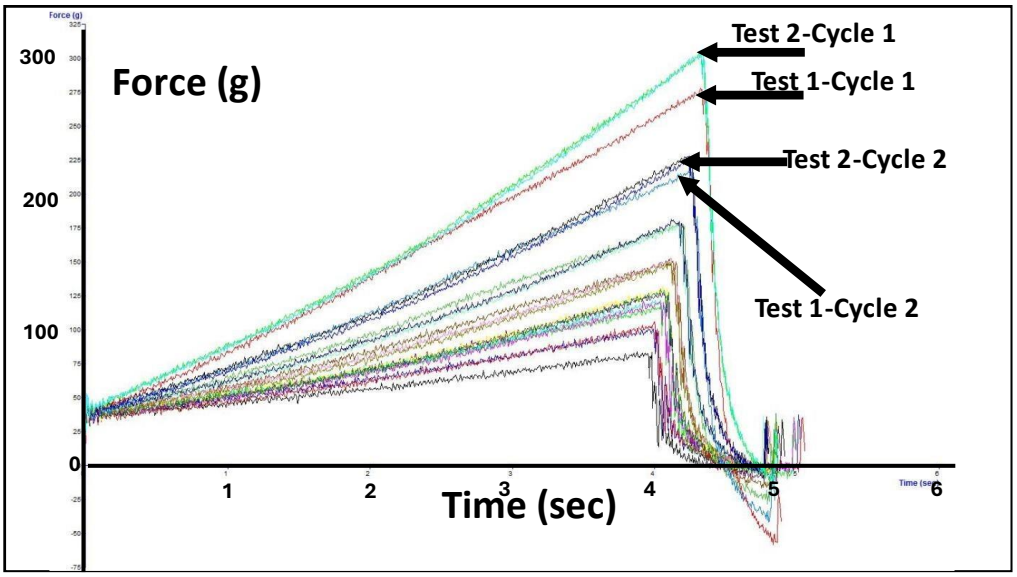

Figure *93*.

One reason for this behaviour may be the knit stitches in the material itself. There is a degree to which stitches randomly change shape when subjected to external effects. Therefore, the main factors affecting the results before the test were the original shape and size of the sample. During the first test, the sample was expanded until it reached the maximum strain; however, after the stretch had been removed, the stitches did not return to their original shape and size. This means that for the subsequent tests, the "history" determining the starting shape has been standardised (based on the previous tensile test). Friction also seems to play a role in this random behaviour. When the starting shape was altered, it affected the consistency and reliability of the results, as variations in the initial configuration introduced inconsistencies in the stress distribution and deformation patterns. These deviations made it more challenging to isolate the effects of other variables being tested.

This hypothesis is supported using a higher pre-strain when the test result of the knitted fabric was affected, even when using different materials. The first test curve was closer to the second

and subsequent sequence test curves because the stitches of the knitted fabric stretched to a higher level and then returned to the pre-original position, which did not require as much force to stretch. While a low strain means that the force was exceedingly small and insufficient for the stitches to stretch freely and return to the first position quickly, the stitches needed more force to stretch again. When the second test was conducted, the textile stretched from the last position that the stitches had reached previously; therefore, it was easier to stretch. To overcome this frictional problem, wax can be used to cover the yarn and reduce friction, as illustrated in Figure 195.

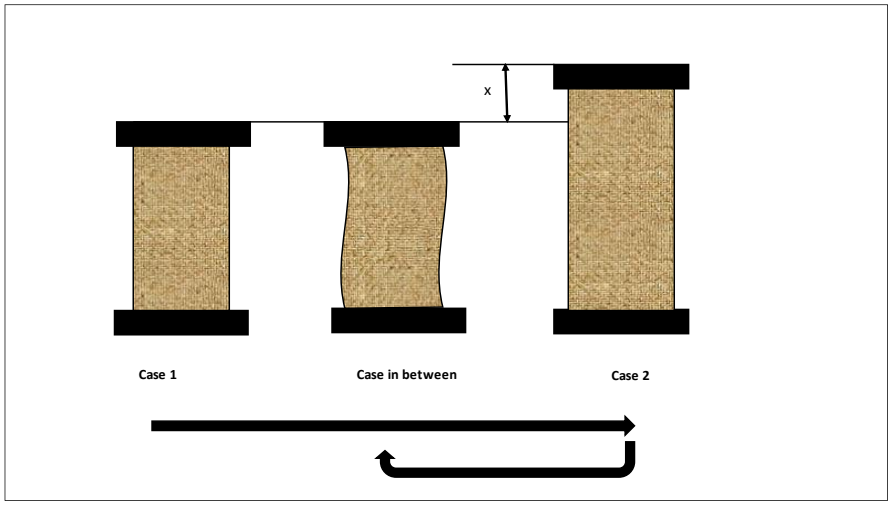

Figure 195: Textile testing process.

Mathematical simulations provided evidence to support this hypothesis. Despite the random distribution of knot positions, the energy minimisation results indicate similar energy levels when friction is factored into the tests. This suggests a consistent pattern in the energy levels, despite the variability in knot positions, highlighting the significant role of friction in these simulations.

The correlation between the experimental findings of the textile analyser machine and the simulation outcomes was robust. When the sample underwent vertical stretching between the top and bottom clamps, various factors interacted to induce its extension. Alterations in yarn length contributed to strain energy, whereas some elongation occurred without changing the initial length. This phenomenon was influenced by the curl weft energy, resulting in slight

curling along the left and right sides even before the test commenced, which is an inherent characteristic.

5.2.2 Significance and Contribution

The unique behaviour observed during the initial test has not been extensively documented in the reviewed literature. This study highlights the importance of acknowledging and incorporating this distinct behaviour into testing protocols for smart textiles made using the knitting technique. Recognising this peculiarity is essential for ensuring accurate and reliable evaluations of the performance and functionality of these textiles.

The possibility of integrating smart knitted textiles as sensors into various products has opened innovative opportunities across multiple fields. These textiles are embedded with sensors that can detect and measure a range of stimuli such as pressure, temperature, moisture, and even motion. Their flexible and adaptable nature allows for comfortable integration into clothing, enabling the real-time monitoring of vital signs, movement patterns, and environmental conditions. This technology holds immense promise in healthcare for continuous health monitoring and sports performance analysis, and even in diverse industries, such as automotive and aerospace, for structural health monitoring. The integration of smart textiles into garments represents a discreet and effective approach to gathering data for a variety of applications, which opens the door to a new era in wearable technology.

This research strongly suggests that textile tensile tests should be repeated several times under the same strain and for the same sample to obtain a clear representation of the relationship between successive tests and to investigate the gap between the first and second tests.

Unlike fibres typically used in smart sensors, natural fibres such as wool include wax-like materials as a preventative agent against biological effects and atmospheric conditions. The addition of silicon wax affects the mechanical behaviour of stitch interactions and knitted fabrics and may improve reproducibility by reducing friction. Kang and Kim (2001) have shown the significant effect that softeners of a surface coating using silicon have on reducing the inter-fibre and yarn friction.

5.3 Comparison of Tensile Behaviour with and without Lycra

5.3.1 Findings and Discussion

Another promising finding of this study was the effects of Lycra on the mechanical behaviour. Lycra is a highly flexible artificial material that is a trademark designation for elastane. These materials can stretch five to eight times their normal size with excellent recovery.

Other studies have found that adding Lycra affects the course and wale density of textiles (Sadek et al., 2012) and the initial elasticity modulus of the yarn (Halim et al., 2019). The research outlined in these papers demonstrates that the presence of Lycra in textiles typically results in fabric compression. This compression effect leads to a decrease in the loop length and a tighter fabric structure owing to increased elastance. Additionally, it was found that the tension generated by Lycra-induced stitch interlacing further contributes to the thickness of the fabric. Specifically, fabrics incorporating Lycra tend to exhibit a higher course density, reducing the number of wales per centimetre, and consequently increasing the fabric's course count per centimetre. Moreover, the fabrics with Lycra exhibited a lower tensile strength along the lengthwise direction, requiring less force to extend. This indicates the distinctive behaviour of the mechanical properties of the fabric, emphasising the impact of Lycra on the structural integrity and stretching characteristics of the fabric (Sitotaw & Adamu, 2017).

The outcomes of incorporating Lycra into the knitted fabric highlight a distinctive pattern: the fabric exhibits reduced tensile strength along its lengthwise direction. This lower strength is accompanied by the requirement for less force to extend the fabric. This behaviour is attributed to the increased elastance imparted by Lycra, which results in a tighter fabric structure.

In this study, plain flat knit and plain tubular knit samples with and without Lycra were tested. The results were obtained for samples with equal courses and wale densities. The unique findings of this study are as follows:

- The addition of Lycra did not remove any differences between the first and second tests.

- By adding Lycra to the stainless-steel knitting fabric for the plain flat knit sample under low strain, the first test curve was longer than the second test curve, and the shape of the curve fluctuated more than the shape of the curve when the test was conducted under higher strain. For the plain tubular knit sample without Lycra, the shape of the test appeared more linear than that of the sample with Lycra because the round shape stretches more easily. In general, a round or tube shape can be comparatively easier to stretch than other shapes, especially if the material is evenly distributed or has a consistent structure. A circular or tubular form often allows for a more uniform distribution of forces when stretched, contributing to a more balanced and manageable stretching experience. This shape minimises the potential weak points that can cause uneven stretching or tearing, particularly when a force is applied uniformly around the circumference. However, the ease of stretching also depends on material properties, thickness, elasticity, and overall structural integrity.
- For the plain flat polyester knit sample with Lycra under low strain, the first test started with a higher force than the second test and took a longer time to stretch but appeared lower than the second test which started with a lower force but reached a higher force to stretch in a shorter time than the first one. For the plain tubular knit sample under low strain, the gap between the first and second tests was large for the Lycra sample; however, in the sample without Lycra, there was a smaller gap between the tests, even though the problem in the second test was still higher than that in the first test, and the problem disappeared when the strain was high.
- In general, for the polyester and stainless-steel samples, the testing shapes, with or without Lycra, showed that a higher strain is more linear and more stable than the testing curve under low strain.
- The rubber sample was also an elastomer (but with a monolithic structure) and did not show a difference between the first and second tests. This is because, when it stretches to a few times its natural length, it returns to its original length once the tensile strain is removed. This is due to the natural behaviour of rubber, since the elastic region (Figure 196) is larger for rubber than for the other materials.

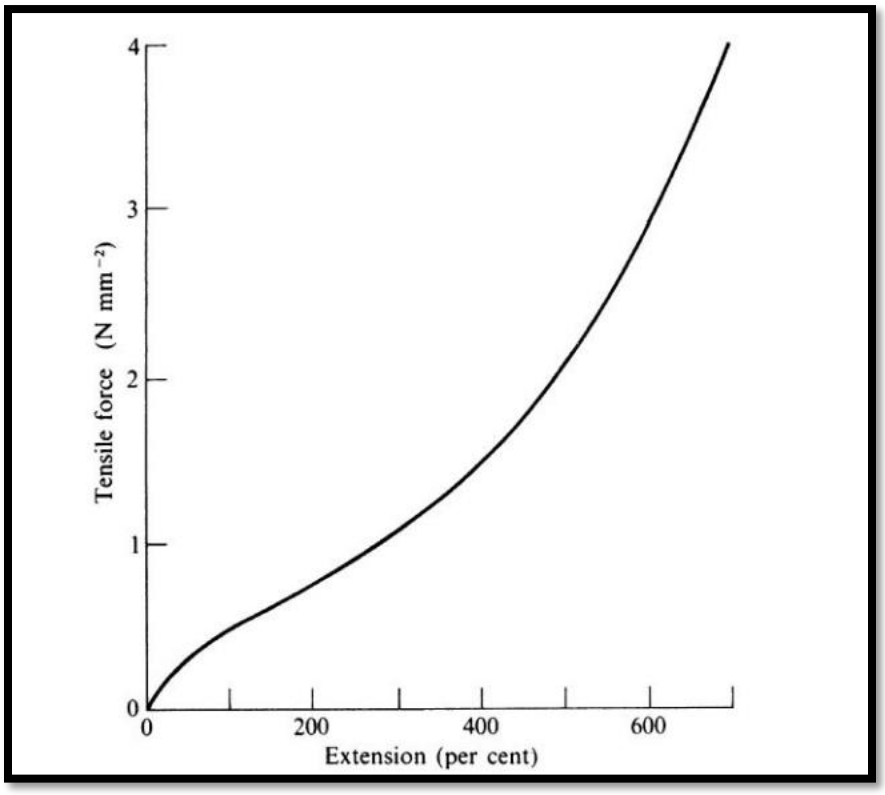

Figure 196: Rubber Elasticity, force-extension curve (Treloar, 2005)

These experimental results can be supported by the findings from the modelling and simulation studies, specifically in relation to the calculations of stain energy and strain length energy as outlined in Equations 11 and 13 (pages 257-260). Adding Lycra to a textile sample can potentially reduce the strain energy under specific conditions. Lycra is an elastomeric material that restricts the stretchability of fabrics. Therefore, if the presence of Lycra decreases the overall stretching capability of the textile compared to the sample without Lycra, it can result in reduced strain energy, this reduction in strain energy would occur when the Lycra component alters the fabric's behaviour, causing it to reach a lower maximum extension or strain compared to the fabric lacking Lycra. Essentially, if the addition of Lycra limits the fabric's ability to stretch to the same degree as the sample without Lycra under similar conditions, it would lead to a reduction in the overall strain energy as well as leading to a reduction of the differences between x and x_o, when Δx is very small compared to the sample without Lycra. The simulation of the experimental result would likely be affected when using high weighting (from

2 and above) to increase the value of the strain energy after adding Lycra, then can overcome a randomness problem as explained in 4.5.1 Strain Energy Weighting.

About the strain length energy, the case is the same as the strain energy because the correlation between the strain length energy and the alteration in length is positive. Adding Lycra to the sample means the differences between L and L_o that are represented by ΔL would be very small and, as a result, the strain length energy would be small, so by reducing the weighting of the energy to a weighting that is less than the value of the other energies, the textile shape would be regular and stable.

5.3.2 Significance and Contribution

In the experimental tests for conductive and nonconductive yarns, a novel contribution to knowledge has been made regarding the behaviour of textiles with and without Lycra in plain flat and plain tubular knit forms. This work examines the first-second test difference, defined as the variation in material performance between the first and second test iterations.

The results demonstrate that Lycra cannot mitigate the first-second test difference. In plain flat knit samples, the addition of Lycra increases resistance to stretch, leading to an irregular and fluctuating first -second curve. This suggests that Lycra introduces inconsistencies in material behaviour, potentially due to elastic recovery properties.

In contrast, the effect of Lycra in a tube samples is less pronounced. The round shape of the tube facilitates easier stretching, reducing irregularities in the first-second test compared to flat samples. However, the extent of this reduction is contingent on the yarn material, emphasising the combined influence of geometry and material properties on textile performance.

5.4 Use of PIV to Characterise Textile Strain Fields

This study demonstrated the use of a new technique to calculate the velocity and strain of textiles. Although particle image velocimetry (PIV) has been previously used in geotextile analysis, this is the first time it has been used for a greater variety of elastic knitted materials. In summary, the findings of PIV research are as follows:

- PIV estimates two velocity components, V and U. The difference between them is that the V component represents the velocity direction from left to right, whereas the U component represents the velocity direction from top to bottom.
- The velocity and strain of the test are indicated by arrows. Some groups of arrows converge, whereas others diverge, and some of the arrows behave randomly in the left and right directions, depending on the strain amount and the effect of the strain on random parts of the sample. If the strain effect is strong in one sample part, it is represented as a convergence of groups of arrows, and vice versa for weaker areas of strain.
- The examination of fabric blends containing stainless steel/Lycra and polyester/Lycra at different strain levels uncovered intricate deformation behaviours, stress distributions, and flow patterns. Utilising Particle Image Velocimetry (PIV) for data visualisation offered crucial insights into the performance and attributes of these textile blends. The findings underscored the durability and fundamental characteristics of polyester knit fabric with Lycra, demonstrating its capacity to endure significant strains. This study underscores the significance of comprehending material responses under varying circumstances and the value of visual tools in improving data analysis for well-founded conclusions in textile research and development.
- The Particle Image Velocimetry (PIV) velocity tests conducted on stainless steel and polyester tube knit fabrics without Lycra unveiled unique flow patterns and velocity characteristics. The visual depictions of velocity vectors offered valuable insights into material behaviour and flow dynamics. These discoveries hold significance for fabric manufacturers and designers seeking to enhance fabric designs tailored to specific requirements, considering factors such as material properties, strain rates, and structural dynamics.

- Analysing the strain test image with Particle Image Velocimetry (PIV) to assess knit fabrics inherently involves the establishment of intricate processes that demand advanced methodologies and high-quality images. However, in the specific case under consideration, the clarity of the image was lacking, making it difficult to distinguish the movement of arrows accurately. Consequently, conducting a thorough analysis using PIV for all knit fabrics posed a significant challenge. This limitation underscores the necessity for further investigation into enhancing image sharpness and arrow movement visibility when analysing strain test images of knit fabrics.

  It is crucial to recognise that employing PIV for assessing strain tests on knit fabrics can be an invaluable asset in unravelling their mechanical characteristics and performance attributes. The insights gained from such analyses can prove instrumental for fabric developers and manufacturers seeking to enhance product quality. Unfortunately, due to the subpar image clarity and ambiguous arrow movements observed in this study, a comprehensive evaluation could not be achieved.

Therefore, this aspect warrants future exploration aimed at refining techniques that surmount these obstacles and yield precise strain test results via PIV analysis on knit fabrics. The absence of clear image quality and distinct arrow movements significantly impeded the thoroughness of this study's analysis on strain tests for knit fabrics using PIV methodology.

5.4.1 Limitations

In this thesis, the Practical Image Velocimetry (PIV) faced several significant limitations that must be acknowledged to fully understand the circumstance and accuracy of the findings.

- **Image quality:**

One of the main challenges faced in this study was the poor quality of the images utilised in the PIV analysis. The images did not have the required sharpness and clarity, which made it challenging to accurately notice the movement of arrows depicting velocity and strain vectors. Since the visibility of these arrows is essential for interpreting the data accurately, this issue meant that a comprehensive and exact analysis could not be conducted.

- **Arrow movement visibility**:
  The analysis of arrow movements in PIV images is hindered by unclear visibility, which complicates the tracking of strain and velocity changes. This lack of clarity, stemming from factors like overlapping vectors and processing artifacts rather than image quality, negatively affects result precision. Improving vector field processing and optimising experimental conditions are suggested to enhance analysis accuracy.
- **Specificity of Findings**:
  The results of the study are only relevant to the fabrics that were used in the experiments – stainless steel/Lycra and polyester/Lycra blends. Therefore, these findings may not be easily applied to other types of textiles. This insufficiency of generalisability limits the application of the results to a wider variety of fabrics.

5.4.2 Future work

To address the current limitations and strengthen the reliability of PIV analysis in textile research, several potential areas for future exploration are suggested:

- **Improving Image Quality**:
  Future research should focus on improving the sharpness and clarity of images used in PIV analysis. By incorporating advanced imaging techniques and higher resolution cameras, there is potential to greatly enhance the visibility of velocity and strain vectors. This would enable more precise data interpretation and analysis.
- **Refining Analysis Techniques:**
  Improving the methodologies used for analysing PIV data could help address visibility issues with arrow movement. Employing machine learning algorithms to automate and improve the accuracy of arrow tracking and interpretation could be especially advantageous.
- **Expanding Material range:**
  To improve the overall applicability of the results, future research should consider a wider variety of textile materials. Examining a range of fabric compositions and structures would deepen our understanding of the mechanical characteristics of different types of smart textiles.

- **Quantitative Validation**:
  For future research, it would be important to validate PIV results quantitatively by comparing them with results obtained from other well-established measurement techniques in textile analysis. This approach would enhance the credibility and reliability of PIV as a tool for analysing textiles.

By addressing these limitations and pursuing these future research directions, more reliable and generalisable insights into the mechanical behaviour of smart textiles could be gained, which would markedly enhance the application of Particle Image Velocimetry (PIV) in textile analysis.

5.5 A Novel Modelling Approach

5.5.1 Findings and Discussion

Several approaches to theoretically and mathematically model the strain behaviour of textiles have been previously published. They were mostly based on mechanical finite element methods. Some modelling approaches also accounted for strain energy in various forms.

This research described the formation of a theoretical mathematical model based on energy method analysis. For each sample, four types of energy were considered (strain energy, length strain energy, curl weft energy, and gravity energy). The results show that each type of energy has an obvious effect on the behaviour of a textile sample when it is stretched. Gravity energy drags the sample down, as expected, but quickly becomes insignificant when the textile is stretched in another direction as well. In this case, other energies, such as the strain energy, were found to have significant weighting.

The mathematical models behaved like the experimental results.

- Strain energy is generated within a material as it deforms in response to an applied force. When the textile sample was stretched, it experienced tensile strain, which caused deformation and sorted energy within the material. This strain energy influenced the

material's mechanical behaviour and contributed to the final shape of the textile after stretching.

- Strain length energy occurs from changes in the shape of a patch due to the elongation of the yarn. If more strain energy is generated, the stitches will become longer and larger than their original state.
- Curl weft energy occurs when the yarn needs to take a linear form but is prevented from doing so by neighbouring loops. Therefore, curling starts at the edges of the textile, and even when the textile is under the influence of other energies, the curl weft energy seems to be the energy that has the greatest impact on the textile shape, as can be noticed by the narrowing, curling ripples, and irregularities shown in the matrices. The approach presented in this thesis is unique in several respects.

- The approach used in this research is different to previous studies because it did not model an individual stitch and did not rely on a repeating unit cell. Instead, it modelled the behaviour of a patch of knitted textiles and mapped the interactions across the fabric.
- The energy components considered in this context encompass broader aspects beyond surface alterations, including factors such as strain energy, strain length energy, curl-weft energy, and gravity energy. The solution procedure utilised in this study has an advantage over finite element modelling for several reasons.

  First, the solution procedure employed offers more practical utility than finite element modelling, owing to its potential for greater adaptability and ease of application. It often provides quicker insights into the overall energy aspects, allowing for a comprehensive understanding of the system behaviour without the computational complexity associated with finite-element modelling.

  Additionally, the solution procedure typically offers a more intuitive and direct approach, facilitating interpretation and analysis of the results. It often simplifies complex phenomena into understandable components, aiding in the identification of critical factors that influence the behaviour of the system under study.

  Moreover, this approach allows for a more holistic view by considering a broader spectrum of energies, encompassing various influential factors that might not be readily accounted for in finite element modelling. Consequently, it provides a more comprehensive understanding of the interplay between different energies and their cumulative effects on the behaviour of the system.

Overall, while finite element modelling has advantages in certain applications, the solution procedure used in the current study stands out for its practicality, ease of implementation, and capacity to swiftly provide comprehensive insight into the impact of diverse energy components on the system's behaviour.

5.5.2 Significance and Contribution

Many papers have reported good agreement between the experimental and theoretical models for tensile tests and stress-strain behaviour, consistent with course-wise and wale-wise directions in an assumed knitted fabric. However, the model presented in this thesis additionally describes the 3D behaviour of the textile and the effect of the energy component on the textile, such as the curl weft energy which curls the edges of the textile on both the right and left sides. The ripple phenomenon results from the curling weft energy. The strain length energy changes the length of the yarn and, hence, the form of the textile. This involves the narrowing of the centre area and the compatibility between the nodes in the middle with an increase in the size of the stitch because of the energies. These phenomena have not been observed in other studies.

Theoretical energy methodologies use mathematical models and calculations to analyse and predict how textiles behave based on their energy levels. These theoretical approaches can help understand and expect different properties.

Experimental data and observations either validate or challenge theoretical models. Comparing theoretical predictions with real-world results allows researchers to refine their understanding of material properties and applications.

- The alignment between theoretical energy methodologies and practical findings is crucial as it validates the accuracy and reliability of theoretical models, ensuring they accurately represent real-world material performance. This validation procedure is essential for building trust in theoretical approaches and using them to decide on material design and engineering.

- The current research has significantly advanced our understanding of textile properties and their practical applications. By linking theoretical and practical findings, the study has enhanced our knowledge of material behaviours and enabled innovative applications in various fields.

Knitted fabrics have various practical uses in multiple fields:

Knitted fabrics are extensively utilised in the textile industry for constructing a variety of garments, such as T-shirts, sweaters, socks, and activewear. The stretchability and breathability of these fabrics make them comfortable for daily use.

In the medical field, knitted textiles are employed for wound dressings and surgical implants. These fabrics can be designed to have specific characteristics like elasticity, making them suitable for various medical applications.

In the sports and athletic wear industry, knitted fabrics are preferred for their flexibility and moisture-absorbing capabilities. They provide comfort and support during physical activities, enhancing performance and movement.

Knitted materials are also used in vehicle internal stuffing and seat covers, offering toughness and the ability to meet specific safety and comfort requirements.

Furthermore, knitted fabrics are utilised in home furnishings, such as curtains, and bedding, providing a soft and warm feeling while being functional and durable.

These examples demonstrate the various applications of knitted fabrics, highlighting their unique properties that contribute to comfort, performance, and functionality in everyday contexts.

Predicting the mechanical behaviour of knitted fabrics with conductive and non-conductive yarns is essential for developing reliable smart textiles. Key benefits include:

- Improving sensor performance: Understanding how the knitted structure deforms under strain allows for designing sensors with desired electro-mechanical properties, such as high sensitivity (gauge factor), low hysteresis, and linearity across a broad strain range. These capabilities would enable precise motion capture and monitoring of human body movements (Warncke et al., 2023).
- Improving durability: Analysing the mechanical behaviour helps identify potential failure modes such as yarn slippage or breakage. This knowledge is needed to enable designers to identify suitable countermeasures such as reinforcing the knitted structure or modifying yarn materials and knit patterns to enhance the durability and longevity of the smart textile.
- Refining stretchability: The mechanical response of knitted fabric is intricately linked to its stretchability. By accurately predicting stretch behaviour, it is possible to tailor fabrics to possess the ideal level of elasticity, ensuring comfortable wearability and optimal conformity to the human body (Jansen, 2020).
- Improving knitting parameters: By establishing correlations between knitting parameters (such as yarn types, stitch density, and knit pattern) and mechanical properties, you can fine-tune the knitting process. This optimisation enables the production of fabrics with precisely tailored electro-mechanical characteristics suited for specific applications.

In summary, predicting mechanical behaviour empowers textile designers to engineer knitted smart textiles with optimal sensor performance, durability, stretchability, and washability. This engineering precision ensures their reliable use across diverse applications such as healthcare, sports, and human-machine interfaces (Shekhar et al., 2023).

The findings of this study featured several variations between the mathematical model and experimental results in some respects. Specifically:

Strain Energy Weighting:

When adjusting the strain energy weighting, the textile shapes predicted by the model were noticeably different from the experimental findings. For instance, with a low strain energy

weighting (0.1), the textile shape seemed random and undulating, whereas higher weightings (up to 2) generated more uniform shapes.

Strain Length Energy Weighting:

Varying the strain length energy weighting resulted in similar changes. Different weightings led to distinct behaviours in the textile material, which did not always match experimental findings.

Combinations of Energy Functions:

The study has also consisted of combinations of various types of energy functions. When differences in energy combinations were used more changes were observed in the predicted variation of textile behaviour compared to the experimental variations, which suggests that the model output differed from the experimental findings.

The study investigated the use of various combinations of energy functions. Differences were observed in the predicted behaviour of textiles when different energy function combinations were employed, suggesting disparities between the model's predictions and the experimental findings.

5.6 Study Limitations and Future Directions

This study investigated the mechanical properties and behaviour of knitted textiles to better inform the development of smart textiles. This included both experimental methods and the use of energy methods for mathematical modelling of weft knitted fabrics. However, the results should be interpreted within the context of these limitations.

The limitations of this study were shaped by the assortment of yarns employed, encompassing two conductive varieties (silver-coated nylon and an 80%-20% polyester/stainless steel blend), alongside a non-conductive option such as polyester. Additionally, this study investigated weft knitting fabrics with varying stitch counts in both the wale and course directions. Plan flat knit samples crafted with silver yarn featured 70 stitches per wale and 40 stitches per course. In

contrast, the polyester and stainless-steel samples were characterised by 70 stitches per wale and 120 stitches per course, examined in both flat and tube configurations. Two different knitting shapes were used to address the problems identified during testing: plain flat knit and plain tubular knit samples. The PIVlab software programme, described in section 3.7 PIV Results, was used to help determine the causes of the first-second test differences and simulate the hypothesis directly to see if it behaved similarly. Some yarns were mixed with Lycra, including both flat and tube samples, whereas others were not. Some used silicon wax to reduce friction during the test and overcome the first-second test problem. All these parameters were necessary limitations in this research to determine small changes and the reproducibility of results by the accuracy and repeatability of the tests.

Empirical testing was conducted under nonspecialist laboratory conditions. The results are limited by the potential association of properties with the effects of environmental factors, such as temperature and humidity, which cannot be controlled or monitored in the laboratory. External perturbations around the texture analyser machine could explain the zigzag "noise" represented in Figure 99, Figure 101, Figure 104, Figure 124, and Figure 125. There is abundant room for further progress in controlling the surrounding circumstances, such as isolating the test from noise and radiant heat and using a test chamber that can provide constant temperature and humidity.

A limited range of sample sizes were investigated (typically 20 x 60 & 40 x 80 courses and wales). Polyester samples with measurements 40 x 70 or 120 × 70 stitches were also tested. However, samples of these sizes may not be representative of the scale of sensor elements used in practical e-textile applications. Furthermore, only a limited set of yarns was tested, and only plain flat knit and plan tubular knit structures were investigated. Only the knit stitch was explored as a stitch type and only tested under uniaxial strain, with a range of strains (2.5, 5, 7.5, and 10%) being limited in this testing. The results indicate significant differences between the testing results, depending on the type of textile, materials, number of stitches, length of the stitches, and shape of the knitted sample. More detailed experiments that investigate the differences between samples with varying stitch lengths or number of stitches under different strain magnitudes would be of interest.

Similarly, the investigation of the mathematical model was confined to nominally flat shapes of small structures (a small number of nodes). Although various phenomena have been reproduced in modelling, the weighting factors have not yet been quantitatively related to experiments or the specific contributions of deformation (such as torsion or bending). Frictional energy was neglected because it is difficult to capture in a quasi-static energy model due to its path-dependent nature. This implies that frictional energy results in a loss of energy from the system, making it no longer conservative.

Advanced research must be conducted to explore the mathematical model by directly comparing it with another method to estimate various types of energy such as frictional or torsional energy. It may also be possible to model ways to overcome practical issues, such as the curling-edge problem when knitting the samples and simulating the effect during tensile tests, which would be an interesting issue for future research.

To develop a full picture of the mechanical characteristics of weft knitted fabrics, additional studies are needed to predict the behaviour of fabrics or materials under strain when stretched along two axes (horizontal x-axis and vertical y-axis) and thus subjected to fabric shear, fabric compression, buckling, and bending. Future work should be able to predict the behaviour based on estimates of measurable properties, such as density, modulus of elasticity (Young's modulus in the fibre direction of the axis), and size of stitches.

This investigation focused on mechanical behaviour. There are still many unanswered questions regarding the electrical modelling of knitted conductive yarns. An important area of future study would be to measure the electrical properties of textiles subjected to mechanical deformation. In this context, testing could be used to estimate the frequency-dependent impedance of conductive textiles.

To improve the practical utility of these results, future investigations could explore different materials, use the same materials but change the knitting structure, or explore other textile structures such as woven samples.

5.7 Conclusion

As discussed in Chapter 1, the main objective of this thesis was to demonstrate the mechanical properties of smart knitted textiles using a theoretical model. Only a few papers investigating the mechanical behaviour of smart knitted textiles have been published, most of which did not consider the differences between their theoretical and experimental results. This study sought to better understand the mechanical properties of plain knitted fabrics represented by conductive yarns, such as silver and stainless steel, and non-conductive yarn-like polyester and to test a mathematical model against experimental results.

The project investigated the use of particle image velocimetry (PIV) to quantify the motion of textiles undergoing mechanical strain and developed a method of modelling mechanical behaviour based on the concept of energy conservation. This study observed the changes in the knitted textile behaviour during repeated extension under the effects of tensile strain and how this is related to the form and material.

The most significant implication of the project findings is that the first tensile test of the textile behaved differently from the second and subsequent tests, indicating that the force produced in the first test was lower than that in the second test. This implementation demonstrated that it was correct for different yarn materials, strain rates, and knitted structures.

The investigations revealed a notable disparity in the behaviour of various materials when subjected to force, particularly highlighting the robustness of polyester yarn compared to knitted fabrics such as silver or stainless steel. Specifically, the first tensile test showed intriguing distinctions: the plain flat knit polyester sample, with or without Lycra, required more force for stretching than the plain tubular knit sample at identical tensile strains. Conversely, the stainless-steel flat sample, regardless of the presence of Lycra, required less force for stretching under similar conditions. These nuanced differences in the initial test behaviour have not been extensively documented in prior studies, which emphasises the necessity to incorporate such behaviour into testing protocols for smart textiles.

This study supports suggestions advocating multiple repetitions of the tensile test under consistent strain and with the same sample. This approach aims to elucidate the relationship between sequential tests and to clarify the discrepancies observed between the initial and subsequent tests. In doing so, it aims to provide a clearer understanding of how materials respond over successive tests and how this behaviour evolves, ensuring a more comprehensive assessment of textile performance.

The study also developed a theoretical model that was based on energy model method analysis. The mathematical model considers that each fabric has four types of energy (strain energy, strain length energy, curl weft energy, and gravity energy). The model assumes that each type of energy has a clear effect on the behaviour of the textile sample when it is stretched. Gravity energy has an obvious effect on the sample at the beginning of the test when it is trying to drag the sample down; however, the effect of this energy gradually becomes insignificant because the effects of the weightings of the other energies increase when a textile is stretched.

In this thesis, the model was used to describe the 3D behaviour of the textile and the effect of the energy component on the textile, such as the ripple phenomenon that results from the curling weft energy. This phenomenon has not been explained in previous studies. This thesis provided data, analysis, and new models of the mechanical behaviour of knitted e-textiles to support the ongoing development and application of e-textiles.

This research has the potential to make a real difference across a variety of industries, including textiles, materials science, medicine, and sports performance. By advancing our understanding of textile properties and their practical applications, this work paves the way for innovations that can enhance comfort, performance, and functionality in everyday life.

Glossary and Abbreviations

PIV	Particle image velocimetry
RUC	Repeated unit cells
FEM	Finite element method
PJN	Pin joint net
KES	Kawabata evaluation system
ACBT	Automatic cyclic bending tester
Denier	Linear density (weight in gram per 1000 m length)
Dtex	1 gram per 10000 m length
Tex	A small unit of linear density
ECG	Electrocardiogram
ANN	Artificial neural network
jamming	"Jamming" is when the threads of a knitted material are closely packed and intertwined, creating a strong and secure framework
Curling couple moment	The forces that cause a fabric to curl
knot	Patch or cluster of stitches, rather than an individual stitch

Bibliography

Abghary, M. J., Hasani, H., & Nedoushan, R. J. (2016). Numerical simulating the tensile behavior of 1×1 rib knitted fabrics using a novel geometrical model. *Fibers and Polymers*, *17*(5), 795–800. https://doi.org/10.1007/s12221-016-5791-6

Abreu, M. J., Carvalho, H., Catarino, A., & Rocha, A. (2010). Integration and Embedding of Vital Signs Sensors and Other Devices into Textiles. In *Medical and Healthcare Textiles* (pp. 381–388). Elsevier. https://doi.org/10.1533/9780857090348.381

Adam Zewe. (2022, July 7). *Smart textiles sense how their users are moving | MIT News | Massachusetts Institute of Technology*. https://news.mit.edu/2022/smart-textiles-sense-movement-0707

Agcayazi, T., Chatterjee, K., Bozkurt, A., & Ghosh, T. K. (2018). Flexible Interconnects for Electronic Textiles. *Advanced Materials Technologies*, *3*(10), 1700277. https://doi.org/10.1002/admt.201700277

Ajeli, S., Jeddi, Ali. A. A., & Rastgo, A. (2009). A three-dimensional analysis of loop knit structure by using a property of the buckled–twisted elastic rod. *Journal of the Textile Institute*, *100*(2), 111–119. https://doi.org/10.1080/00405000701660921

Ajeli, S., Jeddi, Ali. A. A., Rastgo, A., & Gorga, R. E. (2009). An analysis of the bending rigidity of warp-knitted fabrics: A comparison of experimental results to a mechanical model. *Journal of the Textile Institute*, *100*(6), 496–506. https://doi.org/10.1080/00405000801972374

Atalay, O., Kennon, W., & Husain, M. (2013). Textile-Based Weft Knitted Strain Sensors: Effect of Fabric Parameters on Sensor Properties. *Sensors*, *13*(8), 11114–11127. https://doi.org/10.3390/s130811114

ATEX Technologies Inc. (2016). *Braided Medical Fabric | Surgical Yarn Braiding & Medical Textile Braiding*. http://www.atextechnologies.com/medical-textile-what-we-do/medical-fabric-and-technologies/braiding/

Balea, L., Dusserre, G., & Bernhart, G. (2014). Mechanical behaviour of plain-knit reinforced injected composites: Effect of inlay yarns and fibre type. *Composites Part B: Engineering*, *56*, 20–29. https://doi.org/10.1016/j.compositesb.2013.07.028

Banerjee, P. K., & Ghosh, S. (1999). A Model of the Single-jersey Loop-formation Process. *Journal of the Textile Institute*, *90*(2), 187–208. https://doi.org/10.1080/00405009908690622

Barburski, M., & Lomov, S. V. (2016). Influence of oxidation on steel fiber yarn and knitted fabric properties. *Journal of Industrial Textiles*, *45*(6), 1516–1529. https://doi.org/10.1177/1528083714564634

Bassett, R. J., Postle, R., & Pan, N. (1999). Experimental Methods for Measuring Fabric Mechanical Properties: A Review and Analysis. *Textile Research Journal*, *69*(11), 866–875. https://doi.org/10.1177/004051759906901111

Brad Stephenson. (2021, October). *Smart Clothes Are the Future and They're Already Here*. Lifewire. https://www.lifewire.com/what-are-smart-clothes-4176103

Carvelli, V., & Poggi, C. (2001). A homogenization procedure for the numerical analysis of woven fabric composites. *Composites Part A: Applied Science and Manufacturing*, *32*(10), 1425–1432. https://doi.org/10.1016/S1359-835X(01)00041-0

Chen, Y., Battley, M., & Finch, G. (2013, December 20). *Contact Area Analysis of Intelligent Knitted Textiles*. Centre for Advanced Composite Materials, The University of Auckland.

Choi, K. F., & Lo, T. Y. (2003). An Energy Model of Plain Knitted Fabric. *Textile Research Journal*, *73*(8), 739–748. https://doi.org/10.1177/004051750307300813

Choi, K. F., & Lo, T. Y. (2006). The Shape and Dimensions of Plain Knitted Fabric: A Fabric Mechanical Model. *Textile Research Journal*, *76*(10), 777–786. https://doi.org/10.1177/0040517507069030

Choi, K. F., & Tandon, S. K. (2006). An energy model of yarn bending. *Journal of the Textile Institute*, *97*(1), 49–56. https://doi.org/10.1533/joti.2005.0212

Choi, M.-S., & Ashdown, S. P. (2000). Effect of Changes in Knit Structure and Density on the Mechanical and Hand Properties of Weft-Knitted Fabrics for Outerwear. *Textile Research Journal*, *70*(12), 1033–1045. https://doi.org/10.1177/004051750007001201

Choi, W., & Lee, Y. L. (2010). *Development of Three-Dimensional Knit Models through Rib & Purl Structures*. *18*(1), 109–117.

Cohen, R., & Swerdlik, M. (2009). *Psychological Testing and Assessment: An Introduction to Tests and Measurement 7tEditionh* (7th ed.). McGraw-Hill Humanities/Social Sciences/Languages.

CORE-Materials. (2010). *Felt structure* [Photo]. https://www.flickr.com/photos/core-materials/4419853508/

Dabiryan, H., & Jeddi, A. A. A. (2011). Analysis of warp knitted fabric structure. Part I: A 3D straight line model for warp knitted fabrics. *The Journal of The Textile Institute*, *102*(12), 1065–1074. https://doi.org/10.1080/00405000.2010.532624

Dabiryan, H., & Jeddi, A. A. A. (2012). Analysis of warp-knitted fabric structure part IV: Modeling the initial Poisson's ratio in elastic deformation region. *Journal of the Textile Institute*, *103*(12), 1352–1360. https://doi.org/10.1080/00405000.2012.685269

Dabiryan, H., Jeddi, A. A. A., & Rastgoo, A. (2012a). Analysis of warp-knitted fabric structure. Part II: Theoretical study on initial modulus of warp-knitted fabrics (tricot, locknit, and satin).

Journal of the Textile Institute, *103*(9), 997–1011. https://doi.org/10.1080/00405000.2012.654665

Dabiryan, H., Jeddi, A. A. A., & Rastgoo, A. (2012b). Analysis of warp-knitted fabric structure. Part III: Theoretical study on initial modulus of warp-knitted fabrics (reverse locknit, three- and four-needle sharkskin). *The Journal of The Textile Institute*, *103*(11), 1213–1227. https://doi.org/10.1080/00405000.2012.673297

Dabiryan, H., Jeddi, A. A. A., & Rastgoo, A. (2013). Analysis of warp knitted fabric structure. Part V: Experimental study on the initial modulus of warp knitted fabrics. *Journal of the Textile Institute*, *104*(1), 46–56. https://doi.org/10.1080/00405000.2012.693276

Demiroz, A., & Dias, T. (2000a). A Study of the Graphical Representation of Plain-knitted Structures Part I: Stitch Model for the Graphical Representation of Plain-knitted Structures. *Journal of the Textile Institute*, *91*(4), 463–480. https://doi.org/10.1080/00405000008659121

Demiroz, A., & Dias, T. (2000b). A Study of the Graphical Representation of Plain-knitted Structures Part II: Experimental Studies and Computer Generation of Plain-knitted Structures. *The Journal of The Textile Institute*, *91*(4), 481–492. https://doi.org/10.1080/00405000008659122

Dhakal, R. P., & Maekawa, K. (2002). Reinforcement Stability and Fracture of Cover Concrete in Reinforced Concrete Members. *Journal of Structural Engineering*, *128*(10), 1253–1262. https://doi.org/10.1061/(ASCE)0733-9445(2002)128:10(1253)

Ding, C. (2024). Properties of stainless steel and its application in construction. *Applied and Computational Engineering*, *59*(1), 51–56. https://doi.org/10.54254/2755-2721/59/20240748

Dinh, T. D., Weeger, O., Kaijima, S., & Yeung, S.-K. (2018). Prediction of mechanical properties of knitted fabrics under tensile and shear loading: Mesoscale analysis using representative

unit cells and its validation. *Composites Part B: Engineering*, *148*, 81–92. https://doi.org/10.1016/j.compositesb.2018.04.052

DVDVideoSoft. (2017). *Free Video to JPG Converter—Make snapshots from video files*. https://www.dvdvideosoft.com/products/dvd/Free-Video-to-JPG-Converter.htm

Eryuruk, S. H., & Kalaoglu, F. (2016). Analysis of the performance properties of knitted fabrics containing elastane. *International Journal of Clothing Science and Technology*, *28*(4), 463–479. https://doi.org/10.1108/IJCST-10-2015-0120

Eysan_ac. (2019, November 27). Single Jersey Fabric Vs Interlock Fabric. *Eysan Fabrics*. https://www.eysan.com.tw/single-jersey-fabric-vs-interlock-fabric/

Ghapanvari, S., Khoddami, A., & Hasani, H. (2015a). Effect of Weft Knitted Polyester Fabric Structure on its Hydrophobicity after Fluorocarbon Finishing. *Textiles and Light Industrial Science and Technology*, *4*(1), 27–34. https://doi.org/10.12783/tlist.2015.0401.03

Ghapanvari, S., Khoddami, A., & Hasani, H. (2015b). Effect of Weft Knitted Polyester Fabric Structure on its Hydrophobicity after Fluorocarbon Finishing. *Textiles and Light Industrial Science and Technology*, *4*(1), 27–34. https://doi.org/10.12783/tlist.2015.0401.03

Gilmore, C. M. (1998). Advanced Composites Manufacturing By Timothy G. Gutowski. *Materials and Manufacturing Processes*, *13*(4), 626–626. https://doi.org/10.1080/10426919808935286

Go, Y., & Shinohara, A. (1959). CURL IN WOVEN TEXTILE FABRICS. *Sen'i Gakkaishi*, *15*(4), 281–284. https://doi.org/10.2115/fiber.15.281

Grosberg, P. (1964). 3—THE GEOMETRICAL PROPERTIES OF SIMPLE WARP-KNIT FABRICS. *Journal of the Textile Institute Transactions*, *55*(1), T18–T30. https://doi.org/10.1080/19447026408660205

Guler Murat, A. A. H. (2004). *Use of Image Analysis in Determination of Strain Distribution During Geosynthetic Tensile Testing*. *18*. https://doi.org/10.1061/(ASCE)0887-3801(2004)18:1(65)

Halim, abdul, Iftay Khairul Alam, & Akhter, T. (2019). *Comparative study of the effect of Lycra on Single Jersey and 1×1 Rib made from 100% Cotton and Cotton/Lycra Yarns*. *Vol.2, No.2, 2019: 91-100*. https://doi.org/10.5281/ZENODO.3334515

Hamilton, R. J. (1975). *Bending and shear properties of knitted stuctures* [UNSW Sydney]. https://doi.org/10.26190/UNSWORKS/11203

Hamilton, R. J., & Postle, R. (1974). Bending and Recovery Properties of Wool Plain-Knitted Fabrics. *Textile Research Journal*, *44*(5), 336–343. https://doi.org/10.1177/004051757404400503

Hasani, H. (2014a). An Investigation into the Effect of Fabric Structure and Yarn Twist Direction on the Curling Behavior of Single Jersey Weft Knitted Fabrics. *Journal of Fashion Technology & Textile Engineering*, *02*(01). https://doi.org/10.4172/2329-9568.1000107

Hasani, H. (2014b). An Investigation into the Effect of Fabric Structure and Yarn Twist Direction on the Curling Behavior of Single Jersey Weft Knitted Fabrics. *Journal of Fashion Technology & Textile Engineering*, *02*(01). https://doi.org/10.4172/2329-9568.1000107

Hassan, M., Qashqary, K., Hassan, H. A., Shady, E., & Alansary, M. (2012). *Influence of Sportswear Fabric Properties on the Health and Performance of Athletes*. Fibres & Textiles in Eastern Europe*, 4(93)*, 82–88.

Hearle, J. W. S., & Shanahan, W. J. (1978). 11—AN ENERGY METHOD FOR CALCULATIONS IN FABRIC MECHANICS PART I: PRINCIPLES OF THE METHOD. *The Journal of The Textile Institute*, *69*(4), 81–91. https://doi.org/10.1080/00405007808631425

J. Schaefer. (2018). *Mechanical properties of rubber*. https://www.mtec.or.th/wp-content/uploads/2018/04/mechanical-properties_rubber.pdf

Jacques, S., De Baere, I., & Van Paepegem, W. (2014). Application of periodic boundary conditions on multiple part finite element meshes for the meso-scale homogenization of textile fabric composites. *Composites Science and Technology*, *92*, 41–54. https://doi.org/10.1016/j.compscitech.2013.11.023

Jaffe, M., Easts, A. J., & Feng, X. (2020). Polyester fibers. In *Thermal Analysis of Textiles and Fibers* (pp. 133–149). Elsevier. https://doi.org/10.1016/B978-0-08-100572-9.00008-2

Jansen, K. M. B. (2020). Performance Evaluation of Knitted and Stitched Textile Strain Sensors. *Sensors*, *20*(24), 7236. https://doi.org/10.3390/s20247236

Jones, D. (2000). Wide-Width Geotextile Testing with Video Extensometry. In P. Stevenson (Ed.), *Grips, Clamps, Clamping Techniques, and Strain Measurement for Testing of Geosynthetics* (pp. 83-83–86). ASTM International. https://doi.org/10.1520/STP13473S

Joy. (2021, February 25). The Ultimate Guide to Circular Needles—The Yarn Queen NZ. *The Yarn Queen*. https://theyarnqueen.co.nz/the-ultimate-guide-to-circular-needles/

Kabir, S. M. F., Uluturk, I., Pang, R., Khadse, N., Stapleton, S. E., & Park, J. H. (2023). Structure–Property Investigation of Knit Patterns on Thermal Comfort: A Holistic Approach. *ACS Applied Engineering Materials*, *1*(5), 1455–1466. https://doi.org/10.1021/acsaenm.3c00143

Kang, G., Kan, Q., Zhang, J., & Sun, Y. (2006). Time-dependent ratchetting experiments of SS304 stainless steel. *International Journal of Plasticity*, *22*(5), 858–894. https://doi.org/10.1016/j.ijplas.2005.05.006

Kang, T. J., & Kim, M. S. (2001). Effects of Silicone Treatments on the Dimensional Properties of Wool Fabric. *Textile Research Journal*, *71*(4), 295–300. https://doi.org/10.1177/004051750107100403

Kawabata, S. (1980). *The standardization and analysis of hand evaluation* (1 ed). Textile Machinery Society of Japan. https://openlibrary.org/books/OL19767923M/The_standardization_and_analysis_of_hand_evaluation

Kayacan, O., & Kurbak, A. (2008). Basic Studies for Modeling Complex Weft Knitted Fabric Structures Part IV: Geometrical Modeling of Miss Stitches. *Textile Research Journal*, *78*(8), 659–663. https://doi.org/10.1177/0040517507087663

Kelly Mitchell. (2023). Purl Knitting. *Catwalk Yourself*. https://www.catwalkyourself.com/fashion-dictionary/purl-knitting/

Kikuta, M. T. (2003). *Mechanical Properties of Candidate Materials for Morphing Wings* [Master thesis]. https://vtechworks.lib.vt.edu/items/36151628-2eb2-42da-be46-fdad5af65bee

Kiron, M. I. (2014a, February 6). Spirality Correction System (SCS) for Knitted Fabrics. *Textile Learner*. https://textilelearner.net/spirality-correction-system-for-knitted-fabrics/

Kiron, M. I. (2014b, December 12). Spandex Fiber: Properties, Manufacturing Process and Uses. *Textile Learner*. https://textilelearner.net/spandex-fiber-properties-manufacturing/

Kirstein, T. (2013). *Multidisciplinary know-how for smart-textiles developers* (p. 501). https://www.alibris.com/Multidisciplinary-Know-How-for-Smart-Textiles-Developers/book/23725498?qsort=dr#:~:text=Multidisciplinary%20know-how%20for%20smart-textiles%20developers%20provides%20a%20filtered,the%20new%20enabling%20technologies%2C%20commercialisation%20and%20market%20tre

Knitted fabric. (2021). In *Wikipedia*. https://en.wikipedia.org/w/index.php?title=Knitted_fabric&oldid=1025031371

Kun, M., Chan, C., & Ramakrishna, S. (2009). Textile-based scaffolds for tissue engineering. In *Advanced Textiles for Wound Care* (pp. 289–321). Elsevier. https://doi.org/10.1533/9781845696306.2.289

Kurbak, A., & Alpyildiz, T. (2009). Geometrical Models for Cardigan Structures Part I: Full Cardigan. *Textile Research Journal*, *79*(14), 1281–1300. https://doi.org/10.1177/0040517508102258

Kurbak, A., & Amreeva, G. (2006). Creation of a Geometrical Model for Milano Rib Fabric. *Textile Research Journal*, *76*(11), 847–852. https://doi.org/10.1177/0040517507071968

Kurbak, A., & Ekmen, O. (2008a). Basic Studies for Modeling Complex Weft Knitted Fabric Structures Part I: A Geometrical Model for Widthwise Curlings of Plain Knitted Fabrics. *Textile Research Journal*, *78*(3), 198–208. https://doi.org/10.1177/0040517507082352

Kurbak, A., & Ekmen, O. (2008b). Basic Studies for Modeling Complex Weft Knitted Fabric Structures Part I: A Geometrical Model for Widthwise Curlings of Plain Knitted Fabrics. *Textile Research Journal*, *78*(3), 198–208. https://doi.org/10.1177/0040517507082352

Kurbak, A., & Soydan, A. S. (2009). Geometrical Models for Balanced Rib Knitted Fabrics Part III: 2 × 2, 3 × 3, 4 × 4, and 5 × 5 Rib Fabrics. *Textile Research Journal*, *79*(7), 618–625. https://doi.org/10.1177/0040517508096218

Leaf, G. A. V. (1958). A property of a buckled elastic rod. *British Journal of Applied Physics*, *9*(2), 71–72. https://doi.org/10.1088/0508-3443/9/2/305

Liu, H., Jiang, G., & Dong, Z. (2021). Geometric simulation for warp-knitted tubular bandages with the mesh model. *Textile Research Journal*, *91*(21–22), 2612–2623. https://doi.org/10.1177/00405175211013836

Liu, T., Choi, K. F., & Li, Y. (2007). Mechanical Modeling of Singles Yarn. *Textile Research Journal*, *77*(3), 123–130. https://doi.org/10.1177/0040517507074022

Lomov, S. V., Boisse, Ph., Deluycker, E., Morestin, F., Vanclooster, K., Vandepitte, D., Verpoest, I., & Willems, A. (2008). Full-field strain measurements in textile deformability studies. *Composites Part A: Applied Science and Manufacturing*, *39*(8), 1232–1244. https://doi.org/10.1016/j.compositesa.2007.09.014

Lundström, J., & Lu, J. (2021, April 16). Complete Guide To Sewing Knits with a Twin-Needle. *The Last Stitch*. https://www.thelaststitch.com/complete-guide-to-sewing-knits-with-a-twin-needle/

Ma, P., & Gao, Z. (2015). A review on the impact tension behaviors of textile structural composites. *Journal of Industrial Textiles*, *44*(4), 572–604. https://doi.org/10.1177/1528083713503001

Mac Namara, C., Gabriele, A., Amador, C., & Bakalis, S. (2012). Dynamics of textile motion in a front-loading domestic washing machine. *Chemical Engineering Science*, *75*, 14–27. https://doi.org/10.1016/j.ces.2012.03.009

Mathews Donovan. (2023, July 7). *Interlock Fabric—Everything You Need To Know—Bryden Apparel*. https://brydenapparel.com/interlock-double-knit-fabric/

MATLAB. (2023). https://au.mathworks.com/products/matlab.html

Meyer, J., Lukowicz, P., & Troster, G. (2006). Textile Pressure Sensor for Muscle Activity and Motion Detection. *2006 10th IEEE International Symposium on Wearable Computers*, 69–72. https://doi.org/10.1109/ISWC.2006.286346

Miao, Y., Guo, X., & Zhang, X.-J. (2020). Visualization of Fiber Moving in Air Tunnel with Velocity Gradient *. *Chinese Physics Letters*, *37*(3), 034201. https://doi.org/10.1088/0256-307X/37/3/034201

Minapoor, Sh., Ajeli, S., Hasani, H., & Shanbeh, M. (2013a). Investigation into the curling behavior of single jersey weft-knitted fabrics and its prediction using neural network model.

Journal of the Textile Institute, *104*(5), 550–561. https://doi.org/10.1080/00405000.2012.752124

Minapoor, Sh., Ajeli, S., Hasani, H., & Shanbeh, M. (2013b). Investigation into the curling behavior of single jersey weft-knitted fabrics and its prediction using neural network model. *Journal of the Textile Institute*, *104*(5), 550–561. https://doi.org/10.1080/00405000.2012.752124

NC state university. (2021). Kawabata Evaluation System—Textile Protection And Comfort Center—NC State University. *Textile Protection And Comfort Center*. https://textiles.ncsu.edu/tpacc/comfort-performance/kawabata-evaluation-system/

Nikhil Bhosale and Bajirao Jadhav. (2015). *Weft Knitted Fabrics*. Texnote. https://texnote.blogspot.com/2017/01/weft-knitted-fabrics.html

Niu, L., Miao, X., Jiang, G., Wan, A., Li, Y., & Liu, Q. (2020). Biomechanical energy harvest based on textiles used in self-powering clothing. *Journal of Engineered Fibers and Fabrics*, *15*, 155892502096735. https://doi.org/10.1177/1558925020967352

Nocent, O., Nourrit, J.-M., & Remion, Y. (2001). *Towards mechanical level of detail for knitwear simulation*. https://dspace.zcu.cz/handle/11025/11277

Nutting, T. S., & Leaf, G. A. V. (1964). 5—A GENERALIZED GEOMETRY OF WEFT-KNITTED FABRICS. *Journal of the Textile Institute Transactions*, *55*(1), T45–T53. https://doi.org/10.1080/19447026408660207

O'Brien, C., McBride, A., E. Zaghi, A., Burke, K., & Hill, A. (2017). Mechanical Behavior of Stainless Steel Fiber-Reinforced Composites Exposed to Accelerated Corrosion. *Materials*, *10*(7), 772. https://doi.org/10.3390/ma10070772

OCS Team. (2019). *Classification of Fabric Defects*. https://www.onlineclothingstudy.com/2019/02/classification-of-fabric-defects.html

Olofsson, B. (1964). 49—A GENERAL MODEL OF A FABRIC AS A GEOMETRIC-MECHANICAL STRUCTURE. *Journal of the Textile Institute Transactions*, *55*(11), T541–T557. https://doi.org/10.1080/19447026408662245

Paradiso, R., Loriga, G., & Taccini, N. (2005). A Wearable Health Care System Based on Knitted Integrated Sensors. *IEEE Transactions on Information Technology in Biomedicine*, *9*(3), 337–344. https://doi.org/10.1109/TITB.2005.854512

Pavko-Cuden, A., & Sluga, F. (2015). Measuring loop lengths of elasticised knitted fabrics. *The Journal of The Textile Institute*, *106*(3), 225–235. https://doi.org/10.1080/00405000.2014.911998

Pavlović, Ž., & Vrljičak, Z. (2020). Comparing double jersey knitted fabrics made of Tencel and modal yarns, spun by different spinning methods. *Journal of Engineered Fibers and Fabrics*, *15*, 155892502091985. https://doi.org/10.1177/1558925020919854

Peace, G. S. (1993). *Taguchi Methods: S Hands-On Approach*. Reading, Mass. : Addison-Wesley. https://archive.org/details/taguchimethodsha0000peac

Peng, H., & Green, S. I. (2012). PAPER PHYSICS. PIV measurements of flow through forming fabrics. *Nordic Pulp & Paper Research Journal*, *27*(4), 783–789. https://doi.org/10.3183/npprj-2012-27-04-p783-789

Petersen, P., Helmer, R., Pate, M., & Eichhoff, J. (2011). Electronic textile resistor design and fabric resistivity characterization. *Textile Research Journal*, *81*(13), 1395–1404. https://doi.org/10.1177/0040517511404591

Phukan, A. R., & Subramaniam, V. (1995). Degree and Stability of the Flat Set of Plain. Weft Knitted Fabrics: Part I: Effect of Finishing Treatments. *Textile Research Journal*, *65*(8), 471–477. https://doi.org/10.1177/004051759506500806

PIVlab - Digital Particle Image Velocimetry Tool for MATLAB. (2021). What is PIVlab? *What Is PIVlab?* https://pivlab.blogspot.com/p/what-is-pivlab.html

Postle, R., & Munden, D. L. (1967). 25—ANALYSIS OF THE DRY-RELAXED KNITTED-LOOP CONFIGURATION: PART II: THREE-DIMENSIONAL ANALYSIS. *Journal of the Textile Institute*, *58*(8), 352–365. https://doi.org/10.1080/00405006708629881

Rajak, B. (2021, June 7). *What Are the Woven Fabric Parameters that affect Garment Production?* Garments Technology. https://www.technologygmt.com/post/what-are-the-woven-fabric-parameters-that-affect-garment-production

Rattfält, L., Lindén, M., Hult, P., Berglin, L., & Ask, P. (2007). Electrical characteristics of conductive yarns and textile electrodes for medical applications. *Medical & Biological Engineering & Computing*, *45*(12), 1251–1257. https://doi.org/10.1007/s11517-007-0266-y

Ray, S. C. (Ed.). (2012). *Fundamentals and Advances in Knitting Technology* (first). WPI Publishing. https://doi.org/10.1201/b18245

Repon, Md. R., Shiddique, Md. N. A. S., Paul, D., Al Mamun, R. A. M., Shahria, S., & Quayum, M. (2018). *Effect of Yarn Count & Stitch Length on the Fabric Width, GSM, WPI and CPI of 1×1 Rib Fabrics*. *7*(4), 94–100. https://doi.org/10.5923/j.textile.20180704.03

Sadek, R., El-Hossini, A. M., Eldeeb, A. S., & Yassen, A. A. (2012). Effect of Lycra Extension Percent on Single Jersey Knitted Fabric Properties. *Journal of Engineered Fibers and Fabrics*, *7*(2), 155892501200700. https://doi.org/10.1177/155892501200700203

Salar Zohoori. (2017). *Fashion Technology & Textile Engineering Journal—High Impact Factor Journal*. Https://Www.Scitechnol.Com/Fashion-Technology-Textile-Engineering.Php. http://www.scitechnol.com/fashion-technology-textile-engineering.php

Sarker, M. E., Islam, M. R., Mahmud, M. S., Islam, M. Z., Alimuzzaman, S., & Ahmed, A. T. M. F. (2022). Effects of Yarn, Fabric and Machine Parameters on the Dimensional Properties of

Weft Knitted Single Jersey Fabric. *Journal of Natural Fibers*, *19*(17), 15625–15636. https://doi.org/10.1080/15440478.2022.2131682

Scanco. (2018). *Acoustic Envelope Detector | Accesories de textura | Scanco Analytical Instruments*. https://scancotec.com/en/products/acoustic-envelope-detector/

Schröder, A., & Willert, C. (2008). *Particle Image Velocimetry: New Developments and Recent Applications* (Vol. 112). Springer Berlin Heidelberg. https://doi.org/10.1007/978-3-540-73528-1

Senthilkumar, M., Anbumani, N., & Hayavadana, J. (2011). Elastane fabrics—A tool for stretch applications in sports. *Indian Journal of Fibre and Textile Research. 36*, 300–307.

Shanahan, W. J., & Hearle, J. W. S. (1978). 12—AN ENERGY METHOD FOR CALCULATIONS IN FABRIC MECHANICS PART II: EXAMPLES OF APPLICATION OF THE METHOD TO WOVEN FABRICS. *The Journal of The Textile Institute*, *69*(4), 92–100. https://doi.org/10.1080/00405007808631426

Shanahan, W. J., & Postle, R. (1973). Jamming of Knitted Structures. *Textile Research Journal*, *43*(9), 532–538. https://doi.org/10.1177/004051757304300907

Sharma, S. B., & Sutcliffe, M. P. F. (2004). A simplified finite element model for draping of woven material. *Composites Part A: Applied Science and Manufacturing*, *35*(6), 637–643. https://doi.org/10.1016/j.compositesa.2004.02.013

Sheikh, Md. R., Hossain, Md. K., & Khan, M. M. R. (2022). Influence of Lycra Content and Stitch Length on the Dimensional and Physical Characteristics of Lycra Back Plaited Cotton (LBPC) Single Jersey Fabrics. *Journal of Textile Science and Technology*, *08*(04), 203–220. https://doi.org/10.4236/jtst.2022.84015

Shekhar, R., Choudhry, N. A., Islam, S., Ahnood, A., Pirogova, E., & Troynikov, O. (2023). A Novel Elastic Conductive Yarn for Smart Textile Applications. *Advanced Engineering Materials*, *25*(22), 2300572. https://doi.org/10.1002/adem.202300572

Sheryll. (2021, March 11). A Little Bit (OK, A LOT!) About Single Jersey. *Pattern Scissors Cloth*. https://patternscissorscloth.com/2021/03/12/a-little-bit-ok-a-lot-about-single-jersey/

Singhal, K., Mishra, S., & Kumar, B. (2021). A study of curling in rib-knit constructions. *The Journal of The Textile Institute*, *112*(4), 666–675. https://doi.org/10.1080/00405000.2020.1778224

Sitotaw, D. B., & Adamu, B. F. (2017). Tensile Properties of Single Jersey and 1×1 Rib Knitted Fabrics Made from 100% Cotton and Cotton/Lycra Yarns. *Journal of Engineering*, *2017*, 1–7. https://doi.org/10.1155/2017/4310782

Song, J.-H., & Turner, J. D. (1968). Some Aspects of the Geometry of Simple Rib-Tuck Weft-Knitted Wool Fabrics. *Textile Research Journal*, *38*(5), 481–487. https://doi.org/10.1177/004051756803800505

Sperl, G., Narain, R., & Wojtan, C. (2021). Mechanics-aware deformation of yarn pattern geometry. *ACM Transactions on Graphics*, *40*(4), 1–11. https://doi.org/10.1145/3450626.3459816

S.R. Mishra, et al. (2016). *APPLICATION OF IMAGE PROCESSING TECHNIQUE IN WIDE WIDTH TENSILE TESTING OF NONWOVEN GEOTEXTILE*. https://www.researchgate.net/publication/312166877_Application_of_Image_Processing_Technique_in_Wide_Width_Tensile_Testing_of_Nonwoven_Geotextile

staff, E. (2018). *Volt smart yarn*. https://textile-network.com/en/Technical-Textiles/Fasern-Garne/Volt-Smart-Yarns

Stoppa, M., & Chiolerio, A. (2014). Wearable Electronics and Smart Textiles: A Critical Review. *Sensors*, *14*(7), 11957–11992. https://doi.org/10.3390/s140711957

Tamanna, T. A., Shibly, M. A. H., Nurunnabi, Suruj-Zaman, Md., Mondal, B. V., & Saha, P. K. (2017). Investigation of Stretch and Recovery Property of Weft Knitted Regular Rib Fabric. *European Scientific Journal, ESJ*, *13*(27), 400. https://doi.org/10.19044/esj.2017.v13n27p400

Tamke, M., Sinke Baranovskaya, Y., Monteiro, F., Lienhard, J., La Magna, R., & Ramsgaard Thomsen, M. (2021). Computational knit – design and fabrication systems for textile structures with customised and graded CNC knitted fabrics. *Architectural Engineering and Design Management*, *17*(3–4), 175–195. https://doi.org/10.1080/17452007.2020.1747386

Tandon, S. K., Kim, S. J., & Choi, F. K. F. (1995). The Torsional Behaviour of Singles Yarns. Part II: Evaluation. *Journal of the Textile Institute*, *86*(2), 200–217. https://doi.org/10.1080/00405009508631327

Tao, X. (2015). *Handbook of Smart Textiles* (1st ed. 2015). Springer Singapore Springer e-books Imprint: Springer.

Tex Education. (2015, August 18). *Introduction to warp knitting*. https://texeducation.wordpress.com/2015/08/18/introduction-to-warp-knitting/

Thielicke, W. & Eize J. Stamhuis. (2015). *PIVlab—Time-Resolved Digital Particle Image Velocimetry Tool for MATLAB* (p. 0 Bytes) [Computer software]. figshare. https://doi.org/10.6084/M9.FIGSHARE.1092508.V5

Thielicke, W., & Stamhuis, E. J. (2014). PIVlab – Towards User-friendly, Affordable and Accurate Digital Particle Image Velocimetry in MATLAB. *Journal of Open Research Software*, *2*. https://doi.org/10.5334/jors.bl

Treloar, L. R. G. (2005). *The physics of rubber elasticity* (3. ed., repr). OUP Oxford. https://www.google.co.nz/books/edition/The_Physics_of_Rubber_Elasticity/EfCZXXKQ50wC?hl=en&gbpv=0

Tridon hose clamps—Perforated band—Regular clamp. (2022). *Yousta*. https://www.yousta.com.au/product/tridon-hose-clamps-perforated-band-regular-clamp/

Ucar, N. (2000a). Prediction of Curling Distance of Dry Relaxed Cotton Plain Knitted Fabrics. *Journal of Textile Engineering*, *46*(4), 118–122. https://doi.org/10.4188/jte.46.118

Ucar, N. (2000b). Prediction of Curling Distance of Dry-Relaxed Cotton Plain Knitted Fabrics. *Journal of Textile Engineering*, *46*(4), 109–117. https://doi.org/10.4188/jte.46.109

Vassiliadis, S. G., Kallivretaki, A. E., & Provatidis, C. G. (2007). Mechanical simulation of the plain weft knitted fabrics. *International Journal of Clothing Science and Technology*, *19*(2), 109–130. https://doi.org/10.1108/09556220710725711

Vassiliadis, Savvas G. (2007). Geometrical modelling of plain weft knitted fabrics. *CSIR*, *Mar-2007*, 62–71.

Vogue Knitting. (2002). *Vogue Knitting: The Ultimate Knitting Book, Completely Revised and Updated*. https://store.vogueknitting.com/product/vogue-knitting-the-ultimate-knitting-book-completely-revised-and-updated/

Walker, E. M., & Doyle, P. J. (1952). SOME FUNDAMENTAL PROPERTIES OF HOSIERY YARNS AND THEIR RELATION TO THE MECHANICAL CHARACTERISTICS OF KNITTED FABRICS. *Journal of the Textile Institute Proceedings*, *43*(1), P19–P35. https://doi.org/10.1080/19447015208663954

Wang, J., Long, H., Soltanian, S., Servati, P., & Ko, F. (2014a). Electromechanical properties of knitted wearable sensors: Part 1 – theory. *Textile Research Journal*, *84*(1), 3–15. https://doi.org/10.1177/0040517513487789

Wang, J., Long, H., Soltanian, S., Servati, P., & Ko, F. (2014b). Electro-mechanical properties of knitted wearable sensors: Part 2 – Parametric study and experimental verification. *Textile Research Journal*, *84*(2), 200–213. https://doi.org/10.1177/0040517513490057

Warncke, M. N., Böhmer, C. H., Sachse, C., Fischer, S., Häntzsche, E., Nocke, A., Mersch, J., & Cherif, C. (2023). Advancing Smart Textiles: Structural Evolution of Knitted Piezoresistive Strain Sensors for Enabling Precise Motion Capture. *Polymers*, *15*(19), 3936. https://doi.org/10.3390/polym15193936

Weft Knitting Structure. (2013). *Textile Information* [Graphic]. https://textileinformations.com/weft-knitting-structure/

Yan, Y., Jiang, S., & Zhou, J. (2021a). Three-dimensional stretchable knitted design with transformative properties. *Textile Research Journal*, *91*(9–10), 1020–1036. https://doi.org/10.1177/0040517520968281

Yan, Y., Jiang, S., & Zhou, J. (2021b). Three-dimensional stretchable knitted design with transformative properties. *Textile Research Journal*, *91*(9–10), 1020–1036. https://doi.org/10.1177/0040517520968281

Yang, K., Isaia, B., Brown, L. J. E., & Beeby, S. (2019). E-Textiles for Healthy Ageing. *Sensors*, *19*(20), 4463. https://doi.org/10.3390/s19204463

Zhang, H., Tao, X., Wang, S., & Yu, T. (2005). Electro-Mechanical Properties of Knitted Fabric Made From Conductive Multi-Filament Yarn Under Unidirectional Extension. *Textile Research Journal*, *75*(8), 598–606. https://doi.org/10.1177/0040517505056870

Zhang, H., Tao, X., Yu, T., & Wang, S. (2006). Conductive knitted fabric as large-strain gauge under high temperature. *Sensors and Actuators A: Physical*, *126*(1), 129–140. https://doi.org/10.1016/j.sna.2005.10.026